Elucidation of the aerobic respiratory chains in mycobacteria

Limenako Georgina Matsoso

A thesis submitted to the Faculty of Science, University of the Witwatersrand, Johannesburg, in fulfilment of the requirements for the degree of Doctor of Philosophy.

September, 2005

DECLRARATION

I declare that this thesis is my own, unaided work. It is being submitted for the degree of Doctor of Philosophy at the University of the Witwatersrand, Johannesburg. It has not been submitted before for any degree or examination at any other university.

_____ _____

Limenako Georgina Matsoso Date

ABSTRACT

The aerobic respiratory chain of mycobacteria consists of at least two branches, a cytochrome *c* branch terminating in an aa_3-type cytochrome *c* oxidase, and a quinol branch terminating in cytochrome *bd* oxidase. The structure and function of the former branch, leading from the menaquinone-menaquinol pool to the cytochrome bc_1 complex and terminating in the aa_3-type cytochrome *c* oxidase, was characterized in *Mycobacterium smegmatis.* Allelic exchange mutants of *M. smegmatis* in the bc_1 complex (Δ*qcrCAB*::*hyg*) and in subunit II of the aa_3-type cytochome *c* oxidase (Δ*ctaC*::*hyg*) were constructed and analyzed for growth, and gene expression using *lacZ* reporter assays and genome expression profiling by DNA microarray. Both mutants were found to be profoundly growth impaired. Disruption of this pathway resulted in an adaptation of the respiratory network that is characterized by a marked up-regulation of *cydAB*, which encodes the bioenergetically less-efficient and microaerobically induced cytochrome *bd*-type menaquinol oxidase that is required for the growth of *M. smegmatis* under O_2-limiting conditions. Other adaptations to re-routing of the electron flux through the branch terminating in the *bd*-type oxidase were revealed by comparative expression profiling of the bc_1-deficient mutant and its parental wild type strain using a partial-genome microarray of *M. smegmatis* that is enriched in essential genes. The majority of the genes up-regulated in the mutant are involved in intermediary metabolism and respiration. Also induced were several genes including, *uspL* and a homologue of Rv1592c, which were previously shown to be up-regulated by hypoxia in *M. smegmatis* (*uspL*) and *M. tuberculosis* (*uspL* and Rv1592). The cytochrome bc_1-aa_3 branch is required for growth of *M. smegmatis* under aerobic conditions and its disruption results in growth attenuation and up-regulation of cytochrome *bd* oxidase.

DEDICATION

I am proud to dedicate this thesis to the memory of my father

Mpiti B. Matsoso (1922-1989)

Father, I always wish you were here to share in my achievements,

but I do know that you have always been watching over me from Heaven.

ACKNOWLEDGEMENTS

I would like to express my gratitude to my supervisor, Professor Valerie Mizrahi, whose invaluable guidance, and support led me through this study. Val, I learnt a lot from you, and I appreciate everything. Thanks for the opportunities to travel abroad and present my work internationally. I am also grateful to Dr Bavesh Kana, for his input in various aspects of this study. None of these went unnoticed or unappreciated, thank you.

I would like to thank all my colleagues, in the Molecular Mycobacteriology Research Unit, names mentioned or not, for their various contributions to my learning during this study. Edith thanks for repeatedly showing me that computers are not the monsters that I sometimes thought they were. To Julia, thanks for always finding a way to put a smile on my face at times when I would otherwise be frowning. You are more than just a colleague.

I wish to thank Dr. Ross Coppel and his colleagues for their collaboration on the microarray experiments, especially Dr. David Powell (Victorian Bioinformatics Consortium, Monash University, Australia) for his assistance with the analysis of some of the DNA microarray data. I would also like to thank Dr. Harvey Rubin, Dr. Martin Voskuil and Dr. David Sherman for their helpful discussions.

I appreciate the financial support provided by the Howard Hughes Medical Institute (International Research Scholar's grant to Prof. Mizrahi), the Medical Research Council of South Africa and the National Research Foundation of South Africa (grants to Prof. Mizrahi).

To my family- mother ('Mapontso M. Matsoso), my brothers, sisters and their families, thank you all for your love, support and encouragement, and thanks for always believing in me. Special thanks to you mother: I don't have enough words to express my gratitude to you– for being a mother, a "father" and a friend all in one. You have always been the source of love, dignity, courage, strength, and perseverance to me, and I thank God for keeping you.

Above all, I thank God for everything.

PUBLICATIONS FROM THIS THESIS

Matsoso, L. G., B. D. Kana, P. K. Crellin, D. J. Lea-Smith, A. Pelosi, D. Powell, S. S. Dawes, H. Rubin, R. L. Coppel, and V. Mizrahi. 2005. Function of the cytochrome bc_1-aa_3 branch of the respiratory network in mycobacteria and network adaptation occurring in response to its disruption. J. Bacteriol. **187:**6300-6308.

TABLE OF CONTENTS

LIST OF FIGURES

LIST OF TABLES

1. INTRODUCTION

1.1 Mycobacteria and diseases

Mycobacteria are Gram-positive bacteria belonging to the family *Actinomycetales*, members of which include other clinically and industrially important genera such as *Corynebacterium*, *Nocardia*, *Rhodococcus* and *Streptomyces* (Ishikawa *et al*., 2004). Members of this family are characterized by GC-rich DNA and a cell wall that contains mycolic acids (Brennan and Nikaido, 1995; Bott and Niebisch, 2003; Ishikawa *et al*., 2004). The genus *Mycobacterium* comprises more than seventy species of human and animal pathogens as well as non-pathogenic saprophytes (Krzywinska *et al*., 2004). Among the world's most important human pathogens are *Mycobacterium tuberculosis* and *Mycobacterium leprae*, the causative agents of tuberculosis and leprosy, respectively. The naturally non-pathogenic members of the *Mycobacterium avium* complex are increasingly emerging as opportunistic pathogens in immuno-compromised individuals such as AIDS patients (Hou *et al*., 2002). Although the availability of multi-drug therapy and the BCG vaccine helped to reduce the incidence of leprosy, the annual emergence of 690 000 new cases clearly indicates that this disease remains a health concern (Cole *et al*., 2001). However, the scale of infection by *M. tuberculosis* poses an even higher threat world-wide.

1.2 Tuberculosis: a global burden

Tuberculosis (TB) incidences have escalated at an alarming rate over the past two decades, prompting the World Health Organisation (WHO) to declare TB as a global emergency (Ortalo-Magne *et al*., 1996). Approximately one third of the world's population is estimated to be latently infected with *M. tuberculosis* and 2-3 million people die from TB every year, while an estimated 8.2 million new cases were reported per year by 2002 (Raviglione, 2003; Rook *et al*., 2005). The impact of TB is mostly suffered in developing countries, with the highest prevalence in Southeast Asia and sub-Saharan Africa, where the currently available BCG vaccine is failing to control the disease (Rook *et al*., 2005). However, TB is a threat to the whole world as there is no population that is immune to the disease risk (van Helden, 2003).

The battle to bring TB under control is hampered by, among other factors, the overwhelming increase in the spread of human immunodeficiency virus (HIV) infection, with a significant fraction of the TB deaths being attributable to co-infection with HIV (Williams and Dye, 2003; Corbett *et al*., 2003; Andries *et al*., 2004; Ballel *et al*., 2005). The problem is further compounded by the emergence of drug-resistant strains of ***M. tuberculosis***, demonstrating the urgent need to develop new anti-tubercular drugs (Cohen *et al*., 2003; Andries *et al*., 2004; Ballel *et al*., 2005). Nevertheless, there is an even more compelling need to develop drugs that can act against latent ***M. tuberculosis*** as most cases of active TB result from reactivation of latent infections (D. R. Sherman, 6th International Conference on the Pathogenesis of Mycobacterial Infections, Stockholm, 2005).

1.2.1 Tuberculosis prevention and treatment

The BCG vaccine and challenges facing it

An ideal way to control a disease such as TB would be to have a protective vaccine that would prevent infection and progression of disease. The only currently available vaccine for TB, *Mycobacterium bovis* bacille Calmette-Guérin (BCG) – an attenuated deletion mutant of *M. bovis* – (Horwitz *et al*., 2005), is the world's most widely used (Andersen and Doherty, 2005; Horwitz *et al*., 2005) and one of the safest vaccines known (Rook *et al*., 2005). However, this vaccine is failing to control TB. Whereas BCG successfully protects against disseminated forms of TB such as miliary TB in children (Brennan, 2005; Rook *et al*., 2005) and tuberculous meningitis (Andersen and Doherty, 2005; Rook *et al*., 2005), it provides little or no efficacy against adult pulmonary TB (Brennan, 2005; Andersen and Doherty, 2005; Rook *et al*., 2005; Grode *et al*., 2005), with the BCG failure being highest in developing countries where it is most needed (Andersen and Doherty, 2005; Rook *et al*., 2005). Adult pulmonary TB is both the main source of new infections and the main cause of morbidity and mortality (Andersen and Doherty, 2005). This therefore underscores the need for development of new vaccines or improvement of BCG. An example of an improved BCG vaccine has recently been reported, which consists of a urease C-deficient recombinant BCG mutant that expresses listeriolysin, and

it has been shown to display a superior protection against tuberculosis, compared to its parental wild type, in a mouse model (Grode *et al*., 2005).

The question of whether BCG should be improved or replaced remains a subject of debate as some studies have suggested that the low efficacy against adult pulmonary TB may be due to the limited life-span of BCG protection, which is estimated to be 10-20 years (Andersen and Doherty, 2005). This waning BCG protection in adolescence corresponds to the increase in the levels of adult pulmonary TB (Brennan, 2005; Andersen and Doherty, 2005). If correct, this then argues against development of a better vaccine to replace BCG in infant vaccination but instead, favours development of a booster for BCG or a combination of both (Brennan, 2005; Andersen and Doherty, 2005). However, this would require an understanding of why the efficacy of BCG varies so much in human hosts as opposed to animal models. While still a subject of debate, two hypothetical reasons have been proposed to account for the failure of BCG in tropical regions, both of which are linked to exposure of individuals to environmental mycobacteria (Andersen and Doherty, 2005). Firstly, the masking hypothesis suggests that the immunity provided by environmental mycobacteria masks that derived from a subsequent BCG vaccination as the two are superimposed (Andersen and Doherty, 2005). Alternatively, the blocking hypothesis proposes that the pre-existing immune responses derived from exposure to environmental mycobacteria block BCG replication and therefore render the vaccine ineffective. Nonetheless, the two hypotheses are not mutually exclusive (Andersen and Doherty, 2005).

Although a number of vaccines have recently been developed, which have entered or are on their way to clinical trials (Andersen and Doherty, 2005; Rook *et al*., 2005), the main challenge that remains is to determine whether they will also be safe and effective against bacilli in latent TB infections, as these represent the reservoir for the disease (Andersen and Doherty, 2005; Rook *et al*., 2005). It has been suggested that such a vaccine be designed to reduce immunopathology (Andersen and Doherty, 2005). However, the lack of knowledge on the biology of *M. tuberculosis* in latent infections hinders progress towards development of such vaccines (Brennan, 2005).

Antitubercular chemotherapy and drug resistance

TB incidences have continued to rise in spite of the availability, for more than half a century, of chemotherapeutic drugs to treat the disease (Ballell *et al*., 2005). Due to the high drug tolerance exhibited by *M. tuberculosis*, a multidrug regimen has long been introduced for treatment of TB (Morris *et al*., 2005). The regimen involves a daily treatment with the four front-line drugs, isoniazid (INH), rifampin (RIF), pyrazinamide (PZA) and ethambutol (EMB) for 2 months, followed by daily doses of RIF and INH for 4 months (Ballell *et al*., 2005). The escalating figures have been attributed to a number of reasons including coinfection with HIV, and the emergence of multidrug resistance resulting from lack of compliance (Ballell *et al*., 2005; Morris *et al*., 2005) and/or suboptimal drug dosage (Morris *et al*., 2005). To address the problem of non-compliance, the WHO introduced the directly observed therapy, short course (DOTS) strategy (Cohen and Murray, 2004; Ballell *et al*., 2005) a decade ago. This strategy involves supervised administration of the four front-line drugs to sputum-positive TB patients to ensure their compliance, and it has been shown to have cure rates as high as 95%. However, the implementation of DOTS requires substantial infrastructure and is labour-intensive, and therefore has not been fully implemented in all WHO regions, making it difficult to prevent development of multidrug resistant (MDR) *M. tuberculosis* (Ballell *et al*., 2005). This problem is exacerbated by the delay in detecting drug resistance (Cohen and Murray, 2004; Ballell *et al*., 2005).

Although the impact of MDR *M. tuberculosis* emergence on the global TB control remains unknown (Cohen and Murray, 2004), recent mathematical models have paradoxically suggested that successful reduction of wild type drug-sensitive strains of *M. tuberculosis*, where effective treatment programs are in place, paves the way for new infection with the circulating MDR strains (Blower and Chou, 2004; Cohen and Murray, 2004). Therefore, there is a need for development of strategies that will combine high-quality DOTS programs with therapy for MDR TB infections (Cohen and Murray, 2004; Ballell *et al*., 2005). Equally important to the treatment of MDR infections is the eradication of bacilli in latent infections or prevention of such infections to develop into active disease (Lenaerts *et al*., 2005). An approach to address both of these problems calls for development of new drugs that can shorten the length of treatment as pointed out

by the Global Alliance for TB Drug Development (Andries *et al*., 2004; Lenaerts *et al*., 2005). One such drug, a diarylquinoline active against ATP synthase of *M. tuberculosis*, is currently undergoing clinical trials (Andries *et al*., 2004). Another example of a drug that has shown the required properties in preclinical tests is the nitroimidazopyran PA-824 (Lenaerts *et al*., 2005). Development of more potent drugs that will be active against various strains of *M. tuberculosis* in different stages/forms of infection requires an understanding of the biology of these bacilli. However, little is known about the biology of bacilli in latent infections.

1.2.2 Latency

There is growing awareness regarding the way in which the terms latency and persistence were loosely used interchangeably in the past, and the importance of what they mean in the current era of growing insight into the possible physiological differences exhibited by bacilli in latent compared to persistent infections. However, in the context of this study, the term *latency* is used to refer to the state(s) in which tubercle bacilli exist in the host for an extended period of time without causing clinical disease symptoms, following an infection. This excludes bacilli that may remain in the host following chemotherapeutic treatment. Following a primary infection with *M. tuberculosis*, one of a number of outcomes can ensue. The host's innate immune mechanisms may destroy the bacilli (Flynn and Chan, 2001), although the organism is almost never eliminated (Glickman *et al*., 2001; Stewart *et al*., 2003; Monack *et al*., 2004). Alternatively, failure of the innate immunity to control the infection can lead to progression to active disease (Dannenberg and Rook 1994), within 1 to 3 years of infection (Flynn and Chan, 2001; Stewart *et al*., 2003), and this proportion constitutes 5-10% of individuals who are infected with *M. tuberculosis* (Stewart *et al*., 2003; Rook *et al*., 2005).

Individuals who harbour the bacilli but do not develop clinical disease are said to be latently infected (Flynn and Chan, 2001; Flynn and Chan, 2005), and these constitute approximately 90% of the people who are infected with *M. tuberculosis* (Rook *et al*., 2005). The bacilli in such cases can persist undetected in the host for decades before causing active disease (Cosma *et al*., 2004). By mechanisms yet to be elucidated, it is estimated that 5-10% of latent TB infections will reactivate to cause active disease (Flynn

and Chan, 2001; Flynn and Chan, 2005; Boshoff *et al*., 2005). The only clinical evidence in latently infected individuals is the delayed-type hypersensitivity (DTH) reaction as determined by the skin test with the purified protein derivative (PPD) used in screening for TB infection (Dannenberg and Rook 1994; Flynn and Chan, 2001; Glickman *et al*., 2001). The presence of a healing granulomatous structure in the lungs of latently infected individuals has also been noted (Boshoff *et al*., 2005).

Bacilli in a latent infection are thought to be in a "dormant' state, another term that requires contextual definition. In this work *dormancy* refers to the state in which the bacteria exhibit highly reduced or no metabolism, are not (or very slowly) replicating and do not increase in numbers (Wayne and Sohaskey, 2001). Very little is known about the exact location of these dormant bacteria during latent infection (Monack *et al*., 2004), but they are thought to reside mainly in the granulomas where their metabolism and replication remain under the immune surveillance of the host (Cosma *et al*., 2004; Monack *et al*., 2004; Boshoff *et al*., 2005). However, some models hypothesize that the bacilli reside in the caseum, while others propose that they can escape from the granuloma to new sites (Cosma *et al*., 2004).

Containment of latent M. tuberculosis *infection in granulomas*

Although the mechanisms by which latent infection is established and maintained remain largely unknown, there is consensus that an interplay of the *M. tuberculosis* virulence determinants and the host's immune response contribute towards this (Shen *et al*., 2004; Volkman *et al*., 2004; Flynn and Chan, 2005; Wallis, 2005). Formation of granulomas represents an effort by the host's immune system to contain the infection that otherwise cannot be eradicated (Volkman *et al*., 2004; Flynn and Chan, 2005; Salgame, 2005; Wallis, 2005). Granulomas are complex structures composed of tight aggregates of mononuclear phagocytes that form around macrophages infected with *M. tuberculosis* in both latent and active infection (Volkman *et al*., 2004; Salgame, 2005; Wallis, 2005). From the host's side, the tuberculous granuloma is a physical barrier that helps to limit bacterial replication and probably dissemination, while, to the pathogen's advantage, it provides a niche for evading eradication by the immune system (Flynn and Chan, 2005).

Environmental conditions faced by* M. tuberculosis *in latent infections

The granuloma is thought to create a hostile environment for *M. tuberculosis*, in which pH, nutrient availability, oxidative and nitrosative stress are likely to restrict the growth of this organism (Wayne and Sohaskey, 2001; Dahl *et al*., 2003; Timm *et al*., 2003; Wallis, 2005). Of these conditions, the mechanism of physiological adaptation of *M. tuberculosis* to oxygen (O_2) depletion has been most intensively investigated. Whereas a rapid shift from an O_2-rich environment to an O_2-deficient one has been shown to result in death (Wayne and Sohaskey, 2001), the widely accepted Wayne model has demonstrated that a gradual depletion of O_2 from *M. tuberculosis* cultures leads to progression of this organism through two stages of non-replicating persistence (Wayne and Sohaskey, 2001). This model demonstrates that *M. tuberculosis* replication requires O_2. A number of studies that have utilized transcriptional profiling to investigate the metabolic response of *M. tuberculosis* to inhibition of aerobic electron flow by O_2 restriction (Sherman *et al*., 2001; Schnappinger *et al*., 2003; Voskuil *et al*., 2003; Voskuil *et al*., 2004; Boshoff *et al*., 2004) or by other means (Boshoff *et al*., 2004; Voskuil *et al*., 2003) have revealed the importance of the respiratory network in adaptation of *M. tuberculosis*. In order to investigate some of the hypotheses derived from these studies, a more in-depth understanding of the function and regulation of the respiratory network of *M. tuberculosis* is required.

1.3 Respiration

In broad terms, respiration at the level of the organism refers to the exchange of gases between the organism and its environment. However, of relevance to this study is respiration at the cellular level, which generally refers to the process by which cells extract energy from nutrients and conserve it in the biologically useful forms, such as ATP. Respiration comprises a chain of enzyme-mediated reductive-oxidative (redox) reactions in which electrons are transferred in a stepwise fashion from the nutrient (donor) to a terminal oxidant (acceptor). At certain points along the chain, electron transfer is coupled to energy-conserving proton translocation, which drives production of ATP (Payne, 2001). This energy can subsequently be used to support other metabolic activities of the cell. Depending on its environment and the type of biological machinery

it is equipped with, an organism can use one or both of two types of respiration, aerobic or anaerobic respiration. In aerobic respiration, O_2 is used as the terminal oxidant, whereas other organic and inorganic substances such as nitrate are used as terminal oxidants in anaerobic respiration (Poole and Cook, 2000). These two types of respiration differ greatly in terms of energy yield, with more energy produced by aerobic than by anaerobic respiration.

1.3.1 Aerobic respiration

Aerobic respiration is characterized by a stepwise four-electron reduction of O_2 to water (Hansford, 2001; Wikström, 2001). In this multi-step redox process, hydrogen atoms (or their electrons) are transferred from the substrate such as glucose, pyruvate, and fatty acids, to O_2 through a chain of electron carriers (Hansford, 2001). Electron carriers consist of a diverse group of compounds ranging from cytochromes, quinones, NADH ($NAD^+ + H^+ + 2e^-$), flavins, to iron-sulfur proteins and others (Roehm, 2001). Some of these electron carriers act as prosthetic groups for the membrane-bound respiratory proteins while others act as intermediate mobile carriers between such proteins (Roehm, 2001). For electron transfer to proceed spontaneously (without requiring external energy), the reduction potential of the acceptor must be higher than that of the donor, suggesting that electron carriers have to be arranged in order of increasing redox potential (Roehm, 2001). This array of electron carriers forms what is referred to as the electron transport (or respiratory) chain. However, it is important to note that the respiratory proteins may not necessarily be physically arranged in the order of their roles in the membrane.

The passage of hydrogen atoms (or electrons) along the respiratory chain in the series of redox reactions is coupled to ATP formation by a process called oxidative phosphorylation (Hansford, 2001; Solomon ***et al.***, 1993). This process, which only occurs in membrane-bound structures, and is commonly explained by the chemiosmotic model of energy conservation, was initially proposed by Peter Mitchell in 1961 (Solomon ***et al.***, 1993; Hansford, 2001). According to this model, the stepwise oxidation of NADH or $FADH_2$ by oxygen, catalysed by components of the respiratory chain, results in the release of energy that is used to pump protons across the membrane, forming a proton gradient (protonmotive force). This force then draws protons back into the matrix (in the

case of mitochondria) through special channels that occur in the ATP synthase complex, releasing free energy that is used by this enzyme to synthesize ATP from ADP and inorganic phosphate (P_i) (Hansford, 2001; Solomon *et al.*, 1993).

1.3.2 Respiration in eukaryotes

In eukaryotes, respiration occurs in specialized organelles known as mitochondria, whose structure is adapted for its function. Each mitochondrion consists of an inner compartment (the matrix) that is bounded by two membranes – an inner and an outer membrane– (Solomon *et al.*, 1993). The space between the membranes (the intermembrane space) forms another compartment. The mitochondrial respiratory chain consists of four complexes, NADH:ubiquinone oxidoreductase (NADH dehydrogenase, complex I), succinate:ubiquinone oxidoreductase (succinate dehydrogenase, complex II), ubiquinol:cytochrome *c* oxidoreductase or cytochrome bc_1 complex (complex III), and an aa_3-type cytochrome *c* oxidase (complex IV) (Solomon *et al.*, 1993; Cruciat *et al.*, 2000). These protein complexes are embedded in the inner mitochondrial membrane (Cruciat *et al.*, 2000). The smaller respiratory molecules, ubiquinone and cytochrome *c* act as mobile electron carriers between these complexes (Hansford *et al.*, 2001). The fifth complex, ATP synthase (complex V) does not transport electrons but plays a very important role in oxidative phosphorylation.

NADH:ubiquinone oxidoreductase (complex I)

NADH dehydrogenase is the largest enzyme complex of the mitochondrial respiratory chain, consisting of more than 40 protein subunits encoded by the *nuo* operon, one non-covalently bound flavin mononucleotide (FMN) and at least 5 iron-sulfur clusters (Schuler *et al.*, 1999; Tsang *et al.*, 2001). Whereas the mammalian mitochondria contain only type I NADH dehydrogenase (NDH-I), some eukaryotes have been shown to have a single subunit type II alternative NADH dehydrogenase (NDH-II) (Nantapong *et al.*, 2005). This complex catalyses the oxidation of NADH into NAD^+, and links this to reduction of ubiquinone into ubiquinol. At the same time the enzyme translocates protons from the matrix into the intermembrane space. NADH is bound on the module of the protein that protrudes into the matrix, and electrons from it are transferred in a yet

undefined series of steps via the flavin cofactor and iron-sulfur clusters to ubiquinone (Hansford, 2001). The overall reaction can be summarized as follows:

$$NADH + H^+ + \text{ubiquinone} + 4H^+ (\text{in}) \rightarrow NAD^+ + \text{ubiquinol} + 4H^+ (\text{out})$$

where "in" and "out" indicate movement of protons into and out of the matrix, respectively. NDH-I pumps four protons across the mitochondrial inner membrane for every pair of electrons transferred (Hansford, 2001).

Succinate:ubiquinone oxidoreductase (complex II)

This enzyme complex forms an integral part of the mitochondrial membrane, and is composed of 4 protein subunits, a flavin adenine dinucleotide (FAD) and several iron-sulfur clusters (Roehm, 2001; Yankovskaya *et al*., 2003; Hederstedt, 2003). Though part of the Krebs cycle, succinate dehydrogenase also forms part of the respiratory chain (Solomon *et al*., 1993). It catalyzes oxidation of succinate into fumarate in the matrix and simultaneously reduces ubiquinone. Unlike NDH-I, succinate dehydrogenase does not pump protons, as there is not enough free energy released during electron transfer by this complex to drive translocation of protons (Hansford, 2001).

The ubiquinone/ubiquinol pool and other dehydrogenases

Quinones are derivatives of benzoquinone that bear long hydrophobic isoprenoid side chains that render them soluble in the hydrophobic interior of membranes (Roehm, 2001). They can freely move laterally within the membrane, a property that makes them suitable for transfer of electrons between complexes of the respiratory chain (Roehm, 2001). Quinones can carry hydrogen atoms (Solomon *et al*., 1993). In addition to complexes I and II, the ubiquinone pool can also be reduced by electrons coming from oxidation of other metabolites such as acyl-coenzyme A (acyl-CoA; produced by β-oxidation of fatty acids) and α-glycerophosphate by their respective dehydrogenases in the matrix. Reduced ubiquinone transfers the electrons to ubiquinol:cytochrome *c* oxidoreductase (Solomon *et al*., 1993).

Ubiquinol-cytochrome c oxidoreductase or cytochrome bc_1 complex (complex III)

Cytochrome bc_1 complex plays a crucial role in both photosynthetic and respiratory electron transport chains (Zhang *et al*., 1998; Darrouzet and Daldal, 2002). The mammalian mitochondrial complex III consists of 11 subunits, 2 of which form the catalytic core of the enzyme. This complex contains 4 redox centres: 2 heme groups, b_H (high-spin heme *b*) and b_L (low-spin heme *b*) of cytochrome *b* (subunit III), 1 heme group in cytochrome c_1 (subunit IV), and 1 iron-sulfur cluster of Rieske protein (subunit V) (Zhang *et al*., 1998). The enzyme complex transfers electrons from ubiquinol to a water-soluble cytochrome *c*. It is believed that for each pair of electrons transferred, the complex draws 2 protons from the matrix and pumps 4 out into the cytosolic side (Hansford, 2001). The overall redox reaction catalysed by this enzyme complex is as follows:

$$\text{ubiquinol} + 2 \text{ cytochrome } c^{3+} + 2H^+ \rightarrow \text{ubiquinone} + 2 \text{ cytochrome } c^{2+} + 4H^+$$

Cytochrome c oxidase (complex IV)

Cytochrome *c* oxidase is the key enzyme of cellular respiration (Wikström, 2001) and together with other respiratory oxidases is estimated to be responsible for at least 90% of the total consumption of O_2 in the biosphere (Garcia-Horsman *et al*., 1994; Hansford, 2001). The mammalian cytochrome *c* oxidase consists of 2 units each of 13 polypeptides, the 3 largest and most hydrophobic (subunits I, II and III) of which are encoded in the mitochondria, whereas the remaining 10 are encoded in the nucleus (Garcia-Horsman *et al*., 1994; Hansford, 2001). It belongs to the heme-copper oxidase super-family, members of which are characterized by presence of a subunit homologous to the largest subunit I of mammalian enzyme, and have in common a low-spin heme and a binuclear centre composed of a high-spin heme and Cu_B (Garcia-Horsman *et al*., 1998).

This enzyme catalyses the four-electron reduction of O_2 to water, and also couples that to proton translocation. It has four redox-active metal sites, namely, heme *a*, heme a_3, Cu_A and Cu_B (Gennis, 1998; Bränden *et al*., 2001). Subunits I and II contain all the redox cofactors required for catalysis, with subunit I containing the heme a_3- Cu_B binuclear centre where O_2 is bound until it has been fully reduced to H_2O, as well as the low-spin heme *a* (Wikström, 2001). Subunit II contains the unique bimetallic copper

center (two Cu_A atoms) that serves as the primary electron acceptor of the enzyme (Wikström, 2001). Cu_A receives electrons from cytochrome *c* and each electron is transferred via heme *a* to the heme *a*-Cu_B binuclear centre. The sequestration of O_2 in the binuclear centre ensures that release of partially reduced and toxic O_2 intermediates is prevented (Hansford, 2001). Although it is known that cytochrome *c* oxidase can pump protons, the mechanism by which this happens remains unknown in spite of years of study (Wikström, 2004). However, the general consensus is that the enzyme takes up 8 protons from the medium (matrix) and pumps 4 into the intermembrane space per O_2 molecule that is reduced (Gennis, 1998; Wikström, 2001). The overall reaction for O_2 reduction can be presented as follows,

$$4e^{-1} + 8H_i^+ + O_2 \rightarrow 2H_2O + 4H_o^+$$

where "i" and "o" refer to the protons input and output, respectively.

The ATPsynthase (F_0F_1-ATPase; complex V)

Although it does not transport electrons, ATP synthase is responsible for generation of ATP via oxidative phosphorylation. This is a large multi-subunit transmembrane protein comprising peptides encoded in the mitochondrial and nuclear genomes (Hansford, 2001). It uses energy stored in the pH and potential gradients, created by pumping of protons across the membrane by enzymes of the respiratory chain, to synthesize ATP. It is believed that electrons flow back into the mitochondrial matrix down the gradient via a special channel accompanied by conformational changes in the ATP synthase, releasing energy that is used to drive ATP synthesis from ADP and inorganic phosphate (Hansford, 2001; Tran and Cook, 2005).

1.4 Respiration in bacteria

1.4.1 The multiplicity of respiratory pathways

The remarkable ability of bacteria to survive in a wide variety of environments is attributable to their complex respiratory pathways (Poole and Cook, 2000). These systems are believed to have evolved over time, in bacterial progenitors, in response to the changing environmental conditions they were subjected to. Unlike the mitochondrial respiratory chain which is branched at the dehydrogenase end but terminates in only one

oxidase (cytochrome *c* oxidase), the bacterial respiratory chains are equipped with multiple terminal oxidases which can be modulated depending on the prevailing environmental conditions (Poole and Cook, 2000; Winstedt and von Wachenfeldt, 2000). These branched bacterial respiratory pathways enable the organisms to use O_2 as the terminal oxidant (aerobic respiration), or other, alternative terminal acceptors in the absence of oxygen (anaerobic respiration). Bacterial respiratory chains share a number of characteristics, namely (i) branching at both the dehydrogenase and reductase ends, (ii) use of O_2 and other alternative electron acceptors, (iii) presence of numerous cytochromes and quinones, (iv) the possibility of pairing one reductant with several oxidants, and (v) coupled proton translocation and energy transduction (Poole and Cook, 2000).

***The respiratory chain of* Escherichia coli**

The *E. coli* respiratory chain is the best characterized of all bacterial respiratory chains that have been studied to date (Garcia-Horsman, 1994; Poole and Cook, 2000). It consists of a number of dehydrogenases that can oxidize various substrates (e.g. NADH, succinate, malate, lactate and hydrogen) and contribute their reducing equivalents into the quinone pool (Poole and Cook, 2000). At least two types of quinones, ubiquinone and menaquinone, are involved in the respiratory chain of *E. coli*, and they are used selectively depending on the terminal oxidant to which the electrons are destined. It has been proposed that electrons destined to O_2 are transferred through ubiquinone (Poole and Cook, 2000). From ubiquinol, the electrons can be transferred directly to either one of three oxidases, cytochrome bo_3 (encoded by *cyoABCDE*), cytochrome *bd* (encoded by *cydAB*) or possibly to cytochrome *bd* II (encoded by *cbdAB*) (Poole and Cook, 2000; Bebbington and Williams, 2001). This is notably different from the mitochondrial respiratory chain where electrons are transferred from ubiquinol to the terminal oxidase via a cytochrome bc_1 complex and cytochrome *c*. Since they oxidize the ubiquinol pool directly, these *E. coli* terminal oxidases are referred to as quinol oxidases as opposed to the mitochondrial cytochrome *c* oxidase. While the *E. coli* cytochromes bo_3 and *bd* oxidases have been extensively characterized, the function of the third oxidase,

cytochrome *bd* II, has not yet been discerned (Sturr *et al.*, 1996; Poole and Cook, 2000; Bebbington and Williams, 2001).

The two quinol oxidases, cytochrome bo_3 and cytochrome *bd*, differ in their structural and functional properties, including affinity for O_2 (Sturr *et al.*, 1996; Poole and Cook, 2000; Bebbington and Williams, 2001). Cytochrome bo_3 belongs to the heme-copper oxidase superfamily and can pump protons across the plasma membrane, whereas cytochrome *bd* does not. The former oxidase has a low affinity for O_2 and has been shown to be required for growth under O_2-rich conditions. Its ability to pump protons makes it energetically more efficient than cytochrome *bd* oxidase, which has a higher affinity for O_2, and is highly expressed under microaerobic conditions, but cannot pump protons (Sturr *et al.*, 1996; Poole and Cook, 2000; Bebbington and Williams, 2001; Alexeeva *et al.*, 2002). It is noteworthy that though cytochrome *bd* does not pump protons, it does contribute towards generation of a transmembrane electrical potential difference (Zhang *et al.*, 2004; Belevich *et al.*, 2005).

***The respiratory chain of* Corynebacterium glutamicum**

C. glutamicum is gaining increasing recognition as a model organism for studying the certain aspects of the biology of high G+C content Gram-positive bacteria, including pathogens such as *C. diphtheria* and *M. tuberculosis* (Nolden *et al.*, 2002; Niebisch and Bott, 2003). The aerobic respiratory chain of *C. glutamicum* is by far the best-characterized among the nocardioform actinobacteria. It comprises several branches of dehydrogenases that transfer electrons into the menaquinone pool, from where they can be transferred to the terminal electron acceptor O_2 via one of at least two pathways – the cytochrome *c* branch or quinol branch (Bott and Niebisch, 2003). The respiratory chain of *C. glutamicum* is schematically illustrated in Figure 1. The cytochrome *c* branch consists of a cytochrome bc_1 complex that oxidizes menaquinol and passes electrons to the terminal aa_3-type cytochrome *c* oxidase, whereas the quinol branch terminates in a cytochrome *bd*-type menaquinol oxidase. The former branch was shown to be of primary importance for aerobic growth as mutants lacking either cytochrome bc_1 complex or cytochrome aa_3 had severe growth defects (Niebisch and Bott, 2001). The presence of a

third putative terminal oxidase that is cyanide-resistant has been proposed, but its existence has yet to be proven (Bott and Niebisch, 2003; Nantapong *et al*., 2005).

NADH:menaquinone oxidoreductase

Interestingly, *C. glutamicum* synthesizes only one type of NADH dehydrogenase, NDH-II encoded by *ndh*, and its genome does not encode any other NADH dehydrogenase (Bott and Niebisch, 2003; Nantapong *et al*., 2005). In contrast to the mitochondrial NDH-I and the *E.coli* NDH-I, both of which are multi-subunit proton-pumping enzymes specified by the *nuo* operon, *C. glutamicum* NDH-II is a single-subunit enzyme, which does not translocate protons (Bott and Niebisch, 2003; Nantapong *et al*., 2005). In addition to NADH dehydrogenase activity, this enzyme was found to exhibit NADPH oxidase activity, and has been proposed to couple oxidation of NADPH to reduction of O_2 (Nantapong *et al*., 2005). The same study demonstrated that *C. glutamicum* NDH-II was a source of reactive O_2 species such as superoxide and hydrogen peroxide, associated more with oxidation of NADPH than NADH (Nantapong *et al*., 2005).

Succinate:menaquinone oxidoreductase

The genome of *C. glutamicum* contains genes (*sdhCAB*) that encode a three-subunit succinate dehydrogenase. The subunits include a flavoprotein (SdhA), an iron-sulfur protein (SdhB) and a membrane anchor protein (SdhC) (Bott and Niebisch, 2003). This enzyme has not yet been characterized in *C. glutamicum*, but genome comparisons suggest that it belongs to the same class as those of *B. subtilis* and *Wolinella succinogens* (Bott and Niebisch, 2003).

Other dehydrogenases that can reduce menaquinone

In addition to NADH and succinate dehydrogenases, *C. glutamicum* possesses genes encoding at least six other dehydrogenases, malate:menaquinone oxidoreductase (*mqo*), pyruvate oxidase (*poxB*), D-lactate dehydrogenase (*dld*), L-lactate dehydrogenase (*lldD*), glycerol-3-phosphate dehydrogenase (*glpD*) and L-proline dehydrogenase (*putA*) (Bott and Niebisch, 2003). These enzymes allow *C. glutamicum* to utilize various substrates to

generate energy. Electrons from these substrates are used to reduce the menaquinone pool (Bott and Niebisch, 2003).

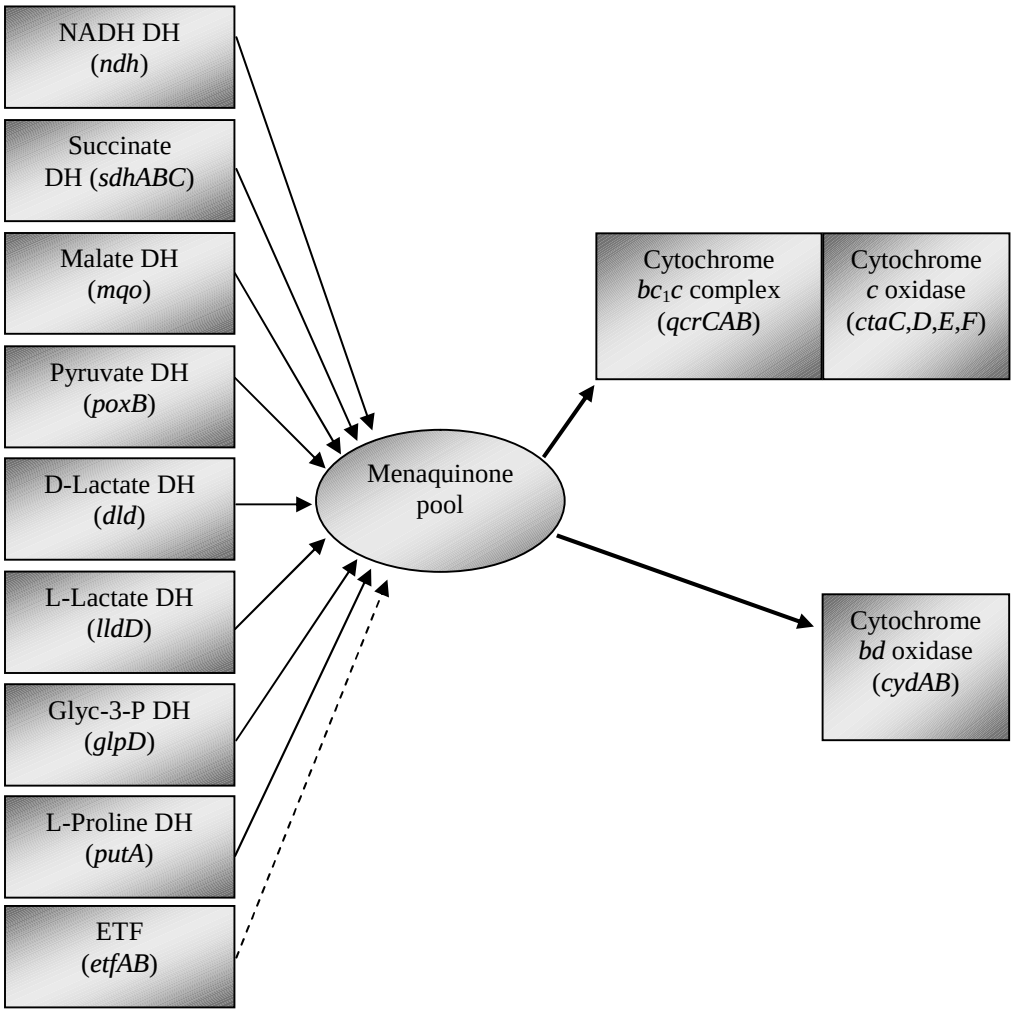

Figure 1. The respiratory chain of *C. glutamicum* (Adapted from Bott and Niebisch, 2003). Boxes represent the various dehydrogenases (DH) (left) or the terminal oxidases (right). The gene(s) encoding each dehydrogenase is shown in brackets. The solid arrows denote electron transfer, and the broken arrow denotes a putative path for electron flow.

Menaquinol:cytochrome c *oxidoreductase or cytochrome* bc_1 *complex*

The quinol-cytochrome *c* oxidoreductases comprise a large superfamily of enzymes found in mitochondrial and bacterial respiratory and photosynthetic electron transfer chains, and which couple electron transfer to proton translocation (Sone *et al.*, 2001). These enzymes accept electrons from quinol and transfer them to a small cytochrome *c*

located in the mitochondrial intermembrane space of eukaryotes or in the periplasmic space of bacteria, from where they are transferred to a cytochrome *c* oxidase (Sakamoto *et al.*, 2001).

The cytochrome bc_1 complex of *C. glutamicum* is encoded by the *qcrCAB* genes which specify cytochrome c_1, Rieske iron-sulfur protein, and cytochrome *b*, respectively (Sone *et al.*, 2001; Niebisch and Bott, 2001). Bioinformatic analysis of the deduced protein sequences and subsequent genetic and biochemical characterization of the proteins revealed a number of features that distinguish the bc_1 complex of *C. glutamicum* from the classical examples of these enzymes (Bott and Niebisch, 2003). The most peculiar of these features is presence of two heme-binding motifs (CXXCH) instead of one, in cytochrome c_1 (QcrC), which is indicative of a diheme c_1-type cytochrome (Sone *et al.*, 2001; Niebisch and Bott, 2001). This was found to be the sole *c*-type cytochrome in aerobically grown cells of *C. glutamicum* (Sone *et al.*, 2001; Niebisch and Bott, 2001), leading to the proposal that the second heme domain of cytochrome c_1 performs the function of a separate cytochrome *c* in the transfer of electrons form the bc_1 complex to the aa_3-type cytochrome *c* oxidase (Niebisch and Bott, 2001). The other differences include a 120 amino acid (aa) extension at the C-terminus of cytochrome *b* (QcrB), and presence of three instead of one transmembrane helices in the Rieske iron-sulfur protein (QcrA) (Bott and Niebisch, 2003). Genome comparisons of the *C. glutamicum qcrCAB* operon and deduced protein sequences with those of other bacteria showed a high similarity with those from *Mycobacterium*, *Streptomyces* (Sone *et al.*, 2001; Niebisch and Bott, 2001), and *Rhodococcus rhodochrous* (Sone *et al.*, 2003).

A *qcrCAB* deletion mutant of *C. glutamicum* was severely attenuated when grown aerobically in glucose minimal medium, indicating that the cytochrome bc_1 complex was important for aerobic growth of this organism (Niebisch and Bott, 2001). Spectral analysis of membranes from this mutant demonstrated that cytochrome c_1 was absent from this strain. In contrast, a peak characteristic of cytochrome aa_3 was not diminished in the mutant, indicating that this mutant could still synthesize the aa_3-type cytochrome *c* oxidase (Niebisch and Bott, 2001).

Cytochrome c *oxidase (cytochrome* aa_3*)*

The aa_3-type cytochrome *c* oxidase of *C. glutamicum* is encoded by *ctaD* (subunit I), *ctaC* (subunit II), *ctaE* (subunit III) and *ctaF* (subunit IV). Whereas subunit I (CtaD) showed all features typical of heme-copper terminal oxidases, subunits II and III displayed some differences from those of other organisms, while subunit IV was found to be unique to actinomycetes (Bott and Niebisch, 2003). Subunit II has an insertion of an extra 30 aa in the substrate-binding domain, which is absent from the mitochondrial and proteobacterial counterparts, and is proposed to play a role in the interaction of this oxidase with the di-heme cytochrome *c* of the bc_1 complex (Sakamoto *et al*., 2001). Subunits I and II form the catalytic core of the enzyme, while the functions of subunits III and IV remain to be elucidated.

Analysis of mutants in the different subunits of aa_3-type cytochrome *c* oxidase (Δ*ctaD* and Δ*ctaF*) showed severe growth defects, demonstrating that like the bc_1 complex, this oxidase is important for aerobic growth of *C. glutamicum* (Niebisch and Bott, 2001; Niebsch and Bott, 2003). Spectral analysis of both Δ*ctaD* and Δ*ctaF* mutants revealed the absence of cytochrome *a*, proving that both *ctaD* and *ctaF* encode subunits of the aa_3-type cytochrome *c* oxidase. In addition, both mutants exhibited a drastically reduced cytochrome c_1 peak (at 550 nm) than the wild type strain, suggesting that cytochrome aa_3 oxidase was important for the stability of cytochrome c_1. Based on these data and the primary structures of cytochromes bc_1 and aa_3, it was postulated that the two complexes associate to form a supercomplex (Niebisch and Bott, 2001). This hypothesis was later confirmed by the co-purification of bc_1- and aa_3-subunits using either streptavidin-tagged QcrB or CtaD (Niebisch and Bott, 2003).

Cytochrome bd *oxidase*

The *bd*-type menaquinol oxidase of *C. glutamicum* is encoded by *cydA* and *cydB* for subunits I and II, respectively (Kusumoto *et al*., 2000; Bott and Niebisch, 2003). These genes form a cluster with the *cydD* and *cydC* genes which are proposed to encode an ABC-type transporter. Based on sequence analysis, subunit I (CydA) of *C. glutamicum* and other high G+C Gram-positive bacteria lack a significant portion of the Q-loop found in *E. coli*, low G+C Gram-positive bacteria, proteobacteria and others (Bott and Niebisch,

2003). The cytochrome *bd* oxidase of *C. glutamicum* contains two heme types, a heme *d* and two heme *b* (high- and low-spin), and it exhibits menaquinol oxidase acivity (Kusumoto *et al*., 2000). This oxidase was found to be dominant in the stationary phase of cells grown aerobically in copper-deficient medium (Kusumoto *et al*., 2000). However, its general induction during stationary phase remains to be investigated (Bott and Niebisch, 2003).

ATP synthase and bioenergetics in C. glutamicum

The genome of *C. glutamicum* encodes an F_1F_0-ATP synthase (*atpI-BEFHAGDC* operon) (Bott and Niebisch, 2003). Whereas the function of the *atpI* gene is not known, *atpB*, *atpE* and *atpF* encode components of the F_0 part, a-, c- and b-subunit, respectively. Components of the F_1 part, δ-, α-, γ-, β- and ε-subunit, are encoded by *atpH*, *atpA*, *atpG*, *atpD* and *atpC*, respectively (Bott and Niebisch, 2003). An ATP synthase mutant with a point mutation in the γ-subunit had a decreased ATP synthase activity. Interestingly, this mutant exhibited an increased glucose consumption and respiration rate. This phenotype was assumed to be due to a shortage of ATP resulting from a defect in oxidative phosphorylation. Low ATP was proposed to increase the glucose catabolism and hence production of NADH, which consequently led to an increase in the rate of respiration by O_2 consumption (Bott and Niebisch, 2003).

The efficiency of oxidative phosphorylation has been shown to be dependent on the electron transfer pathway utilized. In *C. glutamicum* aerobic respiration, electron transfer to O_2 involves three enzymes that contribute towards the generation of an electrochemical proton gradient across the cytoplasmic membrane, namely, cytochrome bc_1 complex, aa_3-type cytochrome *c* oxidase and cytochrome *bd* oxidase (Bott and Niebisch, 2003). It is assumed that one molecule of ATP is synthesized by ATP synthase from every three or four protons transported from the outside to the inside. The cytochrome bc_1-aa_3 supercomplex is estimated to transport a net of six protons per two electrons, whereas the net value for cytochrome *bd* oxidase is two protons per two electrons. Therefore the transfer of electrons from NADH via the cytochrome bc_1-aa_3 branch is estimated to generate approximately three times more ATP than that generated when electrons flow to cytochrome *bd* oxidase. It is expected that transfer of electrons to

the menaquinone pool by lactate dehydrogenase, glycerol-3-phosphate dehydrogenase, proline dehydrogenase and malate:menaquinone reductase would yield similar energy proportions as for NADH dehydrogenase above. In all these enzymes, the protons used for the reduction of menaquinone come from the cytoplasm. In contrast the reduction of menaquinone by succinate dehydrogenase uses protons from the periplasmic side of the membrane and results in a net extrusion of four protons for every two electrons transferred. This translates to formation of approximately 1.3 ATP when electrons are transferred from succinate to O_2 via the cytochrome bc_1-aa_3 branch as opposed to 2 ATP formed when electrons come from NADH dehydrogenase through the same branch. Transfer of electrons from succinate to O_2 via the cytochrome *bd* oxidase results in no net proton extrusion and therefore no ATP synthesis by oxidative phosphorylation (Bott and Niebisch, 2003).

1.4.2 Respiratory inhibitors

Inhibitors of NADH dehydrogenase

In various organisms respiration has been shown to be inhibited by a wide spectrum of chemicals which target different components of the respiratory chain. The availability of such compounds has contributed towards understanding of the roles of the individual respiratory components. Phenothiazines such as chlorpromazine have long been known to inhibit respiration though their precise mode of action was not known. Recent studies have shown that these chemicals inhibit NADH dehydrogenase in *M. tuberculosis* (Boshoff *et al*., 2004; Weinstein *et al*., 2005) and *M. smegmatis* (Boshoff *et al*., 2004), whereas azoles were shown to inhibit succinate dehydrogenase activity (Boshoff *et al*., 2004). Inhibition of NADH dehygrogenase was accompanied by a decrease in the redox potential leading to a decrease in the intracellular ATP levels (Boshoff *et al*., 2004).

Inhibitors of the cytochrome* bc_1 *complex

A number of chemicals have been shown to block electron transfer through the respiratory chain by inhibiting the cytochrome bc_1 complex, and these include myxothiazol, stigmatellin and antimycin (Zhang *et al*., 1998; Ouchane *et al*., 2002). Whereas antimycin binds at the site (Q_i) where the reduction of quinone is postulated to

take place, stigmatellin and myxothiazol inhibit the complex by binding to the Q_o site of quinol oxidation (Zhang *et al*., 1998; Ouchane *et al*., 2002). Recently a novel inhibition at the cytochrome c_1 subunit of the complex by cyanide was reported for ***Rhodobacter capsulatus*** (Osyczka *et al*., 2004). Since cytochrome bc_1 complex is one of the proton coupling sites along the electron transport chain, its inhibition is expected to result in a change in the transmembrane proton gradient and thus lower the production of ATP by oxidative phosphorylation.

Inhibitors of terminal oxidases

The known inhibitors of aerobic respiratory terminal oxidases include nitric oxide (NO), cyanide and azides. NO has long been known to inhibit cytochrome *c* oxidase [reviewed by Cooper (2002)]. At high concentrations, it competes with O_2 by reversibly binding to the reduced iron of the heme a_3/Cu_B binuclear centre, and it binds to the oxidized copper under low concentrations. NO can also reversibly inhibit cytochrome *bd* oxidase, which unlike heme-copper oxidases does not contain Cu_B (Borisov *et al*., 2004). On the other hand, the respiratory inhibitors such as cyanide and azides specifically inhibit cytochrome *c* oxidase, but not cytochrome *bd* oxidase in *M. tuberculosis* (Boshoff *et al*., 2004).

1.4.3 Regulation of expression of the bacterial respiratory chain components

Bacteria respond to changes in the environment by altering the level of expression of genes required for growth or survival under such conditions (Poole and Cook, 2000). Adaptation to the changing conditions often requires coordinated regulation of a set(s) of genes, which often, may be controlled by a single transcriptional regulator (Boshoff *et al*., 2004; Green and Paget, 2004). Bacteria are equipped with a variety of two-component signal transduction regulatory systems, which can sense environmental changes and subsequently regulate a network of target genes. A two-component regulatory system consists of a membrane-bound sensor kinase that can activate a cognate transcriptional regulator by phosphorylation. The activated regulator can then turn a set(s) of genes (regulon) on or off (Himpens *et al*., 2000; Georgellis *et al*., 2001a; Parish *et al*., 2003).

For respiratory metabolism, availability of O_2 or other electron acceptors determines the switch from aerobic to anaerobic respiration (Poole and Cook, 2000). Alternatively, disruption of one or more of the pathways by chemical or genetic means can also lead to the switch. In the presence of adequate O_2, genes required for aerobic respiration may be switched on and those required for anaerobic respiration may be repressed. The converse is true under anoxic conditions (Zientz *et al*., 1998; Green and Paget, 2004). A number of bacterial two-component regulatory systems have been described that are responsible for regulation of respiratory metabolism, and they have been shown to respond to a range of signals, including environmental O_2, the redox states of electron carriers (quinone, NAD^+) and nitrite/nitrate levels. A few examples of these systems will be discussed below (Green and Paget, 2004).

Direct oxygen sensors

The FixLJ system

FixLJ is an oxygen-responsive two-component system that regulates genes involved in nitrogen fixation in bacteria such as *Rhizobium meliloti* (Miyatake *et al*., 2000; Green and Paget, 2004). Bacteria that are equipped with machinery necessary for fixing atmospheric nitrogen to ammonia are able to survive in habitats where fixed nitrogen is limiting. However, nitrogen-fixation is an energy-demanding process and therefore it has to be controlled tightly to avoid unnecessary energy consumption (Grabbe and Schmitz, 2003; Green and Paget, 2004). The sensor kinase FixL contains a kinase domain and a heme domain, and the latter acts as a sensor by binding O_2 (Green and Paget, 2004).

The FixLJ is the only system for which the mechanism for O_2 sensing has been elucidated in detail (Swem *et al*., 2003; Baruah *et al*., 2004). Under aerobic conditions, oxygen binds to the heme domain of FixL and converts its iron to a low-spin state. This causes a conformational change which inhibits the activity of the kinase domain, thus preventing FixL autophosphorylation and promoting the dephosphorylation of the response regulator, FixJ. Conversely, when O_2 is limiting, no O_2 is bound to the sensor (heme) domain and the heme iron changes to a high-spin state, which allows autophosphorylation of FixL and subsequent phosphorylation of FixJ. The activated FixJ

induces expression of FixK and NifA, which control expression of nitrogen-fixation genes (Miyatake *et al*., 2000; Green and Paget, 2004).

The Fnr system

Fnr (fumarate nitrate reduction) system is another example of an O_2 sensor and transcription factor which regulates expression of respiratory genes in response to hypoxia (Geadle and Ratcliffe, 2001). This system functions in close co-operation with the ArcAB system discussed below. In *E. coli* the system is expressed under both aerobic and anaerobic conditions. Under microaerobic conditions, Fnr activates the expression of cytochrome *bd* oxidase and represses that of cytochrome bo_3 oxidase. Whereas Fnr has no effect on the expression of cytochrome bo_3 oxidase anaerobically, it represses the expression of cytochrome *bd* oxidase and activates the nitrate reductase (Swem and Bauer, 2002; Brekasis and Paget, 2003; Green and Paget, 2004).

Fnr contains two domains, an amino terminal sensory domain and a carboxyl DNA-binding domain. The sensory domain contains a cysteine coordinated $[4Fe\text{-}4S]^{2+}$ cluster that is essential for dimerization. Under anaerobic conditions, Fnr is a homodimeric protein containing one $[4Fe\text{-}4S]^{2+}$ per subunit, and in this form it can bind to target promoters and regulate their expression. In the presence of O_2, this cluster is disassembled to a $[2Fe\text{-}2S]^{2+}$ that, probably through conformational changes, causes a switch from the dimeric form to the monomeric form that is unable to bind DNA (Brekasis and Paget, 2003; Green and Paget, 2004).

Redox sensors

The ArcAB system

The *E. coli* Arc (anoxic redox control) system is the best-studied of the bacterial two-component regulatory systems. ArcB is a transmembrane sensor kinase that can autophosphorylate in response to a signal, and then transphosphorylate the cytosolic response regulator, ArcA (Georgellis *et al*., 2001a; Alexeeva *et al*., 2003; Green and Paget, 2004). This system is a global regulator of gene expression under microaerobic and anaerobic conditions (Green and Paget, 2004). Under O_2-limiting conditions, ArcB autophosphorylates at the conserved His292 of the primary transmitter domain, and the

phosphate is relayed to Asp576 in the receiver domain and then to His717 situated in the secondary transmitter domain and subsequently transphosphorylates the response regulator, ArcA, at the conserved Asp54 residue. The phosphorylated ArcA (ArcA~P) activates or represses expression of genes involved in respiratory metabolism (Georgellis *et al*., 2001a; Green and Paget, 2004). Among the genes regulated by ArcA~P are those encoding the terminal oxidases, cytochrome bo_3 and cytochrome *bd*. The major aerobic terminal oxidase cytochrome bo_3 is repressed while the microaerobic cytochrome *bd* oxidase is activated. Similarly, ArcA~P inversely regulates the two quinone reductases, NADH dehydrogenase and succinate dehydrogenase, with the former being activated while the latter is repressed (Liu and de Wulf, 2004; Green and Paget, 2004).

Georgellis *et al* (2001a) used different quinone analogs to demonstrate that ArcB autophosphorylation was inhibited by oxidized forms of quinone during aerobiosis, indicating that ArcB senses the redox state of the quinone pool. Based on these data it was proposed that accumulation of reduced quinol during microaerobic growth would stimulate autophosphorylation of ArcB. This proposal was later supported by data, from the same group, showing that formation of disulphide bonds between ArcB monomers was necessary for inhibition of ArcB autophosphorylation, with quinones probably acting as oxidants of the cysteines involved in bond formation (Malpica *et al*., 2004).

The Arc system is not confined to *E. coli*, but is present in other bacteria. In *Haemophilus influenzae* the ArcB sensor kinase has been demonstrated to autophosphorylate in response to redox conditions despite lacking a PAS domain. Northern blot analysis of the *H. influenzae lctD* gene, a homologue of the *E. coli* L-lactate dehydrogenase gene (*lldD*), demonstrated anaerobic repression of this gene by ArcB, suggesting that the Arc system of *H. influenzae* plays a similar role as that of *E. coli* in response to redox conditions (Georgellis *et al*., 2001b). Another two-component system, BvgAS that responds to the redox status of the quinol pool has been reported in *Bordetella pertussis*. The BvgAS system is involved in the regulation of virulence genes in this organism, including the gene encoding the pertussis toxin (Bock and Gross, 2002).

The RegB-RegA and PrrB-PrrA systems

The RegB-RegA two-component regulatory system of ***Rhodobacter capsulatus*** regulates photosystem and respiratory gene expression under anaerobic conditions. Under these conditions the sensor kinase RegB autophosphorylates and then transphosphorylates its cognate response regulator, RegA (Swem ***et al.***, 2003; Green and Paget, 2004). The activated RegA~P then regulates target genes including those that encode the terminal oxidases cytochrome cbb_3 and ubiquinol oxidase (Swem ad Bauer, 2002; Swem ***et al.***, 2003; Green and Paget, 2004). However, regulation of these oxidases involves other regulatory systems in addition to RegB-RegA. Both are also regulated by FnrL and HvrA, as well as CrtJ and Aer for the ubiquinol oxidase (Swem ad Bauer, 2002).

RegB uses a redox-active cysteine as a mechanism for regulation of gene expression in response to changing oxygen conditions. Under oxidizing conditions, formation of intermolecular disulphide bonds in RegB results in accumulation of the tetrameric form of the protein, which inhibits its autophosphorylation. The disulphide bond formation is mediated by a redox-sensitive Cys265, mutation of which resulted in derepression of photosynthetic genes under aerobic conditions (Swem ***et al.***, 2003).

Another global regulator of anaerobic and photosynthetic gene expression is the PrrBA two-component system of ***Rhodobacter sphaeroides*** (Oh and Kaplan, 2000; Oh and Kaplan, 2002). This system has been shown to sense O_2 levels indirectly by monitoring electron flow through the cytochrome cbb_3 oxidase, generating an inhibitory signal for the PrrBA. The magnitude of electron flow through the cbb_3 oxidase determines the strength of the inhibitory signal generated by the oxidase to alter the PrrB activity from the kinase mode to a phosphatase mode, which would inhibit activation of the photosynthesis genes (Oh and Kaplan, 2002). The ability of the cbb_3 terminal oxidase to directly stimulate the dephosphorylation of PrrB, thereby resulting in inactivation of PrrA, has recently been shown (Green and Paget, 2004).

The DosR-DosS/DosT (DevR-DevS/DevT) system

The alarming increase in the incidence of TB world-wide has prompted an urgent need for development of new drugs and vaccines, but the success in winning this battle hinges on an understanding of the physiology of ***M. tuberculosis*** and how it adapts to its

intracellular environment. In an attempt to understand the way *M. tuberculosis* responds to changing conditions as well as to identify potential drug targets, considerable effort has been placed on investigating its various regulatory systems. The genome of *M. tuberculosis* encodes 11 two-component regulatory systems (Cole *et al*., 1998; Zahrt and Deretic, 2001), of which the DosR-DosS/DosT (dormancy survival) system is the best studied, This system consists of two histidine sensor kinases, DosS (Rv3132c) and DosT (Rv2027c), and a response regulator, DosR (Rv3133c) (Dasgupta *et al*., 2000; Roberts *et al*., 2004). The genes encoding this system were first isolated by subtractive hybridization as differentially expressed in virulent (*dev*) *vs.* avirulent strains of *M. tuberculosis* (Dasgupta *et al*., 2000). The Dos system belongs to the LuxR family of two-component regulatory systems, members of which include NarL, FixJ, BvgA, and UhpA (Dasgupta *et al*., 2000). The functionality of the DosR-DosS as a two-component system was analyzed by *in vitro* phosphorylation assays, which demonstrated the ability of DosS to autophosphorylate and to phosphorylate DosR, thus proving that DosS is a functional kinase for this system (Roberts *et al*., 2004; Saini *et al*., 2004). Similarly, the alternative kinase, DosT was demonstrated to be a *bona fide* sensor kinase for the Dos system (Roberts *et al*., 2004). Based on its constitutive expression under hypoxia, DosT was suggested to respond initially leading to amplification of DosS expression and hence, the hypoxic response (Roberts *et al*., 2004).

DNA microrarray analysis of hypoxically-grown cultures of *M. tuberculosis* revealed a 47-gene set that was induced under these conditions, among which were ***dosR*** (Rv3133c) and ***dosS*** (Rv3132c), and the hypoxia-responsive α-crystallin homologue, ***hspX*** (Rv2031) (Sherman *et al*., 2001). HspX is one of the proteins that had previously been demonstrated to be required for low-O_2-induced stationary survival of *M. tuberculosis* (Yuan *et al*., 1996; Cunningham and Spreadbury, 1998; Purkayastha *et al*., 2002; Rosenkrands *et al*., 2002). It is responsible for the cell wall thickening that has long been shown to characterize Wayne's model of non-replicating persistence (Wayne and Hayes, 1996; Wayne and Sohaskey, 2001). Mutational studies of ***dosS***, ***dosR*** and the gene immediately upstream of ***dosR***, Rv3134c, confirmed that the Dos system was required for hypoxic induction of ***hspX***, suggesting that this two-component regulatory system was involved in mycobacterial latency (Sherman *et al*., 2001). Further extensive studies on

the DosR-DosS/DosT system demonstrated that it is required for induction of an approximately 48-gene regulon by hypoxia (Voskuil *et al.*, 2003; Park *et al.*, 2003; Bacon *et al.*, 2004; Karakousis *et al.*, 2004; Kendall *et al.*, 2004; Muttucumaru *et al.*, 2004; Saini *et al.*, 2004; Voskuil *et al.*, 2004) and low concentrations of NO (Voskuil *et al.*, 2003; Schnappinger *et al.*, 2003). Computational analyses revealed a conserved palindromic sequence[1] upstream of nearly all hypoxically-induced DosR-regulated genes (Florczyk *et al.*, 2003; Park *et al.*, 2003), and DosR binding to this promoter region was demonstrated using *hspX* (Park *et al.*, 2003).

The DosR-DosS/DosT system has attracted considerable interest owing to its involvement in the regulation of genes required for adaptation to hypoxia and NO, the conditions to which *M. tuberculosis* is proposed to be subjected in the granuloma (Voskuil *et al.*, 2003; Park *et al.*, 2003; Schnappinger *et al.*, 2003). Some members of the DosR regulon encode universal stress proteins (USPs), suggesting that this class of proteins may be involved in the development and survival of dormancy during latent TB infections (O'Toole and Williams, 2003b). By analogy to their *E. coli* counterparts, it has also been speculated that the mycobacterial USPs may protect the organism from NO, oxidative and acid stress during its survival in the macrophage (O'Toole and Williams, 2003b). The virulence of *M. tuberculosis* DosR mutants was found to be attenuated *in vivo* in guinea pig (Maholtra *et al.*, 2004) and rabbit models (D. R. Sherman, 6th International Conference on the Pathogenesis of Mycobacterial Infections, Stockholm, 2005).

Despite extensive studies, the mechanisms of signal sensing and transduction by the DosR-DosS/DosT system are still not known. Induction of the DosR regulon by signals arising from either O_2 depletion or the presence of low amounts of NO led Voskuil *et al* (2003) to propose that the major aerobic terminal oxidase, aa_3-type cytochrome *c* oxidase, or alternatively another heme-containing enzyme, might be the sensor of O_2 and NO. This proposal was based on the previous reports showing that: (i) the mitochondrial counterpart of this oxidase could reversibly be inhibited by low concentrations of NO; and (ii) the yeast cytochrome *c* oxidase (Kwast *et al.*, 1999) and the *R. sphaeroides* cytochrome cbb_3 (Oh and Kaplan, 2000) act as O_2 sensors. Unless the

[1] Some genes have two copies of this palindromic sequence recognized by DosR.

specificity of interactions of the mycobacterial cytochrome *c* oxidase with NO or other inhibitors determines the type of signal generated, it would be tempting to propose that other inhibitors of cytochrome *c* oxidase would result in the induction of the DosR regulon. However, treatment of the *M. tuberculosis* oxidase with inhibitors such as cyanide and azide did not induce such a response, arguing against the notion that cytochrome *c* oxidase might be the sensor of O_2 (Boshoff *et al*., 2004). Boshoff *et al.* (2004) also reported that there was no correlation between the induction of the dormancy regulon and the menaquinone/menaquinol or NADH/NAD^+ ratios in *M. tuberculosis*, but could not rule out the possibility that the redox state of another electron carrier signaled this response (Boshoff *et al*., 2004).

Although proposed to play an important role in the pathogenesis of *M. tuberculosis*, the DosR-DosS/DosT system is also present in the non-pathogenic *M. smegmatis* (Mayuri *et al*., 2002; O'Toole *et al*., 2003a). This is consistent with its role in the establishment and/or maintenance of oxygen-depletion induced dormancy, a phenomenon that has been demonstrated for both pathogenic (reviewed in Wayne and Sohaskey, 2001) and non-pathogenic mycobacteria (Dick *et al*., 1998). However, the dormancy regulon of *M. smegmatis* has not yet been fully defined. Analysis of the then unfinished genome sequence of *M. smegmatis* revealed the presence of homologues of the genes encoding *hspX* and the DosR-DosS/DosT system, and their hypoxia-responsiveness was demonstrated by RNA and protein analysis (Mayuri *et al*., 2002; O'Toole *et al*., 2003a). In addition, analysis of a *dos*R mutant of *M. smegmatis* revealed that DosR was required for hypoxia induction of *hspX* (MSMEG3937)[2], *uspL* (MSMEG3944), *uspM* (MSMEG3945), *uspN* (MSMEG4368), and *acg* (MSMEG5231) (O'Toole *et al*., 2003). Together, these data suggest that the transcriptional and/or physiological response to hypoxia is broadly conserved in *M. tuberculosis* and *M. smegmatis*. In support of this proposal, hypoxia-induced expression of the *M. tuberculosis dosR* and Rv3133c promoters was successfully achieved in *M. smegmatis*, suggesting that *M. smegmatis* can be used as a model for studying the dormancy response of *M. tuberculosis* (Bagchi *et al*., 2003).

[2] This gene annotation is obtained from the complete genome sequence of *M. smegmatis* mc^2155 site at TIGR (http://www.tigr.org/tigr-scipts/CMR2/CMRHomePage.spl).

The SenX3-Reg3 system

Despite being the first reported example of a *M. tuberculosis* two-component regulatory system (Wren *et al*., 1992), and contrary to the better-studied DosR system discussed above, the mycobacterial SenX3-RegX3 system has only been partially characterized. Based on homology searches, this system is proposed to be an orthologue of the *E. coli* ArcB-ArcA system, which regulates expression of aerobic genes (Rickman *et al*., 2004). Independent studies that used *M. tuberculosis* mutants in the *senX3* and/or *regX3* demonstrated that these mutants were attenuated for virulence in mouse models (Parish *et al*., 2003; Rickman *et al*., 2004). Moreover, microarray analysis of a *senX3-regX3* mutant revealed that *cydB*, encoding subunit II of cytochrome *bd* oxidase was among the genes possibly regulated by this two-component system (Parish *et al*., 2003).

The SenX3-RegX3 system is not restricted to *M. tuberculosis*, but is found in other mycobacteria including *M. leprae*, which has retained only four of the 11 two-component regulatory present in *M. tuberculosis*, suggesting that this system may be necessary for survival in the harsh environment of the host (Rickman *et al*., 2004). The ability of SenX3 to autoregulate and transphophorylate RegX3 was demonstrated using a recombinant SenX3 from *Mycobacterium bovis* BCG overexpressed in *E. coli* (Himpens *et al*., 2000). The authors further showed that RegX3 can bind to the *senX3-regX3* promoter and positively regulate the operon.

1.5 Respiration in mycobacteria

Although respiration in mycobacteria has long been proposed to play an important role in the success of some mycobacterial species as pathogens, very little is known about the respiratory chains of these organisms. Bioinformatic analyses of those mycobacteria for which the complete or partial sequence information is available have revealed that as in many other bacteria, mycobacteria possess a branched aerobic respiratory chain, terminating in at least two oxidases. Electrons flow from NADH dehydrogenase and succinate dehydrogenase, and possibly other dehydrogenases, into the menaquinone-menaquinol pool, from where they can be transferred to the terminal electron acceptor, O_2, through either of two branches, the cytochrome *bd*-type menaquinol oxidase branch

or the cytochrome *c* oxidase branch. In the former branch, electrons flow directly for menaquinol to the terminal cytochrome *bd* oxidase, whereas in the latter, electrons are transferred from menaquinol to the aa_3-type cytochrome *c* oxidase via a cytochrome bc_1 complex (Kana *et al*., 2001; Weinstein *et al*., 2005; Boshoff *et al*., 2005). Genome comparisons have revealed a high resemblance of the mycobacterial respiratory chain to that of *C. glutamicum* shown in Figure 1 though some of the dehydrogenases seem to be absent in mycobacteria.

1.5.1 Respiration in *M. smegmatis*

In a pioneering genetic study on the mycobacterial respiratory chain, the branch terminating in cytochrome *bd* oxidase in *M. smegmatis* was previously shown to be important for microaerobic respiration in this organism (Kana *et al*., 2001). Spectral analysis of *cydA*::*aph* and *cydB*::*aph* mutants in comparison to their parental wild type strain revealed loss of a heme-*d* signature, confirming the presence, in *M. smegmatis*, of a γ-proteobacterial type cytochrome *bd*-type oxidases as well as providing evidence that this oxidase is encoded by the *cydAB* genes (Kana *et al*., 2001). Although the *cydA*::*aph* mutant did not show any growth defects under aerobic conditions, it displayed significant growth impairment when air saturation was dropped below 1%, suggesting that this oxidase was required for microaerobic growth. This observation was further confirmed by expression analysis of the *M. smegmatis cyd* promoter under oxystatic growth conditions, which revealed a more than two-fold increase in *cyd* expression between 5 and 0.5% air saturation (Kana *et al*., 2001). The mutant also displayed cyanide sensitivity when co-cultured with the wild type, suggesting that the alternative oxidase(s) functional in this mutant was inhibited by cyanide (Kana *et al*., 2001). Together, these data suggested that the alternative branch terminating in the aa_3-type cytochrome *c* oxidase was the major respiratory route under aerobic conditions. However, this remains to be proven experimentally.

1.5.2 Respiration in *M. tuberculosis*

Evidence is accumulating that the success of *M. tuberculosis* as a pathogen depends largely, if not entirely, on its ability to switch its metabolism to adapt to the prevailing

conditions within its host (Boshoff *et al*., 2005). A large amount of data emerging from transcriptome analyses of *M. tuberculosis* have generated promising hypotheses that can guide towards a better understanding of the incredibly flexible adaptation exhibited by this bacterium (Boshoff *et al*., 2005). At the centre of metabolic adaptation of *M. tuberculosis* is its ability to generate cellular energy, by oxidative phosphorylation, to maintain basic cellular processes (Weinstein *et al*., 2005). While the respiratory chain has partially been characterized in *M. smegmatis*, very little is known about the respiratory chain of *M. tuberculosis*. The information currently available came from studies that have utilized inhibitors of respiratory metabolism as well as biochemical analyses, highlighting the functionality of some components of the respiratory chain (Boshoff *et al*., 2004; Weinstein *et al*., 2005), and suggesting possible roles for them in the pathogenesis of *M. tuberculosis* (Boshoff *et al*., 2005). Based on their data on inhibition of NADH dehydrogenase activity by phenothiazines, and previous studies that have shown the dispensability of the type I NADH dehydrogenase (NDH-I), Weinstein *et al* (2005) suggested that the type II NADH dehydrogenase (NDH-II) is the sole NADH dehydrogenase in the aerobically grown *M. tuberculosis*. Spectral analysis of *M. tuberculosis* membrane preparations confirmed presence of the cytochrome components of the cytochrome bc_1 complex and aa_3-type cytochrome *c* oxidase (Weinstein *et al*., 2005). Boshoff *et al.* (2004) used inhibitors of aa_3-type cytochrome *c* oxidase to show that disruption of electron flow to this terminal oxidase resulted in up-regulation of the alternative *bd*-type menaquinol oxidase encoded by *cydABDC*, which was also responsive to hypoxia and changes in the transmembrane proton gradient.

1.6 Aims and objectives of this study

The long-term goal of this study was to understand how *M. tuberculosis* uses its respiratory chain to modulate its metabolic activities under various environmental conditions during an infection. The aim was to use a genetic approach to elucidate the composition and functionality of the aerobic respiratory chains of mycobacteria. To achieve this goal, an understanding of the conserved genetic, biochemical and physiological aspects of the mycobacterial respiratory chain was initially explored in the fast-growing non-pathogenic species, *M. smegmatis*. Although concerns have previously

been expressed regarding the suitability of *M. smegmatis* for studying the physiology of *M. tuberculosis* (Barry, 2001), *M. smegmatis* has proved useful in studying the conserved areas of mycobacterial physiology (Reyrat and Kahn, 2001; Tyagi and Sharma, 2002; Murray and Rubin, 2005). In support of this, the recently completed genome sequence of this organism has revealed that it contains a high repertoire of genes found in pathogenic cousins, particularly *M. tuberculosis*. The respiratory chains of these two organisms are highly conserved, and therefore provide ground for using *M. smegmatis* to guide investigations in *M. tuberculosis*.

Following a previous characterization of the respiratory branch terminating in cytochrome *bd* oxidase by Kana *et al* (2001), the focus of this study was to investigate the cytochrome bc_1-cytochrome aa_3 branch of the respiratory chain, terminating in cytochrome aa_3 oxidase in *M. smegmatis*. The ultimate goal was to use the findings of this study to guide a more in-depth investigation of the respiratory chain of *M. tuberculosis*.

Against this background, the specific aims and objectives of this study were as follows:

1. To generate *M. smegmatis* and *M. tuberculosis* mutant strains deficient in the cytochrome bc_1 complex and aa_3-type cytochrome *c* oxidase.
2. To determine the effects of such mutations on the growth of the organisms.
3. To investigate the effects of loss of the cytochrome bc_1 complex and aa_3-type cytochrome *c* oxidase on the expression of the alternative oxidase, cytochrome *bd* in *M. smegmatis* under conditions of varying O_2 tension.
4. To determine the general adaptive responses, at the transcriptional level, of *M. smegmatis* as a result of loss of functionality in the cytochrome bc_1-cytochrome aa_3 branch.
5. To determine the effects of known respiratory inhibitors on the expression profile of the *M. smegmatis* cytochrome bc_1 complex and aa_3-type cytochrome *c* oxidase mutants.

2. MATERIALS AND METHODS

2.1 General recombinant DNA methods and reagents

Standard molecular biology techniques were performed as previously described by Sambrook and Russell (2001). The suppliers of all reagents used in this work are listed in parentheses within the text. Unless otherwise stated, all enzymes were obtained from Roche Biochemicals. Solutions and media are detailed in Appendix B.

2.1.1 Bacterial strains and plasmids

The bacterial strains and plasmids used in this study are detailed in Tables 1 and 2, respectively. Restriction maps of the plasmids are shown in Appendix C. *E. coli* strains were stored at -70°C in LB plus 50% glycerol. *M. smegmatis* and *M. tuberculosis* strains were stored at -70°C in 50% DUBOS (Difco, Becton Dickinson, USA).

2.1.2 Bacterial culture conditions and selective agents

E. coli DH5α used for cloning procedures was grown in Luria broth (LB) or agar (LA) containing 100 µg/ml ampicillin (Ap), 50 µg/ml kanamycin (Km) or 200 µg/ml hygromycin (Hyg) where necessary. Liquid cultures were grown at 37°C with shaking (350 rpm). To avoid plasmid rearrangements, *E. coli* strains carrying large constructs (≥8000 bp) were incubated at 30°C with slow shaking (100 rpm). *M. smegmatis* strains were grown in LB or MADC-Tw [Middlebrook 7H9 broth (Difco, Becton Dickinson, USA) supplemented with 0.085% NaCl, 0.2% glucose, 0.2% glycerol, and 0.05% Tween 80 (Jacobs *et al.*, 1991)] or on LA for solid medium. Where necessary, antibiotic supplements were added to the following concentrations: Km - 10 µg/ml (solid medium) or 25 µg/ml (liquid medium) and Hyg - 50 µg/ml. Unless otherwise stated, cultures were grown in Erlenmeyer conical flasks at 37°C with shaking (350 rpm). Specific growth conditions for analyses of *M. smegmatis* mutant strains are described in section 2.2.3. For *M. tuberculosis* culturing was carried out in a Biosafety Level 3 (BSL 3) laboratory and bacilli manipulations were performed under negative pressure (180 kPa) in a Class II flow cabinet. Strains were grown at 37°C in Middlebrook 7H9 medium supplemented with 10% v/v ADC (Difco, Becton Dickinson, USA), 0.2% glycerol and 0.05% Tween 80

in roller bottles or as stirred cultures. For solid medium, Middlebrook 7H10 agar supplemented with 10% v/v OADC (Difco, Becton Dickinson, USA) and 0.5% glycerol was used. Antibiotic supplements were as defined for *M. smegmatis* above. For DNA extraction, *M. tuberculosis* strains were grown on LJ slants supplemented with the relevant antibiotics. Other selective agents used were sucrose (Suc) at 5% for *E. coli* and 2% for mycobacteria, and X-Gal (5-bromo-4-chloro-3-indolyl-β-D-galactopyranoide), at a concentration of ca. 40 μg/ml for all strains.

Table 1. Bacterial strains used in this study

Strain	Characteristics	Source / Reference
E. coli		
DH5α	*supE44 ΔlacU169 (Φ80lacZΔM15) hsdR17 recA1 endA1 gyrA96 thi-1 relA1*	Hanahan, 1983
M. tuberculosis		
H37Rv	Laboratory strain (ATCC 27294)	Laboratory collection
M. smegmatis		
mc^2155	High frequency transformation mutant of ATCC 607	Snapper *et al*., 1990
Δ*qcrCAB*::*hyg*	*qcrCAB* deletion-insertion mutant of mc^2155; Hyg^R	This work
Δ*ctaC*::*hyg*	*ctaC* deletion-replacement mutant of mc^2155; Hyg^R	This work
$ctaD^{+/-}$	Derivative of mc^2155 with one wild type *ctaDI* and one *ctaDI*::*hyg* allele; Hyg^R	This work
Δ*ctaDII*::*hyg*	*ctaDII* deletion-replacement mutant of mc^2155; Hyg^R	This work
Δ*ctaC*::*hyg attB*::*ctaC*	Δ*ctaC*::*hyg* complemented with *M. tuberculosis ctaC* integrated at the *attB* locus; Hyg^R, Km^R	This work
Δ*qcrCAB*::*hyg*::pBK4	Δ*qcrCAB*::*hyg* carrying pBK4 integrated at *cyd* locus; Hyg^R, Km^R	This work
mc^2155::pBK4	mc^2155 carrying pBK4 integrated at *cyd* locus; Km^R	Kana *et al*., 2001
ΔDR	Derivative of mc^2155 that has lost the entire chromosomal duplication	D. F. Warner, PhD thesis

Hyg^R, hygromycin resistant; Km^R, kanamycin resistant

Table 2. Plasmids used in this study

Plasmid[a]	**Characteristics**	**Source or reference**
pGEM3Z(+)f	*E. coli* cloning vector; Ap^R	Promega
pGEMTeasy	*E. coli* vector for cloning PCR products; Ap^R	Promega
pCR2.1-TOPO	*E. coli* vector for cloning PCR products; Km^R, Ap^R	Invitrogen
p2NIL	*E. coli* vector for cloning homologous recombination substrates; Km^R	Parish & Stoker, 2000

Plasmid[a]	Characteristics	Source or reference
pGOAL17	Vector carrying P_{Ag85}-*lacZ* P_{hsp60}-*sacB* as a *Pac*I marker cassette; Ap^R	Parish & Stoker, 2000
pOLYG	*E. coli-Mycobacterium* replicating shuttle vector; Hyg^R	O'Gaora *et al*., 1997
pIJ963	*E. coli* vector carrying *hyg* cassette	Blondelet-Roualt et al., 1997
pY6002	*E. coli* vector carrying *aph* cassette from transposon Tn903; Ap^R, Km^R	Husson *et al*., 1990
pBK4	p2NIL containing the *M. smegmatis cydA*'::*lacZ* fusion cassette; Hyg^R	Kana *et al*., 2001
pMV306K	*E. coli-Mycobacterium* integrating shuttle vector; Km^R	Stover *et al*., 1991
pCYDAKO	Knockout vector carrying *M. smegmatis cydA*::*aph* allele; Km^R	Kana *et al*., 2001
pQCRTBKO	Knockout vector carrying *M. tuberculosis* Δ*qcrCAB* allele; Hyg^R, Km^R	This work
pCTACTBKO	Knockout vector carrying *M. tuberculosis* Δ*ctaC*::*hyg* allele; Hyg^R, Km^R	This work
pQCRSMKO	Knockout vector carrying *M. smegmatis* Δ*qcrCAB*::*hyg* allele; Hyg^r, Km^r	This work
pCTADISMKO	Knockout vector carrying *M. smegmatis* Δ*ctaDI*::*hyg* allele; Hyg^R, Km^R	This work
pGEMCTADIKO	Knockout vector carrying *M. smegmatis* Δ*ctaC*::*aph* allele in pGEM3Z; Km^R, Amp^R	This work
pCTADIISMKO	Knockout vector carrying *M. smegmatis* Δ*ctaDII*::*hyg* allele; Hyg^R, Km^R	This work
pCTACSMKO	Knockout vector carrying *M. smegmatis* Δ*ctaC*::*hyg* allele; Hyg^R, Km^R	This work
pMVCTAC	Complementing vector carrying *M. tuberculosis ctaCF* genes on a 2892 bp *Kpn*I fragment, cloned into pMV306K; Km^R	This work

[a] The intermediary plasmids constructed in this study are not shown in this Table, but are listed instead in Appendix C.

2.1.3 DNA extraction

Plasmid preparation from E. coli

For small scale plasmid preparations, single colonies harbouring plasmids of interest were inoculated into 2 ml LB containing an appropriate antibiotic and grown to stationary phase at 37°C with shaking (350 rpm). Cells were harvested in microcentrifuge tubes by centrifuging for 1 min at 10 000 × g and then resuspended in 100 µl of solution I (50 mM Tris-HCl, pH 8.0; 10 mM EDTA) by vortexing. To lyse the cells, 200 µl of solution II (0.2 M NaOH; 1% SDS) was added and the mixture was incubated at room temperature for 5 min, before neutralizing with 150 µl of solution III (3 M potassium acetate, pH 5.5;

11.5% glacial acetic acid). Following 10 min incubation on ice, the mixture was centrifuged at 9 000 × g for 5 min (4°C) and the supernatant decanted into a clean Eppendorf tube. To remove contaminating RNA, ribonuclease A was added to a final concentration of 10µg/ml and the mixture was incubated at 42°C for 10 min. DNA was precipitated with 260 µl of isopropanol and collected by a 10 min centrifugation at room temperature (10 000 × g). The pellet was washed with an equal volume of ethanol and then dried under vacuum. DNA was resuspended in an appropriate volume of sterile distilled water. For large scale preparations, bacterial cultures were grown overnight in 100 ml LB as previously described. Cells were collected by centrifugation at 1100 × g for 5 min in a Beckman J2-21 rotor. DNA extraction was carried out using a Nucleobond®AX kit (Macherey-Nagel, Germany) according to the manufacturer's instructions.

Chromosomal DNA extraction from mycobacteria

CTAB method. Cultures were grown to stationary phase in liquid media for ***M. smegmatis*** or on LJ slants for ***M. tuberculosis*** and then heat-killed at 100°C for 10 min. [For ***M. tuberculosis***, all the steps up to chloroform/isoamyl alcohol extraction were done in a Class II flow cabinet at negative pressure (180 kPa) in the BSL 3 laboratory]. The cells were harvested by centrifugation (10 000 × g for 1 min) and then resuspended in 500 µl of TE (10 mM Tris; 1 mM EDTA, pH 7.6) containing 1 µg/µl of lysozyme. The mixture was incubated at 37°C for 1 h and then 70 µl of 10% SDS and 6 µl of proteinase K (10 mg/ml) were added, followed by incubation at 37°C for 2 h. To this, 100 µl of 5 M NaCl and 80 µl CTAB/NaCl solution (10% CTAB [N-cetyl-N,N,N-trimethylammonium bromide] in 0.7 M NaCl) were added and the mixture was incubated at 65°C for 10 min. To separate DNA from protein, 750 µl $CHCl_3$/IAA was mixed in and centrifuged for 5 min at 10 000 × g. The aqueous phase was transferred to a clean Eppendorf tube and DNA was extracted with an equal volume of isopropanol. The DNA pellet was washed with 70% ethanol, dried and then resuspended in an appropriate volume of sterile distilled water.

Phenol-chloroform method. Cells were harvested by centrifugation (10 000 × g for 1 min) and then resuspended in 500 µl TES buffer (10 mM Tris-HCl, pH 8; 1 mM EDTA; 150 mM NaCl). Seven hundred µl of phenol were added and cells were shaken for at least 1 h at 37°C (100 rpm). The phenol and DNA layers were separated by centrifuging for 10 min at 10 000 × g. The top (DNA) layer was aspirated and an equal volume of $CHCl_3$/IAA was added and centrifuged at room temperature for 1 min. The top layer was aspirated again and the DNA was precipitated with 2.5 volumes of ethanol and 0.1 volume of 3 M NaOAc. The DNA pellet was collected by centrifugation at 10 000 × g, washed with 70% ethanol, dried and resuspended in an appropriate volume of sterile distilled water.

DNA purification from agarose gels or enzymatic reactions

DNA from excised gel slices or enzymatic reactions was purified using GeneClean®III kit (BIO 101, CA, USA) or Nucleospin® kit (Macherey-Nagel, Germany), according to the manufacturer's instructions.

2.1.4 DNA manipulations

Restriction enzyme digests

Plasmid or chromosomal DNA was digested with the appropriate enzyme as specified by the manufacturer. Reactions were incubated at appropriate temperatures for a period of 1 to 16 h. When double digests could not be performed in a common buffer, DNA was cut with one enzyme, ethanol precipitated and then digested with the second enzyme. DNA fragments were fractionated on agarose gels by electrophoresis.

Dephosphorylation of 5' ends

Linearised plasmid DNA was treated with calf intestine alkaline phosphatase (CIP; Roche Biochemicals, Germany) or shrimp alkaline phosphatse (SAP; Roche Biochemicals, Germany) to remove the 5'-phosphate. One unit of enzyme was added to the DNA in the presence of 1/10 v/v reaction buffer and incubated at 37°C for 2 h (CIP) or 30 min (SAP). The phosphatase was heat-inactivated and DNA was recovered by ethanol precipitation for use in ligation reactions.

Modification of 5' and 3' overhangs

Enzyme-restricted DNA fragments with 5' overhangs were filled in using Klenow enzyme (Roche Biochemicals, Germany) to produce blunt ends. The reaction mixture consisted of 1/10 vol. reaction buffer, 0.8 mM each of dATP, dCTP, dGTP and dTTP, and 1 U klenow enzyme. Samples were incubated at 37°C for 20-40 min. To remove 3' overhangs, the linearized DNA fragments were treated with 1 U of T4 DNA polymerase.

Ligation reactions

DNA ligations were carried out using the Fast Link ligation kit (Epicenter Technologies, Madison, USA) according to the manufacturer's instructions with incubation times ranging from 15 min to 3 h. Ligation reactions (or aliquots thereof) were used directly in *E. coli* transformation reactions.

2.1.5 Polymerase Chain Reaction (PCR)

Thermocycling was carried out in a MasterCycler gradient 5331 (Eppendorf, Hamburg, Germany) or a PCR Express (Hybaid, Middlesex, UK) machine. For preliminary PCR analysis, a Faststart Taq polymerase (Roche Biochemicals, Germany) was used, whereas the high-fidelity Expand PCR system (Roche Biochemicals, Germany) was used for the generation of PCR products to be used for cloning purposes. Fifty µl reactions containing 2 µl of genomic DNA template, 1/10 volume reaction buffer, 2 mM $MgCl_2$, 0.2 mM dNTPs, 5% DMSO, 1 µM of forward and reverse primers, and 2.5 U of polymerase were set up on ice. With modifications suited to the various templates, the thermal cycling program generally included an initial denaturation step at 94°C for 5 min, followed by elongation in 30 cycles of 60 s at 94°C, 60 s at 60°C (or other primer-specific annealing temperatures, T°, as calculated in Appendix B; in the range of 52-65°C), and 60 s at 72°C, terminating in 1 cycle of 5 min at 72°C. For PCR reactions using Expand PCR system, the elongation step was extended by 5 s per cycle. Following thermal cycling, the samples were kept at 4°C, frozen at -20°C or used immediately. PCR following reverse transcription is described in section 2.2.6.

2.1.6 DNA sequencing

Automated DNA sequencing was performed by the Inqaba Biotec sequencing facility (Pretoria, South Africa), on a Spectrumedix 2410 Capillary Electrophoresis automated DNA sequencer. For this purpose a Big Dye DNA sequencing kit was used and results were analysed on the Big Dye Terminator v3.1 software from ABI. Plasmids, PCR products or linear DNA fragments were purified with a Nucleospin kit (Macherey-Nagel, Germany), resupended in sterile distilled water and then provided to Inqaba Biotec together with the relevant DNA sequencing primers. The sequences obtained were then analysed using EditSeq and SeqMan™ II modules of the Lasergene suite of programs (DNASTAR, Madison, WI). Each sequence was aligned with the original sequence downloaded from the relevant site (http://genolist.pasteur.fr/TubercuList/ or http://www.tigr.org/tigr-scripts/CMR2/CMRHomePage.spl), and then scanned for mutations.

2.1.7 Agarose gel electrophoresis

Agarose gels were prepared in 1 × TAE buffer (40 mM Tris; 1 mM EDTA, pH 8.0; 0.1% glacial acetic acid). For large DNA fragments (≥ 1 kb), 1% gels were prepared from high-melting agarose powder (SeaKem), while smaller fragments (≤ 1 kb) were analysed on 2 - 3 % low-melting agarose (Nusieve® GTG) gels. Thirty ml of molten agarose containing 1.5 µl of 10 mg/ml ethidium bromide for DNA visualization was poured into a gel casting tray (Hoeffer, Amersham Pharmacia, USA) and gels were allowed to set at room temperature or at 4^{o}C (low-gelling agarose). Once the gels had set, samples containing a tracking dye (0.025% bromophenol blue in 30% glycerol) were loaded and the gels were run in cold 1 × TAE buffer at 80-120 volts. Gels were viewed and scanned on a Gel Doc 2000 system (BIO-RAD, Johannesburg, South Africa).

2.1.8 Southern blot analysis

Preparation of probes

DNA probes were labelled with [α-^{32}P]dCTP using the Random Primed Labelling kit (Roche Biochemicals, Germany). Nine µl of probe DNA was denatured at 95°C for 10 min and then snap-cooled on ice before adding the labelling reagents as recommended by

the manufacturer. To terminate the reaction, 80 µl of TE buffer was added and unincorporated nucleotides were removed by fractionation through a Sephadex G-25 spin column equilibrated with TE buffer. The probe was either used immediately or frozen at -20°C for later use within a period of up to 7 days.

Electroblotting

Enzyme-restricted DNA of interest was separated on a 1% agarose gel by electrophoresis at 80 volts. DNA was depurinated by soaking the gel in 0.25 M HCl for 15 min followed by a 15 min denaturation in 0.5 M NaOH/1.5 M NaCl solution, with a brief rinse in distilled water in between the two steps. The gel was equilibrated in 1 × TBE buffer (0.178 mM Tris; 17.8 mM boric acid; 2 mM EDTA, pH 8.0) before a nylon membrane (Hybond^{TM}-N) was placed on top of the gel. The gel overlaid with membrane was placed between two double sheets of 3MM Whatman blotting paper and TBE-soaked sponges, and then placed in a blotting cassette. DNA transfer was carried out in a Mini Transfer (Hoeffer scientific) system for 2 h at 0.5 A. The DNA was then cross-linked to the membrane by UV-irradiation in a UV Stratalinker 1800 (Stratagene), using the autocross-link program.

Hybridization

Membranes were pre-hybridized, for 2 h at 42°C, with 10 µg/ml heat-denatured salmon sperm DNA in a pre-hybridization buffer (0.5% SDS; 6× SSC; 5× Denhardts; 50% deionised formamide) in Techne Hybridiser HB-1 roller bottles. The probe was heat-denatured, added to the pre-hybridization buffer and then incubated at 42°C for 16-18 h. The hybridization buffer was discarded and the membranes were washed twice in wash solution I (2 × SSC; 0.1% SDS) for 15 min at 42°C, once in wash solution II (0.5 × SSC; 0.1% SDS) for 15 min at 42°C, once in wash solution III (0.1 × SSC; 0.1% SDS) for 15 min at 42°C and finally in solution IV (0.1 × SSC; 1.0% SDS) for 30 min at 65°C. The membranes were wrapped in plastic and then exposed to X-ray film at -70°C before the films were developed in an XP400 developer (Peromac Medical Services, South Africa).

2.1.9 Transformations

Rubidium chloride transformation of E. coli DH5α

The method used was obtained from Dr P. Stolt. For preparation of competent cells of *E. coli* DH5α, a single colony was picked from a fresh plate, inoculated in 5 ml LB and shaken overnight at 37°C. This pre-culture was used to inoculate 200 ml of LB and the culture was grown for about 4-6 h to an OD_{600} of 0.6. The culture was divided into 40 ml aliquots and then incubated on ice for 15 min before harvesting in a pre-chilled Beckman J2-21 rotor (1100 × g, 15 min). Cells were resuspended in one-third of the original volume of buffer RF1 (30 mM potassium acetate, 100 mM rubidium chloride, 10 mM calcium chloride, 50 mM manganese chloride, 15% glycerol v/v, pH 5.8) and left on ice for 30 min. To collect cells, samples were centrifuged at 3000 rpm for 15 min. Finally cells were resuspended in one-twelfth of the original volume of buffer RF2 (10 mM MOPS, 75 mM calcium chloride, 10 mM rubidium chloride, 15% glycerol v/v, pH 6.5) and incubated for 15 min on ice. The cell suspension was aliquoted into Eppendorf tubes and stored at -70°C. Competent cells were thawed on ice. DNA was mixed with 100-200 µl cells and incubated on ice for 15 min. Cells were heat-shocked at 42°C for 90 s and then rapidly cooled on ice for 2 min before adding 500 µl of 2× TY medium. Cells were incubated at 37°C for at least 30 min to allow for phenotypic expression, and then plated on LA containing appropriate antibiotics. Transformants were recovered after an overnight incubation at 37°C.

Electroporation of mycobacteria

Electroporations were carried out as previously described (Larsen, 2000; Gordhan and Parish, 2001). A 100 ml culture of ***M. smegmatis*** was grown to an OD_{600} of between 0.9 and 1.5 and then chilled on ice for at least 15 min before harvesting in a pre-cooled Beckman J2-21 rotor (1100 × g for 10 min). Cells were washed twice in ice-cold 10% glycerol, first in 25 ml followed by 10 ml, and finally resuspended in 1 ml of 10% glycerol. Two- to four-hundred µl aliquots of the electro-competent cells were mixed with 10 µl of salt-free DNA (ca.1 µg precipitated twice in ethanol to remove excess salts) and incubated on ice for 5 min. The mixture was then transferred into chilled 0.2 cm BIO-RAD electroporation cuvettes. Electroporation was carried out in a Gene Pulser I

model (BIO-RAD, Johannesburg, South Africa) or Gene Pulser Xcell™ (BIO-RAD) under the following conditions: voltage 2.5 kV, capacitance 25 μF and resistance 1000 Ω. The cells were rapidly rescued in 1 ml of LB, transferred into a sterile Eppendorf tube and incubated at 37°C for at least 2 h to allow for phenotypic expression. Cells were plated on LA containing appropriate supplements and plates were incubated at 30°C for at least 3 days.

For *M. tuberculosis* strains, the procedure was carried out as described for *M. smegmatis* with the following modifications. Glycine was added to the culture about 16 h before harvest, to a final concentration of 1.5%, and all the glycerol washes were carried out at room temperature. The DNA (*ca.* 5 μg) was UV-irradiated (100 mJ/cm^2) before mixing with the cells. Cells were plated on Middlebrook 7H10 plates supplemented with 0.5% glycerol, 10% v/v OADC and appropriate antibiotics. Plates were incubated at 37°C for at least 21 days.

2.2 Cloning and characterization of the cytochrome bc_1 and aa_3 knockout mutants of *M. smegmatis* and *M. tuberculosis*

2.2.1 Construction of knockout vectors for *qcrCAB, ctaC, ctaDI* and *ctaDII* genes of *M. smegmatis*

PCR amplification and cloning of deletion allele substrates

M. smegmatis homologues of genes in the cytochrome bc_1-aa_3 pathway were identified by BLAST searching (Altschul *et al*., 1990) of the unfinished genome sequence of strain mc^{2}155 (http://www.tigr.org/ufmg/) using the corresponding *M. tuberculosis* genes as query sequences. The *M. smegmatis* sequences were used to design PCR primers for amplification of DNA segments that would be used in the construction of deletion alleles for the target genes. For each gene (or operon, in the case of *qcrCAB*), two sets of PCR primers were designed to amplify upstream and downstream flanking segments of DNA that include between 69 and 239 bp of 5'- and 3'-ends of the target gene(s). Unique restriction sites were engineered into the PCR primers to facilitate subsequent cloning of the PCR products. The primer sequences and sizes of the corresponding PCR products are detailed in Table 3. Amplification was carried out as described above using Expand

High Fidelity PCR system (Roche Biochemicals, Germany). PCR products were individually cloned into pGEMTeasy (Promega, Madison, USA) or pCR2.1-TOPO (Invitrogen, UK) and completely sequenced (Inqaba Biotec, Pretoria, South Africa) before further use.

The upstream and downstream fragments were simultaneously sub-cloned into p2NIL (Parish and Stoker, 2000) using the engineered restriction sites, effectively resulting in a deletion of most of the internal region of the gene(s) of interest. In the case of the 4404-bp *ctaE-qcrCAB* operon, ligation of the up- and downstream fragments in p2NIL resulted in the deletion of an internal segment of 3472 bp to produce plasmid p2QCR. In the case of the 1026 bp *ctaC* gene, an internal region of 757 bp was deleted resulting in p2CTAC. Similarly, plasmids p2CTADI and p2CTADII carried mutant alleles containing 1506 bp and 1295 bp deletions within the *ctaDI* (1689 bp) and *ctaDII* (1752 bp) genes, respectively. Maps of these plasmids are shown in Appendix C.

Cloning of marker cassettes

To mark the deletion alleles in each case, a Hyg resistance (Hyg^R) gene carried on a 1758 bp *Bgl*II cassette was inserted at the junction site of the two PCR products (upstream and downstream segments), creating plasmids p2QCRH, p2CTACH, p2CTADIH and p2CTADIIH. Further selection markers were introduced by cloning of a *lacZ-sacB* cassette from pGOAL17 (Parish and Stoker, 2000) in the unique *Pac*I site of p2NIL, to produce the suicide vectors pQCRSMKO, pCTACSMKO, pCTADISMKO and pCTADIISMKO for knockout of the *qcrCAB*, *ctaC*, *ctaDI* and *ctaDII* genes, respectively (Table 2). An additional knockout vector for deletion-insertion mutagenesis of the *ctaDI* gene (pGEMCTADIKO) was constructed by excising an *Eco*RI-*Hin*dIII fragment bearing the deletion allele from plasmid p2CTADI, and then cloning into pGEM3Zf(+). A 1264 bp *Bam*HI cassette bearing the Km resistance (Km^R) gene was then cloned into the junction site, followed by cloning of the *lacZ-sacB* cassette from pGOAL17 to produce plasmid pGEMCTADIKO. This plasmid was used in experiments aimed at inactivating the second copy of *ctaDI* either in the *hyg*-marked $ctaDI^{+/-}$ or ΔDR strains of *M. smegmatis* (Table 1). Prior to use in *M. smegmatis*, all of the suicide plasmids were tested

for their ability to confer Suc sensitivity (Suc^S) and to produce a blue color in *E. coli* cells plated on LA supplemented with sucrose and X-gal, respectively.

2.2.2 Allelic replacement of the *qcrCAB*, *ctaC*, *ctaDI* and *ctaDII* genes of *M. smegmatis*

Delivery of knockout constructs into M. smegmatis

The knockout constructs (Figure 2; Table 2) described above, were electroporated into *M. smegmatis* mc^2155, with the exception of pGEMCTADIKO which was later electroporated into strains *ctaDI*$^{+/-}$ and ΔDR. An *E. coli-M. smegmatis* replicating shuttle vector, pOLYG, was also included as a control to assess transformation efficiency of the cells, whereas a no DNA control was used to exclude contamination in the cells. Electroporation was carried out as described in section 2.1.9 and cells were plated on LA containing Hyg, Km and X-Gal.

Selection and genotypic analysis of mutants

Blue, Km^R, Hyg^R *M. smegmatis* transformants (potential single crossover recombinants; SCOs) were picked from the electroporation plates and grown to late log phase in LB containing Hyg and Tween. Serial dilutions of these cultures were plated on LA containing Hyg, X-Gal and 5% Suc and incubated at 37°C for at least 5 days to allow a second crossover to occur. White, Hyg^R, Suc-resistant (Suc^R) colonies (potential double crossover recombinants; DCOs) were isolated and patched on fresh medium containing Km to test for Km-sensitivity (Km^S). This was used as a criterion to confirm loss of the intervening vector sequence. To confirm site-specific integration of the inactivated allele(s) in the candidate knockout mutants that displayed the expected phenotype (white, Hyg^R, Suc^R and Km^S), Southern blot analysis was carried out as described in section 2.1.8. Genomic DNA was isolated from these clones and digested with appropriate restriction enzyme(s). Either the upstream or downstream PCR product used in the knockout construct was used as a probe. For validation, the blot was stripped of the bound probe and then hybridized with a different probe, or a different enzyme was used to digest the genomic DNA.

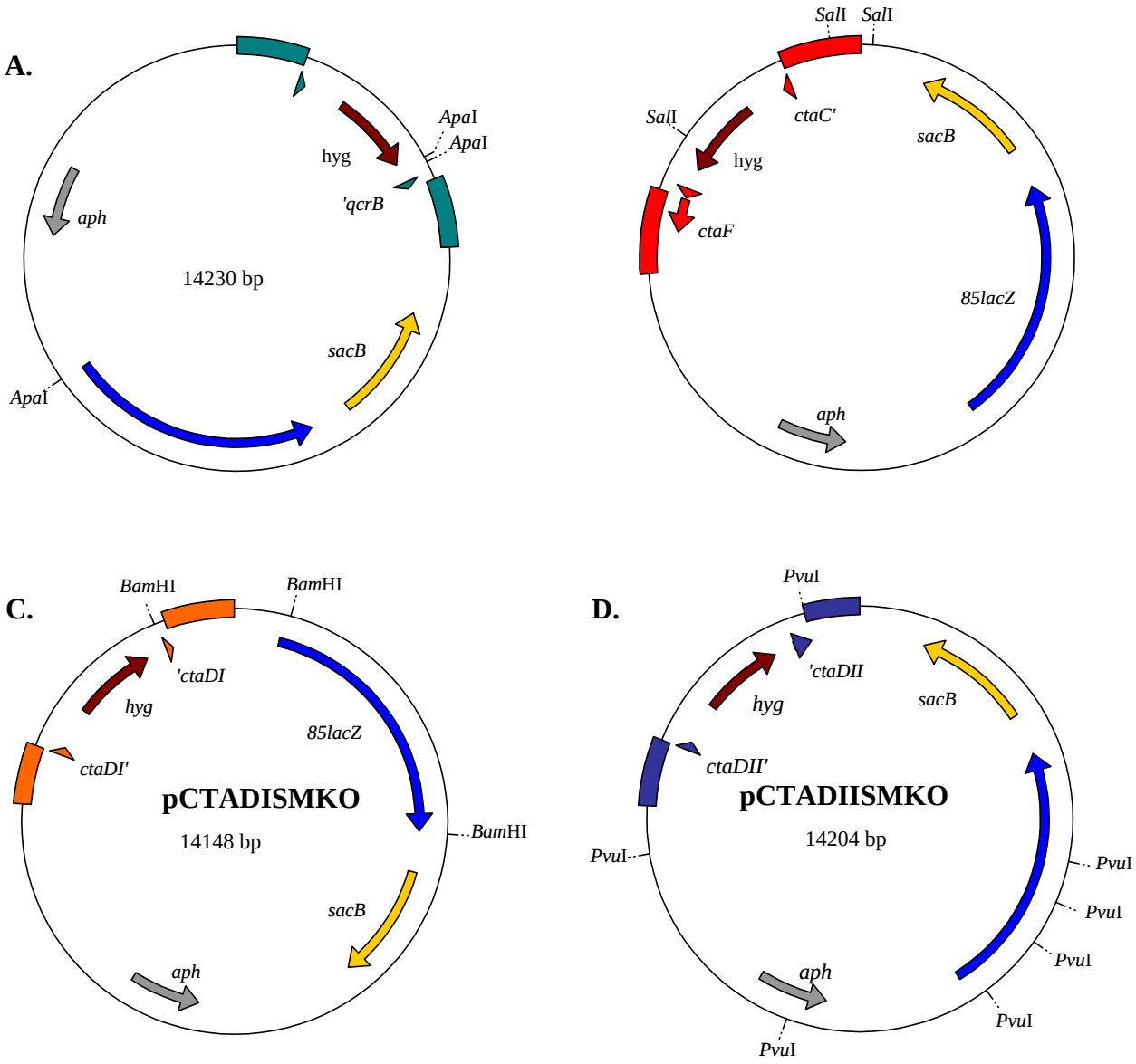

Figure 2. Knockout constructs used for inactivation of the *M. smegmatis* aerobic respiratory genes. **(A)** *qcrCAB*; **(B)** *ctaCF*; **(C)** *ctaDI*; **(D)** *ctaDII*. Shown on the maps are enzymes used for Southern blot analyses of the mutants. An apostrophe on the right or left of a gene name indicates truncation at the 3' and 5', respectively.

Table 3. Oligonucleotides used for construction of knockout vectors

Gene(s)	Oligonucleotide pairs used to construct knockout vectors		
	Oligonucl-eotide[a]	**Sequence (5'-3')**[b]	**Region amplified**
M. smegmatis qcrCAB	QCRF1 QCRR1	GGGCCGGAAGCttATGGGAACGGCTGGGAAGGT CTGCCAGACgGATCcGCAGCAGAAGCCCTGCTGACA	878 bp product including 114 bp of 5'-end of *qcrC*
	QCRF2 QCRR2	CGCTCACCGgGATCcCGCATGCGTCCGAGCACA GCTGTCGGgtACCTGTGCGCTGGGCGTGGC	863 bp product including 104 bp of 3'-end of *qcrB*
M. smegmatis ctaC	CTACF1 CTACR1	TTCGGGACGAgGTACCGCGTCACCTCGGGTGC TTGCCTCAGGGGgGATcCCCGTTGGCCAGCCGAGT	1038 bp product including 130 bp of 5'-end of *ctaC*
	CTACF2 CATCR2	CAAGGCCTACATgGATCcGCGCAACGCCGG TCACGCGCGACGAGAAGCttTACCGACGCCACG	1100 bp product including 139 bp of 3'-end of *ctaC*
M. smegmatis ctaDI	CTAD1F1 CTAD1R1	ACCTCGTCGgGTACCGAGGCAGGCAGCCCGGCG ACTACCCGCACATGGTCGAGCGGATcCGGGCCGA	883 bp product including 114 bp of 3'-end of *ctaDI*
	CTAD1F2 CTAD1R2	TGAACAGCGCCAgGAtcCCGCCGACCAGGAAGAA AATACGACGGCTGCGCGTCCGAAgCTtCGGGCAG	787 bp product including 69 bp of 5'-end of *ctaDI*
M. smegmatis ctaDII	CTAD2F1 CTAD2R1	ACCCGGAGGaaGCTtGCTGGCTGTGTCCGGCGCT AACTGCAGGCCGGGATCCGCCAACTCGGTGCGGA	859 bp product including 217 bp of 5' end of *ctaDII*
	CTAD2F2 CTAD2R2	TCACGGTCGAgGATCCGTGGGGCTACGGCAACT CGCGTTTGGgGTAccTCTCCAGATCCCAACCGA	844 bp product including 239 bp of 3'-end of *ctaDII*
M. tuberculosis ctaC	TBCTACF1 TBCTACR1	GGCCATCTCGTGGAAGCttCTACCCAGGTCC TCGTGGGCCACTGCGtCtAGATGTGTGGCAC	1903 bp product including 221 bp of 3'-end of *ctaC*
	TBCTACF2 TBCTACR2	AGCATTGCTGCGAGCGCCAGCTcTaGAAGACCAC GTACTTGGTGGTGGTACGGGTaAgCTTGGCGCCC	1994 bp product including 111 bp of 5'-end of *ctaC*

[a] F, forward primer; R, reverse primer.

[b] Restriction sites used for cloning are underlined (*Hin*dIII, *Bam*HI *Kpn*I) and bases changed to introduce the sites are given in lower case.

2.2.3 Phenotypic characterization of *M. smegmatis* mutants

Preparation of M. smegmatis seed stocks

All *M. smegmatis* cultures used for growth and expression analyses were seeded from frozen stocks prepared as follows. A single colony was inoculated in 5 ml of broth (MADC-Tw) and grown to mid-log phase in a 25 ml Erlenmeyer flask. This culture was diluted in 100 ml of MADC-Tw, and grown to an OD_{600} of 2.0 at 37°C with shaking (350 rpm). The culture was mixed with an equal amount of Dubos medium containing 15% v/v glycerol, divided into 8 ml aliquots (seed stocks) in sterile Bijou bottles, and stored at -70°C. Each seed stock was thawed on ice and used to inoculate a pre-culture for growth in shaking flasks or in a bioreactor, as described below.

Growth in shaking flasks

To determine the effects of mutations in the various components of the cytochrome bc_1-aa_3 pathway on growth, the *M. smegmatis* mutants and their parental wild type were grown under aerobic conditions in shaking flasks. Starter cultures (OD_{600} ~0.013) were prepared by diluting an overnight pre-culture (OD_{600} ~2.0) in 100 ml of MADC-Tw and incubating at 37°C with shaking (350 rpm). The cultures were grown in 500 ml Erlenmeyer conical flasks, giving a head space ratio of 1:4 to allow for adequate aeration. Optical density was monitored at 3 h intervals for a period of 42-60 h.

Growth in a bioreactor under oxystatic conditions

For gene expression analysis by DNA microarray, RT-PCR, and β-galactosidase assays, *M. smegmatis* strains were grown in a bioreactor under defined O_2 tensions. Oxystatic cultures were grown in a New Brunswick Scientific (NBS) Bioflow 110 fermentor in batches. This system is similar to the Braun BIOSTAT B bioreactor culturing system that was employed previously for the batch growth of *M. smegmatis* under oxystatic conditions (Kana *et al.*, 2001), with minor differences. The NBS system consists of a thermo-jacketed 2 liter vessel fitted with a baffle, two six-bladed impellers, a ring sparger, a water cooling coil, a sampling port, a temperature probe and a dissolved O_2 probe (Mettler Toledo), as well as a pH probe. The probes, water cooling coil and thermo jacket were connected to the fermentor control unit, through which all the variables (with

the exception of airflow rate) were adjusted and monitored. Air was supplied into the system by sparging compressed air through a rotometer and a 0.22 μm sterile filter. The rotometer allowed air supply to be manually controlled from 0 to 150 ml/min, depending on the desired air saturation. Vapour from the culture was allowed to escape through an exhaust fitted at the tip with a 0.22 μm sterile filter. Temperature was maintained at the set level by interplay of the thermo jacket and the circulatory water cooling system. An over-head motor connected to the impellers through a shaft was used to control stirring, with agitation speeds ranging from 50 to 1200 rpm. The fermentor control unit could be set to a dissolved O_2 cascade mode, which linked the stirring rate to the dissolved O_2 level, hence maintaining air saturation at the required level. Experimental conditions were monitored through a BioCommand Plus Bioprocessing software (New Brunswick Scientific), which was linked to the fermentor control unit.

For growth of reporter strains, the fermentor was autoclaved with 990 ml of Middlebrook 7H9 plus 2 ml glycerol. Autoclaved glucose (0.2%) and NaCl (0.085%) were added as the vessel cooled down, bringing the final volume to 1.0 liter. The vessel was allowed to equilibrate overnight, before the dissolved-O_2 probe was calibrated. The O% air saturation level was set by sparging the medium with 100% nitrogen and the 100% air saturation level was set by sparging with 100% compressed air. The medium was inoculated with 200 ml of pre-culture (OD_{600} ~2.0) to yield a starting culture of ca. 10^7 CFU/ml. Sterile Tween 80 (0.05%) and 700 ul of an organic antifoam 204 (Sigma, USA) were added to the medium together with the inoculum.

2.2.4 *cyd* expression analysis in a *ΔqcrCAB::hyg* mutant using a *lacZ* reporter

Construction of a cyd reporter strain

To monitor expression of the *cydAB*-encoded cytochrome *bd* oxidase in a cytochrome bc_1 mutant, plasmid pBK4 was electroporated into *M. smegmatis* strain Δ*qcrCAB*::*hyg* to obtain the reporter strain Δ*qcrCAB*::*hyg*::pBK4. This plasmid carries a *cydA*'::*lacZ* transcriptional fusion that expresses the *lacZ* gene under the control of the *cyd* promoter (Kana *et al.*, 2001). Single crossovers were selected on media containing Km and X-Gal and site-specific recombination was confirmed by Southern blot analysis.

Oxystatic growth of the reporter strains

The reporter strain, Δ*qcrCAB*::*hyg*::pBK4, was grown under oxystatic conditions in a New Brunswick Scientific Bioflow 110 fermentor as described above. For comparison of *cyd* expression in the *qcrCAB* mutant and its parental wild type, a reporter strain mc^2155::pBK4 (Kana *et al*., 2001), carrying the same *lacZ* fusion at the *cyd* locus of wild type mc^2155, was also grown under the same conditions as the Δ*qcrCAB*::*hyg*::pBK4 strain. Each strain was analyzed at least twice at each of 1, 5 and 21% air saturation levels. For each biological replicate experiment, 200 ml of pre-culture was started from the same amount of seed stock[3] and grown overnight to an OD_{600} of 2.0.This pre-culture was used to inoculate 1 liter of MADC-Tw containing 700 µl antifoam 204. Cultures were grown for 6 h and 2 ml duplicate samples were drawn at 2-h intervals, starting from time zero, therefore generating four samples (each in duplicate) per experiment.

β-Galactosidase Assays

Assays were performed on cell extracts as described by Ghanekar *et al* (1999) with a few modifications (Kana *et al*., 2001). Cells were harvested from 2 ml samples by centrifuging at 1500 × g for 5 min. The cell pellets were resuspended in 900 µl of ice-cold Z-buffer (60 mM Na_2HPO_4, 40 mM NaH_2PO_4, 10 mM KCl, 1 mM $MgSO_4$, 50 mM β-mercaptoethanol) and transferred to 2 ml screw cap Lysing Matrix B tubes containing beads (Southern Cross Biotechnology). Cells were lysed in a Savant BIO101 Fastprep cell disruptor in 2 cycles of 15 s at speed 4. Samples were cooled for 2 min on ice in between the pulses. The samples were transferred to Eppendorf tubes and the cell debris was pelleted by centrifuging at 1500 × g and the lysate was decanted into clean Eppendorf tubes. The assay reaction consisted of 50 to 100 µl of soluble cell extract and 0.8 mg/ml of 2-nitrophenyl-β-D-galactopyranoside (ONPG), in a total volume of 1 ml (volume adjusted with Z-buffer). Samples were incubated at 37°C for 80 min, and the reaction was stopped by addition of 500 µl of 1 M Na_2CO_3 bringing the total volume to 1.5 ml. To exclude enzyme activity in the reagents used, a negative control containing all the reagents but no cell extract was also assayed. Absorbance of the samples was

[3] Preparation of seed stocks is described in section 2.2.3.

measured at 420 nm against Z-buffer. The units of β-galactosidase in the samples were calculated in the following steps:

(i) Conc. of product (M) = $A_{420}/ЄL$ where Є = 4500 for ONPG, L = 1 cm for cuvettes used.

(ii) Number of moles (n) = M × v/1000 where v = volume of sample.

(iii) β-galactosidase units (U) = μmoles/t where t= incubation time in min.

Bradford assay

Protein concentrations in the cell extracts were determined using a Bradford-based BIO-RAD reagent according to the manufacturer's instructions. Two hundred μl of the cell extract was made up to 800 μl with Z-buffer and 200 μl of Bio-rad reagent was mixed in. The samples were incubated at room temperature for approx. 10 min, and the absorbance was read at 595 nm against a negative control containing all the reagents but no cell extract. To obtain a standard curve for determination of the unknown protein quantity in the cell extracts, known amounts of purified BSA (Amersham) in the range of 2-14 μg were also assayed in duplicate as described for the cell extracts. The averaged A_{595} values for BSA were plotted against the corresponding protein quantities (μg), and the equation of the slope of the graph was used to calculate the amount (μg) of protein in the cell extracts. Expression of the *cydA'*::*lacZ* fusion was measured as specific activity (SA) of the enzyme *β-galactosidase*. SA values in each sample were calculated as follows:

SA = amount of protein (mg)/enzyme units (mU).

SA values of samples taken at different time points were averaged within an experiment, and then between experimental replicates. Unpaired *t* tests were performed on the data to determine statistical significance, using GraphPad Instat version 3.00 (www.graphpad.com).

2.2.5 Genome expression profiling of the bc_1 and aa_3 mutants using DNA microarray

Sources of DNA microarrays

Two different sets of *M. smegmatis* DNA microarrays were used in this study. The first was a partial-genome amplicon array constructed, in collaboration with V. Mizrahi's

group (Molecular Mycobacteriology Research Unit [MMRU], University of the Witwatersrand, South Africa), by Coppel and colleagues (Monash University, Australia). This array consists of 1822 genes constituting *M. smegmatis* mc^2155 homologues of 1327 *M. leprae* genes (Cole *et al*., 2001), 95 homologues of selected *M. tuberculosis* genes (Cole *et al*., 1998) and 4 *M. smegmatis* genes absent in both *M. tuberculosis* and *M. leprae*. Included in this selection are homologues of genes involved in respiration (Table 4), DNA metabolism, cobalamin biosynthesis, hypoxic response, some members of the dormancy regulon and others. Briefly, PCR amplicons of all the above genes were evaluated for specificity by gel electrophoresis and then printed in triplicate on Corning Gaps II slides using a Genetic Microsystems Inc GMS 417 Arrayer. Slides were hydrated at 100°C for 5 s, cross-linked in a Stratagene UV Stratalinker 1800, baked at 80°C for 2 h and then boiled for 2 min before storage. More details on the array production are provided elsewhere (Matsoso *et al*., 2005) and the MIAME compliance file can be downloaded at http://vbc.med.monash.edu.au/~powell/M.smegmatis. The second set of array was a full genome microarray consisting of 6746 seventy-mer oligonucleotides representing 6746 ORFs from *M. smegmatis* mc^2155. Each ORF is printed in duplicate on the array. This array was obtained as a grant to V. Mizrahi from the TIGR Pathogen Functional Genomics Resource Center (http://pfgrc.tigr.org/).

RNA extraction

M. smegmatis wild type and mutant strains were grown oxystatically at full aeration (21% air saturation) in a bioreactor as described in section 2.2.3. A 200 ml pre-culture was inoculated from a seed stock (described in section 2.2.3), grown to OD_{600} ~ 2.0 and then used to inoculate 2 liter of MADC-Tw to a starting OD_{600} of approx. 0.2. The culture was grown to an OD_{600} of 0.6 and then harvested. RNA extraction was performed as previously described (Betts *et al*., 2002). Briefly, cell pellets were suspended in 1 ml Trizol reagent (Invitrogen, UK) and transferred to 2 ml screw cap Lysing Matrix A tubes containing beads (Southern Cross Biotechnoloy). Cells were lysed in a Savant BIO101 Fastprep cell disrupter for three cycles (20 s at speed 6) with cooling between pulses. Cell debris was separated by a 45 s centrifugation and the supernatant was transferred to 2 ml Phase Lock gel tubes (Eppendorf, Hamburg, Germany) containing 300 µl

chloroform/isoamyl alcohol (24:1). Samples were inverted rapidly for 15 s and then periodically for 2 min before centrifugation (10 000 × g for 5 min). Nucleic acids were precipitated from the top aqueous phase with 600 µl isopropanol and incubated overnight at 4°C. The RNA pellets were collected by centrifugation (9 000 × g for 20 min at 4°C), washed in 1 ml 70% ethanol and air-dried. RNA samples were resuspended in nuclease-free water (DEPC water) and then treated with DNase I (Ambion) for 30 min at 37°C. RNA was further purified using RNeasy kit (Qiagen, Germany) according to the manufacturer's instructions.

Table 4. *M. smegmatis* respiratory genes present on the partial-genome amplicon array

ID	Gene	Function
ctaB	*ctaB*	aa_3-type cytochrome *c* oxidase assembly factor
ctaC	*ctaC*	aa_3-type cytochrome *c* oxidase subunit II
ctaD	*ctaD*	aa_3-type cytochrome *c* oxidase subunit I
ctaE	*ctaE*	aa_3-type cytochrome *c* oxidase subunit III
ML0876	*ctaF*	aa_3-type cytochrome *c* oxidase subunit IV
qcrA	*qcrA*	Rieske iron-sulfur protein
qcrB	*qcrB*	ubiquinol-cytochrome *c* reductase cytochrome *b* subunit
qcrC	*qcrC*	ubiquinol-cytochrome *c* reductase cytochrome *c* subunit
Rv1542c	*glbN*	Hb-like oxygen carrier
Rv3145	*nuoA*	NADH dehydrogenase chain A
Rv3146	*nuoB*	NADH dehydrogenase chain B
Rv2392	*cysH*	3-phosphate adenylylsulfate reductase
Rv2899c	*fdhD*	formate dehydrogenase family accessory protein
Rv1161	*narG*	nitrate reductase subunit
Rv1162	*narH*	nitrate reductase subunit
Rv2391	*nirA*	probable nitrite reductase
Rv0252	*nirB*	nitrite reductase flavoprotein
Rv1623c	*cydA*	cytochrome *bd* oxidase subunit I
Rv1622c	*cydB*	cytochrome *bd* oxidase subunit II
Rv1620c	*cydC*	ABC transporter
Rv1621c	*cydD*	ABC transporter
(ctaDII)	*ctaDII*	aa_3-type cytochrome *c* oxidase chain I (second allele)
(ythA)	*ythA*	YthA (homolgoue of CydA)

Preparation of labeled cDNA probes

Probe preparation and hybridization were carried out using previously described methods (Boshoff *et al.*, 2004). RNA from the control experiment was labelled with Cy3-dCTP (Amersham Pharmacia Biotech, USA) and hybridized against Cy5-dCTP-labelled subject RNA. The 25 µl labeling reaction contained 2 µg of RNA (control) or 4 ug of RNA

(subject), 60 µM random primers, 0.5 mM each of dATP, dGTP and dTTP, and 0.05 mM dCTP, 10 mM DTT, 1 nmol of either Cy3-dCTP or Cy5-dCTP (Amersham Pharmacia Biotech) and 200 units reverse transcriptase Superscript II (Invitrogen^{TM} Life Technologies). The primers were annealed to the RNA by heating to 70°C for 10 min and snap-cooling on ice before adding the remaining reaction components. The sample was incubated for 10 min at 25°C followed by 90-min incubation at 42°C. To stop the reaction, the sample was heated to 72°C, 5 µl of a 1 M NaOH was added and the mixture incubated for 15 min. The pH was neutralized by addition of 5 µl of 1M HCl. To remove unincorporated nucleotides and Cy-dye, the Cy3- and Cy5-labelled cDNA samples to be compared were combined run through a microcon filter (Millipore). The sample was added to a microcon filter tube containing 400 µl of TE and centrifuged at 10 000 × g for ca. 10 min. The wash step was repeated and the sample was finally eluted in a volume of *ca*. 11 ul.

Microarray hybridization

For the partial amplicon array, slides were first boiled in 95°C deionised water for 2 min followed by a rinse in 95% ethanol and quick-dried by centrifugation at 36 × g for 5 min prior to hybridization. For all arrays, the slides were pre-hybridized for 1 hr at 42°C in a buffer containing 5× SSC, 1% BSA and 0.1% SDS. Pre-hybridization was carried out under a glass coverslip in a humidified Corning hybridization chamber submerged in a 42°C water bath. Prior to addition of labeled probes, the pre-hybridized slides were removed from hybridization chambers and coverslips were removed in distilled water. The slides were washed twice in isopropanol (2 min each) and then dried by centrifuging at 36 × g for 5 min. Labeled probes were mixed with blocking reagents (4 µg yeast tRNA, 1.9 µg Herring sperm DNA) and made up to a total of 24 µl (for the partial-genome DNA microarray) or 48 µl (for the full genome DNA microarray) in hybridization buffer (5 × SSC, 25% formamide, 0.1% SDS). Samples were denatured at 98°C for 2 min, snap-cooled on ice and applied to the array. Hybridization took place under a glass coverslip in a humidified slide chamber (Corning) submerged in a 42°C water bath for approximately 16 h. Cover slips were removed in wash buffer I (1 × SSC, 0.05% SDS) and slides were washed once in buffer I and twice in buffer II (0.1 × SSC) for 2 min each at room

temperature before being dried by centrifugation (36 × g, 5 min). Slides were scanned using a GenePix 4000B instrument (Axon Instruments).

Data analysis

After capture with the GenePix 4000B scanner, the image was analyzed with GenePix Pro 4.1 (Axon Instruments). Although the program was allowed to automatically flag bad spots, a manual flagging was also performed based on visual inspection. The results were normalized such that the ratio of medians of all the feature pixels was equal to 1. For a spot to be included in the analysis, at least one of the two channels (Cy3 or Cy5) median intensities had to be ≥ 1000 (or a background-subtracted median intensity of at least 600). However, these cut-offs were decreased in the analysis of the TIGR full genome oligonucleotide array as the spot intensities were generally lower with this array than they were with the partial genome amplicon array. A gene was considered significantly differentially expressed if the $\log_2$ of the ratio of medians of the two channels was ≥ 1. Results were exported into Microsoft Excel and the $\log_2$ values of duplicate spots were averaged per array, before data from biological replicates was collated.

An independent data analysis was performed by D. Powell (Victorian Bioinformatics Consortium, Australia) on some of the microarrays to validate the results (Matsoso *et al*., 2005). Images obtained from the GenePix 4000B scanner were analyzed and quantified using Imagene 6.0 (BioDiscovery) to determine spot integrity, and further analyzed using Bioconductor (Dutoit and Yang, 2003) and Limma (Smyth, 2004) packages. Spot intensities were background corrected by subtracting the background median from the foreground mean. Any resulting non-positive values were replaced with half the minimum of all positive corrected intensities for that array. The normalization to remove various biases involved two parts. Firstly, each array was normalized independently using print-tip loess normalization (Yang *et al*., 2001). Secondly, diagnostic plots suggested a variation in scale between arrays, so the log-ratios were scaled in such a way that each array had the same median-absolute-deviation (MAD). The normalized data were then used to fit a linear model (Yang *et al*., 2001) for each gene using generalized least-squares which takes into account the correlation between duplicate spots (Smyth *et al*., 2005). The coefficient of the fitted model for each gene

describes the inferred difference in RNA expression between wild-type and mutant. Empirical Bayes was then used to calculate the moderated t-statistics and associated *P*-values. The *P*-values were adjusted for multiple testing using false-discovery-rate (FDR), and a cut-off of 1% FDR was used to define a set of differentially expressed (DE) genes.

2.2.6 Effects of chlorpromazine on the transcriptome of a bc_1 mutant of *M. smegmatis*

DNA microarray

Cultures were grown oxystatically at 21% air saturation, in a New Brunswick Scientific Bioflow 110 fermentor as described above, to an OD_{600} of 0.6 and then rapidly harvested into a pre-warmed flask (37°C). The culture was then divided into two 200 ml samples in pre-warmed 1 liter flasks. To one flask, 200 µl of chlorpromazine (CPZ, [50mg/ml stock in DMSO]) was added, and 200 µl DMSO was added to the other flask as a control. Both cultures were shaken at 350 rpm for 1 h at 37°C. Cells were harvested and frozen in Trizol reagent or used immediately for RNA isolation. The RNA was analyzed on the partial-genome amplicon DNA microarray.

Semi-quantitative RT-PCR

RNA samples were treated with DNA-free kit (Ambion) according to the manufacturer's instruction, to remove contaminating DNA. Reverse transcription was carried out in 20 µl reactions containing 0.5 µg of total RNA, 0.3 mM gene-specific reverse primers (Table 5), 0.8 mM each of dATP, dGTP, dCTP and dTTP, and Enhanced Avian HS reverse transcriptase (Sigma). The primers were annealed to the RNA by heating to 94°C for 90 s, followed by 3 min at 65°C and then 57°C for 3 min. Samples were snap-cooled on ice before adding the remaining components and then incubated at 60°C for 30 min, followed by a 5 min heating step at 95°C. The resulting cDNA was either used immediately or frozen at -20°C. Five-fold serial dilutions of the cDNA were prepared and 2 µl from each dilution used as template for PCR. The 50 µl reaction mixture contained 4 mM $MgCl_2$, 0.4 mM each of dATP, dCTP, dGTP and dTTP, 0.4 µM primers, 0.5 mg/ml BSA, 10% DMSO, reaction buffer and 2.5 U of FastStart Taq polymerase (Roche). Samples were heated to 94°C for 10 min before cycling for 14 cycles of 94°C for 30 s, 65°C for 30 s,

72°C for 30 s, followed by 24 cycles of 94°C for 30 s, 57°C for 30 s and 72°C for 30 s. The PCR products were analyzed on a 3% agarose gel.

Table 5. Oligonucleotides used in RT-PCR

M. smegmatis gene	H37Rv homologue	Oligonucl-eotide	Sequence (5'-3')	Product length (bp)
MSMEG5229	*devR* / Rv3133c	3133L 3133R	GCCTGATGCTCACGTCGTTC CTTGACCACGTATCCGCTCG	80
MSMEG3937	*hspX* / Rv2031c	2031L 2031R	GACGGTGGTTACGAACTGCG TCGGCCTTGATGGTCAACAC	98
MSMEG5231	*acg* / Rv2032	2032L 2032R	ACATGGACACCCTCGGTGAG GGCGAGTTCGGAATGGTAGG	104
MSMEG5230	*uspL* / Rv2028c	2028L 2028R	GACGCACCGCTTTCGGTGAT GAGTTCGGGATACCGCTTGC	144
MSMEG3957	*uspM* / Rv2026c	2026c1L 2026c1R	TCGACGTCGGTGACATTCCT GGATAGCGTTCCTGCCAACC	106
MSMEG5708	*uspN* / Rv2026c	2026c2L 2026c2R	CGTCATCGACTGGGAAGGTG TCGACGTAGCACTTCGCCTC	108
MSMEG2759	*sigA* / Rv2703	SigA-F1 SigA-R1	TCTACGCCACGCAGAAGCTG GTTCGCCTCCAGCAGATGGT	124

2.2.7 Complementation of the *M. smegmatis ctaC* knockout mutant

In order to determine if the growth defect of the *M. smegmatis ctaC* mutant could be complemented by presence of a functional *ctaC* gene from *M. tuberculosis*, a complementing vector, pMVCTAC, was constructed (Figure 3B). A 2892 bp *Kpn*I fragment from *M. tuberculosis* H37Rv was cloned into the *Kpn*I site of plasmid pMV306K. This fragment carried the entire *ctaCF* operon (1520 bp) plus 530 bp and 842 bp of the 5' and 3' flanking sequences. The resulting plasmid, pMVCTAC, was electroporated into *M. smegmatis ctaC* mutant, Δ*ctaC*::*hyg*. Integration of this construct at the *attB* locus of the mutant was confirmed by PCR amplification if the resulting *attL* and *attR* regions. The following primer pairs were used: attBS2 (5'-ACAGGATTTGAACCTGCGGC-3') and attL4 (5'-AATTCTTGCAGACCCCTGGA-3') for *attL*, and attBS1 (5'-ACGTGGCGGTCCCTACCG-3') and attL2 (5'-CTTGGATCCTCCCGCTGCGC-3') for *attR*. The primers were kindly supplied by S. Barichievy (MMRU). Growth of the complemented strain under aerobic conditions was compared to that of Δ*ctaC*::*hyg* and its parental wild type under the same conditions.

2.2.8 Attempts to construct a cytochrome *bc*$_1$-*bd* double mutant of *M. smegmatis*

The viability of a *M. smegmatis* mutant lacking both known aerobic electron routes terminating in cytochrome *aa*$_3$ and cytochrome *bd* oxidases, was investigated. Plasmid pCYDAKO used to generate a knockout mutant of cytochrome *bd* in *M. smegmatis* (Kana *et al*., 2001), was electroporated into a cytochrome *bc*$_1$ mutant, Δ*qcrCAB*::*hyg* (this work). Selection of recombinants was carried out as described above.

2.2.9 Attempts to construct a *ctaC* mutant of *M. tuberculosis*

Cloning and delivery of the knockout substrate

To investigate the effects of blocking the cytochrome *bc*$_1$-*aa*$_3$ pathway in *M. tuberculosis*, the gene encoding subunit II (*ctaC*) of the *aa*$_3$-type cytochrome *c* oxidase was targeted for deletion. A knockout vector for the *M. tuberculosis ctaC* was made using the same strategy described for *M. smegmatis* genes above. Two PCR products amplified from the up- and downstream flanking regions of *M. tuberculosis* H37Rv *ctaC* were individually cloned into pGEMTeasy and sequenced. These fragments, which included 111-bp of the 5'- and 221-bp of the 3'- ends of *ctaC*, respectively, were subsequently cloned into p2NIL (Parish and Stoker, 2000), effectively deleting an internal 760-bp region of *ctaC*. The deletion mutation was marked by insertion of a hyg gene at the deletion junction. The *lacZ-sacB* cassette was then cloned in the *Pac*I site of p2NIL, as described above, to create the knockout construct, p2CTACTBKO (Table 2; Figure 3A). This plasmid was electroporated into *M. tuberculosis* H37Rv and plated on Middlebrook 7H10 supplemented with glycerol, OADC, Km, Hyg and X-Gal. Plates were incubated for 21 days at 37°C.

Selection of recombinants

Blue Hyg- and Km-resistant colonies were recovered and genotyped by Southern blot analysis to confirm that they resulted from a site-specific SCO recombination at the *ctaC* locus. The SCOs were streaked onto fresh plates containing Hyg and X-Gal and grown for 22 days at 37°C to allow for a second cross to occur. Serial dilutions of the white Hyg^r colonies were prepared and plated on media containing Hyg, X-Gal and 5% sucrose.

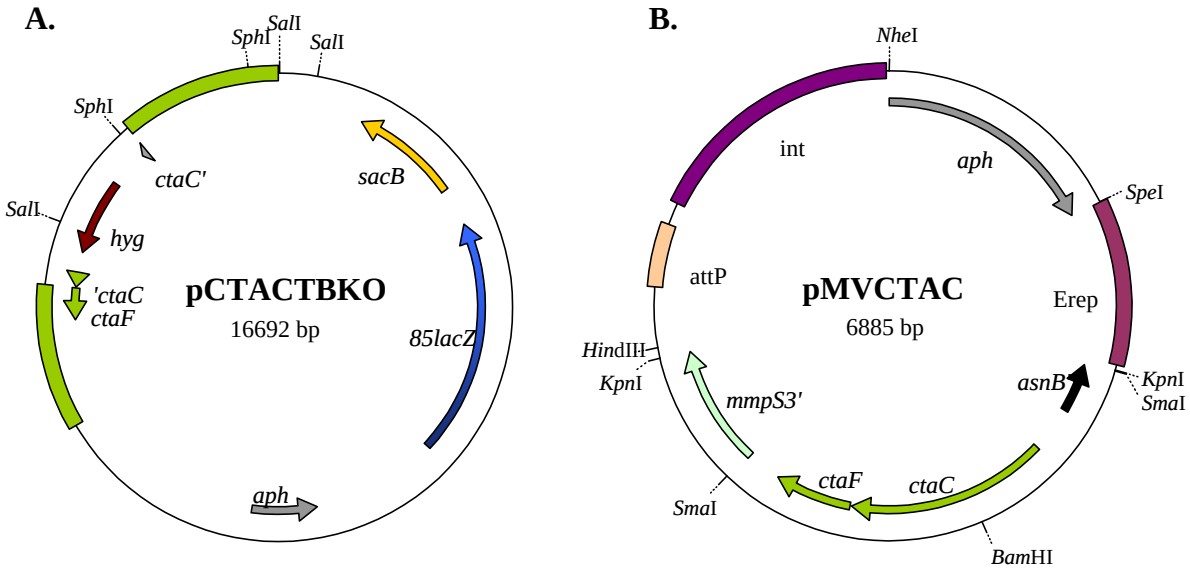

Figure 3. *M. tuberculosis ctaC* constructs. **(A)** Knockout construct used for attempted gene replacement of *ctaC* in *M. tuberculosis* H37Rv. **(B)** a vector used for complementation of a *ctaC* mutant in *M. smegmatis*. This vector carries the *M. tuberculosis ctaCF* operon plus flanking sequence. An apostrophe to the left or right of a gene name means a truncation at the 5' or 3' end of the gene, respectively.

Since it was hypothesized that the mutant in this gene, if viable, would be retarded in growth, the plates were incubated for a total period of 54 days to increase the chances of isolating such a mutant. After this period plates started drying out. All white Hyg^R, Suc^R colonies were isolated from the plates were tested for Kan-sensitivity (potential DCOs).

3. RESULTS

Function of the cytochrome bc_1-aa_3 branch of the respiratory network in mycobacteria

In order to gain insight into how *M. tuberculosis*, which is considered an obligate aerobe, survives the environments of variable oxygen availability during latent and active infections, it is necessary to investigate the functioning of the mycobacterial respiratory chain. The states of functionality of the different components of the respiratory chain may determine the mode of adaptation of the bacilli under existing conditions. In an attempt to dissect the roles played by the various respiratory components in growth and survival of mycobacteria, genes encoding such were selected for targeted gene knockout and the effects thereof studied. The major genetic and physiological aspects of this study were carried out in *M. smegmatis* and based on the insights gained from this work further investigations were subsequently performed in *M. tuberculosis*.

3.1 Identification of the aerobic respiratory genes in the genome of *M. smegmatis*

This work was initiated before the release of the complete genome sequence of *M. smegmatis* strain mc^2155. Therefore to identify the complement of *M. smegmatis* genes involved in aerobic respiration, the unfinished genome sequence of *M. smegmatis* strain mc^2155 (http://www.tigr.org/ufmg/) was initially analyzed by BLAST searching (Altschul *et al*., 1990) using *M. tuberculosis* aerobic respiratory genes as query sequences (Cole *et al*., 1998; Fleischmann *et al*., 2002). These included genes that encode the various aerobic respiratory enzyme complexes such as NADH dehydrogenase (*nuoABCDEFGHIJKLMN*; *ndh*; *ndhA*), and succinate dehydrogenases (*sdhCDAB*), menaquinol:cytochrome *c* oxidoreductase (cytochrome bc_1 complex; *qcrCAB*), and the terminal oxidases, cytochrome aa_3 (*ctaD*, *ctaCF*, *ctaE*) and cytochrome *bd* (*cydAB*) as detailed in Table 6.

Table 6. Genes encoding components of the aerobic respiratory chain of *M. smegmatis*

Origin of query sequence(s)[a]	**Gene / operon name**	**H37Rv ORF #**	**Homologue(s) in smeg**	**Function**	**TIGR annotation**
M. tuberculosis	*nuoABCDEF GHIJKLMN*	Rv3145-Rv3158	*nuoABCDEFGHIJKLMN*	Type I NADH dehydrogenase	MSMEG2064-MSMEG2051
M. tuberculosis	*ndh*	Rv1854c	*ndh*	Type II NADH dehydrogenase	MSMEG3627
M. tuberculosis	*ndhA*	Rv0392c	*ndhA*	Type II NADH dehydrogenase	MSMEG3463
M. tuberculosis	*sdhCDAB*	Rv3316-Rv3319	*sdhBADC*	succinate dehydrogenase	MSMEG1666-MSMEG1669
M. tuberculosis	*qcrCAB*	Rv2194-Rv2196	*qcrCAB*	cytochrome bc_1 complex	MSMEG4264-MSMEG4266
M. tuberculosis	*ctaD*	Rv3043c	*ctaDI* (two copies)[c]	cytochrome *c* oxidase subunit I	MSMEG1027 & MSMEG2320
			ctaDII (2nd homologue)[b]	cytochrome *c* oxidase subunit I	MSMEG4435
M. tuberculosis	*ctaC*	Rv2200c	*ctaC*	cytochrome *c* oxidase subunit II	MSMEG4271
M. tuberculosis	*ctaE*	Rv2193	*ctaE*	cytochrome *c* oxidase subunit III	MSMEG4263
M. tuberculosis	*ctaF*	Rv2199c	*ctaF*	cytochrome *c* oxidase subunit IV	MSMEG4270
M. tuberculosis	*cydA*	Rv1623c	*cydA*	cytochrome *bd* oxidase, subunit I	MSMEG3243
M. tuberculosis	*cydB*	Rv1622c	*cydB*	cytochrome *bd* oxidase, subunit I	MSMEG3240
M. tuberculosis	*cydDC*	Rv1621c-Rv1620c	*cydDC*	ABC transporter	MSMEG3241-MSMEG3240
B. subtilis	*ythA*	None	*ythA* (*cydA* homologue)	cytochrome *bd*' oxidase, subunit I	MSMEG5584
B. subtilis	*ythB*	None	*ythB* (*cydB* homologue)	cytochrome *bd*' oxidase, subunit II	MSMEG5585

[a] Sequences were obtained from Tuberculist (http://genolist.pasteur.fr/TubercuList/) for *M. tuberculosis* and Subtilist (http://genolist.pasteur.fr/SubtList/).
[b] *M. smegmatis* has two homologues of the *M. tuberculosis ctaD* gene.
[c] *M. smegmatis ctaD* located on the previously reported duplicated region of the chromosome (Galamba *et al*., 2001; http://www.tigr.org/tigr-scripts/CMR2/CMRHomePage.spl

To identify genes that may be present in *M. smegmatis* but not in *M. tuberculosis*, homologues of other known aerobic genes such as those of *E. coli*, and *B. subtilis* were also searched for in the *M. smegmatis* genome sequence. Although the genome of *M. smegmatis* was found to contain a full complement of all the known *M. tuberculosis* aerobic genes, some notable differences between these two species were identified. In particular, *M. smegmatis* has more than one homologue of the *ctaD* gene and its genome sequence also contains an additional putative cytochrome *bd*-type terminal oxidase, encoded by homologues of the *B. subtilis ythAB* genes (Table 6).

3.1.1 Occurrence of multiple *ctaD* homologues in *M. smegmatis*

BLAST searches of the unfinished genome sequence of *M. smegmatis* mc^2155 (http://www.tigr.org/ufmg/) revealed presence of two distinct *ctaD* homologues. Of these, one is located within a region of the genome that has been reported to be duplicated (Galamba *et al*., 2001), and as a result, this strain carries a total of three *ctaD*-type genes. The duplicated *ctaD* homologue, designated in this work as *ctaDI*, shows 86% amino acid (aa) identity with *M. tuberculosis ctaD* and is located in the same chromosomal context as its *M.* tuberculosis counterpart (Table 5; MSMEG1027 and MSMEG2320). In all the *Mycobacterium* species for which complete genome sequences are available a *serB2* gene is found immediately downstream of *ctaD*, in an apparently operonic arrangement. A similar arrangement is also seen in other nocardioform actinomycetes, such as *Nocardia farcinica* and *C. glutamicum* (though not operonic with *ctaD* in this species), but not in non-nocardioform actinomycetes such as *Streptomyces coelicolor*. The second *M. smegmatis ctaD* homologue, designated herein as *ctaDII* (Table 6; MSMEG4435), shows 85% identity with *M. tuberculosis ctaD* at the amino acid level, but is located in a completely different chromosomal context compared to its *M. tuberculosis* counterpart (Figure 6B).

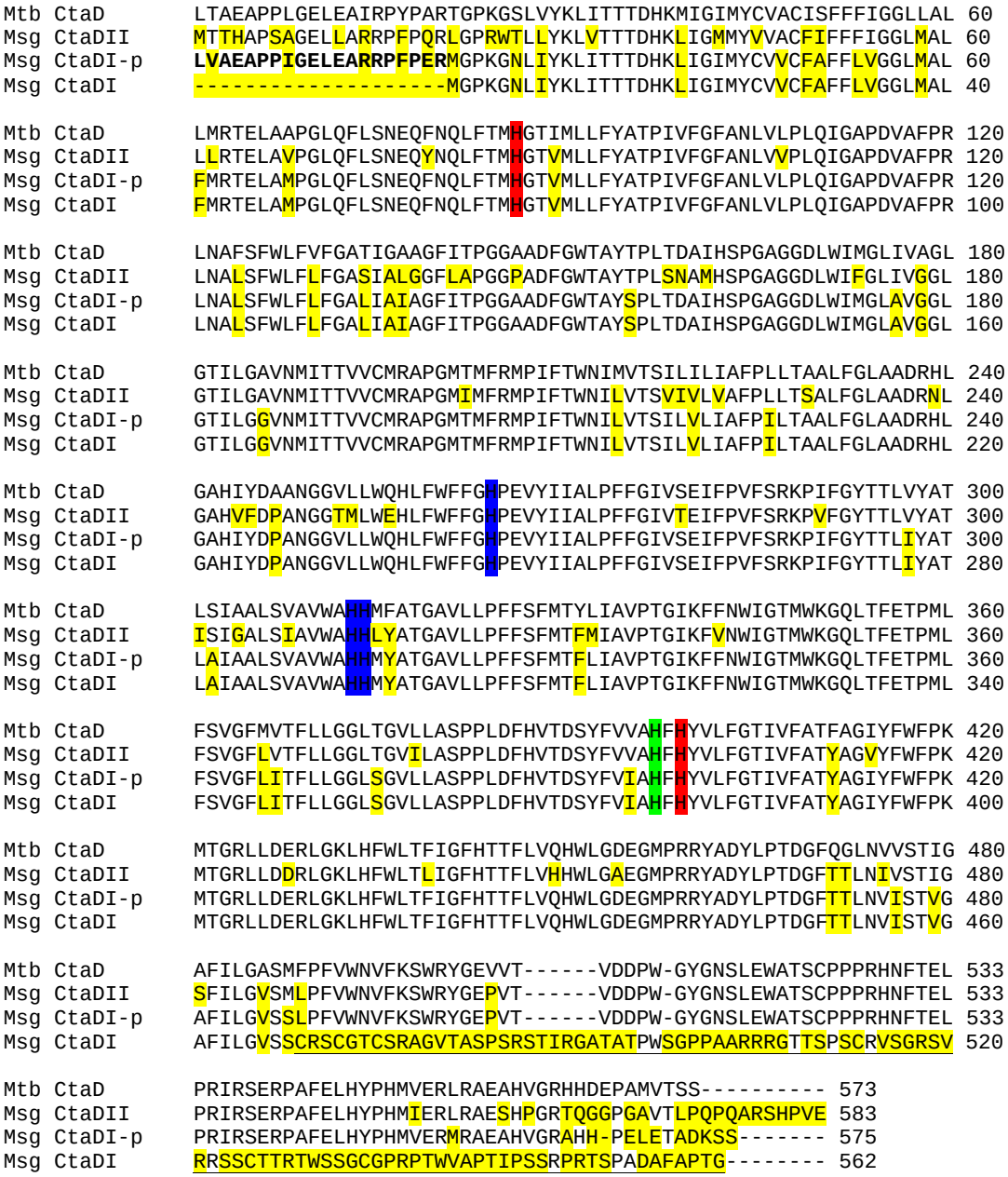

Figure 4. Comparison of subunit I of cytochrome *c* oxidase (CtaD) from *M. tuberculosis* and *M. smegmatis*. The alignment was generated with ClustalW version 1.8 (http://www.ebi.ac.uk/clustalw/). Sequences were obtained from http://genolist.pasteur.fr/TubercuList for *M. tuberculosis* (Mtb CtaD) and http://www.tigr.org/tigr-scripts/CMR2/CMRHomePage.spl for *M. smegmatis* (Msg CtaDI and Msg CtaDII). Msg CtaDI-p is a variant of Msg CtaDI, in which a probable frame-shift (underlined) starting at residue 469 has been corrected and a *Leu* residue 20aa (in bold) upstream of the Msg CtaDI *Met* start codon was proposed as the start site. *M. smegmatis* amino acid residues that differ from the *M. tuberculosis* CtaD are highlighted in yellow. Marked on the sequences are the histidine residues that putatively serve as ligands for Cu_B (blue), heme *a* (red) and heme a_3 (green) (Niebisch and Bott, 2001).

Analysis of the M. smegmatis *CtaD homologues reveals a possible frame-shift in* ctaDI

A comparison of the two different ***M. smegmatis*** CtaD protein sequences to each other and to that of ***M. tuberculosis*** CtaD, highlighting the similarities and divergence, is shown in Figure 4. Alignment of these sequences revealed a frame-shift in the coding sequence of ***M. smegmatis ctaDI*** (both identical copies; MSMEG1027 and MSMEG2320) caused by a probable DNA sequencing error that resulted in a missing nucleotide base (either a C or a T) at position 1405 of the nucleotide sequence. This frame-shift resulted in complete divergence of the last 94aa at the carboxyl end of ***M. smegmatis*** CtaDI from the ***M. tuberculosis*** CtaD (Figure 4; Msg CtaDI).

Also apparent from these alignments is the possibility that a leucine (Leu) 20aa upstream of the TIGR-annotated methionine (Met) start codon in both copies of CtaDI (MSMEG1027 and MSMEG2320 [http://www.tigr.org/tigr-scripts/CMR2/CMRHomePage.spl]) may serve as a start codon. This inference is based on the high homology (75% and 65%) of this 20aa region to the amino end of ***M. tuberculosis*** CtaD and ***M. smegmatis*** CtaDII, respectively (Figure 4). Both the possible missing 20aa N-terminal region and the frame-shift were corrected in the CtaDI sequence, generating Msg CtaDI-p (Figure 4). Although start site mapping would be necessary in order to determine the likelihood of such a proposed sequence, Msg CtaDI-p was used as the ***M. smegmatis*** CtaDI sequence in further comparative analyses with other actinomycetes CtaD sequences (Figure 5; Table 7).

The occurrence of multiple ctaD *alleles is not uncommon in actinomycetes*

The presence of two different ***ctaD*** alleles in ***M. smegmatis*** prompted an interest to investigate this occurrence in other actinomycetes. Although distinct ***ctaD*** alleles were only identified in ***M. smegmatis*** and not any other sequenced mycobacterial species, BLAST searches on the sequenced genomes of other actinobacteria (http://www.tigr.org/tigr-scripts/CMR2/CMRHomePage.spl) revealed that the occurrence of two or more distinct ***ctaD*** alleles was not uncommon. Two species of ***Streptomyces*** and one of ***Nocardia*** were also found to possess two distinct ***ctaD*** homologues with similarity to the ***M. smegmatis ctaD*** genes (Figure 5 and Table 7).

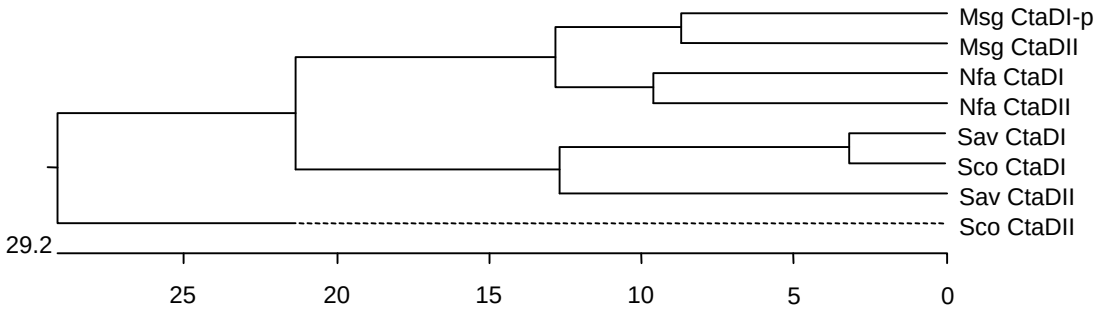

Figure 5. Phylogenetic relationship of CtaD proteins from sequenced actinomycetes bearing multiple *ctaD* alleles. The tree was constructed using ClustalW (http://www.ebi.ac.uk/clustalw/). A similar tree was obtained with the MegAlign module of the Lasergene suite of programs (DNASTAR, Madison, WI). Abbreviations are as follows, Msg: *M. smegmatis*; Nfa: *Nocardia farcinica*; Sav: *Streptomyces avermitilis*; Sco: *S. coelicolor*. With the exception of Msg CtaDI-p (explained in Figure 4), the sequences were obtained from http://www.tigr.org/tigr-scripts/CMR2/CMRHomePage.spl for Sav and Sco, and Nfa. The tree indicates a much closer evolutionary relationship between *M. smegmatis* and *N. farcinica* CtaDs than the *Streptomyces* CtaDs.

Table 7. Sequence distances between various actinomycete CtaD polypeptides

Percent Identity[a]											
Divergence[b]		**1**	**2**	**3**	**4**	**5**	**6**	**7**	**8**		
	1	***	84	80.9	78.3	67.7	67.9	69.8	67.4	**1**	Msg CtaDI-p
	2	17.4	***	75.8	75.2	64.5	65.6	66.5	65.7	**2**	Msg CtaDII
	3	20.7	27.2	***	82.3	65.7	65.8	68.4	66.4	**3**	Nfa CtaDI
	4	24.8	30.3	19.2	***	66.2	65.6	66.8	66.9	**4**	Nfa CtaDII
	5	42	45.7	42.5	43.8	***	78	93.3	72.6	**5**	Sav CtaDI
	6	41.1	44.3	44	45.2	24.6	***	77.1	74.6	**6**	Sav CtaDII
	7	37.7	42.4	37.6	42.7	6.3	26.2	***	72.8	**7**	Sco CtaDI
	8	41.5	44.7	42.7	42.3	33.6	29	33.3	***	**8**	Sco CtaDII
		1	**2**	**3**	**4**	**5**	**6**	**7**	**8**		

[a,b] Sequence identities and divergence, respectively, as generated with MegAlign (DNASTAR) using a clustal method.
Msg, *M. smegmatis*; Nfa, *N. farcinica*; Sav, *S. avermitilis*; Sco, *S. coelicolor*.

Phylogenetic analysis of these various actinobacterial CtaD proteins grouped the *M. smegmatis* and *N. farcinica* CtaD sequences together showing that they share a much more recent common ancestor than the link to their *Streptococcus* counterparts (Figure 5). This is consistent with the classification of the genera *Mycobacterium* and *Nocardia* together as nocardioform actinomycetes (Goodfellow and Minnikin, 1977; Finnerty 1992; Ishikawa *et al*., 2004).

3.1.2 Genetic composition and organization of the aerobic respiratory chain of *M. smegmatis*

The genome analysis revealed presence of an aerobic respiratory chain consisting of at least three branches, namely a cytochrome *c* branch terminating in an aa_3-type cytochrome *c* oxidase, and two quinol branches terminating in cytochrome *bd* and *bd'* oxidases, encoded by *cydAB* and homologues of *ythAB*, respectively (Figure 6). With the exception of the *ythAB*-encoded cytochrome *bd*' oxidase (nomenclature based on the corresponding *B. subtilis* homologues; Table 6), which is absent in *M. tuberculosis*, the aerobic respiratory chain of *M. smegmatis* was found to closely resemble that of *M. tuberculosis*. This composition was later confirmed by searching the complete genome sequence of *M. smegmatis* which became available during the course of this study (http://www.tigr.org/tigr-scripts/CMR2/CMRHomePage.spl).

While the role of the alternative *bd*' (*ythAB*) quinol oxidase has yet to be investigated, the *cydAB*-encoded *bd* oxidase was previously characterized in *M. smegmatis* and was shown to be highly expressed under microaerobic conditions (Kana *et al*., 2001). A *cydA*::*aph* mutant was attenuated for growth under these conditions, suggesting that the pathway terminating in cytochrome *c* oxidase may serve as the major route for respiration under aerobic growth conditions. Therefore the cytochrome bc_1-cytochrome aa_3 pathway became the focus of investigation in this study.

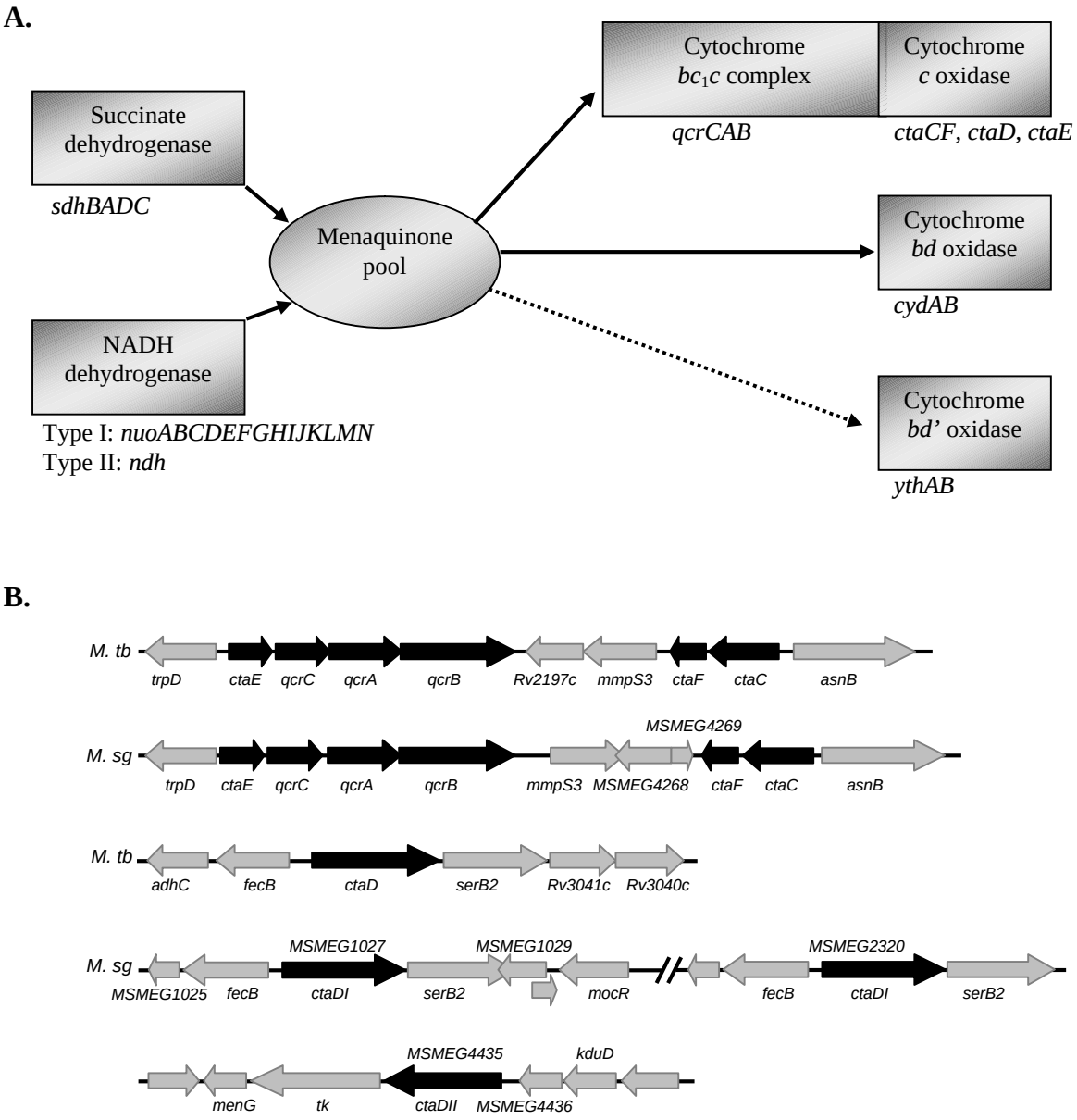

Figure 6. Genetic composition and organization of the aerobic respiratory chain of *M. smegmatis*. **(A)** Proposed pathway of electron flow. Solid arrows indicate established pathways and dashed arrows represent putative pathways. Various enzyme complexes are denoted by boxes. The cytochrome bc_1 complex contains a diheme cytochrome c_1 (represented as c_1c; encoded by *qcrC*), and together with cytochrome *c* oxidase this complex is proposed to form a supercomplex (fused boxes) as is the case in *C. glutamicum* (Niebisch and Bott, 2001). **(B)** Genomic organization of the genes encoding cytochrome bc_1-aa_3 pathway. The arrows denote the respiratory pathway (black) and neighbouring (grey) genes. The annotation for *M. tuberculosis* H37Rv is taken from Tuberculist (http://genolist.pasteur.fr/TubercuList/), and the annotation for *M. smegmatis* mc^2155 is from the TIGR Comprehensive Microbial Resource (http://www.tigr.org/tigr-scripts/CMR2/CMRHomePage.spl).

Genetic structure of the M. smegmatis *cytochrome* bc_1-aa_3 *pathway*

The sequences of the ***M. smegmatis*** genes in the cytochrome ***bc*$_1$-*aa*$_3$** pathway were obtained as described above. The pathway consists of a ***qcrCAB***-encoded menaquinol-cytochrome ***c*** oxidoreductase (cytochrome ***bc*$_1$**), that transfers electrons to the terminal cytohrome ***aa*$_3$**-type cytochrome ***c*** oxidase (cytochrome ***aa*$_3$**) encoded by ***ctaC***, ***ctaD*** (two distinct alleles of which have been found; section 3.1.1), ***ctaE*** and ***ctaF***. As demonstrated for ***C. glutamicum*** (Niebisch and Bott, 2001) and proposed for ***M. tuberculosis*** (Weinstein ***et al***., 2005), the cytochrome ***bc*$_1$** complex of ***M. smegmatis*** contains a diheme cytochrome ***c*$_1$** and is also proposed to form a supercomplex with cytochrome ***aa*$_3$**. The genomic context of these genes (http://www.tigr.org/tigr-scripts/CMR2/CMRHomePage.spl) and the organization of their encoded complexes as determined by their roles in electron transfer are illustrated in Figure 6.

3.2 Targeted knockout of genes in the cytochrome *bc*$_1$-*aa*$_3$ pathway in *M. smegmatis*

Based on previous studies in other organisms, it was proposed in this study that mutants in the components of the cytochrome ***bc*$_1$-*aa*$_3$** pathway would provide tools to investigate the role of individual components of this pathway in growth and control of respiration in ***M. smegmatis***. Different mechanisms have previously been proposed that describe the role of aerobic respiratory components in sensing and responding to oxygen. In one such mechanism it was proposed that when oxygen is not used as the terminal electron acceptor, the reduced quinones react with oxygen to form reactive oxygen species, sending signals to regulators of oxidative stress (Chandel ***et al***., 2000). A ***M. smegmatis*** mutant lacking cytochrome ***bc*$_1$** would provide a tool to probe this mechanism as it is proposed in this work that blockage of cytochrome ***bc*$_1$** may result in an increase in the reduced quinones. Based on their study in ***M. tuberculosis***, Voskiul et al (2003) suggested another mechanism in which they proposed that the terminal oxidase, cytochrome ***aa*$_3$** is itself the sensor of oxygen availability. The basis for this proposal was the observation that the dormancy (DosR) regulon of ***M. tuberculosis*** was induced as a result of hypoxia or low-dose NO treatment, suggesting a common signal transduction for both. Similar proposals had previously been based on studies on paralogous oxidases in yeast (Kwast ***et***

al., 1999) and *Rhodobacter sphaeroides* (Oh and Kaplan, 2000), both of which demonstrated the involvement of cytochrome oxidase in oxygen-sensing and signaling for hypoxia-induced genes. Therefore it was proposed in the current study that cytochrome aa_3 mutants would help to investigate whether a similar mechanism exists in *M. smegmatis*.

3.2.1 Construction of a cytochrome bc_1 mutant of *M. smegmatis*

Initially the *qcrCAB*-encoded cytochrome bc_1 was targeted for disruption by allelic exchange mutagenesis. The hypothesis was that disruption of this complex would block electron flow to the major terminal oxidase, cytochrome aa_3, and therefore have a severe impact on the growth of the organism under aerobic conditions. Electroporation of pQCRMSKO into *M. smegmatis* mc^2155 gave rise to 3 blue colonies (potential single crossovers, SCOs). The clones were analyzed by Southern blot and 2 were confirmed to be SCOs (Figure 7), one resulting from a recombination event upstream of *qcrCAB* and the other one from a downstream recombination event. This confirmed that in both clones the knockout vector had been site-specifically integrated at the *qcrCAB* locus of *M. smegmatis*.

SCO 1 (downstream) was subjected to a counter-selection against the *sacB* gene to identify the product of a second recombination event in which the intervening vector sequence was eliminated from the merodiploid strain to produce a DCO recombinant. Counter selection by plating on sucrose yielded a total of 5 white, Hyg^R, Suc^R, Kan^S colonies that were potential double crossovers (DCOs). Interestingly, these colonies did not emerge at the same time, and they generally took much longer than the usual time (about 3-5 days) to emerge as compared to wild type *M. smegmatis*. The first colony became visible after ±8 days, whereas the other 4 emerged after approximately 14 days from the date of plating. All 5 of the DCOs looked morphologically different from *M. smegmatis* wild type colonies, displaying a glossier and smoother appearance compared to the usual rough surface morphology of the wild type strain.

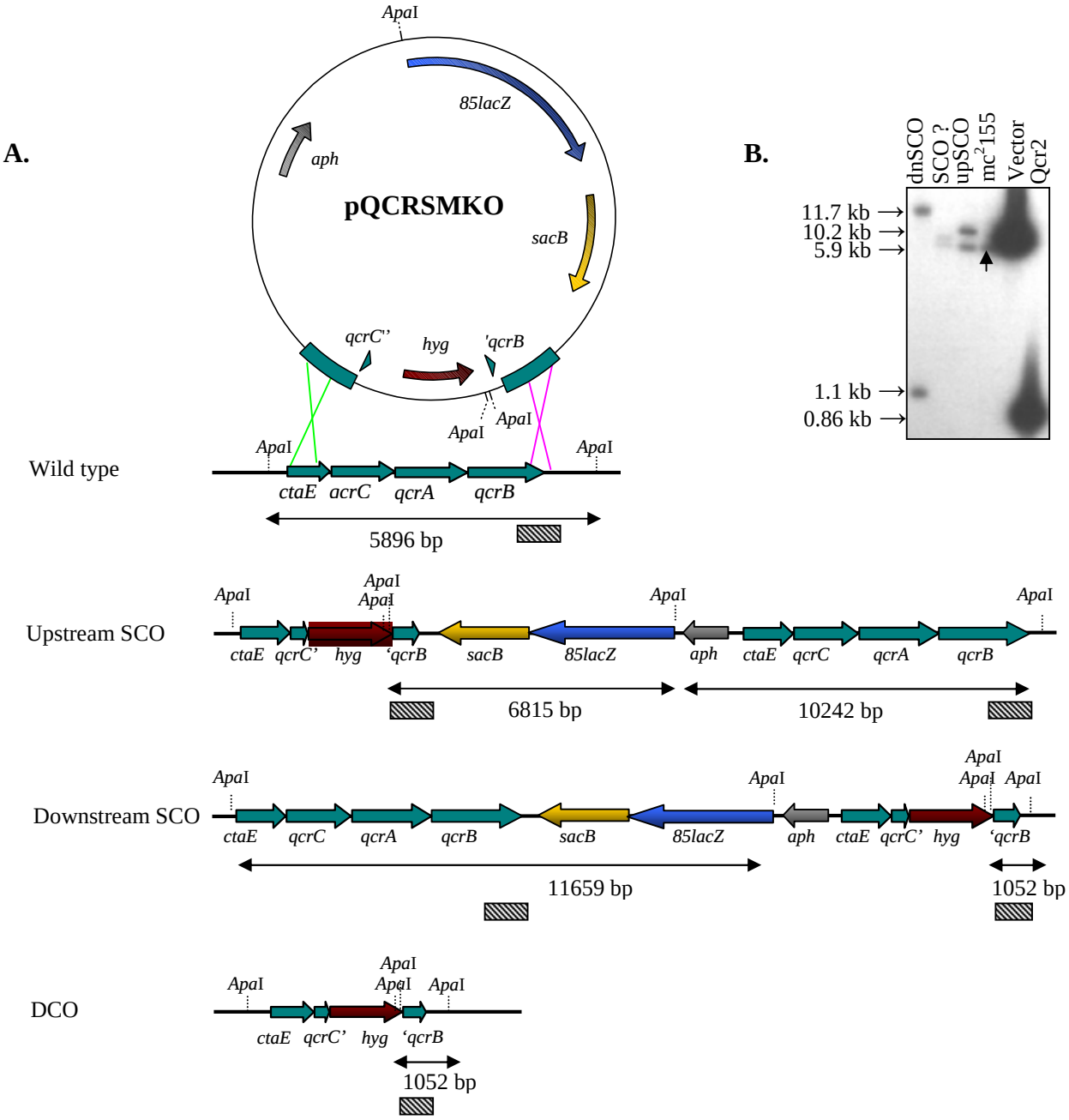

Figure 7. Site-specific integration of the *M. smegmatis qcrCAB* knockout vector, pQCRSMKO, in the chromosome. **(A)** A diagrammatic illustration of recombination at the *qcrCAB* locus (not drawn to scale). Recombination either upstream (light-green cross) or downstream (pink cross) of the operon results in integration of the entire vector into the chromosome, producing upstream or downstream SCO mutant strains, respectively. A subsequent crossover event on the opposite side of the operon in either SCO would result in loss of the intervening vector sequence, producing a DCO. Double headed arrows indicate *Apa*I fragments that would cross-hybridize to the 863-bp downstream PCR product, dnQcr (hatched box) in a Southern blot. **(B)** Southern blot analysis of *Apa*I-digested genomic DNA from the three SCOs obtained from electroporation of pQCRSMKO into *M. smegmatis* mc^{2}155, hybridized to Qcr2. SCO1 (lane 1; bands 11.7 and 1.1 kb) and SCO3 (lane 3; bands 10.2 and 6.8 kb) were confirmed to be downstream and upstream SCOs, respectively, based on the *ApaI* fragments obtained. The genotype of SCO2 (lane 2) could not be confirmed. The wild type band is slightly masked by leakage from the control band and is indicated by an arrow.

Genotypic analysis of the DCO mutants

The 5 white colonies (potential DCOs) were grown up and characterized genotypically by Southern blot analysis. On the wild type *M. smegmatis* chromosome, the *qcrCAB* operon is flanked on both sides by *Apa*I restriction sites, enclosing the genes on a 5896 bp *Apa*I fragment. Two more *Apa*I sites were introduced into the mutant allele by insertion of a *hyg* cassette at the deletion site within *qcrCAB* (Figures 7A and 8A). Therefore digestion of the genomic DNA with this enzyme would be expected to yield a 5896 bp fragment from the wild type, and 3012 bp, 1052 bp and 57 bp fragments in the mutant, at this locus. *Apa*I-digested chromosomal DNA from the 5 candidate *qcrCAB* mutant (referred to from here on as Δ*qcrCAB*::*hyg*) clones was hybridized with the 878 bp upstream PCR product (upQcr) used in the construction of the knockout vector. The results confirmed site-specific replacement of the wild type *qcrCAB* allele with the mutant allele, Δ*qcrCAB*::*hyg*, in all the 5 clones (Figure 8B). To validate the results, the blot was stripped of the bound probe and then hybridized with the downstream PCR product, dnQcr. The results of this analysis were consistent with those of the first Southern blot (Figure 8C).

3.2.2 Targeted knockout of cytochrome aa_3 oxidase subunit I of *M. smegmatis*

Based on the high degree of similarity of the mycobacterial cytochrome bc_1-aa_3 pathway to that of the closely related and better studied *C. glutamicum*, it was proposed that a knockout of the terminal oxidase, cytochrome aa_3 would have a similar effect as a Δ*qcrCAB*::*hyg* mutant, on the growth of *M. smegmatis* as was the case in *C. glutamicum*, in which both Δ*qcrCAB* and Δ*ctaD* mutants were growth impaired (Niebisch and Bott, 2001; Bott and Niebisch, 2003). In an effort to generate additional tools with which to probe the function of this pathway, the genes encoding the major subunit of cytochrome aa_3 (subunit I, encoded by *ctaD*) were also targeted for disruption. Together with the *ctaC*-encoded subunit II, the CtaD subunit is believed to form the functional core of the enzyme, bearing all the redox centers. Subunit I of cytochrome aa_3 contains the heme a_3-Cu_B binuclear site where binding and reduction of oxygen occurs, whereas the unique

Cu_A of subunit II provides the primary electron entry point into the enzyme (Hansford, 2001; Wikström, 2002).

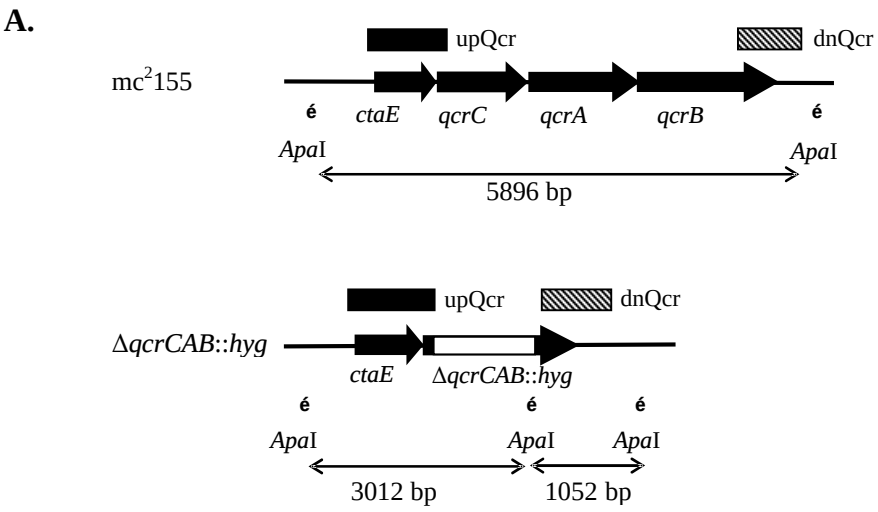

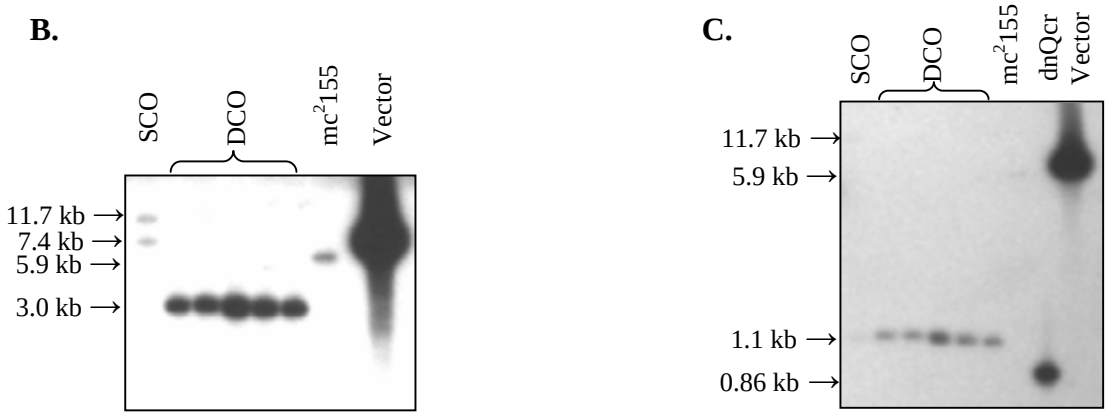

Figure 8. Allelic replacement of *M. smegmatis qcrCAB* with the mutant Δ*qcrCAB*::*hyg*. **(A)** Schematic representation of the wild type (top) and mutant (bottom) alleles, not drawn to scale. An internal deletion (3472 bp) that removed the whole of *qcrA*, most of the 3' end of *qcrC* and 5' end of *qcrB* (black arrows) was replaced by the inserted *hyg* marker (white block). Locations of the probes used for genotypic characterization of the mutants are shown by the black (upQcr) and hatched (dnQcr) boxes above the maps. Chromosomal DNA from an upstream SCO (Figure 7), five double crossovers (DCO) and parental wild type (mc^2155) was digested with *Apa*I and hybridized with upQcr **(B)** or dnQcr **(C)**.

Targeted knockout of ctaDI *in* M. smegmatis *mc²155*

As described above (section 3.1), genome sequence analysis of ***M. smegmatis*** mc²155 revealed presence of two distinct ***ctaD*** homologues, ***ctaDI*** and ***ctaDII,*** in this strain, one of which (***ctaDI***) exists on the duplicated region of the chromosome. Based on the percentage identity to the ***M. tuberculosis ctaD*** and on the similarity in their chromosomal context, ***M. smegmatis ctaDI*** was proposed to be the principal ***ctaD*** allele encoding subunit I of cytochrome aa_3, and therefore was initially targeted for disruption. Specific PCR primer sets were designed to clone knockout substrates for allelic exchange mutagenesis of this ***M. smegmatis ctaD*** homologue. Construction of the knockout vector, pCTADISMKO, was carried out as described earlier. The same principle of homologous recombination illustrated in Figure 7A applies to all the knockout mutants constructed in this study. Electroporation of pCTADISMKO into ***M. smegmatis*** mc²155 yielded 1 SCO, which upon counter-selection against the ***sacB*** gene, gave rise to 2 DCOs. Southern blot analysis of these DCOs confirmed site-specific integration of the vector at the ***ctaDI*** locus, as well as duplication of this gene in ***M. smegmatis*** mc²155 (Figure 9A).

The analysis revealed the presence, in the mutant isolates, of two cross-hybridizing bands of 4.6 and 2.6 kb in size, corresponding to the wild type (***ctaDI***) and mutant (Δ***ctaDI***::***hyg***) alleles respectively (Figure 9A). Due to the duplication of ***ctaDI***, in this mutant allelic exchange has occurred at only one of the two ***ctaDI*** loci, leaving the second locus (4.6 kb band) intact. This mutant strain, with one inactivated and one wild type ***ctaDI*** alleles, is referred to in this study as ***ctaDI***$^{+/-}$. In wild type ***M. smegmatis*** mc²155, the band intensity indicated that this band was a doublet, consistent with presence of two copies of the ***ctaDI*** gene in this strain (Figure 9A, last lane).

Although the first copy of the ***ctaDI*** gene could be readily inactivated, attempts to create a null ***ctaDI*** mutant of ***M. smegmatis*** by inactivation of the second copy in strain ***ctaDI***$^{+/-}$ were not successful. An ***aph***-marked deletion-insertion allele carried on plasmid pGEMCTADIKO was delivered into ***ctaDI***$^{+/-}$ (carrying one Δ***ctaDI***::***hyg*** allele and one wild type allele; Figure 9A), yielding 20 blue colonies (potential SCOs).

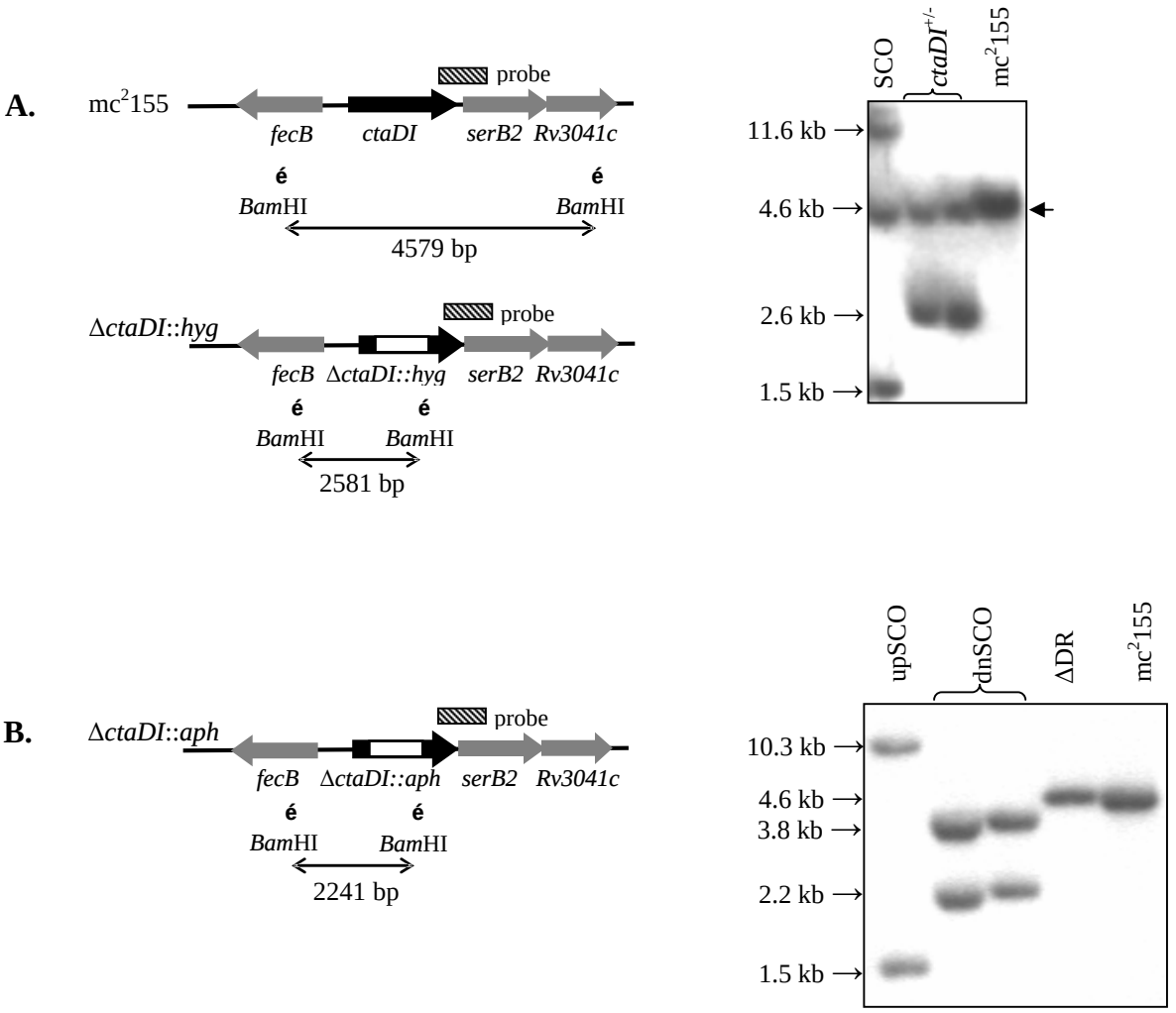

Figure 9. Genotypic analysis of *ctaDI* mutants of *M. smegmatis* mc^{2}155 and ΔDR. Each panel shows a schematic representation of the wild type and/or predicted genotypes of mutant alleles (not drawn to scale). The gene in which an internal deletion was made is denoted by a black arrow, the inserted *hyg* or *aph* marker is symbolized by a white block, and the neighboring genes are shown as grey arrows. The positions of the restriction enzymes used for Southern blot analysis (right) are indicated by vertical arrows, and the probes used are shown as hatched boxes above each map. **(A)** Knockout of one copy of *ctaDI* in mc^{2}155 to produce strain *ctaDI*$^{+/-}$ (carrying one inactivated *ctaDI* allele and one wild type allele). The arrow on the right of the blot indicates the doublet band in mc^{2}155. N. B. Equal amounts of digested genomic DNA were assayed in each lane. **(B)** SCOs obtained in an attempt to create a null *ctaDI* mutant in strain ΔDR using the *aph*-marked knockout vector, pGEMCTADIKO. The genotype of these SCOs confirms presence of only one copy of *ctaDI* in this strain, as only two instead of three (panel A) bands were obtained.

The *aph*-marked plasmid pGEMCTADIKO was used instead of the other plasmid pCTADISMKO (*hyg*-marked), used for knockout of the first *ctaDI* copy in mc^{2}155, to avoid recombination between the *hyg* sequence in pCTADISMKO and that at the Δ*ctaDI*::*hyg* locus of strain *ctaDI*$^{+/-}$. Sixteen of the 20 blue colonies were genotyped and 3 were confirmed to be site-specific SCOs, 2 upstream and 1 downstream of the wild type *ctaDI* locus of strain *ctaDI*$^{+/-}$ (data not shown). The remaining clones were the unwanted products of futile recombination at the previously inactivated *ctaDI* locus (*ctaDI*::*hyg*) in *ctaDI*$^{+/-}$. Both up- and downstream SCOs were subjected to *sacB* counter-selection on sucrose, but none of them yielded the desired DCOs. Candidate DCOs were found to be a mixture of futile recombinants and spontaneous *sacB* mutants as assessed by Southern blot analysis (data not shown). Because of the differences in the sizes of the *hyg* and *aph* cassettes used in the knockout vectors as well as the restriction sites available in each, Southern blot analysis enabled differentiation between recombinants at either site by the sizes of bands obtained, making it easier to distinguish desired crosses from the unwanted crosses.

Attempts to create a null ctaDI *mutant in* M. smegmatis Δ*DR*

To try and overcome the complication of unwanted crosses presented by the presence of two *ctaDI* loci, the *M. smegmatis* strain, ΔDR, which is a derivative of mc^{2}155 that has lost the 56-kb genome duplications (D.F. Warner & V. Mizrahi, unpublished), was used as the host strain for *ctaDI* gene knockout. Since the *ctaDI* gene is located within the genome duplication, the ΔDR strain carries only one copy of this gene. Numerous blue colonies were obtained from electroporation of ΔDR with the knockout vector, pGEMCTADIKO, and 16 of these colonies were genotyped by Southern blot analysis. Of the 16 blue colonies, 8 were found to be upstream SCOs and 5 were downstream SCOs. The genotype of the remaining 3 could not be identified (data not shown), suggesting that they may have resulted from rearrangement of the integrated suicide vector. Southern blot analysis of the site-specific SCOs revealed the presence of only one chromosomal copy of the *ctaDI* gene (2 cross-hybridizing bands in Figure 9B, lanes 1-3), thus providing independent support for the conclusion that ΔDR had lost one of the 56-kb genome duplications present in mc^{2}155 (3 cross-hybridizing bands in Figure 9A, lane 1).

One of each type of SCO was then subjected to *sacB* counter-selection to obtain DCOs. Approximately 425 blue colonies and only 4 white colonies were obtained from sucrose plates of the upstream SCO, and 65 blue colonies (no white colonies) from the downstream SCO. Southern blot analysis of these 4 colonies suggested that they were spontaneous *sacB* mutants and not DCOs. The failure to create a null *ctaDI* mutant of *M. smegmatis* in both *ctaDI*$^{+/-}$ and ΔDR strains suggested that the gene may be essential. Alternatively, this may suggest that the mutation has polar effects on the possibly essential *serB2* gene (Sassetti *et al*., 2003) found immediately downstream of *ctaDI*. The *serB2* gene is involved in the biosynthesis of serine. In order to explore the possibility that a null mutant of *ctaDI* could not be obtained due to polar effects on *serB2* and hence a possible serine auxotrophy of such a mutant, *sacB*-based counter-selection against upstream SCOs from both *ctaDI*$^{+/-}$ and ΔDR strains was carried out by plating on media that contained a serine supplement (100 μg/ml) in addition to sucrose. However, the presence of the serine supplement had no effect on the outcome of the counter-selection step, as no DCOs were obtained from either type of SCO recombinant.

Construction of a ctaDII *mutant of* M. smegmatis *mc*^{2}*155*

Although the *ctaDI* gene described above was proposed to be the principal allele coding for subunit I of cytochrome *aa*$_3$, the possibility that the second homologue *ctaDII* may code for the same function or another function important for the growth of *M. smegmatis* could not be excluded based on genome analysis. Therefore in an attempt to dissect the role of this alternate subunit I, the *ctaDII* gene was also targeted for disruption. Contrary to the results obtained with *ctaDI*, a Δ*ctaDII*::*hyg* mutant was readily obtained. Approximately 103 blue colonies were obtained from electroporation of plasmid pCTADIISMKO into *M. smegmatis* mc^{2}155, 8 of which were genotyped and confirmed to be upstream (2) and downstream (6) SCOs. Counter selection against a downstream SCO yielded 5 candidate DCOs all of which were confirmed by Southern blot analysis to be Δ*ctaDII*::*hyg* mutant clones (Figure 10). The mutant displayed no discernible growth phenotype, suggesting that the *ctaDII* gene is dispensable for the growth of *M. smegmatis*.

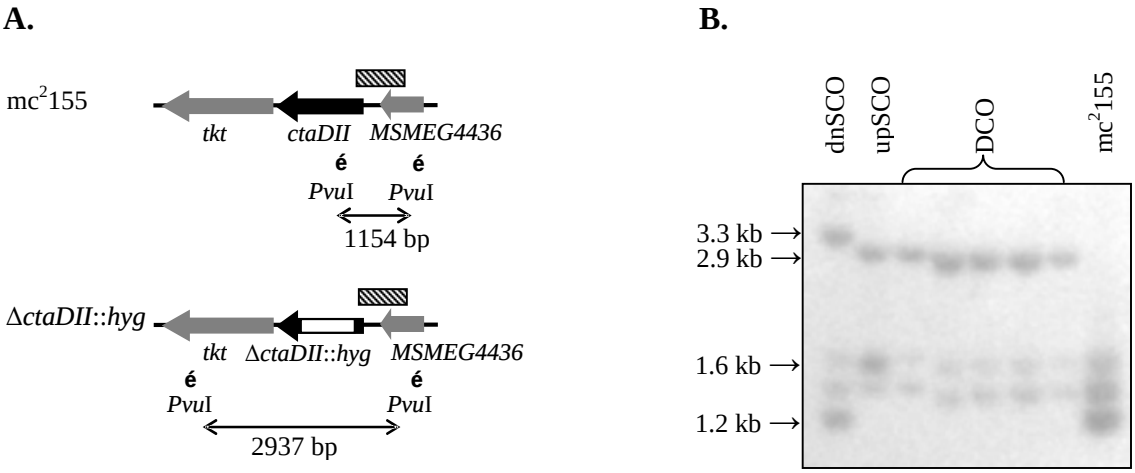

Figure 10. Allelic exchange mutagenesis of *ctaDII* in *M. smegmatis* mc^{2}155. **(A)** A schematic representation of the wild type and mutant alleles (not drawn to scale). The gene in which an internal deletion was made is denoted by a black arrow, the inserted *hyg* marker is symbolized by a white block, and the neighboring genes are shown as grey arrows. The positions of the restriction enzyme, *Pvu*I, used for Southern blot analysis **(B)** are indicated by vertical arrows. The location of the probe, upD2 (upstream PCR product used in the construction of the knockout vector, pCTADIISMKO), is shown as hatched boxes above each map. N.B. The two bands (1.6 and 1.3 kb) present in all the lanes are due to a partial digestion with *Pvu*I. The clones were independently confirmed in another Southern blot using *Nru*I (data not shown).

3.2.3 Construction of a *M. smegmatis* cytochrome aa_3 knockout mutant lacking subunit II (CtaC)

Given the difficulties in inactivating the *ctaDI* gene, an alternative strategy was used to disrupt the aa_3-type cytochrome *c* oxidase of *M. smegmatis*, which involved knockout of the *ctaC* gene, which encodes subunit II of this enzyme. A similar experimental approach as was used for allelic exchange mutagenesis of the *qcrCAB* and *ctaD* genes was employed to construct a *hyg*-marked *ctaC* mutant using the knockout vector, pCTACSMKO (Table 2). Both up- and downstream SCOs were obtained from electroporation of the vector into *M. smegmatis* mc^{2}155 (Figure 11). Sucrose selection from a downstream SCO yielded 10 potential DCOs, only 2 of which showed the correct phenotype (white, Hyg^R, Suc^R and Kan^S). These 2 candidate clones were confirmed by Southern blot analysis to be Δ*ctaC*::*hyg* mutants (Figure 11).

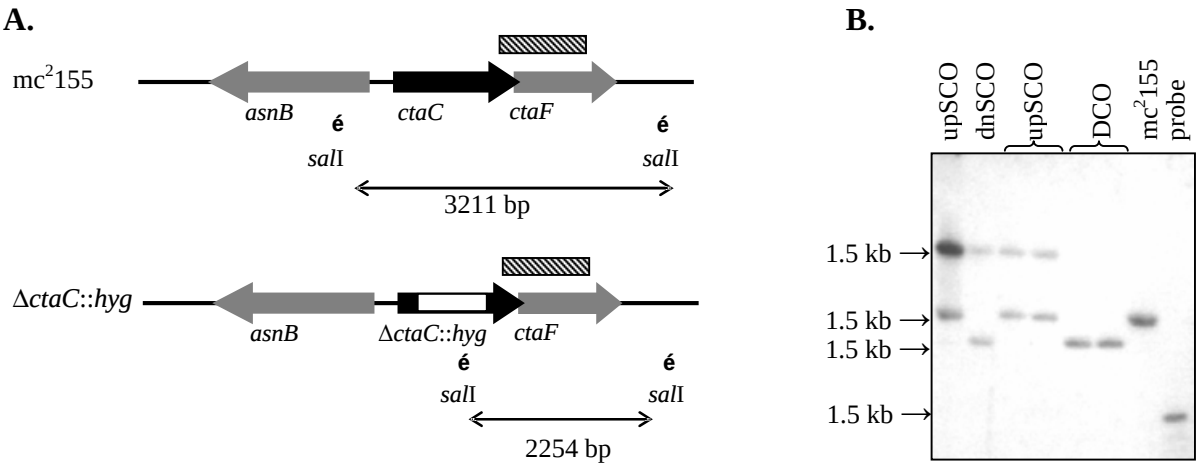

Figure 11. Construction of a *ctaC* deletion mutant of *M. smegmatis*. **(A)** A schematic representation of the wild type and mutant *ctaC* alleles, not drawn to scale. A deletion in the wild type gene (top; black arrow) was replaced by insertion of a *hyg* marker cassette (bottom; white block). Locations of the enzyme and probe (hatched box) used for Southern blot analysis are shown on the map. **(B)** Genotypic confirmation of mutants by Southern blot analysis. *Sal*I-digested chromosomal DNA from up- and downstream single crossover recombinants (upSCO and dnSCO, respectively), double crossover (DCO) mutants and the parental wild type (mc^2155) was hybridized to a 1.1 kb downstream PCR product (dnCtaC) used in the construction of the knockout vector.

3.2.4 Targeted knockout of genes in the cytochrome bc_1-aa_3 respiratory pathway in *M. tuberculosis*

The above results have demonstrated that the *M. smegmatis* cytochrome bc_1 complex and cytochrome *c* oxidase can be inactivated. Therefore, the ultimate goal was to generate equivalent mutants in *M. tuberculosis* and use these to probe the function of this pathway and its possible role in *M. tuberculosis* pathogenesis. Previous attempts to create a *qcrCAB* deletion mutant of *M. tuberculosis* in an independent study had failed. Although SCO recombinants on both sides of the locus were obtained, no DCOs were recovered following counter-selection against an upstream SCO (Matsoso *et al*., 2005). To increase the likelihood of identifying potentially growth-impaired mutants in this pathway, the *ctaC*-encoded subunit II of *M. tuberculosis* cytochrome *c* oxidase was targeted for allelic exchange mutagenesis.

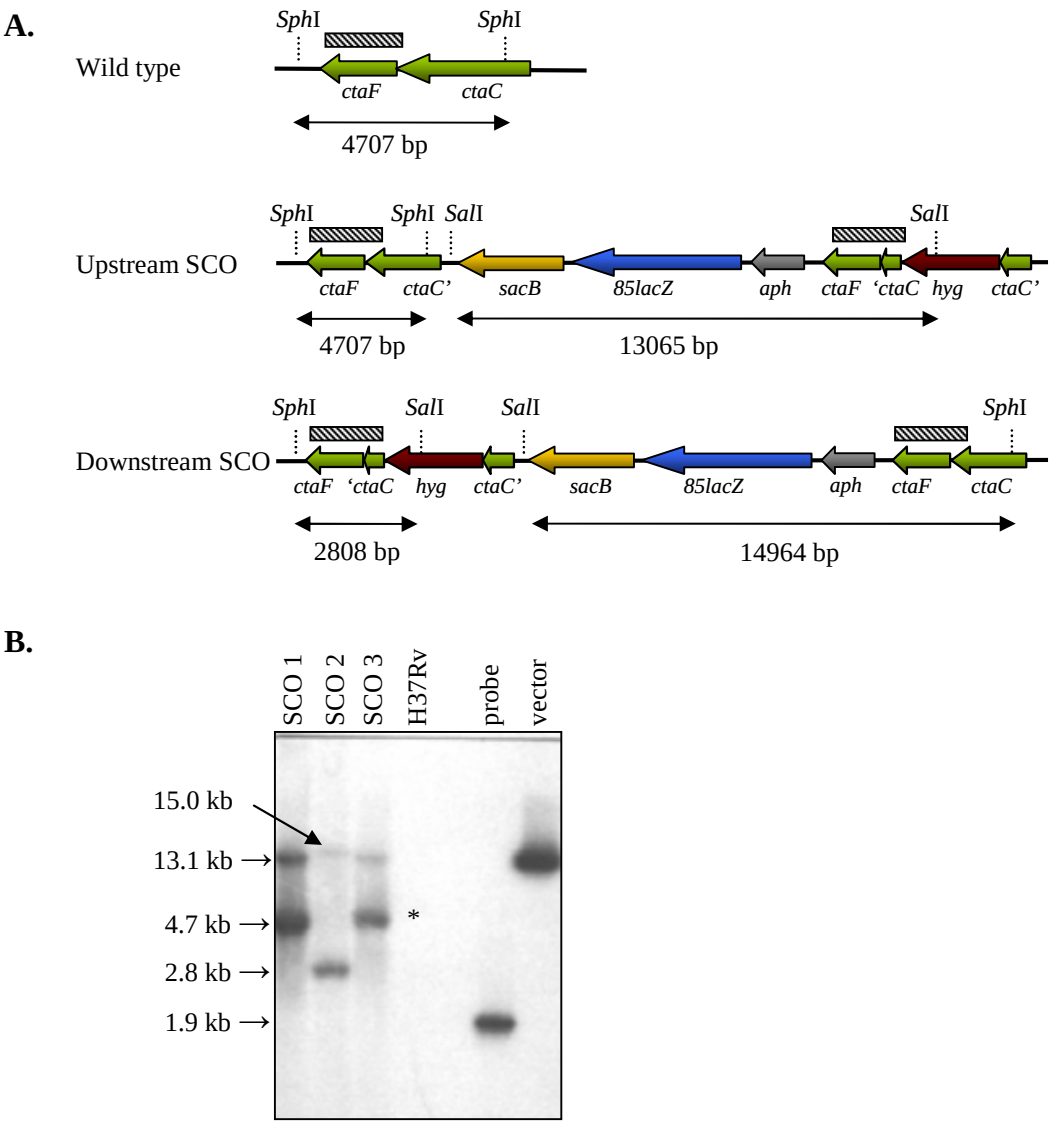

Figure 12. Targeted knockout of cytochrome *c* oxidase subunit II (encoded by *ctaC*) in *M. tuberculosis* H37Rv. **(A)** A schematic representation of the wild type *ctaC* allele on the chromosome (top), and the two types of single crossovers (SCO) (bottom) resulting from homologous recombination of the knockout vector, pQCRTBKO, upstream or downstream of *ctaC* , respectively. Shown on the maps are locations of restriction enzymes and probe (hatched box) used in Southern blot analysis. **(B)** Genotypic characterization of SCO by Southern blot analysis. Chromosomal DNA from three SCOs (SCO 1-3) and wild type (H37Rv) was digested with *Sal*I and *Sph*I, and hybridized to a 1.9 kb downstream PCR product (probe) used in the knockout construct (vector). N.B Due to a very weak signal, the wild type band (*) was not visible on the scan.

Following electroporation of the knockout vector, pQCRTBKO (Table 2), into ***M. tuberculosis*** H37Rv, approx 328 potential SCOs were obtained, and 3 of them were genotyped using Southern blot analysis. Two were confirmed to be upstream SCOs whereas the third one was a downstream SCO (Figure 12). All 3 SCOs were subjected to counter-selection on plates containing sucrose and Hyg, and plates were incubated at 37°C for more than twice the normal length of time (54 vs 21 days). However, no DCOs were recovered; all clones obtained from upstream (25/25) and downstream SCOs (40/40) were Km^R, suggesting that they were all spontaneous ***sacB*** mutants.

3.3 Phenotypic analysis of *M. smegmatis* cytochrome bc_1 and aa_3 mutants

3.3.1 Δ*qcrCAB*::*hyg* and Δ*ctaC*::*hyg* mutants are attenuated for growth

To ascertain whether the loss of cytochrome bc_1 or aa_3 complexes affected the growth of *M. smegmatis*, the bc_1-aa_3 pathway mutants (Δ*qcrCAB*::*hyg* and Δ*ctaC*::*hyg*) and their parental wild type strain (mc^2155) were grown as liquid cultures in MADC-Tw under aerobic conditions on a rotary shaker (350 rpm, 37°C). Growth was assessed by monitoring the optical density of the culture at 600 nm. The Δ*qcrCAB*::*hyg* (Figure 13A and B) and Δ*ctaC*::*hyg* (Figure 13B) mutants both showed growth impairment under these conditions, with a more than two-fold decrease in the growth rate compared to their parental wild type. The growth defect was exacerbated on solid medium, with pin-prick colonies taking a minimum of 6 days (Figure 13D). In a separate experiment, 2 of the 5 different isolates of Δ*qcrCAB*::*hyg* (Figure 8B) were grown independently alongside the wild type to ensure that the phenotype observed was consistent in both isolates (Figure 13A). Both Δ*qcrCAB*::*hyg* isolates tracked one another closely through all stages of growth, demonstrating that the growth defect observed was indeed a result of the *qcrCAB* mutation, and clone 2 was selected for further experiments.

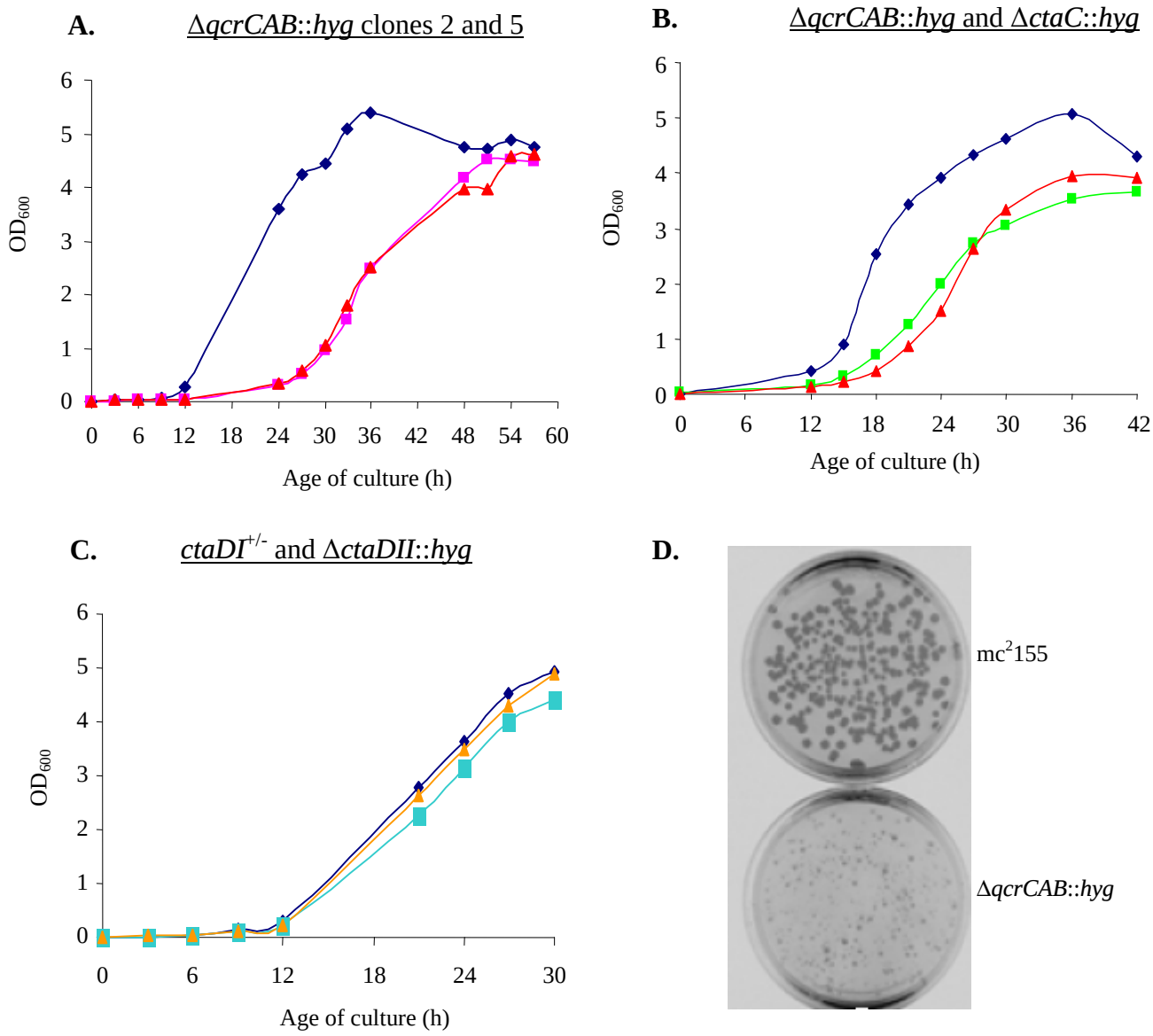

Figure 13. Growth of cytochrome bc_1 and aa_3 mutants of *M. smegmatis* under aerobic conditions. (A to C) Growth in liquid medium. Strains were grown at 37°C in shaking flasks (350 rpm) in MADC-Tw medium and growth was followed by monitoring the absorbance at 600 nm (OD_{600}). Δ*qcrCAB*::*hyg* clones 2 (▲) and 5 (■); Δ*ctaC*::*hyg* (■); *ctaDI*$^{+/-}$ (■); *ctaDII*::*hyg* (▲); wild type mc^{2}155 (♦). Initially two independent Δ*qcrCAB*::*hyg* isolates were analyzed to ensure that the phenotype was indeed a result of the mutation (**A**). Subsequently growth of Δ*ctaC*::*hyg* is compared to that of Δ*qcrCAB*::*hyg* and their parental wild type (**B**). The growth curves are representative of at least two independent experiments. (**C**) Growth of the single *ctaD* mutants (*ctaDI*$^{+/-}$ and *ctaDII*::*hyg*) was also compared to that of the wild type. (**D**) Growth of Δ*qcrCAB*::*hyg* on solid medium. Strains were grown oxystatically (21% air saturation) in MADC-Tw in a New Brunswick Scientific Bioflow 110 fermentor and aliquots were withdrawn and plated on LA. Plates were incubated at 37°C for 3 d (wild type) or 6-8 d (mutant).

In contrast, growth of the *ctaDI* single mutant (*ctaDI*$^{+/-}$) and the *ctaDII* mutant (Δ*ctaDII*::*hyg*) was found to be indistinguishable from that of the wild type as already mentioned above (Figure 13C). Nonetheless, this observation was not unexpected as both mutants still have a functional copy of *ctaDI*, implying that they were still able to synthesize a functional cytochrome *c* oxidase.

3.3.2 Complementation of the *M. smegmatis ctaC* mutant with *M. tuberculosis ctaC*

The *M. smegmatis ctaC* gene shows 77% identity to its *M. tuberculosis* homologue at the amino acid level, suggesting a close functional relationship between these two proteins. In order to investigate the feasibility of reversing the growth defect of the *M. smegmatis* cytochrome aa_3 mutant, Δ*ctaC*::*hyg*, a complementing vector carrying a functional *M. tuberculosis ctaCF* operon plus flanking sequence was electroporated into this mutant. Integration of the vector at the *attB* locus was confirmed by PCR analysis (Figure 14A). The resulting merodiploid strain, Δ*ctaC*::*hyg attB*::*ctaC*, was analyzed under the same conditions in which the Δ*ctaC*::*hyg* mutant strain had been shown to be attenuated in growth. Genetic complementation of Δ*ctaC*::*hyg* partially reversed the growth phenotype (Figure 14B).

3.3.3 Over-expression of cytochrome *bd* oxidase compensates for loss of the bc_1 complex

In a previous study from this laboratory, Kana *et al.* (2001) showed that *M. smegmatis* possesses a *cydAB*-encoded cytochrome *bd* oxidase which is induced under microaerobic conditions. A reporter strain that carried a *cydA*'::*lacZ* transcriptional fusion integrated at the *cyd* locus of *M. smegmatis* was analyzed oxystatically over a range of oxygen tensions to determine the dependence of *cyd* expression on air saturation. This transcriptional fusion carries a promoter-less *lacZ* gene under the control of the *cyd* promoter. *cyd* expression was found to increase two- to three-fold between 5% and 0.5% air saturation (Kana *et al*., 2001).

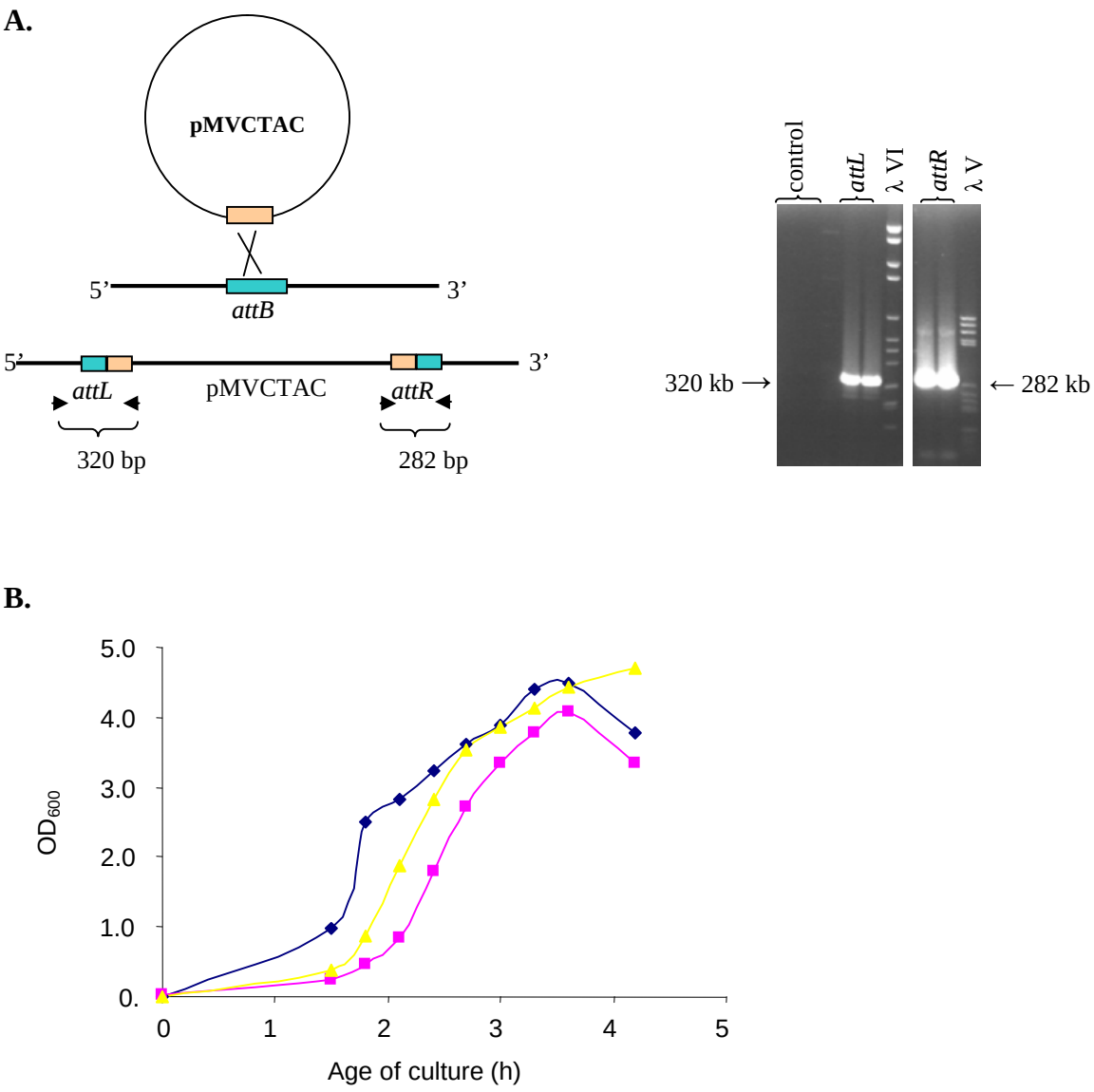

Figure 14. Complementation of *M. smegmatis ctaC* mutant with *M. tuberculosis ctaC* gene carried on pMVCTAC. **(A)** Diagrammatic illustration of the integration of the vector at the *attB* locus of *M. smegmatis* Δ*ctaC*::*hyg* mutant (left). Site-specific integration of pMVCTAC was confirmed by PCR amplification of the resulting *attL* and *attR* regions (right). Locations of primers used to amplify *attL* and *attR* are shown as black arrow heads below the map. **(B)** Growth analysis of the complemented strain, Δ*ctaC*::*hyg attB*::*ctaC*, under aerobic conditions. Strains were grown at 37°C in shaking flasks (350 rpm) in MADC-Tw medium and growth was followed by monitoring the absorbance at 600 nm (OD_{600}). ▲, Δ*ctaC*::*hyg attB*::*ctaC*; ■, Δ*ctaC*::*hyg*; ♦, wild type mc^2155.

Based on genome analysis, *M. smegmatis* contains at least three terminal oxidases – the aa_3-type cytochrome *c* oxidase demonstrated in this study as the major oxidase under aerobic conditions, cytochrome *bd* oxidase previously demonstrated to be required for microaerobic growth (Kana *et al.*, 2001), and the putative cytochrome *bd*', whose function has yet to be investigated. Having established the viability, albeit severe attenuation, of the cytochrome bc_1 and cytochrome aa_3 mutants, it was imperative to investigate the effects, on the expression of the *bd*-type quinol oxidase, of the loss of functionality in the cytochrome bc_1-aa_3 pathway under various oxygen tensions.

To determine the effect of loss of the bc_1 complex on expression of cytochrome *bd* oxidase, a similar approach as described above was adopted. A reporter strain that carries a *cydA*'::*lacZ* transcriptional fusion (Kana *et al.*, 2001), site-specifically integrated at the *cyd* locus of the *M. smegmatis* Δ*qcrCAB*::*hyg* mutant, was constructed. The reporter plasmid, pBK4, used in the analysis of *cyd* expression in wild type mc^2155 (Kana *et al.*, 2001) was electroporated into the Δ*qcrCAB*::*hyg* strain. The genotype of 7 Km^R transformants recovered from the electroporation was confirmed by Southern blot analysis (Figure 15A) and one clone was selected for further analysis.

Levels of β-galactosidase in the recombinant strain Δ*qcrCAB*::*hyg*::pBK4, were analyzed under aerobic and microaerobic conditions (21, 5 and 1% air saturation, respectively) and were compared with those observed in the control strain, mc^2155::pBK4, in which the same transcriptional fusion was integrated at the *cyd* locus of the parental wild type (Kana *et al.*, 2001). Both strains were grown oxystatically in a New Brunswick Scientific Bioflow 110 fermentor as described in section 2.2.4. For each reporter strain, at least two independent experiments were performed at each air saturation level and specific activity was determined based on four time points (samples in duplicate at each time point) per experiment.

Up-regulation of the *cyd* promoter was observed in the wild type strain under micoraerobic conditions (Figure 15B). This observation was consistent with previous results (Kana *et al.*, 2001). Importantly, a marked increase in expression of the *cyd* operon was observed in the Δ*qcrCAB*::*hyg* mutant over the air saturation range tested (1-21%). The difference in the level of *cyd* expression between the wild type and mutant strain was significant under all conditions tested ($P < 0.0001$).

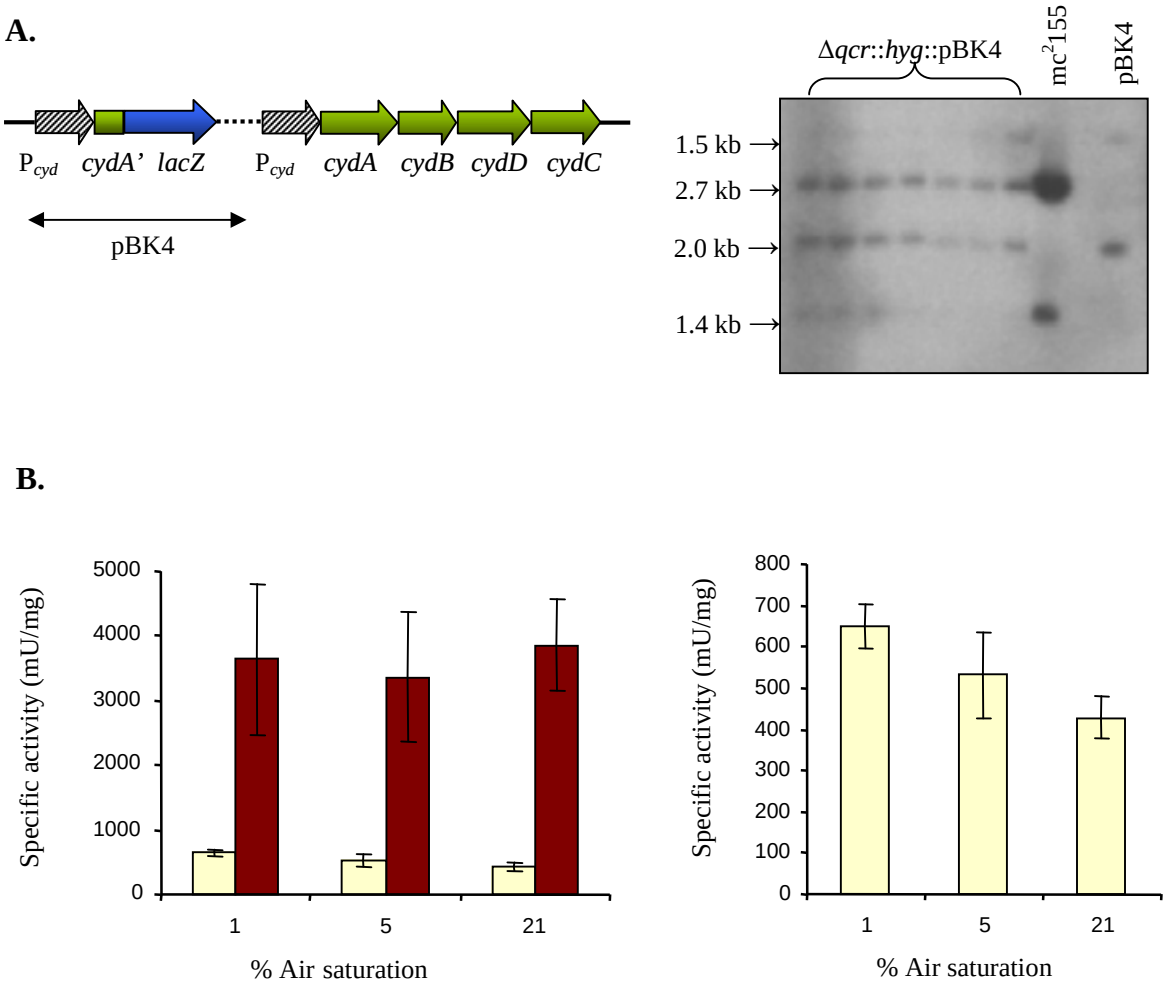

Figure 15. Effect of cytochrome bc_1 disruption on expression of the *cyd* operon in *M. smegmatis*. **(A)** Genotypic characterization of the *cyd* reporter strain, Δ*qcrCAB*::*hyg*::pBK4. Genetic organization of the *cydA-lacZ* fusion construct at the *cyd* locus of Δ*qcrCAB*::*hyg* is schematically illustrated to the left of the panel. The hatched arrows denote the putative *cyd* promoter, P_{cyd}, carried both on the reporter construct and natively on the chromosome. Southern blot analysis was carried out to confirm site-specificity of pBK4 integration into the chromosome (right). Chromosomal DNA from 7 candidate clones of Δ*qcrCAB*::*hyg*::pBK4 and mc^{2}155 was digested with *Eco*RI and *Sph*I, and then probed with a 2.6 kb *Pst*I fragment from the *cyd* locus of *M. smegmatis* mc^{2}155. **(B)** Expression analysis of the *cyd* operon in the wild type (yellow bars) and Δ*qcrCAB*::*hyg* (dark red bars) strains. The same data for wild type were plotted on a different scale (to the right of the panel). Specific activity was assessed at 21, 5 and 1% air saturation. All assays were performed in duplicate and the data shown represent the averages and SD of at least two independent experiments. Unpaired *t* tests were performed on the data to determine statistical significance ($p<0.0001$).

However, comparison of *cyd* expression levels in the mutant strain under conditions of varying O_2 availability revealed no induction under microaerobic conditions above the basal expression level observed under full aeration. These results confirm that the loss of cytochrome bc_1 resulted in constitutive over-production of the *bd*-type oxidase, and suggest that electron flow from the menaquinone pool is re-routed through the quinol oxidase pathway of the aerobic respiratory chain in this mutant.

3.3.4 Attempts to construct a cytochrome bc_1/ cyotochrome *bd* double mutant of *M. smegmatis*

Based on the compensatory over-expression of the cytochrome *bd* oxidase observed in mutants lacking the bc_1 complex (Δ*qcrCAB*::*hyg*; Figure 15) and the severe growth defect exhibited by this mutant, it was proposed that a mutant in which both the cytochrome bc_1-aa_3 and *bd* branches of the respiratory chain were blocked would be non-viable. To test this hypothesis, attempts were made to create such a double mutant. The cytochrome bc_1 mutant, Δ*qcrCAB*::*hyg*, was electroporated with the knockout vector, pCYDAKO, previously used to create a cytochrome *bd* mutant of *M. smegmatis* (Kana *et al*., 2001), and 2 SCOs were obtained. Both SCOs were confirmed to be site-specific by Southern blot analysis (data not shown), and were both passaged through sucrose selection. Despite incubating the plates for an extended period of time (20 days), no white Suc^R colonies were obtained from either SCO but only several blue colonies, suggesting that the double mutant was not viable. If this is true, it implies that the other putative cytochrome *bd* oxidase (encoded by *ythAB* homologues), if at all functional, may not be able to sustain aerobic growth of *M. smegmatis* on its own.

3.3.5 Genome expression profiling of the cytochrome bc_1 (Δ*qcrCAB*::*hyg*) and cytochrome aa_3 (Δ*ctaC*::*hyg*) mutants

To gain insight into the consequences of blockage of the cytochrome bc_1-aa_3 aerobic respiratory pathway in *M. smegmatis*, comparative expression profiling of the mutant strains was performed by DNA microarray analysis. A partial-genome microarray containing the *M. smegmatis* homologues of all *M. leprae* genes and a selection of other genes, including the homologues of *M. tuberculosis* genes not found in *M. leprae* as well

as genes which have no homologues in either *M. tuberculosis* or *M. leprae*. The subset of respiratory pathway genes included on this array is listed in Table 4. During the course of this study, a full genome oligonucleotide array became available from the Pathogen Functional Genome Resource Center (PFGRC) at TIGR (http://pfgrc.tigr.org/). The same samples as used with the partial-genome amplicon array were therefore analyzed using the whole-genome oligo array. The results obtained with both types of array are presented below. Data analysis of the three replicate arrays (partial amplicon arrays) on Δ*qcrCAB*::*hyg* mutant was carried out as described in Section 2.2.5, and subsequently confirmed by an independent analysis, which was performed by Dr. D. Powell, Victorian Bioinformatics Consortium, Australia, as described in Section 2.2.5. The results summarized in all of the tables except for Tables 8, D1 and D2 (which were produced on the basis of Dr. D. Powell's analysis) were analyzed and produced by the investigator as described in Section 2.2.5.

*Differential gene expression profiling of the Δ*qcrCAB*::*hyg *mutant of* M. smegmatis *using a partial-genome amplicon microarray*

Cultures of the mutant and wild type strains were grown oxystatically at full aeration (21% air saturation) to an OD_{600} of 0.6 and RNA was extracted. For each experiment, Cy5-labeled cDNA of the mutant was hybridized against Cy3-labeled cDNA from the wild type. The data from the biological replicates were analyzed, and the analysis was subsequently validated by Dr D. Powell. Importantly, both analysis methods produced a comparable list of differentially expressed (DE) genes. According to Powell's analysis, a total of 78 genes were found to be DE in the Δ*qcrCAB*::*hyg* mutant, 42 of which were up-regulated and 36 down-regulated. The top ranked genes with expression fold change greater than or equal to 1.8 are listed in Table 8. The complete lists of up-regulated (Table D1) and down-regulated (Table D2) genes are provided in Appendix D.

The majority of the up-regulated genes (52%) are involved in intermediary metabolism and respiration. Importantly, the presence of *cydA* in this group of DE genes was independently validated by the marked induction of *cyd* expression in the Δ*qcrCAB*::*hyg* mutant strain, as had been deduced using the *cydA*'::*lacZ* reporter assay (Figure 15). Other up-regulated genes included *uspL* and the *M. smegmatis* homolog of

MSMEG3205 (Rv1592c), which were previously shown to be induced in response to hypoxia in *M. tuberculosis* (*uspL* and Rv1592c; Sherman *et al*., 2001; Boshoff *et al*., 2004; Park *et al*., 2003) and in *M. smegmatis* (*uspL*; O'Toole *et al*; 2003a). The marked up-regulation of *mihF* in the Δ*qcrCAB*::*hyg* mutant was also notable as this gene is up-regulated in *M. smegmatis* just prior to stationary phase and may be involved in the expression of genes required for stationary phase survival (Pedulla and Hatfull, 1998). Because of the stringency of the statistical analysis applied to generate the list of DE genes shown in Tables 8, D1 and D2, some of the genes that were found to be significantly DE by my analysis were excluded on statistical grounds (data not shown). Among these excluded genes were ML2440 (*senX3*), which was significantly up-regulated in 2 of the 3 biological replicates. Since the analysis method (Powell's) used to generate the above-mentioned Tables calculated significance based on the number of replicate spots, inclusion of the third biological replicate rendered the differential expression of this gene insignificant. Similarly, some members of the DosR regulon such as *dosR*, *hspX* and *acg* were also DE on the partial-genome amplicon array based on my analysis, but failed to meet statistical requirements for inclusion on this list.

In contrast, many of the down-regulated genes (Tables 8 and D2) are involved in information pathways (transcription and DNA repair) and in cell wall and cell processes. The most highly down-regulated gene was *lytB* (MSMEG5208). This gene is involved in the non-mevalonate pathway for the biosynthesis of terpenoids (Rohdich *et al*., 2002) and its down-regulation may thus affect the biosynthesis of menaquinone in the Δ*qcrCAB*::*hyg* mutant. The principal sigma (σ) factor-encoding gene, *sigA* (Gomez *et al*., 1998), was also markedly down-regulated in the Δ*qcrCAB*::*hyg* mutant, which is significant in light of the down-regulation of *sigA* that occurs in *M. tuberculosis* during anaerobiosis (Kendall *et al*., 2004; Boshoff *et al*., 2005).

Table 8. Genes differentially expressed in aerobically grown Δ*qcrCAB*::*hyg* mutant of *M. smegmatis* (as analyzed by D. Powell)

ID[a]	Gene	TIGR annotation[b]	Function[c]	M[d]	*P* value	Class[e]
Upregulated genes						
ribA	*ribA2*	MSMEG3082	GTP cyclohydrolase II, riboflavin biosynthesis	-2.301	0.0020	7
ML2274		MSMEG3498	Probable conserved secreted protein	-1.914	0.0072	3
mihF	*mihF*	MSMEG3063	Putative integration host factor	-1.764	0.0003	2
glgC	*glgC*	MSMEG5067	glucose-1-phosphate adenyl-transferase	-1.753	0.0072	7
ML1835		MSMEG6527	CHP	-1.556	0.0030	10
ML0510		MSMEG3035	probable oxidoreductase	-1.444	0.0004	10
ML0886		MSMEG4257	possible glycosyl transferase	-1.430	0.0024	7
ML1312		MSMEG4598	CHP	-1.229	0.0001	10
argD-g	*argD*	MSMEG2446	probable acetylornithine aminotransferase	-1.027	0.0033	7
gabD-q	*gabD*	MSMEG2554	probable aldehyde dehydrogenase	-1.005	0.0052	7
Rv3134c	*uspL*	MSMEG5230	Universal stress protein	-0.990	0.0098	10
Rv1623c	*cydA*	MSMEG3243	Cytochrome *bd* oxidase subunit I	-0.931	0.0069	7
ML1926		MSMEG0828	putative tuberculin-related protein	-0.915	0.0058	3
Rv1592c		MSMEG3205	CHP	-0.878	0.0016	10
ML1783		MSMEG4344	Possible transcriptional regulatory protein	-0.849	0.0080	9
Downregulated genes						
lytB2	*lytB*	MSMEG5208	probable LytB-related protein, LytB2	3.316	0.0002	3
xseA	*xseA*	MSMEG5210	exo-deoxyribonuclease VII, large subunit	2.737	0.0003	2
ML2088-a		MSMEG4807	putative cytochrome P450	2.039	0.0004	7
ctpC-a		MSMEG5384	cadmium-translocating P-type ATPase	1.789	0.0081	3
rpoT	*sigA*	MSMEG2759	RNA polymerase sigma factor, SigA	1.513	0.0000	2
rplE	*rplE*	MSMEG1464	ribosomal protein L5	1.198	0.0002	2
ML2661-e	*fadD7*	MSMEG3702	Fatty acid CoA ligase, FadD7	1.197	0.0051	1
Fpg	*fpg*	MSMEG2417	formamidopyrimidine-DNA glycosylase	0.961	0.0078	7
ML1750		MSMEG2202	CHP	0.922	0.0098	10

[a] Gene identifier as defined in the MIAME compliance file (http://vbc.med.monash.edu.au/~powell/M.smegamtis).
[b] TIGR annotation (http://www.tigr.org/tigr-scripts/CMR2/CMRHomePage.spl).
[c] Function as per Tuberculist and Leproma (http:genolist.pasteur.fr). [d] M, log base 2 of the fold ratio
[e] Functional class as per Tuberculist: 1, Lipid metabolism; 2, Information pathways; 3, Cell wall & cell processes; 6, PE/PPE; 7, Intermediary metabolism & respiration; 9, Regulatory proteins; 10, Conserved hypothetical protein (CHP).

Differential gene expression profiling of the Δ*qcrCAB*::*hyg mutant using a whole-genome oligo array of* M. smegmatis

To obtain a broader reflection of the adaptations of ***M. smegmatis*** in response to blockage of cytochrome bc_1 complex, the same RNA samples used for the amplicon array were then analyzed using the whole-genome oligo array from TIGR, using the same method of labeling, hybridization and slide preparation as was used for the amplicon array, with only one modification. Whereas the amplicon array slides were boiled for 2 min prior to pre-hybridization (section 2.2.5), this step was skipped with the TIGR array slides as it was found to cause streaking of the spots. However, a significant number of spots were found to be missing or bad on the TIGR array and there was relatively lower spot intensity as well as higher background hybridization on these slides than on the amplicon arrays, rendering a lot of spots unusable. Two of the three biological replicates of the Δ*qcrCAB*::*hyg* mutant ***vs*** wild type were analyzed on the whole-genome array. The list of DE genes was in agreement with the results obtained from the amplicon array, with several more genes found to be DE on the whole-genome TIGR array. A list of the top 29 genes up-regulated in the mutant in both biological replicates is shown in Table 9. Of these 29 genes, 11 have previously been shown to be induced by hypoxia in ***M. tuberculosis*** (***nadA***, ***acg***, ***hspX***, ***uspL***, MSMEG5215 [Rv1738][4], MSMEG3958 [Rv3127], MSMEG5228 [Rv3129], ***tgs1*** [Rv3130c] (Sherman ***et al.***, 2001 and Park ***et al.***, 2003); MSMEG0364 [Rv0241c], MSMEG3847 [Rv1628c] (Sherman ***et al.***, 2001, supplementary data); and ***glgE*** [Rv1327c], (Park ***et al.***, 2003, supplementary data)). Seven of these hypoxically induced genes require the transcription factor DosR for induction (***acg***, ***hspX***, ***uspL***, Rv1738, Rv3127, Rv3130c (Park et al., 2003; Kendall ***et al.***, 2004); and Rv3129 (Park et al., 2003; Voskuil et al., 2004)). The eighth gene, ***dosT***, encodes an alternative sensor kinase that can autophosphorylate in response to hypoxia and subsequently activate the cognate regulator ***dosR*** in ***M. tuberculosis*** (Roberts ***et al.***, 2004). DosR-dependent hypoxia-induction of some of these genes – ***acg***, ***hspX***, ***uspL*** - and four others, ***dosR***, ***dosS***, ***uspM*** and ***uspN***, has also been reported in ***M. smegmatis*** (***hspX***, ***uspL***, (Mayuri ***et al.***, 2002 and O'Toole ***et al.***, 2003a); ***dosR***, ***dosS*** (Mayuri ***et al.***,

[4] Where gene names are not known, the MSMEG numbers and their corresponding Rv homologues are given for cross-referencing.

2002); *acg*, *uspM*, and *uspN* (O'Toole *et al*., 2003a)). Also substantiated on these arrays is the up-regulation of *cydA* in the Δ*qcrCAB*::*hyg* mutant, once again demonstrating the constitutive expression of this gene as observed in the reporter analysis and on the partial-genome amplicon microarray. Due to missing spots on all the TIGR arrays used, the up-regulation of *senX3* and *mihF* observed on the amplicon arrays could not be confirmed.

Table 9. Genes induced in aerobically grown Δ*qcrCAB*::*hyg* mutant of *M. smegmatis* as analyzed on the whole-genome microarray (TIGR)

Name	Gene	Description (as per TIGR)	LR[a]	SD[b]	Closest Rv #[c]	BLAST[d] E-value
ORFA06621		conserved hypothetical protein	6.44	0.74	Rv3127	[3e-87]
ORFA02305		alcohol dehydrogenase II	4.68	0.16	Rv1808	[0.036]
ORFA06592	*hspX*	heat shock protein, Hsp20 family	4.26	0.13	Rv2031c	[2e-46]
ORFA02970		STAS domain protein	3.22	0.07	Rv0516c	[4e-07]
ORFA10188		hypothetical protein	3.11	0.08	Rv1638	[0.52]
ORFA08628	*dosT*	GAF domain protein	3.03	0.06	Rv2027c	[1e-162]
ORFA08635	*uspL*	universal stress protein family domain protein	2.93	0.06	Rv2028c	[1e-48]
ORFA08106	*glgE*	probable glucanase GlgE	2.81	0.19	Rv1327c	[0.0]
ORFA02989		conserved hypothetical protein	2.76	0.12	Rv1111c	[0.040]
ORFA11060		hypothetical protein	2.63	0.11	Rv2228c	[0.55]
ORFA05331	*treY*	glycosyl hydrolase, family 13	2.54	0.27	Rv1563c	[1e-128]
ORFA10672		hypothetical protein	2.50	0.04	Rv0683	[2.4
ORFA08629	*tgs1*	triacyl glycerol synthase	2.32	0.06	Rv3130c	[1e-127]
ORFA08613		conserved hypothetical protein	2.30	0.00	Rv1738	[8e-04]
ORFA10419		conserved hypothetical protein	2.28	0.05	Rv1210	[0.86]
ORFA05419	*cydA*	Cytochrome BD-I oxidase subunit I	2.20	0.03	Rv1623c	[0.0]
ORFA00097	*cfp10*	10 kDa culture filtrate antigen Lhp (CFP10)	2.18	0.38	Rv3874	[5e-21]
ORFA08382	*glgC*	glucose-1-phosphate adenylyltransferase	2.17	0.04	Rv1213	[0.0]
ORFA04061		4-aminobutyrate aminotransferase	2.16	0.05	Rv3329	[6e-52]
ORFA01654	*trcR*	response regulator DrrA	2.14	0.02	Rv1033c	[9e-41]
ORFA05358	*nadA*	quinolinate synthetase complex, A subunit	1.93	0.05	Rv1594	[1e-172]
ORFA00098	*esat6*	early secretory antigen target	1.72	0.13	Rv3876	[2e-29]
ORFA08113		4-hydroxyphenylpyruvate dioxygenase C terminal	1.48	0.05	Rv1322	[7e-60]
ORFA00617		MaoC domain protein	1.44	0.01	Rv0241c	[1e-112]
ORFA09559		metallo-beta-lactamase superfamily domain	1.37	0.07	Rv0786c	[3e-55]
ORFA08638	*acg*	conserved hypothetical protein	1.33	0.04	Rv2032	[2e-95]
ORFA05950	*bfrA*	Bacterioferritin	1.15	0.01	Rv1876	[3e-78]
ORFA08631		probable aminotransferase	1.15	0.00	Rv3129	[5e-30]
ORFA00682		hypothetical protein	1.09	0.05	Rv1628c	[0.87]

[a] LR, log base 2 of the fold ratio
[b] SD, standard deviation
[c,d] BLAST search results for the *M. tuberculosis* H37Rv homologues of the *M. smegmatis* genes on the TIGR array was kindly provided by Prof. N. Stoker (Royal Veterinary College, London, UK).

Table 10. Genes induced in aerobically grown Δ*ctaC*::*hyg* mutant of *M. smegmatis* (partial-genome array)

ID[a]	Gene	Function as per Leproma & TubercuList	LR[b]	SD[c]
Induced genes				
ml0886 *	*pimA*	alpha-mannosyl transferase	2.82	0.11
ML2440*	*senX3*	two-component sensor histidine kinase	2.81	0.28
ml1312*		CHP	2.33	0.52
ML0778		CHP	1.73	0.96
mihF*	*mihF*	putative host integration factor	1.66	0.48
Rv1592c*		CHP	1.64	0.16
ftsW	*ftsW*	putative cell division protein	1.61	0.19
ml0893*		probable integral membrane protein	1.56	0.37
ribA	*ribA*	probable riboflavin biosynthesis protein	1.55	0.81
Rv1623c*	*cydA*	cytochrome bd oxidase subunit I	1.48	0.44
polA-a	*polA*	DNA polymerase	1.46	0.27
ml1103-b		probable oxidoreductase	1.45	0.47
ML1030		CHP	1.28	0.36
ML2010*		CHP	1.26	0.10
thrC		probable threonine synthase	1.25	0.10
ml2137		CHP	1.24	0.10
ML2568		possible transcriptional regulatory protein (TetR family)	1.23	0.10
ML1165		CHP	1.23	0.26
yrbE1-b		conserved hypothetical integral membrane protein	1.21	0.36
ml0596-a*	*csd*	probable cysteine desulfurase	1.19	0.28
ML1391*		CHP	1.19	0.09
Rv1622c	*cydB*	cytochrome bd oxidase subunit II	1.14	0.33
ml0759	*fbiA*	probable F420 biosynthesis protein	1.13	0.13
ml1835		CHP	1.11	0.13
PPE-b*	*PPE68*	PPE family domain	1.11	0.10
ml1714		CHP	1.10	0.07
ML0271		possible conserved transmembrane protein	1.07	0.18
pstA1	*pstA1*	phosphate-transport integral membrane ABC transporter	1.01	0.32
ml2631-c		CHP	1.00	0.14
ML0158		34 kDa antigen	0.97	0.06
menD	*menD*	bifunctional menaquinone biosynthesis protein	0.94	0.13
Rv3134c*	*uspL*	universal stress protein	0.93	0.16
glnA2-e	*glnA2*	probable glutamine synthetase	0.91	0.21
Rv2028c*	*uspL*	universal stress protein	0.89	0.04
rhlE-a	*rhlE*	probable ATP-dependent RNA helicase	0.82	0.14
Repressed genes				
rnpA*	*rnpA*	ribonuclease P protein	-4.50	1.12
rplE		ribosomal protein L5	-1.63	0.78
gabD-k	*gabD*	probable aldehyde dehydrogenase	-1.42	0.18
argD-a	*argD*	probable acetylornithine aminotransferase	-1.16	0.33
ML2609		CHP	-1.08	0.08
ML1115	*lprB*	possible lipoprotein	-1.05	0.14
rpsC	*rpsC*	ribosomal protein S3	-1.02	0.12

* DE in all three biological replicates, whereas the rest of the genes are DE in at least two of the three replicates

[a] Gene identifier as defined in the MIAME compliance file (http://vbc.med.monash.edu.au/~powell/M.smegamtis).

[b] LR, log base 2 of the fold ratio. [c] SD, standard deviation

Transcriptome analysis of the cytochrome aa_3 mutant using the amplicon array

Comparative expression profiling of aerobically grown Δ*ctaC*::*hyg* mutant and its parental wild type was carried out using the partial-genome amplicon array. As was observed for the Δ*qcrCAB*::*hyg* mutant, this analysis also revealed a significant up-regulation of the *cydAB* genes in the Δ*ctaC*::*hyg* mutant strain, demonstrating that blockage of the cytochrome bc_1-aa_3 pathway at either complex generates a common signal that results in up-regulation of *cydAB.* This induction was accompanied by an even more profound up-regulation of *senX3* (ML2440) in all the three biological replicates (Table 10). In general, a comparable list of DE genes was obtained for both the Δ*qcrCAB*::*hyg* and Δ*ctaC*::*hyg* mutants, with a few exceptions. Among the common DE genes in the two mutant strains was *mihF*, which was previously shown to be required for stationary phase survival and viability of *M. smegmatis* (Pedulla *et al*., 1998). Also observed in both mutants (Tables 10, and D1 [Appendix D]) was an induction of PPE2, a *dosR*-dependent gene previously reported to be induced in standing cultures of *M. tuberculosis* (Kendall *et al*., 2004). Interestingly the most highly down-regulated gene in the Δ*qcrCAB*::*hyg* mutant, *lytB2*, was not DE in the *DctaC::hyg* mutant. As mentioned earlier, this gene is involved in the synthesis of menaquinone, and its down-regulation in the Δ*qcrCAB*::*hyg* mutant but not Δ*ctaC*::*hyg* mutant may highlight the different effects, on the quinone pool, of electron backup at different points along the cytochrome bc_1-aa_3 pathway.

3.3.6 Effects of chlorpromazine on the transcriptomes of the bc_1 and aa_3 mutants

Analysis by DNA microarray

The phenothiazine, chlorpromazine (CPZ), has previously been shown to act on the respiratory chain of *M. tuberculosis* (Boshoff *et al*., 2004; Weinstein *et al*., 2005), by inhibiting the activity of the *ndh*- and *ndhA*-encoded type II NADH dehydrogenases (Weinstein *et al*., 2005). To investigate the effects of altering the redox state of the menaquinone pool on gene expression in the bc_1-aa_3 pathway mutants, the Δ*qcrCAB*::*hyg* and Δ*ctaC*::*hyg* mutants were treated for 1 h with 50 μg/ml of CPZ before harvesting for RNA extraction. This concentration of drug was chosen based on the observation that the

growth of *M. smegmatis* is inhibited by CPZ in a dose-dependent manner, with a minimum inhibitory concentration (MIC) of 9.23 μg/ml, whereas four-fold this concentration (35.5 μg/ml) completely inhibited growth over 48 h (H. Rubin and E. D. Weinstein *et al*, unpublished). Therefore, it was proposed in this study that treating *M. smegmatis* with a higher dose (50 μg/ml) of the drug for a shorter period of time (1 h) would be enough to disrupt the flow of electrons from NADH into the menaquinone pool, without killing the organism. The effects of this treatment on gene expression in the mutant strain were analyzed by comparative gene expression profiling of the CPZ-treated culture against an untreated control using the partial-genome amplicon array. Cy5-labeled cDNA from the CPZ-treated mutant strain was co-hybridized with Cy3-labeled cDNA from the untreated mutant control. Among the genes whose expression was significantly up-regulated by CPZ in the Δ*qcrCAB*::*hyg* mutant were *cydA*, *cydB* and *senX3*, suggesting that the signal leading to up-regulation of these genes, all three of which were already up-regulated in the untreated mutant strain, was intensified by CPZ treatment (Table 11 and Appendix D, Table D3).

Interestingly, three *M. smegmatis* homologs of *M. tuberculosis* genes previously shown to be part of the DosR regulon (*uspL*, *acg*, *dosS*) and two others shown to be DosR-regulated in *M. smegmatis* (*uspM* and *uspN*; Table 12), as well as other *M. smegmatis* homologues of *M. tuberculosis* hypoxia-induced genes (*groEL*, *gltA2*) were down-regulated in response to CPZ. These data support the hypothesis that blockage of electron flow upstream of the menaquinone pool affected the signal that led to the modest over-expression of these genes observed in the untreated bc_1 mutant. Another gene whose expression was negatively affected in the Δ*qcrCAB*::*hyg* mutant by CPZ treatment was *mihF*. In addition to the genes mentioned above, a large number of genes encoding ribosomal proteins and others involved at various levels of gene expression (such as *rpoA*, *tsf*, *infA*;) are also down-regulated in response to CPZ, suggesting that growth and hence metabolic activity of the organism is significantly reduced (Tables 12 and 13).

Table 11. Genes up-regulated in response to CPZ in the Δ*qcrCAB*::*hyg* mutant (partial-genome array)

ID	Gene	Function (as per Leproma & TubercuList)	LR	SD
ML0778*		CHP	4.49	0.70
gabD-q	*aldA*	probable aldehyde dehydrogenase (NAD-dependent)	4.44	0.51
ML1030*		CHP	3.53	0.68
metH*	*metH*	methionine synthase	3.19	1.07
xseB	*xseB*	probable exodeoxyribonuclease VII, large subunit	3.16	0.74
aroE	*aroE*	probable shikimate 5-dehydrogenase	3.04	0.51
ml0798*		CHP	2.71	0.64
pbpB	*pbpB*	probable penicillin-binding membrane protein	2.67	1.27
tpi-a	*tpi*	probable triosephosphate isomerase	2.60	0.11
nrdF*	*nrdF*	ribonucleoside-diphosphate reductase beta chain	2.58	0.29
ML0956		putative integral membrane protein	2.53	0.43
ribA*	*ribA2*	probable riboflavin biosynthesis protein	2.47	0.29
glnA2-a*	*glnA2*	probable glutamine synthetase	2.44	0.24
fdxA*	*fdxA*	probable ferredoxin	2.44	0.12
Rv1623c*	*cydA*	cytochrome bd oxidase subunit I	2.33	0.64
htpX	*htpX*	probable protease transmembrane protein	2.24	0.41
metS*	*metS*	methionine synthase	2.17	0.32
clpB	*clpB*	probable endopeptidase ATP-binding protein	2.09	0.16
ml1312*		CHP	2.05	0.43
ML1254		CHP	2.04	0.20
ML2691		CHP	2.04	0.13
menG*	*menG*	demethylmenaquinone methyl transferase	2.00	0.61
ml1328-b	*paf*	probable proteasome associated factor	1.98	0.21
ML0904*		CHP	1.93	0.46
ml0594		CHP	1.89	0.18
hisB	*hisB*	probable imidazole glycerol-phosphate dehydrogenase	1.88	0.19
pgsA-b*	*pgsA*	probable diacylglycerol phosphatidyl transferase	1.87	0.43
fabG4*	*fabG4*	probable oxoacyl-(acyl carrier protein) reductase	1.85	0.15
ml2661-d	*fadD7*	probable fatty acid CoA ligase	1.85	0.05
ML0335*		CHP	1.77	0.50
ML2440	*senX3*	two-component sensor histidine kinase	1.73	0.27
ml0818*		CHP	1.71	0.59
ml2435		CHP	1.70	0.20
ML0079		probable phosphoglycerate mutase	1.70	0.15
ml2550-b		CHP	1.68	0.26
Rv1592c*		CHP	1.67	0.33
ML0322*	*ispF*	methyl erythritol cyclodiphospahte synthase	1.67	0.47
ml0886		possible glycosyl transferase	1.66	0.20
thrB*	*thrB*	probable homoserine kinase	1.65	0.25
ml2272	*pimB*	Mannosyltransferase	1.64	0.32
ML1367		putative initiation inhibitor	1.62	0.15
glbO*	*glbO*	possible globin (oxygen-binding protein)	1.60	0.37
leuC-a	*leuC*	conserved integral membrane protein (Leu & Ala rich)	1.59	0.37
argD-g*	*argD*	probable acetylornithine aminotransferase	1.59	0.22
modD	*modD*	possibly involved in molybdate uptake	1.57	0.13
lsr2	*lsr2*	probable iron-regulated protein	1.55	0.23
Rv1622c*	*cydB*	cytochrome bd oxidase subunit II	1.53	0.55
ml0510*		CHP	1.52	0.15

ID	*Gene*	Function (as per Leproma & TubercuList)	LR	SD
trxB-b	*trxB*	probable thioredoxin	1.52	0.06
ML1446		CHP	1.51	0.33
thrC*	*thrC*	probable threonine synthase	1.50	0.17
ml2088-f*	*cyp140*	probable cytochrome p450 140	1.48	0.10
mraY-b*	*mruX*	UDP-N-acetylmuramoyl pentylpeptide transferase	1.47	0.39
ribH	*ribH*	riboflavin synthase, beta subunit	1.47	0.17
ml2409*	*ccsA*	possible cytochrome c-type biogenesis protein	1.46	0.33
Rv2578c		CHP	1.46	0.10
ML2111*		CHP	1.46	0.33
Rv3841	*bfrB*	Bacterioferritin	1.45	0.07
uspA	*uspA*	sugar ABC transporter	1.43	0.15
ML0174	*mprA*	mycobacterial persistence regulator	1.39	0.42
tyrS	*tyrS*	tyrosyl-tRNA synthase	1.33	0.48
ml0606*		CHP	1.33	0.25
ML2531*	*cfp7*	low molecular weight portein antigen 7	1.33	0.14
ML0031		probable secreted proline rich protein	1.31	0.42
ml1332*	*tatC*	probable Sec-independent protein translocase	1.31	0.36
ml0759	*fbiA*	probable F420 biosynthesis protein	1.29	0.12
ML1077		CHP	1.28	0.08
dnaJ	*dnaJ*	probable chaperone protein	1.26	0.25
ml1946		CHP	1.24	0.18
polA-a	*polA*	DNA polymerase I	1.24	0.15
ribC	*ribC*	riboflavin synthase, alpha subunit	1.23	0.17
bccA-a*	*bccA*	biotincarboxy carrier protein & carboxyl transferase	1.23	0.30
rplN	*rplN*	50S ribosomal protein L14	1.22	0.08
ML1560*		CHP	1.22	0.25
ml2489		possible conserved secreted protein	1.22	0.24
moaB	*moaB*	molybdopterin biosynthesis protein	1.22	0.18
ml1089	*sugC*	sugar-transport ATP-binding membrane protein	1.21	0.18
ilvG-a	*ilvG-a*	probable acetolactate synthase	1.18	0.02
ml0596-b	*csd*	probable cysteine desulfurase	1.18	0.09
ml0115		CHP	1.17	0.08
ftsX	*ftsX*	putative cell division protein	1.17	0.10
ML0049	*esxA/esat6*	probable 6 kDa early secreted antigenic target	1.17	0.02
ml2491-a		CHP	1.16	0.27
ml2305		probable anion transporter ATPase	1.14	0.21
uvrB	*uvrB*	probable excinuclease ABC, subunit B	1.09	0.11
Rv0233	*nrdB*	ribonucleoside-diphosphate reductase	1.06	0.04
mce1A-a	*mce1A*	virulence factor	1.05	0.17
glcB	*glcB*	probable malate synthase	1.04	0.05
sucD	*sucD*	probable succinyl-CoA synthetase	1.03	0.08
ML1526		probable conserved membrane protein	1.02	0.15
ML0376		possible membrane protein	1.01	0.13

* DE in all three biological replicates, whereas the rest of the genes are DE in at least two of the three replicates

[a] Gene identifier as defined in the MIAME compliance file (http://vbc.med.monash.edu.au/~powell/M.smegamtis).

[b] LR, log base 2 of the fold ratio

[c] SD, standard deviation

Table 12. Genes down-regulated in response to CPZ in the Δ*qcrCAB*::*hyg* mutant (partial-genome array)

ID	Gene	Function (as per Leproma & TubercuList)	LR	SD
rplX	*rplX*	50S ribosomal protein L24	-3.53	0.19
rpmC	*rpmC*	50S ribosomal protein L29	-3.46	0.17
rpsQ*	*rpsQ*	ribosomal protein S17	-3.19	0.68
cysS	*cysS*	cysteinyl-tRNA synthetase	-3.17	1.82
rplP*	*rplP*	ribosomal protein L16	-3.14	0.15
sdhB	*sdhB*	succinate dehydrogenase	-3.07	0.18
argD-a*	*argD*	probable ornithine transferase	-2.87	0.24
rpsC*	*rpsC*	ribosomal protein S3	-2.84	0.16
infA*	*infA*	probable translation initiation factor	-2.78	0.23
uvrA-a*		excinuclease ABC, subunit A	-2.69	0.33
yrbE1-b*		CHP	-2.66	0.20
mntH-a*	*mntH*	divalent cation-transport integral membrane protein	-2.66	0.17
Rv2028c	*uspL*	universal stress protein	-2.60	0.51
ml0703*		CHP	-2.55	0.97
rplC*	*rplC*	ribosomal protein L3	-2.54	0.18
accD4-c*	*accD4*	propionyl-CoA carboxylase beta chain	-2.41	0.28
rplS*	*rplS*	ribosomal protein L19	-2.36	1.09
ml2687*		probable conserved transmembrane protein	-2.34	0.34
ml0593*		CHP	-2.34	0.22
rplE	*rplE*	50S ribosomal protein L5	-2.34	0.22
rhlE-b*	*rhlE*	probable ATP-dependent RNA helicase	-2.33	0.36
Rv3134c	*uspL*	universal stress protein	-2.33	0.27
rpsI*	*rpsI*	ribosomal protein S9	-2.32	0.13
lpd-a*	*lpd*	Lipoprotein	-2.24	0.48
ml0691-b*	*dacB*	probable D-alanylalanine carboxypeptidase	-2.21	0.17
ML0068*		CHP	-2.20	0.15
ml0734*		probable conserved transmembrane protein	-2.20	0.37
ML2640		CHP	-2.14	0.04
ML1439*		CHP	-2.13	0.58
ML1115*	*lprB*	possible lipoprotein	-2.13	0.52
ML0386*		CHP	-2.13	0.15
ml1544-a*		probable conserved membrane protein	-2.12	0.12
pdc-a*	*pdc*	probable pyruvate decarboxylase	-2.11	0.34
ml1714*		CHP	-2.10	0.05
aroG	*aroG*	deoxy arabino heptulosonate phosphate synthase	-2.10	0.45
lipG	*lipG*	probable lipase	-2.06	0.04
rpsL*	*rpsL*	ribosomal protein S12	-2.06	0.20
rplR*	*rplR*	ribosomal protein L18	-2.06	0.42
Rv2032	*acg*	putative nitroreductase	-2.04	0.42
Rv2191*	*polC*	DNA polymerase III, alpha subunit	-2.01	0.11
rpsN*	*rpsN*	ribosomal protein S14	-1.97	0.40
mihF*	*mihF*	putative mycobacterial integration host factor	-1.97	0.84
uspE	*uspE*	universal stress protein	-1.88	0.23
PPE-b*	*PPE*	PPE family protein	-1.83	0.33
ML2487*	*pyrE*	probable orotate phosphoribosyl transferase	-1.80	0.49
ml2639-f*		probable aldehyde dehydrogenase	-1.73	0.25
leuB-c	*leuB*	probable isopropyl malate dehydrogenase	-1.73	0.26
ml2661-e	*fadD7*	probable fatty acid CoA ligase	-1.69	0.42
fadD2-i*	*fadD2*	fatty acid CoA synthetase	-1.69	0.29
Rv2392*	*cysH*	probable phosphoadenylsulfate reductase	-1.67	0.45
rpsE*	*rpsE*	ribosomal protein S5	-1.66	0.40

ID	Gene	Function (as per Leproma & TubercuList)	LR	SD
ml2699*		putative secreted protein	-1.66	0.30
ML2297*	*ephE*	possible epoxide hydrolase	-1.65	0.18
rpoA*	*rpoA*	DNA-directed RNA polymerase	-1.64	0.20
glnA2-e	*glnA2*	glutamine synthetase	-1.63	0.72
pstC2*	*pstC2*	phosphate-transport integral membrane ABC transporter	-1.62	0.21
ml1306*		CHP	-1.55	0.23
ml1835*		CHP	-1.53	0.24
ml1720*		CHP	-1.51	0.12
groEL-c*	*groEL*	heat shock protein	-1.50	0.33
ansA	*ansA*	possible aspartate aminotransferase	-1.49	0.49
tsf*	*tsf*	probable elongation factor	-1.48	0.27
eftB	*eftB*	electron transfer flavoprotein, beta subunit	-1.47	0.38
ML2274*		probable consrved secreted protein	-1.46	0.18
cobT*	*cobT*	dimethyl-benzimidazole transferase	-1.43	0.15
gabD-l	*gabD*	succinate-semialdehyde dehydrogenase	-1.40	0.15
mscL*	*mscL*	large-conductance ion mechanosensitive channel	-1.37	0.12
ksgA*	*ksgA*	dimethyl adenosine transferase	-1.36	0.20
atpH*	*atpH*	ATP synthase	-1.35	0.35
phoH-a*	*phoH*	probable phosphofructokinase	-1.34	0.18
ml1706*		CHP	-1.33	0.32
ctpC-a*	*ctpC*	cadmium-transporting P-type ATPase	-1.32	0.26
sucC*	*sucC*	succinyl hydroxy cyclohexadiene carboxylase synthase	-1.31	0.12
ddlA*	*ddlA*	D-alanylalanine synthetase	-1.29	0.14
ML0321	*ispD*	methylerythritol phosphate cytidyltransferase	-1.26	0.32
ftsH	*ftsH*	membrane-bound protease	-1.26	0.09
ml0093*	*glfT*	bifunctional UDP-galactofuranosyl transferase	-1.26	0.22
accD4-b*	*accD4*	propionyl-CoA carboxylase beta chain	-1.26	0.34
ml1538-b	*mycP5*	serine protease	-1.25	0.07
ml2156		CHP	-1.24	0.24
glnA2-b	*glnA2*	glutamine synthetase	-1.24	0.16
mtf1	*mtf1*		-1.23	0.27
atpB*	*atpB*	ATP synthase	-1.22	0.21
ruvB	*ruvB*	probable Holliday junction helicase	-1.22	0.03
murC*	*murC*	probable UDP-N-acetylmuramate-alanine ligase	-1.20	0.18
rnpA	*rnpA*	ribonuclease P protein	-1.17	0.04
ML1138		possible integral membrane protein	-1.17	0.07
ml2400*		probable conserved transmembrane protein	-1.17	0.16
gltA2-a*	*gltA2*	probable citrate synthase	-1.16	0.10
ml0430*		probable conserved integral membrane protein	-1.14	0.23
Rv3132c	*dosS*	two-component sensor histidine kinase	-1.13	0.16
ML2549*		CHP	-1.12	0.13
sodA-a	*sodA*	superoxide dismutase	-1.09	0.14
ml0893		probable integral membrane protein	-1.09	0.13
gabD-k*	*gabD*	aldehyde dehydrogenase	-1.07	0.25
valS	*valS*	valyl-tRNA synthase	-1.04	0.16
gabD-p	*gabD*	succinate-semialdehyde dehydrogenase	-0.99	0.14
ml2692		Glucocycloaldolase	-0.99	0.15
ML2647	*msrA*	protein-methionine-S-oxide reductase	-0.96	0.03
purH	*purH*	probable bifunctional purine biosynthesis protein	-0.92	0.03
fadA-b	*fadA*	probable beta ketoacyl CoA thiolase	-0.91	0.06

* DE in all three biological replicates, whereas the rest of the genes are DE in at least two of the three replicates

[a] Gene identifier as defined in the MIAME compliance file (http://vbc.med.monash.edu.au/~powell/M.smegamtis).

[b] LR, log base 2 of the fold ratio

[c] SD, standard deviation

Table 13. Genes down-regulated in response to CPZ in the Δ*qcrCAB*::*hyg* mutant (TIGR arrays)

Name on array	Gene	Description (TIGR)	LR[a]	SD[b]	Closest Rv #[c]	E-value[d]
ORFA02397	*rpmC*	Ribosomal protein L29	-6.46	2.37	Rv0709	[1e-33]
ORFA02387	*rplD*	Ribosomal protein L4/L1 family	-5.62	1.63	Rv0702	[1e-103]
ORFA10253*		alcohol dehydrogenase II	-5.47	1.43	Rv0405	[0.75]
ORFA02442	*rplF*	probable ribosomal protein	-5.44	2.03	Rv0719	[2e-88]
ORFA08638	*acg*	Conserved hypothetical protein	-5.36	1.29	Rv2032	[2e-95]
ORFA11432*		hypothetical protein	-5.19	1.66	Rv2426c	[2e-54]
ORFA08631*		Conserved hypothetical protein	-5.13	2.55	Rv3129	[5e-30]
ORFA02531	*rpsK*	probable ribosomal protein S11	-5.07	1.65	Rv3459c	[3e-64]
ORFA02437	*rplE*	Ribosomal protein L5	-5.02	0.76	Rv0716	[1e-81]
ORFA11325*	*rpsF*	Ribosomal protein S6	-5.02	0.78	Rv0053	[3e-47]
ORFA02389	*rplW*	Ribosomal protein L23	-4.99	1.10	Rv0703	[6e-34]
ORFA02396*	*rplP*	Ribosomal protein L16	-4.90	0.72	Rv0708	[3e-74]
ORFA02391*	*rpsS*	Ribosomal protein S19	-4.82	1.10	Rv0705	[3e-51]
ORFA09487	*cysA3*	thiosulfate sulfurtransferase	-4.81	0.35	Rv3117	[1e-147]
ORFA02317	*rpsG*	Ribosomal protein S7	-4.74	0.40	Rv0683	[9e-84]
ORFA02443	*rplR*	Ribosomal protein L18	-4.65	0.55	Rv0720	[3e-40]
ORFA02254*	*rplJ*	ribosomal protein L10	-4.64	1.08	Rv0651	[3e-69]
ORFA11322	*rpsR1*	Ribosomal protein S18	-4.63	0.87	Rv0055	[2e-40]
ORFA07122	*glnA1*	Glutamine synthetase, type I	-4.53	1.31	Rv2220	[0.0]
ORFA02435	*rplX*	Ribosomal protein L24	-4.50	0.51	Rv0715	[8e-51]
ORFA02591	*rplM*	Ribosomal protein L13	-4.32	0.16	Rv3443c	[3e-70]
ORFA02255	*rplL*	Ribosomal protein L7/L12	-4.31	1.24	Rv0652	[1e-32]
ORFA02316*	*rpsL*	Ribosomal protein S12	-4.31	0.14	Rv0682	[4e-66]
ORFA02320*	*fusA1*	translation elongation factor EF-G (fusA)	-4.29	0.17	Rv0684	[5e-93]
ORFA10100*	*cspA*	probable cold shock protein	-4.29	0.60	Rv3648c	[4e-34]
ORFA11402*	*rpsO*	Ribosomal protein S15	-4.24	0.30	Rv2785c	[1e-32]
ORFA06348	*rplT*	Ribosomal protein L20	-4.24	0.28	Rv1643	[5e-64]
ORFA02323*	*tuf*	translation elongation factor Tu	-4.19	0.26	Rv0685	[0.0]
ORFA08635*	*uspL*	universal stress protein	-4.18	2.52	Rv2028c	[1e-48]
ORFA02796	*amiB*	probable amidase	-4.13	0.62	Rv3306c	[4e-80]
ORFA02592	*rpsI*	Ribosomal protein S9	-4.13	0.44	Rv3442c	[4e-58]
ORFA08560*	*mpt70*	Osteoblast specific factor 2-related protein	-4.11	1.17	Rv2875	[1e-29]
ORFA08144		vrlB protein	-4.05	2.52	Rv1304	[3e-15]
ORFA02214*	*rpmG2*	Ribosomal protein L33	-3.90	0.85	Rv0634	[3e-27]
ORFA07185	*kasA*	beta-ketoacyl-ACP synthase	-3.87	1.04	Rv2245	[1e-38]
ORFA02799		Conserved hypothetical protein	-3.81	0.10	Rv2839c	[0.15]
ORFA11093*	*glpK*	glycerol kinase	-3.75	0.42	Rv3696c	[0.0]
ORFA02566*		aldehyde dehydrogenase family protein	-3.73	0.35	Rv0458	[0.0]
ORFA04190	*rpsB*	Ribosomal protein S2	-3.71	0.42	Rv2890c	[1e-133]
ORFA08937	*rplY*	ribosomal 5S rRNA E-loop binding protein Ctc/L25/TL5	-3.68	2.09	Rv1015c	[4e-68]
ORFA07184	*acpM*	acyl carrier protein	-3.65	0.49	Rv2244	[2e-30]
ORFA00098*	*esat6*	early secretory antigen target	-3.62	0.38	Rv3875	[2e-29]
ORFA07656	*rplU*	Ribosomal protein L21	-3.54	0.55	Rv2442c	[1e-45]
ORFA01727	*adhC*	oxidoreductase, zinc-binding	-3.49	0.47	Rv3045	[1e-134]

Name on array	Gene	Description (TIGR)	LR[a]	SD[b]	Closest Rv #[c]	E-value[d]
ORFA10505*	*fbpA*	esterase, putative, antigen 85-A	-3.45	0.98	Rv3804c	[1e-122]
ORFA06347	*rpmI*	Ribosomal protein L35	-3.42	0.79	Rv1642	[3e-27]
ORFA06619	*uspM*	universal stress protein	-3.31	0.87	Rv2026c	[6e-97]
ORFA01603	*pknE*	mspA-Gen	-3.28	1.37	Rv1743	[0.007]
ORFA03933	*ilvC*	ketol-acid reductoisomerase	-3.26	0.65	Rv3001c	[1e-156]
ORFA11096*	*glpD2*	glycerol-3-phosphate dehydrogenase	-3.25	0.77	Rv3302c	[1e-173]
ORFA03010	*accD5*	Propionyl-CoA carboxylase, beta subunit	-3.23	0.04	Rv3280	[0.0]
ORFA01465	*groEL*	60 kd chaperonin , fragment	-3.19	0.43	Rv0440	[0.0]
ORFA11091*		glycerol uptake facilitator protein	-3.18	1.45	Rv3299c	[0.066]
ORFA11401*	*rpmJ*	hypothetical protein	-3.13	0.30	Rv3461c	[9e-18]
ORFA02258	*rpoB*	DNA polymerase (rpoB)	-3.13	2.92	Rv0667	[0.0]
ORFA01360		hypothetical protein	-3.11	0.87	Rv1699	[0.074]
ORFA00097*	*lhp*	10 kDa culture filtrate antigen Lhp (CFP10)	-3.09	0.35	Rv3874	[5e-21]
ORFA02572		B12-dependent glycerol dehydrogenase	-3.06	1.00	Rv3825c	[0.018]
ORFA02804		allantoin permease family protein	-3.03	0.77	Rv0936	[0.23]
ORFA08143*	*atpE*	ATP synthase c chain	-3.01	0.09	Rv1305	[1e-19]
ORFA09090*	*sucC*	carbamoyl-phosphate synthase, large subunit	-2.84	1.02	Rv0951	[0.0]
ORFA04224	*frr*	ribosome recycling factor	-2.79	0.40	Rv2882c	[1e-86]
ORFA02800		YER057c/YjgF/UK114 family protein	-2.78	0.51	Rv2704	[4e-10]
ORFA04425	*gpsI*	polyribonucleotide nucleotidyltransferase	-2.70	0.40	Rv2783c	[0.0]
ORFA09410	*uspN*	universal stress protein	-2.69	1.45	Rv2026c	[4e-29]
ORFA06349	*infC*	translation initiation factor IF-3	-2.69	0.35	Rv1641	[4e-88]
ORFA06414	*rpsA*	rpsA	-2.63	1.18	Rv1630	[0.0]
ORFA07077*	*ctaC*	cytochrome c oxidase, subunit II, putative	-2.47	0.85	Rv2200c	[1e-147]
ORFA06997	*wag31*	cell division protein DivIVA	-2.45	0.00	Rv2145c	[1e-103]
ORFA02224*	*rpl1*	Ribosomal protein L1	-2.44	0.73	Rv0641	[1e-110]
ORFA02634	*groES*	chaperonin, 10 kDa	-2.42	0.50	Rv3418c	[2e-52]
ORFA01395	*sodC*	superoxide dismutase (sodC), Cu-Zn family	-2.39	0.44	Rv0432	[9e-84]
ORFA07655	*rpmA*	Ribosomal protein L27	-2.34	0.40	Rv2441c	[5e-38]
ORFA02529*	*infA*	translation initiation factor IF-1	-2.34	0.89	Rv3462c	[7e-38]
ORFA10554*	*sodA*	superoxide dismutase (mn)	-2.31	0.57	Rv3846	[1e-102]
ORFA07065*	*ctaE*	Cytochrome c oxidase subunit III	-2.22	0.85	Rv2193	[1e-103]
ORFA10746		hypothetical protein	-2.21	0.04	Rv2943	[0.074]
ORFA10741		anti-anti-sigma factor, putative	-2.19	1.22	Rv0516c	[0.009]
ORFA09321	*gltA2*	citrate synthase I	-2.19	1.01	Rv0896	[0.0]
ORFA02698		hypothetical protein	-2.03	0.71	Rv2944	[1.1]
ORFA02223*	*rplK*	Ribosomal protein L11	-2.02	0.83	Rv0640	[3e-54]
ORFA09975*		Conserved hypothetical protein	-1.99	0.07	Rv2451	[0.095]
ORFA05827		probable secreted protein [imported]	-1.87	0.29	Rv0559c	[2e-21]
ORFA00657	*nrp*	peptide synthetase	-1.71	0.52	Rv0101	[0.0]
ORFA09778		Conserved hypothetical protein	-1.66	0.03	Rv0236c	[0.080]
ORFA10514	*pirG*	hypothetical protein	-1.60	0.49	Rv3810	[1e-53]
ORFA00915	*cspA*	cold shock protein	-1.60	0.48	Rv3648c	[3e-25]
ORFA05828		probable secreted protein [imported]	-1.59	0.46	Rv0455c	[1e-32]
ORFA08112	*fadA4*	acetyl-CoA acetyltransferase	-1.44	0.39	Rv1323	[0.0]
ORFA03892	*fixB*	electron transfer flavoprotein, alpha subunit	-1.43	0.68	Rv3028c	[1e-135]
ORFA08162*	*rpmE*	Ribosomal protein L31	-1.39	1.14	Rv1298	[5e-31]
ORFA05511	*cysA1*	Polyamine ABC transporter	-1.33	0.22	Rv2397c	[8e-57]

Name on array	Gene	Description (TIGR)	LR[a]	SD[b]	Closest Rv #[c]	E-value[d]
ORFA06045	*apa*	hypothetical protein	-1.03	0.04	Rv1860	[5e-58]

* DE in all three biological replicates, whereas the rest of the genes are DE in at least two of the three replicates

[a] LR, log base 2 of the fold ratio

[b] SD, standard deviation

[c,d] BLAST search results for the *M. tuberculosis* H37Rv homologues of the *M. smegmatis* genes on the TIGR array was kindly provided by Prof. N. Stoker (Royal Veterinary College, London, UK).

Analysis of effects of CPZ on the bc_1 *mutant using RT-PCR*

In order to verify the microarray results, semi-quantitative RT-PCR was performed on a selection of the genes that were found to be DE in the Δ*qcrCAB*::*hyg* mutant as a result of CPZ treatment. These comprised 6 members of the *M. smegmatis* DosR regulon (*dosR*, *uspL*, *uspM*, *uspN*, *acg* and *hspX*; O'Toole *et al*., 2003), and *sigA* as a control (Table 5). To exclude DNA contamination in RNA samples, control samples containing all the reaction components except reverse transcriptase were included in the reverse transcription step, and subsequently PCR amplified using *sigA* primers. Absence of PCR product on gel electrophoresis was an indication for lack of DNA contamination. Although poor or no amplification was obtained for some of the genes due to technical problems (data not shown), the results obtained for those genes for which amplification was obtained were in agreement with the microarray observation that some members of the DosR regulon were down-regulated in response to CPZ (Figure 16). There was visibly less amplified product of these genes (*uspM*, *uspL*, *hspX*, *dosR*), except for *acg* whose expression did not seem different, in the CPZ-treated samples than in the untreated samples. In contrast, no change in the amount of amplicon derived from the control *sigA* gene was observed between the two samples, confirming that the different effects observed with the above-mentioned genes were not a result of unequal amounts of starting total RNA or cDNA in the RT or PCR reactions, respectively.

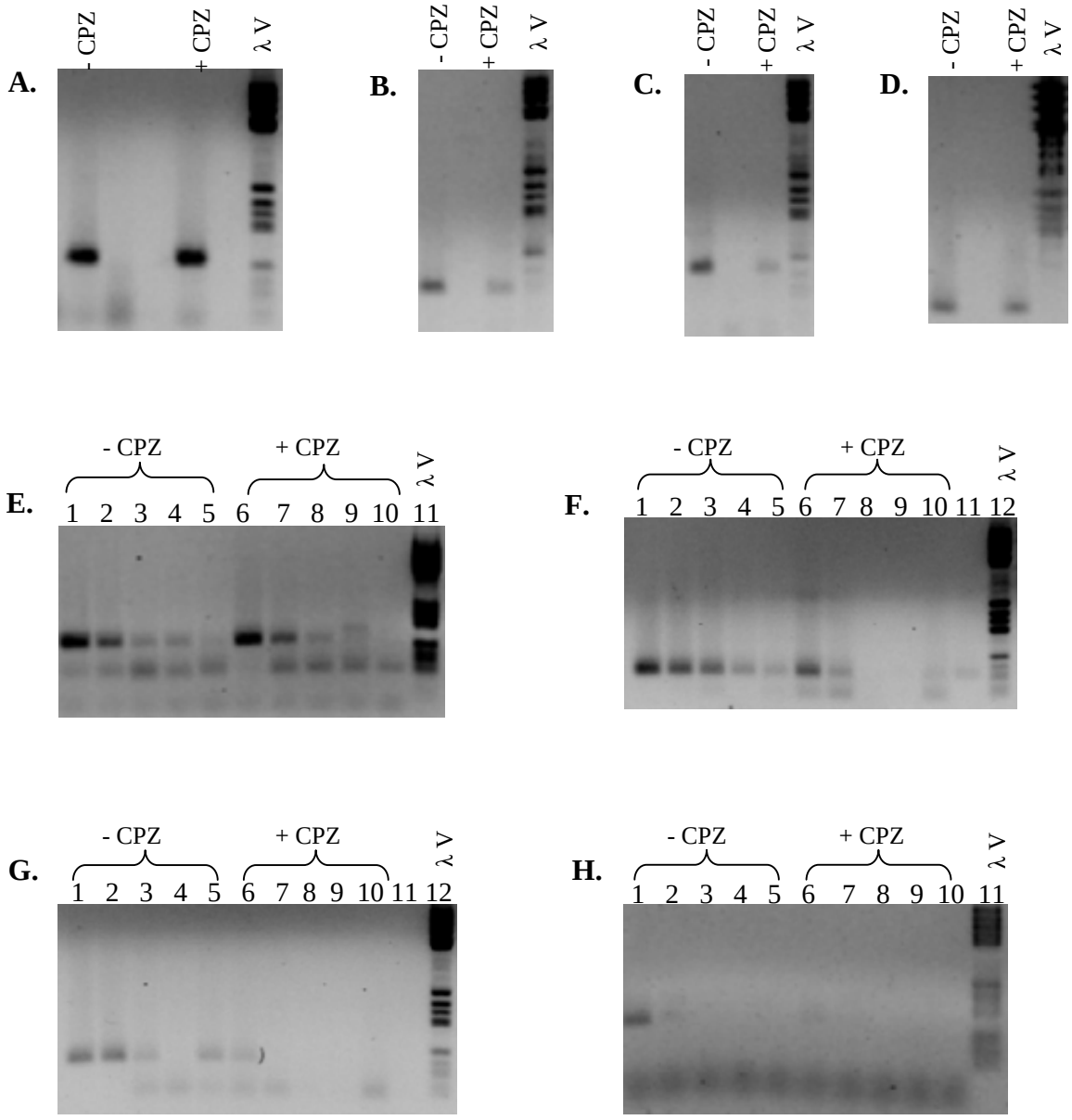

Figure 16. Expression analysis, as assessed by semi-quantitative RT-PCR, of sentinel genes differentially expressed in response to CPZ in a Δ*qcrCAB*::*hyg* mutant of *M. smegmatis*. 1 μg of RNA from CPZ-treated and untreated cultures of Δ*qcrCAB*::*hyg* was reverse-transcribed and the undiluted cDNA (A to D) or five-fold serial dilutions of the cDNA (E to H) were used in PCR to amplify portions of *sigA* (A and E), *dosR* (B and F), *uspM* (C), *acg* (D), *hspX* (G) and *uspL* (H), using primers described in Table 2.4. (A to D) PCR product of undiluted cDNA from untreated (lane 1) or treated (lane 2), and DNA molecular marker V (lane 3). (E to H) Lanes 1 to 5 contain PCR products of serial dilutions of DNA from untreated culture, lanes 6 to 10 are from treated culture, DNA molecular marker V is in lane 11 (E and H) or lane 12 (F and G), and no DNA control in lane 11 (F and G). [N.B lanes 8 and 11 in panel F are swapped]. Arrows indicate the expected bands. Bands below those of interest are primer dimers.

4. DISCUSSION

Genomic organization of the cytochrome *bc*$_1$-*aa*$_3$ pathway in *M. smegmatis*

BLAST searches of the genome sequence of *M. smegmatis* mc^{2}155 (pre- and post-sequence completion) revealed the genetic composition and organization of the components of this branch of the aerobic respiratory chain, and also allowed for comparison with their counterparts in other bacterial species. As has been proposed for *M. tuberculosis* (Kana *et al*., 2001; Weinstein *et al*., 2005), the pathway consists of a *qcrCAB*-encoded cytochrome *bc*$_1$ complex, which transfers electrons to the terminal oxidase, cytochrome *aa*$_3$, that ultimately reduces O_2 to water.

Cytochrome bc$_1$ *complex*

The chromosomal arrangement of genes (*qcrCAB*) encoding cytochrome *bc*$_1$ complex is conserved in actinomycetes such as *Streptomyces, Mycobacterium, Nocardia*, *Corynebacterium* (http://www.tigr.org/tigr-scripts/CMR2/) and *Rhodococcus* (Sone *et al*., 2003), which is consistent with the close evolutionary relationship between these genera (Ishikawa *et al*., 2004). Components of the *qcrCAB* operon, which is preceded by a *ctaE* (encoding subunit III of the *aa*$_3$-type cytochrome *c* oxidase) in all these genera, specify the cytochrome *c*, Rieske iron-sulfur protein and cytochrome *b* subunits of the menaquinol:cytochrome *c* oxidoreductase (cytochrome *bc*$_1$ complex), respectively. As has previously been shown through sequence alignments, the primary structures of these components are highly homologous within the actinomycetes, with some peculiar features apparently unique to these organisms (Bott and Niebisch, 2003; Sone *et al*., 2003). The most important of these features are the presence of two heme-binding motifs in the cytochrome *c*$_1$ (QcrC) subunit of this complex, and the apparent absence of a gene encoding a separate cytochrome *c* in the genomes of these organisms. These features suggest that the cytochrome *c*$_1$ performs the function of a separate cytochrome *c* in electron transfer to the terminal *aa*$_3$-type cytchrome *c* oxidase.

Cytochrome c *oxidase*

The mycobacterial genes encoding the aa_3-type cytochrome *c* oxidase are located at non-contiguous positions on the chromosome, with the exception of *ctaCF* (encoding subunits II and IV, respectively) which form an operon. These two genes are separated by two genes downstream from the *ctaE-qcrCAB* operon, while *ctaD* (for subunit I) is located at a totally different position on the chromosome. Whereas the genomic context of all these genes is conserved within mycobacteria, the arrangement differs between the actinomycete genera mentioned above. However, the high sequence similarity of these genes across the genera indicates that they are functionally equivalent, consistent with the relatedness of the organisms (Niebisch and Bott, 2001; Niebisch and Bott, 2003).

The apparent essentiality of the *M. smegmatis ctaDI* gene

Several attempts to obtain a null *ctaDI* mutant of *M. smegmatis* failed, suggesting a possible essentiality of this gene, which encodes subunit I of aa_3-type cytochrome *c* oxidase. However, the ability to knock out the gene encoding subunit II (*ctaC*) of this oxidase suggested that the inability to inactivate *ctaDI* may have been due to a polar effect on the downstream *serB2* gene, which appears to be operonic with *ctaDI*, rather than due to the essentiality of *ctaDI*. In *M. tuberculosis* and *M. bovis* BCG *serB2*, and not *serB*, was shown to encode an essential phosphoserine phosphatase as determined by high-density mutagenesis using a transposon site hybridization (TraSH) method (Sassetti *et al*., 2003). Like *M. tuberculosis* and *M. bovis* BCG, *M. smegmatis* also possesses both *serB* and *serB2* genes, so by analogy, *serB2* is probably also essential in this organism.

The failure to recover a null *ctaDI* mutant using serine supplementation could be due to any one of a number of possible reasons. (i) If the null *ctaDI* mutant was a serine auxotroph, either the concentration of serine supplement used (100 μg/ml) may not have been sufficient or its uptake by *M. smegmatis* failed to meet the serine demand of this organism. In *M. tuberculosis*, it was demonstrated that a high concentration of exogenous L-arginine was required to restore the growth rate of an *argF* mutant (defective in arginine biosynthesis) to an optimum level, suggesting that this organism had a high arginine demand (Gordhan *et al*., 2002). (ii) The enzyme encoded by *serB2* (phosphoserine phosphatase) is not only required for serine biosynthesis, but also for

glycine and cysteine biosynthesis (Sassetti *et al*., 2003). Therefore it is possible that loss of *serB2* function could confer pleiotropic effects (multiple amino acid auxotrophy) that are not simply reversible by serine supplementation.

The occurrence of two *serB* genes and the location of one (designated herein as *serB2* by analogy to the mycobacterial counterparts), downstream of *ctaD* in the closely related actinobacterium *C. glutamicum*, suggested that these genes may have similar roles as in mycobacteria. However, the *serB2* gene of *C. glutamicum*, unlike its mycobacterial counterpart, does not form an operon with *ctaD*, but is located 200 bp downstream of *ctaD* (http://www.tigr.org/tigr-scripts/CMR2/ CMRHomePage.spl). This suggests that the *C. glutamicum serB2* may have its own promoter, and would explain the viability of a deletion mutant of this organism in *ctaD* (Niebisch and Bott, 2001).

Are there isoenzymes of *aa*$_3$-type cytochrome *c* oxidase in *M. smegmatis*?

The occurrence of two distinct *ctaD* genes in the genome of *M. smegmatis* as revealed by the genome sequence and confirmed by targeted mutagenesis raises a question about the possible existence of isoenzymes of *aa*$_3$-type cytochrome *c* oxidase in this organism. Although distinct *ctaD* alleles could only be identified in the genome of *M. smegmatis* and not any other sequenced mycobacterial species, two distinct *ctaD* homologues were identified in the genomes of three other actinobacteria, *N. farcinica*, *S. coelicolor* and *S. avermitilis* (http://www.tigr.org/tigr-scripts/CMR2/). Similarly, two *ctaD* alleles (with 90% identity) have previously been reported for *Paracoccus denitrificans* (Raitio *et al*., 1990; van der Oost *et al*., 1991), suggesting that a multiplicity of *ctaD* genes is reasonably common occurrence in bacterial genomes. Subunit I (CtaD) is the only component of *aa*$_3$-type cytochrome *c* oxidase that is apparently encoded by more than one allele in these species, suggesting that either one of the encoded CtaDI or CtaDII subunit can combine with the other subunits to form functional isoforms of *aa*$_3$-type cytochrome *c* oxidase[5]. Consistent with this, *ctaDI* and *ctaDII* were separately expressed to complement a double mutant (Δ*ctaDI*/*ctaDII*) in *P. denitrificans*, demonstrating that they were isoforms of subunit I of cytochrome *c* oxidase (de Gier, *et al*., 1994). However,

[5] Note that the genes designated as *ctaDI* and *ctaDII* in *M. smegmatis* are not necessarily the functional counterparts of the genes given this nomenclature in *P. denitrificans*

ctaDI could only be expressed if maintained on a plasmid, suggesting that there was a gene dosage or repressor titration effect (Baker *et al*., 1998) whereas *ctaDII* was shown to encode the primary subunit I of the enzyme (Baker *et al*., 1998; Otten *et al*., 2001a). Whether the *M. smegmatis ctaDI* and *ctaDII* encode isoforms of subunit I, as is the case in *P. denitrificans*, remains to be investigated.

In this study, *ctaDI* is proposed to be the principal *ctaD* allele of *M. smegmatis* under aerobic conditions for the following reasons. (i) *ctaDI* displays the highest homology to its *M. tuberculosis* counterpart than exhibited by *ctaDII*. (ii) *ctaDI* but not *ctaDII* exists in the same chromosomal context as *ctaD* genes of other mycobacteria. (iii) If CtaDII was a component of the principal aa_3-type cytochrome *c* oxidase, which should include CtaC (subunit II, encoded by only one gene), the loss of either *ctaC* or *ctaDII* would be expected to confer the same phenotype. However, the Δ*ctaDII*::*hyg* mutant showed no growth phenotype when cultured under the same conditions under which the Δ*ctaC*::*hyg* mutant was impaired for growth. (iv) The expression of *ctaDII* under aerobic conditions was not affected by disruption of the cytochrome bc_1 complex (Δ*qcrCAB*::*hyg*) or cytochrome *c* oxidase (Δ*ctaC*::*hyg*). Taken together, these data suggest that *ctaDI* encodes the principal subunit I of aa_3-type cytochrome *c* oxidase in *M. smegmatis*.

Growth attenuation of the cytochrome bc_1 (Δ*qcrCAB*::*hyg*) and aa_3-type cytochrome *c* oxidase (Δ*ctaC*::*hyg*) mutants of *M. smegmatis*

In an earlier study from this laboratory, a *cydAB*-encoded cytochrome *bd*-type quinol oxidase of *M. smegmatis* was demonstrated to be required for growth under microaerobic conditions (Kana *et al*., 2001). Although severely growth impaired at and below 1% air saturation, a *cydA*::*aph* mutant of *M. smegmatis* showed no discernible phenotype when grown under high aeration (Kana *et al*., 2001), suggesting that the cytochrome bc_1-aa_3 branch was the main route of electron flow under aerobic conditions in this organism. The results presented here support this hypothesis as both the Δ*qcrCAB*::*hyg* and Δ*ctaC*::*hyg* mutants were severely attenuated for growth under these conditions. A more than two-fold decrease in the growth rate of the two mutants compared to their parental wild type was observed during the logarithmic growth in liquid medium, demonstrating

the importance of this branch of the respiratory chain for the aerobic growth of *M. smegmatis*. The delayed emergence of mutant colonies on solid medium was indicative of a longer lag phase in these strains compared to the wild type, which was also reflected in the growth curves. A similar observation has been reported for *C. glutamicum*, in which Δ*qcrCAB* and Δ*ctaC* mutants were severely defective in growth in glucose minimal medium (Niebisch and Bott, 2001; Bott and Niebisch, 2003). In *P. denitrificans*, an analogous growth defect was also reported in which mutants lacking cytochrome bc_1 displayed lower maximum cell numbers compared to the wild type (Otten *et al*., 2001b). However, the viability of the cytochrome bc_1-aa_3 pathway mutants in these organisms suggested that the loss of functionality in this pathway could be compensated by re-routing of the electron flow through alternate pathways.

Over-expression of cytochrome *bd* oxidase compensates for loss of the bc_1 complex or aa_3-type cytochrome *c* oxidase

Disruption of the *M. smegmatis* cytochrome bc_1-aa_3 pathway at the level of the bc_1 complex (in a Δ*qcrCAB*::*hyg* mutant) or the aa_3-type cytochrome *c* oxidase (in a Δ*ctaC*::*hyg* mutant) resulted in a marked up-regulation of the *cydAB*-encoded cytochrome *bd* oxidase as determined by *lacZ* reporter assays and/or DNA microarray analysis. These results indicated that in both mutants, electron flow to the major terminal oxidase, cytochrome aa_3 was re-routed to the bioenergetically less-efficient cytochome *bd*-type quinol oxidase. An analogous observation was made in *P. denitrificans* where expression of the *qox* promoter, controlling expression of the quinol oxidase cytochrome ba_3, increased up to 11-fold in strains lacking cytochrome bc_1 complex or cytochrome aa_3 oxidase (Otten *et al*., 2001a). To corroborate this result in *P. denitrificans*, aerobically grown cytochrome ba_3-deficient mutants were unable to respire when treated with myxothiazol (Otten *et al*., 2001a), a specific inhibitor of the bc_1 complex, demonstrating that aerobic respiration could not proceed when both pathways were blocked. Nonetheless, the severe growth defect of the *M. smegmatis* cytochrome bc_1 and aa_3 mutants suggested that the compensatory effect of the cytochrome *bd* oxidase was not energetically sufficient to sustain growth to levels comparable to the wild type.

The pathways terminating in aa_3-type cytochrome *c* oxidase and cytochrome *bd* oxidase differ greatly in their bioenergetic efficiency. Although both oxidases couple electron transfer to the generation of an electrochemical proton gradient, which may then be used for the synthesis of ATP, the coupling efficiency of aa_3-type cytochrome *c* oxidase is higher than that of the *bd* oxidase and therefore resulting in a higher ATP yield (Garcia-Horsman *et al*., 1994; Bott and Niebisch, 2003; Belevich *et al*., 2005).

Cytochrome *bd*' oxidase (YthAB) is not differentially expressed in the mutants

The genome of *M. smegmatis* contains a pair of genes, designated herein as *ythAB*, which are homologous to *cydAB*, and may thus encode an alternate cytochrome *bd*-type quinol oxidase. Based on microarray analyses of the *M. smegmatis* Δ*qcrCAB*::*hyg* and Δ*ctaC*::*hyg* mutants, the *ythAB* genes were not differentially expressed in either mutant, suggesting that these genes are not required for aerobic growth of *M. smegmatis*. However, the presence of a signal from these genes in both wild type and mutant strains on the array provided the first evidence that these genes are expressed, at least at the RNA level, in *M. smegmatis*. The failure to recover a double mutant of *M. smegmatis* in which the pathways terminating in both aa_3-type cytochrome *c* oxidase and the *cydAB*-encoded quinol oxidase are disrupted suggested that YthAB is unable to substitute functionally for the *cydAB*-encoded oxidase. Therefore, there currently is no experimental evidence to suggest that an alternate, *bd*-type oxidase is indeed expressed in *M. smegmatis*. Interestingly, *M. smegmatis* is the only sequenced mycobacterial species carrying *ythAB* homologues. In *B. subtilis*, the *ythAB* genes have been proposed to be required for sporulation (Winstedt and Wachenfeldt, 2000; Schau *et al*., 2004). Although both *M. smegmatis* and *B. subtilis* are soil bacteria, there is no documented knowledge of spore formation in *M. smegmatis*. Therefore, the role of *ythAB* in respiration and/or some other cellular function in *M. smegmatis* remains unknown.

Induction of hypoxia-responsive genes in the cytochrome bc_1-aa_3 pathway mutants of *M. smegmatis*

Disruption of the cytochrome bc_1-aa_3 pathway resulted in up-regulation of several hypoxia-responsive genes including *cyd*A, *cydB, hspX*, *uspL*, *uspM*, *acg*, *dosT*,

MSMEG5227 (Rv3130c), MSMEG5228 (Rv3129), MSMEG3958 (Rv3127), MSMEG5215 (Rv1738)[6]. Based on previous studies, these genes can be classified into two independent, but mutually non-exclusive groups (Boshoff *et al*., 2004). The *cydAB* genes are sentinel members of one group, and the implication of their constitutive induction in the mutants has been discussed above. The remaining genes belong to the second group, which includes several DosR-regulated genes of *M. smegmatis* (*hspX*, *uspL*, *uspM*, *acg*; O'Toole *et al*., 2003) and *M. smegmatis* homologues of the *M. tuberculosis* DosR-regulated genes, *dosT*, MSMEG5227 (Rv3130c), MSMEG5228 (Rv3129), MSMEG3958 (Rv3127) and MSMEG5215 (Rv1738). However, it is important to note that the induction of these genes was more significant in the Δ*qcrCAB*::*hyg* mutant than in the Δ*ctaC*::*hyg* mutant. Although the *M. smegmatis* DosR regulon has only been partially characterized (Mayuri *et al*., 2002; O'Toole *et al*., 2003) and therefore, the full complement of DosR-regulated genes is unknown, up-regulation of the above genes suggests that there is an overlap in the type of signal(s) and/or signal transduction system(s) resulting from either disruption of the cytochrome bc_1-aa_3 pathway or O_2 starvation (hypoxia). This finding is consistent with previous studies in which components of the respiratory system were proposed to be involved in the signaling of the DosR system of *M. tuberculosis* (Voskuil *et al*., 2003; Boshoff *et al*., 2004).

Proposed changes in the redox states of electron carriers in the cytochrome bc_1-aa_3 pathway mutants

The proposed changes in the redox states of the $NADH/NAD^+$ and menaquinol/menaquinone (MKH_2/MK) pools resulting from disruption of the cytochrome bc_1-aa_3 pathway are summarized schematically in Figure 17. Under aerobic conditions, NADH in the wild type *M. smegmatis* is proposed to be rapidly re-oxidized to NAD^+ by the NADH dehydrogenase as has been demonstrated in *Streptomyces coelicolor* (Brekasis and Paget, 2003; Green and Paget, 2004), resulting in a low $NADH/NAD^+$ ratio (Figure 17A). Concomitant with this proposal, Vilchèze *et al* (2005) recently

[6] The *M. tuberculosis* H37Rv counterparts of the *M. smegmatis* genes are given in brackets for the purposes of cross-referencing.

demonstrated that the NADH/NAD^+ ratio in wild type *M. smegmatis* was approximately 0.7. An arbitrary representation of an approximately 1:1 ratio of the MKH_2/MK pool has been shown only for the purpose of illustrating the relative changes proposed to occur in response to disruption of the pathway, and it does not represent the actual ratio as such has not been measured in *M. smegmatis*.

Disruption of the cytochrome bc_1-aa_3 pathway at either the level of the bc_1 complex or cytochrome aa_3 is proposed to increase the reduced state of both the NAD+/NADH and MKH_2/MK pools (Figure 17B). When the pathway is blocked upstream of the MK(H_2) pool by treatment with, chlorpromazine (CPZ), which has previously been demonstrated to inhibit the type II NADH dehydrogenase (NDH-II) of *M. tuberculosis* (Boshoff *et al*., 2004; and Weinstein *et al*., 2005), the NADH/NAD^+ ratio is proposed to increase further (Figure 17C). CPZ The ratio is estimated based on the previous report that *ndh* (NDH-II) mutants of *M. smegmatis* had a higher NADH/NAD^+ ratio than the wild type [≥1.0 in *ndh* mutant strains vs. 0.7 in wild type; Vilchèze *et al*., 2005)].

Effects of chlorpromazine on the transcriptome of the cytochrome bc_1 mutant

Inhibition of NDH-II disrupts the flow of electrons from NADH into the MKH_2/MK pool. It was therefore predicted that such a perturbation would affect the responsiveness of some of the genes that were differentially regulated in the Δ*qcrCAB*::*hyg* mutant of *M. smegmatis*. Inhibition of NDH-II by CPZ treatment was found to have opposing effects on the genes that were differentially expressed in the untreated mutant, with some being down-regulated and others up-regulated (Figure 17B and C). Among the up-regulated genes were *senX3* and *cydAB* which were constitutively up-regulated in the untreated mutant strain, and were further up-regulated by CPZ treatment. These results are in accordance with those previously reported for *M. tuberculosis*, in which the expression of cytochrome *bd* oxidase was up-regulated in the wild type *M. tuberculosis* treated with CPZ and other phenothiazines (Boshoff *et al*., 2004). The implications of these findings for the regulation of the *cydAB* genes are discussed in the next section. Other genes whose induction in the mutant was further elevated by CPZ include *ribA2* and *fbiA*, the function of which will be discussed below.

(A) Wild type

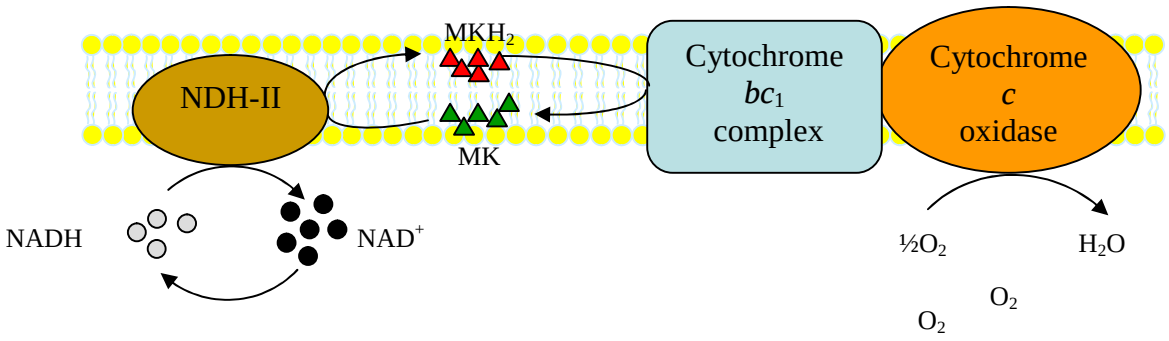

(B) bc_1-aa_3 pathway mutants

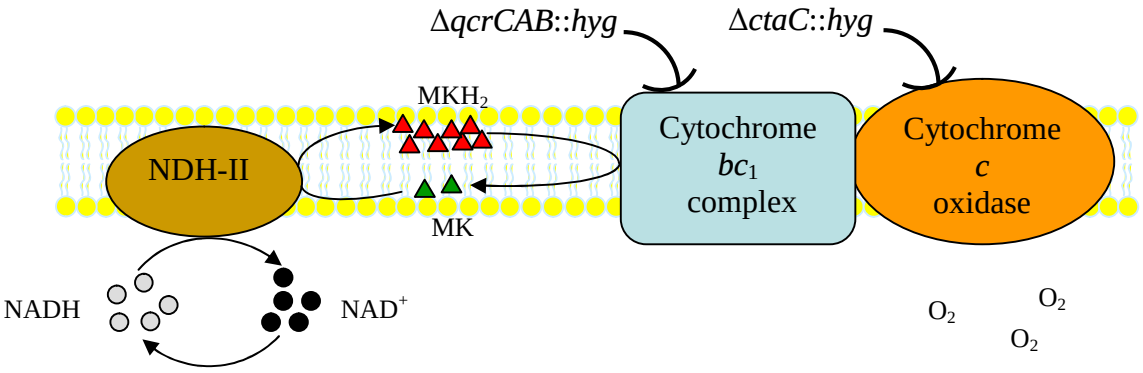

Up-regulated group 1:	**Up-regulated group 2:**	**Up-regulated group 3:**
cydA, *senX3*	*hspX*, *uspL*, *uspM*, MSMEG5227, MSMEG5215, MSMEG3958, *dosT*, *acg*, MSMEG5228	*ribA2*, *fbiA*, *mihF*, *esat6*, *cfp10*, *PPE68*

(C). CPZ-treatment of bc_1-aa_3 pathway mutants

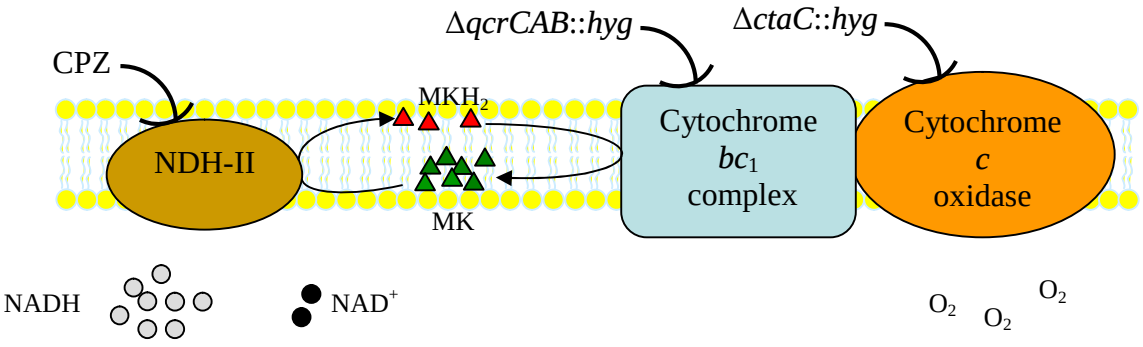

Up-regulated:	**Down-regulated group 1:**	**Down-regulated group 2:**
cydA, *senX3*, *ribA2*, *fbiA*	*hspX*, *uspL*, *uspM*, MSMEG5227, MSMEG5215, MSMEG3958, *dosT*, *acg*, MSMEG5228	*mihF*, *esat6*, *cfp10*, *PPE68*

Figure 17. Aerobic respiration through the cytochrome bc_1-aa_3 pathway in *M. smegmatis*, and effects of its disruption on the redox states of the cofactors NAD(H) and MK(H_2), and on gene expression. For the sake of simplicity, the type I NADH dehydrogenase, succinate dehydrogenase and the pathway terminating in cytochrome *bd* oxidase have not been shown. The NADH (●) / NAD^+ (●) and MKH_2 (▲) / MK (▲) ratios are not representative of the actual ratios as these were not measured, but are used to illustrate the differences proposed to occur in response to disturbance of electron flow. **(A)** In the wild type, the NADH/NAD^+ ratio is approximately 0.7 (Vilchèze *et al*., 2005). Electrons are passed from NADH into the MKH_2/MK pool from where they are passed, via the cytochrome bc_1 complex, to cytochrome aa_3 oxidase, which reduces O_2 to H_2O. **(B)** Disruption of the pathway at level of either the cytochrome bc_1 complex (Δ*qcrCAB*::*hyg* mutant) or cytochrome aa_3 oxidase (Δ*ctaC*::*hyg* mutant) blocks electron flow to O_2, resulting in an increase in the reduced forms of the cofactors NADH and MKH_2, and up-regulation of the three groups (boxes) of genes. **(C)** Treatment of the mutants with CPZ is proposed to have opposing effects on the cofactors as well as on the differentially expressed genes (boxes). The NADH/NAD^+ ratio is further increased while the MKH_2/MK ratio is proposed to drop.

Among the genes down-regulated in response to CPZ treatment were genes that are known to be DosR-regulated in *M. smegmatis* and which appear to be expressed at slightly elevated levels in the untreated mutant strain (Figure 17B, group 2 and Figure 17C, group 1). This reversed expression resulting from blockage of electrons into the MKH_2/MK pool as opposed to disruption of electron flow out of the MKH_2/MK pool indicated that the genes were responding to a change in the redox state of the respiratory chain, or to the secondary effects of such a change. These data suggest a cofactor whose redox state changes, in the Δ*qcrCAB*::*hyg* mutant, in response to blockage of electrons into the MK(H_2) pool. Whereas the NADH/NAD^+ ratio of the mutant is expected to increase further in the presence of CPZ, the MKH_2/MK ratio is proposed to decrease relative to the untreated mutant (Figure 17B and C). Based on this, it is tempting to speculate that the DosR-DosS/DosT system senses a change in the redox state of the MKH_2/MK pool or indirect effects thereof. However, Boshoff *et al* (2004) did not find any correlation between induction of the DosR regulon and changes in the MKH_2/MK ration in *M. tuberculosis*, suggesting that the redox state of other electron carriers such as cytochromes, flavoproteins and iron-sulfur proteins may be sensed instead. Such possibilities remain to be investigated. Other genes whose expression was reversed by disruption of electron flow into the MKH_2/MK pool include *mihF*, *esat6*, *cfp10* and *PPE68*, the implications of which are discussed below.

The overall effect of CPZ on the Δ*qcrCAB*::*hyg* mutant was indicative of a reduction in the metabolic activity of this organism, with more than 30% of the down-regulated genes encoding ribosomal proteins, as well as a number of genes involved in gene expression (transcription and translation). The reduced metabolic activity may be indicative of a reduced availability of energy to support the metabolic activities of the cell, which is also demonstrated by the accompanying down-regulation of some of the genes that encode F_0F_1 ATP synthase (*atpH*, *atpB*, *atpE*).

The regulation of cytochrome *bd* oxidase in *M. smegmatis*

A possible role for SenX3-RegX3 in the regulation of cytochrome bd *oxidase*

Although the *cyd* genes encoding cytochrome *bd* oxidase have been shown to be up-regulated in response to O_2 depletion in mycobacteria (Kana *et al*., 2001; Boshoff *et al*., 2004; Voskuil *et al*., 2004), these genes do not form part of the dormancy (DosR) regulon, whose induction has been proposed to be mediated by changes in the redox state of the cell (Boshoff *et al*., 2004). The constitutive up-regulation of cytochrome *bd* oxidase in the Δ*qcrCAB*::*hyg* and Δ*ctaC*::*hyg* mutants confirmed that this oxidase does respond to change(s) in the electron flux through the respiratory chain, but in a manner that is independent of DosR. The concomitant induction of *senX3* alongside *cydAB* in aerated cultures of both the Δ*qcrCAB*::*hyg* and Δ*ctaC*::*hyg* mutants of *M. smegmatis* (Figure 17B, group 1) was interesting in light of the fact that *cydB* was previously reported to be up-regulated in a *senX3-regX3* mutant of *M. tuberculosis* grown to late exponential phase under aerobic conditions, which suggested that this gene may be part of the SenX3-RegX3 regulon (Parish *et al*., 2003). The co-induction of the *senX3* and *cyd* genes in the Δ*qcrCAB*::*hyg* and Δ*ctaC*::*hyg* mutants (this work) would suggest that this two-component regulatory system activates expression of the *cyd* genes in response to a change in the electron flux through the respiratory chain, such as that caused by blockage of electron flow through the cytochrome bc_1-aa_3 pathway.

The proposed signal for SenX3-RegX3

The nature of the signal sensed by SenX3 is not yet known. Blockage of electron flow through the cytochrome bc_1-aa_3 pathway is proposed to cause an increase in the NADH and MKH_2 cofactors relative to their oxidized forms as discussed above (Figure 17B). Therefore, the possibility that both *senX3* and *cydAB* were up-regulated in response to the redox state(s) of either one or both of these cofactors is discussed in this section. A number of transcriptional regulators of *cydAB* gene expression that sense the redox states of the above cofactors have been described in other bacteria. In *E. coli*, the ArcB-ArcA system has been demonstrated to activate expression of the cytochrome *bd* oxidase in response to an increase in the reduced quinol form (Georgellis *et al*., 2001a; Alexeeva *et al*., 2003; Malpica *et al*., 2004). Interestingly, the *senX3-regX3* genes in mycobacteria have been shown to exhibit the highest homology to those encoding the ArcB-ArcA system in *E. coli*, suggesting that SenX3-RegX3 may similarly respond to the oxidative stress generated through respiration (Rickman *et al*., 2004). Another example of a redox sensor that regulates *cyd* gene expression is the Rex repressor found in *S. coelicolor*, which modulates expression of cytochrome *bd* oxidase in response to an increase in the $NADH/NAD^+$ ratio (Brekasis and Paget, 2003). Although no *rex* homologues have been found in the genomes of mycobacteria (Brekasis and Paget, 2003), the possibility of existence of a regulator that responds to the redox state of the $NADH/NAD^+$ pool cannot be excluded.

The results obtained with the expression analysis of CPZ-treated Δ*qcrCAB*::*hyg* and Δ*ctaC*::*hyg* mutants of *M. smegmatis* in this study are more in favor of the proposal that SenX3 senses the redox state of the $NADH/NAD^+$ pool than that of the MKH_2/MK pool. The constitutive up-regulation of *cyd* genes in the above mutants under highly aerobic conditions, suggests that the signal to which these genes (and probably *senX3-regX3*) respond – a change in the redox state of electron carriers and/or a change in the transmembrane potential in the respiratory chain – is sustained, but can be modulated by CPZ-mediated disruption of electron flow into the MKH_2/MK pool. The observed increase in the magnitude of induction of both *senX3* and *cydAB* in the Δ*qcrCAB*::*hyg* and Δ*ctaC*::*hyg* mutants in response to CPZ treatment suggested that the signal to which these genes responded was amplified by CPZ treatment. The increased signal is

consistent with the proposed increase in the NADH/NAD^+ ratio (Figure 17B and C). In contrast, CPZ treatment would prevent further reduction of the MKH_2/MK pool, and may therefore result in a decreased MKH_2/MK ratio in the CPZ treated mutant compared to the untreated mutant, which is proposed to have an opposing effect to what was observed of the ***senX3*** and ***cydAB*** expression. Nonetheless, the possibility that these genes may respond to a change in the redox states of cofactors other than these two cannot be excluded.

Other adaptations to re-routing the electron flux through cytochrome *bd* oxidase

A significant number of genes up-regulated in both the Δ***qcrCAB***::***hyg*** and Δ***ctaC***::***hyg*** mutants are involved in intermediary metabolism and respiration, including genes such as ***ribA2*** and ***fbiA***. The up-regulation of genes of this type suggests that the mutants adapt by switching on or increasing the availability of alternative electron carriers. ***ribA2*** is the most highly up-regulated gene in the Δ***qcrCAB***::***hyg*** mutant and is also highly up-regulated in the Δ***ctaC***::***hyg*** mutant. This gene encodes an important bifunctional enzyme of the riboflavin biosynthesis pathway, GTP cyclohydrolase II/3,4-dihydroxy-2-butanone-4-phosphate synthase. The ***ribA2*** gene has been shown to be essential in the pathogenic actinomycete ***Rhodococcus equi*** (Ashour ***et al.***, 2003) and suggested to be essential in ***M. tuberculosis*** (Sassetti ***et al.***, 2003). Riboflavin is a precursor of the flavin coenzymes FMN (flavin mononucleotide) and FAD (flavin adenine dinucleotide), which form important components in some of the electron transport chain enzymes, including most if not all of the dehydrogenases that transfer reducing equivalents to the MKH_2/MK pool. The deazaflavin cofactor F420 encoded for by ***fbiA*** has been proposed to be involved in low-redox potential electron transfer reactions associated with anaerobiosis in ***M. tuberculosis*** (Boshoff and Barry, 2005). It is proposed that ***M. smegmatis*** may switch to such electron transfer reactions as a result of blockage of its aerobic respiratory pathways. Similar to ***cydAB*** and ***senX3***, the magnitude of the expression of ***ribA2*** and ***fbiA*** further increased in response to CPZ treatment (Figure 17B and C), suggesting that there was an increase in the demand for flavin-containing enzymes under the conditions tested.

The marked up-regulation of ***mihF*** in these mutants is also notable as this gene has been reported to be up-regulated in ***M. smegmatis*** and ***M. bovis*** BCG prior to

stationary phase (Pedulla and Hatfull, 1998). *mihF* has been shown to be essential in *M. smegmatis* (Pedulla and Hatfull, 1998) and is inferred as essential in *M. tuberculosis* (Sassetti *et al*., 2003). Since intracellular MihF protein levels peaked just prior to entry into stationary phase and then dropped in both *M. smegmatis* and *M. bovis* BCG, it was proposed that this protein may be involved in the regulation of genes required for stationary phase survival, as had been suggested for the *E. coli* orthologue (Pedulla and Hatfull, 1998). The up-regulation of this gene in the Δ*qcrCAB*::*hyg* and Δ*ctaC*::*hyg* mutants suggests that blockage of the bc_1-aa_3 respiratory pathway generates a cellular environment that resembles in at least some respects, that occurring during entry into the stationary phase.

Also of note is the up-regulation of *esat6* and *cfp10* in both the Δ*qcrCAB*::*hyg* and Δ*ctaC*::*hyg* mutants. These genes are found within the RD1 region of *M. tuberculosis*, the loss of which has been shown to mimic the attenuation observed in *M. bovis* BCG (Lewis *et al*., 2003). These genes encode secreted proteins, which are strongly immunogenic (Lewis *et al*., 2003; Brodin *et al*., 2005; Fortune *et al*., 2005; Renshaw *et al*., 2005). The proteins form a tight complex (Brodin *et al*., 2005; Fortune *et al*., 2005; Renshaw *et al*., 2005) whose specific binding to the host cell surface is proposed to signal modulation of the host cell behavior to the pathogen's advantage (Renshaw *et al*., 2005). A region syntenous with the RD1 region of *M. tuberculosis* was recently reported in *M. smegmatis* and has been implicated in regulation of DNA transfer in this organism (Flint *et al*., 2004). Complementation of the conjugation suppression phenotype of *M. smegmatis* RD1 mutants with the *M. tuberculosis* RD1 suggested that the RD1 regions of both organisms are functionally equivalent (Flint *et al*., 2004). The *M. smegmatis* homologue of *PPE68* (Rv3873) was also up-regulated in both bc_1-aa_3 pathway mutants. This gene is located immediately upstream of *cfp10* within the RD1 loci of both *M. tuberculosis* and *M. smegmatis*, and it has been proposed to be involved in the export of ESAT-6 and CFP-10 proteins (Brondin *et al*., 2004). Interestingly, the up-regulation of *PPE68*, *esat6* and *cfp10* was reversed by CPZ in both Δ*qcrCAB*::*hyg* and Δ*ctaC*::*hyg* mutants. The molecular and physiological link between expression of these genes and perturbation of the respiratory chain in *M. smegmatis* is presently unclear, but may be associated with ATP synthesis, since export of ESAT-6 and CFP-10 has been proposed to involve an

ATPase encoded within the RD1 locus by Rv3870, Rv3871 and Rv3877, in an ATP hydrolysis dependent process (Brodin *et al*., 2004).

Evidence for reduced metabolic activity in the cytochrome bc_1-aa_3 *pathway mutants*

A significant number of up-regulated genes in both the Δ*qcrCAB*::*hyg* and Δ*ctaC*::*hyg* mutants encoded hypothetical proteins, making it difficult to interpret the full extent of the adaptive changes that occur in response to re-routing of electron flux through the menaquinol oxidase. Nevertheless, most of the genes whose expression was down-regulated in both mutants are involved in information pathways (transcription and DNA repair) and cell wall and cell processes, suggesting that inactivation the cytochrome bc_1-aa_3 pathway is associated with an overall metabolic shift-down. This is consistent with a lower availability of energy due to a switch to the bioenergetically less-efficient cytochrome *bd* oxidase.

Differences in the transcriptomes of the cytochrome bc_1 and aa_3 mutants

Although the transcriptomes of these two mutants were highly comparable, there were some notable differences. For example, the *lytB2* gene is down-regulated in the Δ*qcrCAB*::*hyg* mutant but not Δ*ctaC*::*hyg* mutant. *lytB2* is involved in the nonmevalonate pathway for the biosynthesis of terpenoids, and hence, in the biosynthesis of menaquinone (Rohdich *et al*., 2002). Similarly, the most highly down-regulated gene, *rnpA* (which encodes a ribonuclease P protein) in the Δ*ctaC*::*hyg* mutant is not differentially regulated in the Δ*qcrCAB*::*hyg* mutant. Another notable difference, which would, however, require validation by RT-PCR, is that seen in the expression of the DosR-regulated genes in these two mutants, where the expression appeared to be higher in the Δ*qcrCAB*::*hyg* than in the Δ*ctaC*::*hyg* mutant One possible explanation for this difference is that in the cytochrome aa_3 mutant, electron flow can be reversed through the bc_1 complex, as has been shown for *P. denitrificans* (van der Oost *et al*., 1995).

What can be learnt about mycobacterial respiration from this study?

This study has provided the first experimental evidence for the presence and functionality of the mycobacterial aerobic respiratory pathway that transports electrons from the

MKH_2/MK pool to aa_3-type cytochrome *c* oxidase via the cytochrome bc_1 complex (Figure 3.3; results section). The branch terminating in the aa_3-type cytochrome *c* oxidase is the major aerobic respiratory pathway in mycobacteria and its disruption leads to severe growth attenuation that is accompanied by a marked constitutive up-regulation of cytochrome *bd* oxidase. Characterization of mutants in this pathway allowed for speculation about the possible signals that may lead to the expression of the branch terminating in the alternate, *bd*-type oxidase.

Expression profiling of the bc_1-aa_3 pathway mutants suggested that there might be an overlap in the signals and/or regulatory networks that govern adaptation of *M. smegmatis* to re-routing of electron flow through the cytochrome *bd* oxidase and hypoxia. The primary or secondary signal(s) for all of these responses appear to derive from changes in the redox status of the cell resulting from use of alternative respiratory pathways. However, the full extent and significance of this overlap can only be established once the complete hypoxia responses of this organism have been defined. A significant number of differentially regulated genes in the mutants encode proteins of unknown functions (hypotheticals) therefore obscuring what may be important adaptations that would probably improve our understanding of the metabolism of this organism.

Although caution has to be exercised in extrapolating findings from the fast-growing non-pathogenic *M. smegmatis* to the slow-growing pathogen, *M. tuberculosis*, it is tempting to speculate that the respiratory chain of *M. tuberculosis* plays a very important role in modulating the metabolic activities of this organism in response to changing environmental conditions. Based on the high degree of sequence similarity and the relatedness in the adaptive responses reported for *M. smegmatis* in this work to those reported previously for *M. tuberculosis*, the respiratory chains of both organisms are proposed to be equivalent in function. As observed in *M. smegmatis*, disruption of electron flow through the cytochrome bc_1-aa_3 branch of *M. tuberculosis* using inhibitors of cytochrome *c* oxidase resulted in up-regulation of cytochrome *bd* oxidase (Boshoff *et al*., 2004). This demonstrates that in both organisms, the latter oxidase compensates for the loss of functionality of the main aerobic branch. The failure to recover allelic exchange mutants in the cytochrome bc_1-aa_3 pathway of *M. tuberculosis* H37Rv suggests

that they were severely impaired for growth or nonviable under the conditions tested. In support of this conclusion, the transposon mutations in the genes encoding the bc_1 complex (*qcrCAB*) and the aa_3-type cytochrome *c* oxidase (*ctaC, ctaD, ctaE*) were under-represented in high-density mutagenized libraries of *M. tuberculosis*, as determined by transposon site hybridization (Sassetti *et al.*, 2003). This apparent essentiality of the cytochrome bc_1-aa_3 pathway in *M. tuberculosis* may be due to an inability of its respiratory network to adapt in a manner analogous to that of *M. smegmatis*. However, *cyd* gene expression in *M. tuberculosis* has been shown to be highly responsive to interference with the machinery that maintains the proton motive force, as evidenced by its up-regulation by inhibitors of aa_3-type cytochrome *c* oxidase and chemicals that affect its maturation (Boshoff *et al*., 2004), during adaptation to hypoxia (Boshoff *et al*., 2004; Voskuil *et al.*, 2004), by growth on palmitate (Boshoff *et al*., 2004), and by protonophores (Boshoff *et al*., 2004).

The role of the respiratory chain in the pathogenesis of *M. tuberculosis*

The respiratory chain of *M. tuberculosis* has been proposed to play an important role in the pathogenesis of this organism (Boshoff *et al.*, 2005). The picture that has emerged from differential gene expression analysis of bc_1-aa_3 pathway mutants of *M. smegmatis* supports this view. The induction of homologues of genes previously shown to be involved in *M. tuberculosis* virulence in response to disruption of the respiratory chain of *M. smegmatis* suggests that the respiratory chain may play a central role in guiding and maintaining survival of *M. tuberculosis* in the host. While the general response is indicative of a metabolic shift-down, part of which may be aimed at conserving energy, up-regulation of the genes implicated in virulence such as ESAT-6, CFP-10, PPE68, SenX3, and Rv3130c, suggests that *M. tuberculosis* may rely on changes in its respiratory chain components to detect its environment. For instance, Rv3130c (*tgs1*), encoding a triacylglycerol synthase with the highest activity in *M. tuberculosis* exposed to hypoxia or NO (Schnappinger *et al*., 2003; Daniel *et al*., 2004), was shown to be one of the first genes induced during phagosome formation. *M. tuberculosis* stores triacylglycerols as a source of fatty acids, which may later be used for energy production during persistence

(Daniel *et al*., 2004; Boshoff *et al*., 2005). ESAT-6 and CFP-10 have been proposed to be required for *M. tuberculosis* escape from the phagosome (Fortune *et al*., 2005).

Future studies

The present study has confirmed the presence of the cytochrome bc_1-aa_3 branch of the aerobic respiratory chain in *M. smegmatis* and demonstrated its importance for the growth of this organism. While the genetic methods employed assisted in unraveling to a large extent the genetic components of this pathway and the effects on gene expression of disrupting such, the biochemical aspect of these effects are not yet fully understood. Studies aimed at analyzing the concentrations of the different components of the respiratory chain, such as proteins, quinones and cofactors, can help to determine the physiological relevance of each component. Spectral analysis of membrane fractions for cytochrome composition would help to determine, for instance, whether the assembly of cytochrome bc_1 requires presence of a functional cytochrome *c* oxidase as been reported to be the case for *C. glutamicum* (Niebisch and Bott, 2003). The concentrations of quinones and cofactors such as NAD(H) would answer the questions of whether or not their redox states serve as signals for induction of the DosR-DosS/DosT and SenX3-RegX3 two-component regulatory systems. Finally, further studies will be required in order to elucidate the functions of the *ctaDII* and *ythAB* genes in the respiratory chain of *M. smegmatis*.

5. APPENDICES

APPENDIX A: Abbreviations

aa	amino acid
ADC	albumin dextrose catalase
Amp	ampicillin
aph	aminoglycoside phosphotransferase gene (Km-resistance)
ATP	adenosine triphosphate
BCG	bacille Calmette-Guerin
bla	β-lactamase gene (Ap-resistance)
bp	base pair
BSA	bovine serum albumin
CbdO	cytochrome *bd* oxidase
CcO	cytochrome *c* oxidase
CFU	colony forming units
$CHCl_3$/IAA	choloroform/isoamyl alcohol
CHP	conserved hypothetical protein
CPZ	chlorpromazine
CTP	cytosine triphosphate
cyt	cytochrome
DCO	double cross over
DE	differentially expressed
DMSO	dimethylsulphoxide
DNA	deoxyribonucleic acid
dNTPs	deoxyribonuceotide triphosphates
DOTS	directly observed therapy, short-course
DTT	dithiothreitol
EDTA	ethylenediaminetetraacetic acid
Fe-S	iron-sulphur
HIV	human immunodeficiency virus
Hyg	hygromycin

hyg	Hyg-resistance gene
IPTG	isopropyl-β-D-galactopyranoside
kb	kilobase(s)
Km	kanamycin
KO	knockout
LA	(see Appendix C)
lacZ	β-galactosidase gene
MADC-Tw	(see Appendix C)
MDR	multidrug resistance
MMRU	Molecular Mycobacteriology Research Unit
NaOAc	sodium acetate
NO	nitric oxide
NRP	nonreplicating persistence
O_2	oxygen
OADC	oleic albumin dextrose catalase
OD	optical density
OD_{600}	optical density at wavelength 600 nm
ONPG	2-nitrophenyl-β-galactopyranoside
ORF	open reading frame
^{r}	resistant
RNA	ribonucleic acid
RNase	ribonuclease
RNIs	reactive nitrogen intermediate
ROI	reactive oxygen intermediate
sacB	*B. subtilis* levansucrase
SCO	single cross over
SDS	sodium dodecyl laurel sulphate
TB	tuberculosis
Tween	polyoxyethylene sorbitan monooleate
X-Gal	5-bromo-4-chloro-3-indolyl-β-D-thiogalactopyranoside

APPENDIX B: Media and solutions

Media

Luria Bertani broth (LB)

1% tryptone, 0.5% yeast extract, 0.5% sodium chloride.

Luria Bertani agar plates (LA)

1% tryptone, 0.5% yeast extract, 0.5% sodium chloride, 1.5% agar.

2 × TY broth

1.6% tryptone, 1% yeast extract, 0.5% sodium chloride.

Middlebrook-Tween broth (MADC-Tw) for *M. smegmatis*

0.47% Middlebrook 7H9, 0.2% glycerol, 0.085% sodium chloride, 0.2% glucose, 0.05% Tween 80. [Sodium chloride and glucose were autoclaved separately, Tween was filter sterilized separately as a 20% stock, and the components were added to the autoclaved Middlebrook 7H9 plus glycerol].

Middlebrook-Tween broth (MADC-Tw) for *M. tuberculosis*

0.47% Middlebrook 7H9, 0.2% glycerol, 10% Middlebrook ADC, 0.05% Tween. [sterile Middlebrook ADC and Tween were added to the autoclaved Middlebrook 7H9 plus glycerol after cooling to approx. 60°C].

Middlebrook 7H10 agar plates

1.8% Middlebrook 7H10, 0.5% glycerol, 10% Middlebrook OADC. [Sterile OADC was added to the autoclaved media after cooling to approx. 60°C].

Solutions

Antiobiotic stocks

Ampicillin: 35 mg/ml in 50% ethanol.

Kanamycin: 50 mg/ml in water.

Hygromycin B: 50 mg/ml in phosphate buffered saline (as supplied by Roche).

50 × Denhardt's reagent

1% Ficoll (Type 400), 1% polyvinylpyrrolidone, 1% BSA. Filter sterilized.

20 × SSC

17.53% NaCl, 8.82% sodium citrate; adjust pH to 7.0 with HCl.

DEPC-water

0.1% diethylpyrocarbonate (DEPC) in double distilled water; incubated overnight in fume hood and then autoclaved.

RNA loading buffer

50% glycerol, 1 mM sodium EDTA, 0.4% bromophenol blue; in DEPC-water.

Calculation for PCR primer-pair annealing temperature, T°

$T° = [(T_{m1} + T_{m2})/2] -6$

where $T_m = 2(A+T) + 4(G+C)$

T_{m1} = forward primer and T_{m2} = reverse primer.

APPENDIX C: Plasmid Maps

Vectors commercially available and those obtained from other research groups:

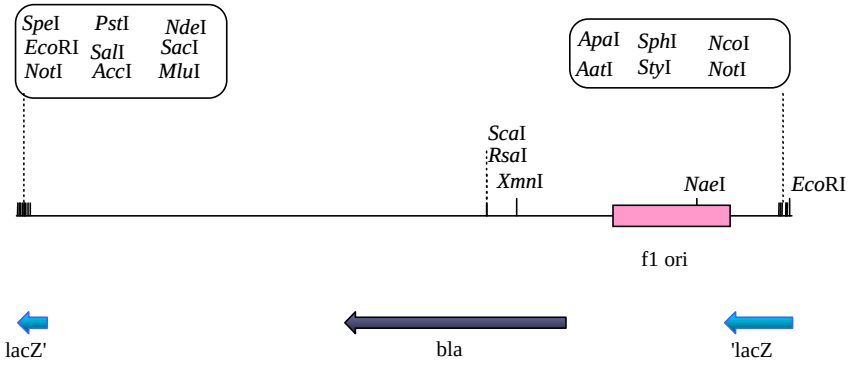

pGEMTEasy (3017 bps)

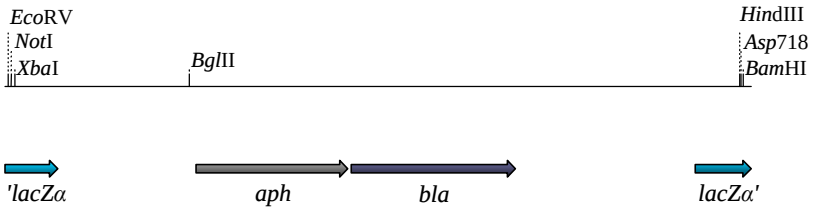

pCR2.1-TOPO* (3908 bp)

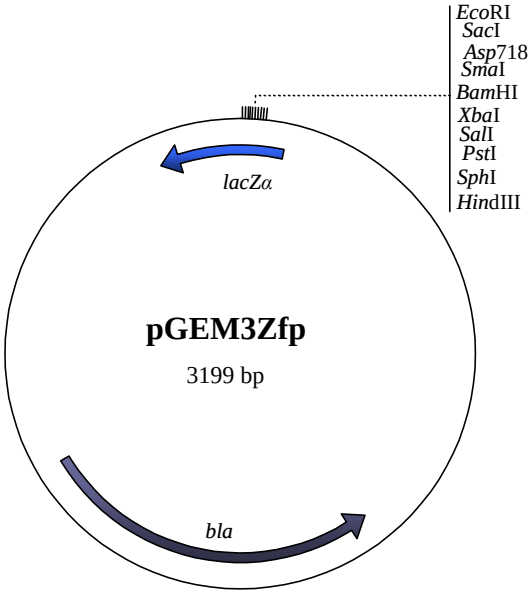
EcoRI
SacI
Asp718
SmaI
BamHI
XbaI
SalI
PstI
SphI
HindIII
lacZα
pGEM3Zfp
3199 bp
bla

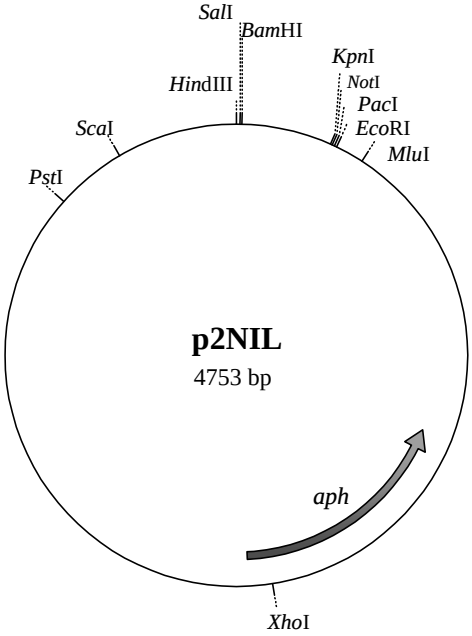
SalI
BamHI
KpnI
NotI
HindIII
PacI
EcoRI
ScaI
MluI
PstI
p2NIL
4753 bp
aph
XhoI

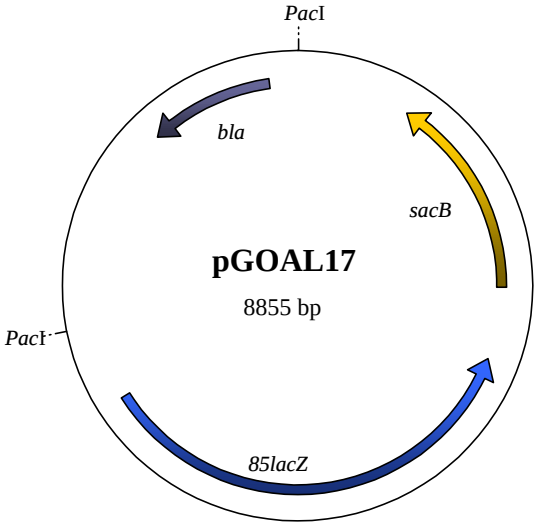
PacI
bla
sacB
pGOAL17
8855 bp
PacI
85lacZ

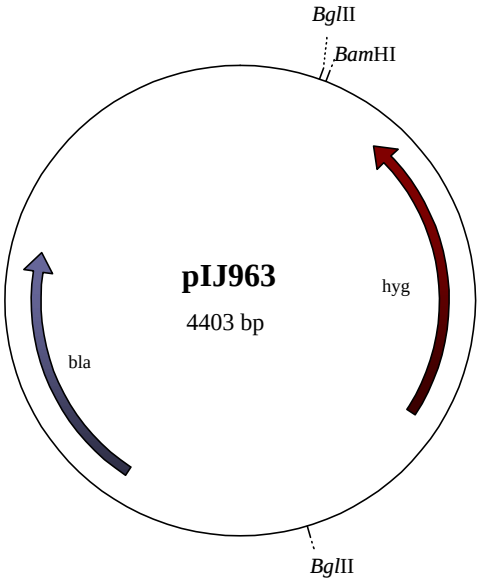
BglII
BamHI
pIJ963
4403 bp
hyg
bla
BglII

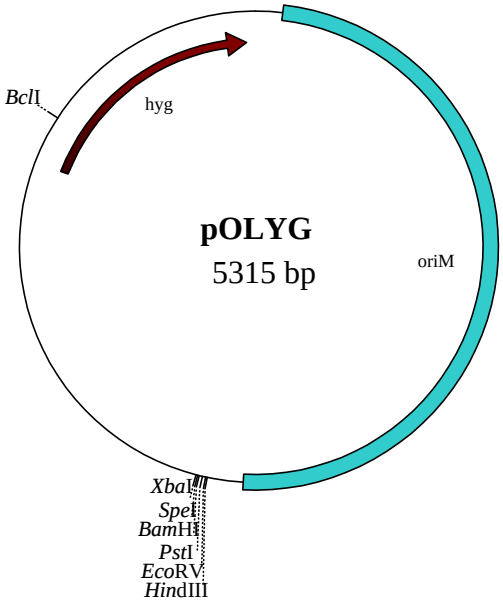
BclI
hyg
pOLYG
5315 bp
oriM
XbaI
SpeI
BamHI
PstI
EcoRV
HindIII

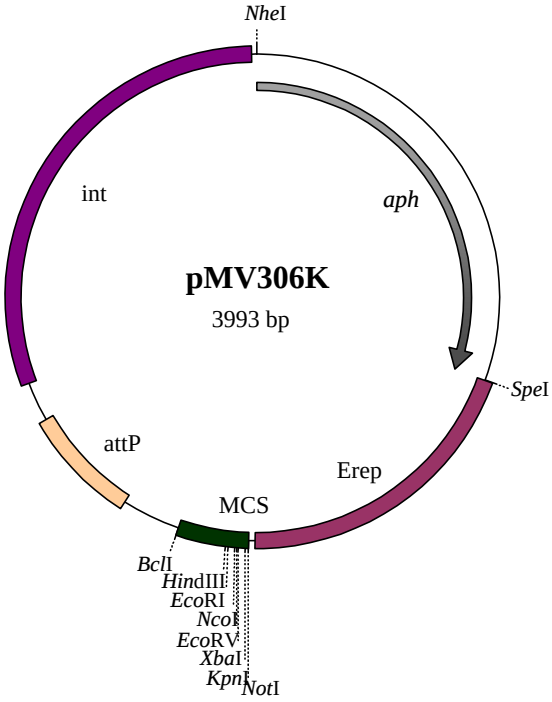
NheI
int
aph
pMV306K
3993 bp
SpeI
attP
Erep
MCS
BclI
HindIII
EcoRI
NcoI
EcoRV
XbaI
KpnI
NotI

Intermediate plasmids constructed in this study:

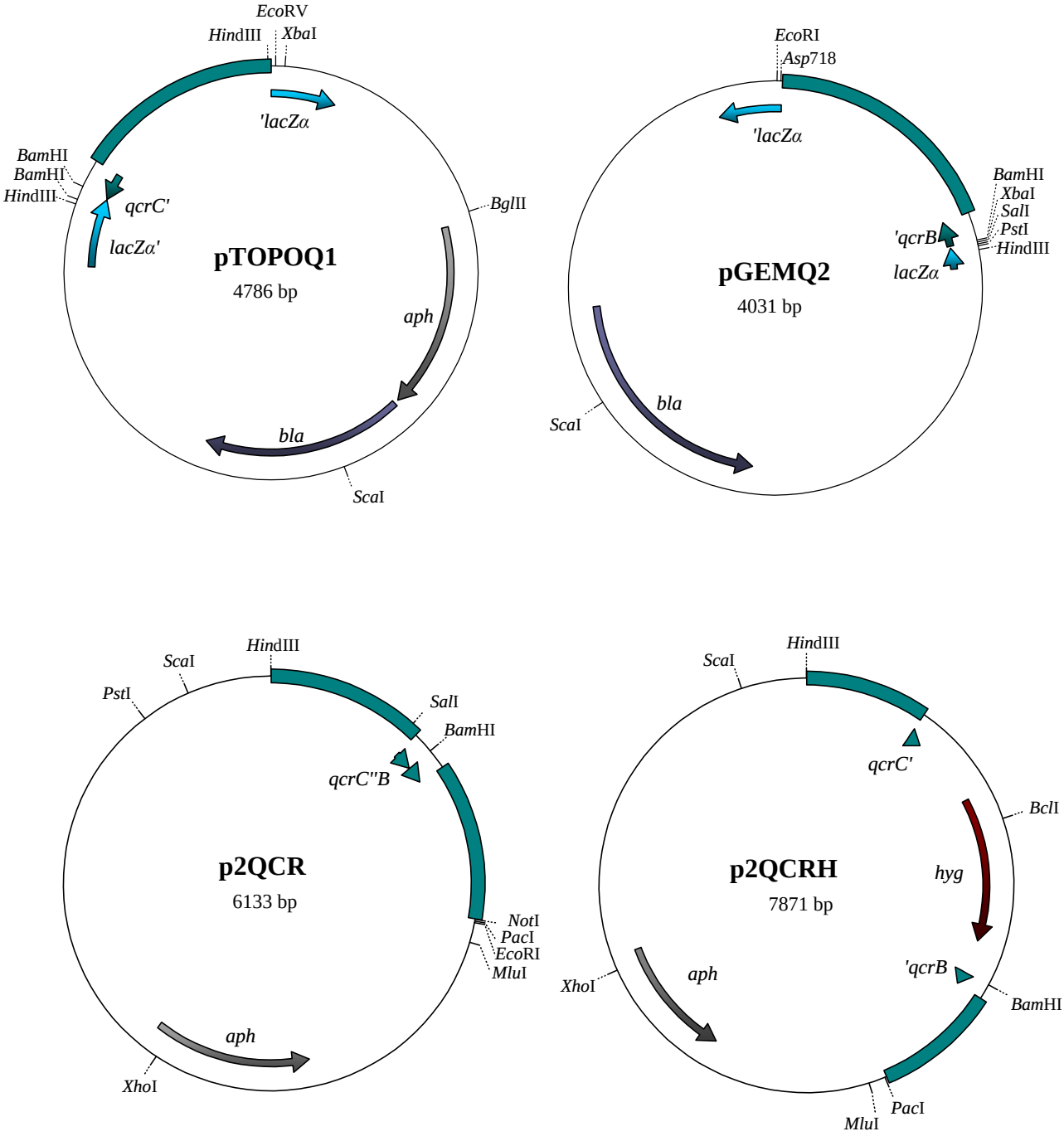

For construction of M. smegmatis qcrCAB knockout vector

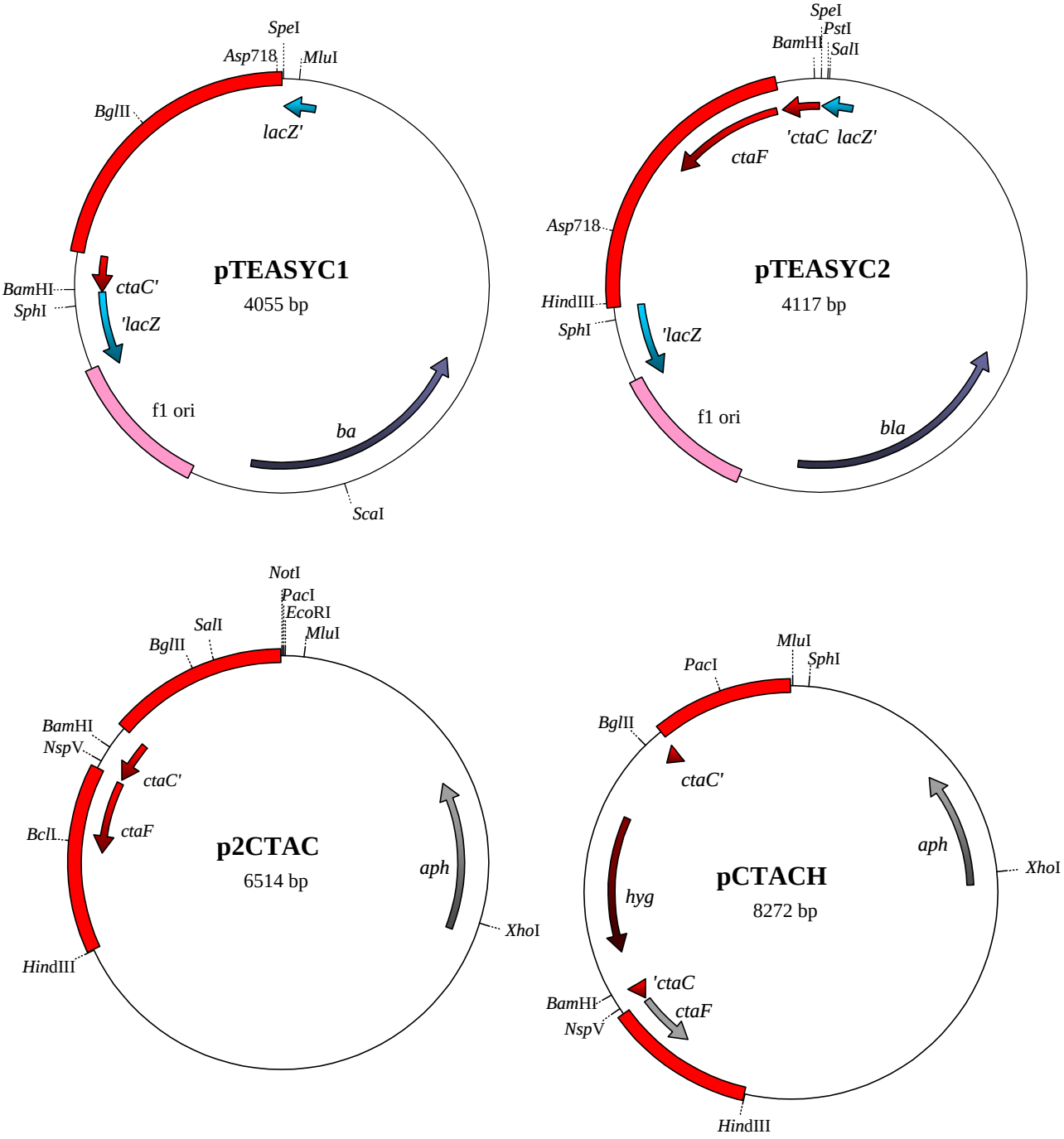

For construction of M. smegmatis ctaC knockout vector

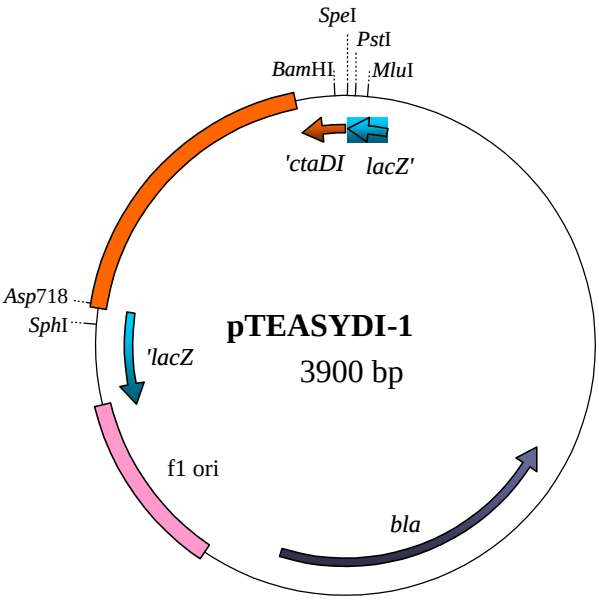

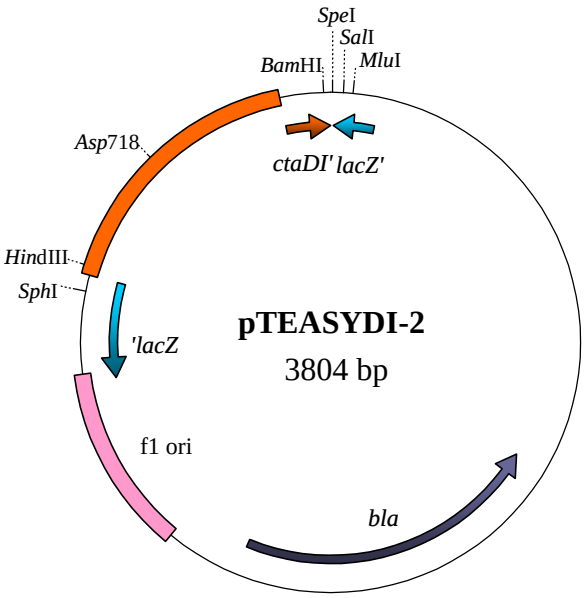

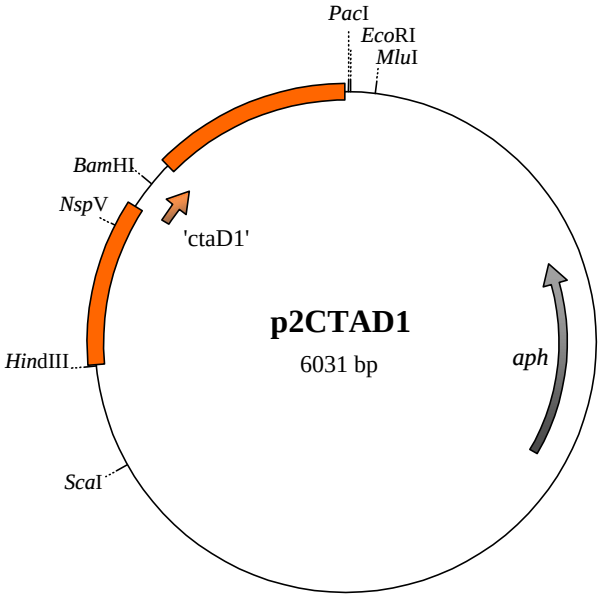

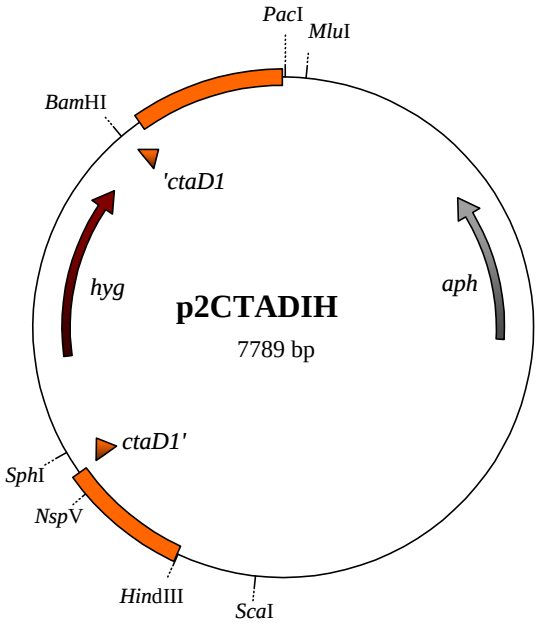

For construction of M. smegmatis ctaDI knockout vector

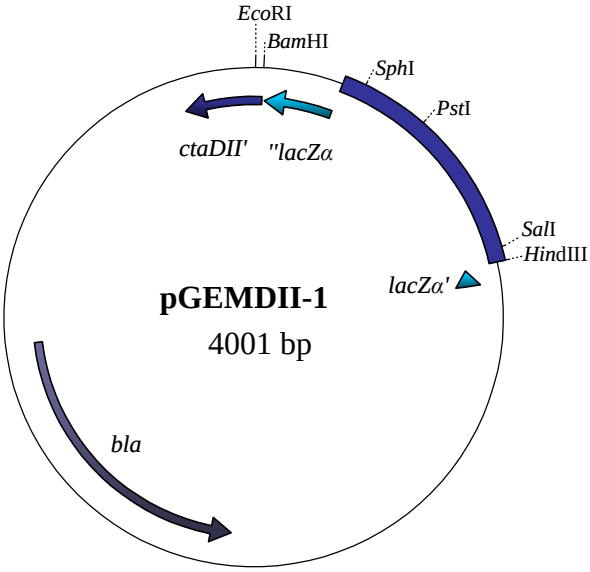

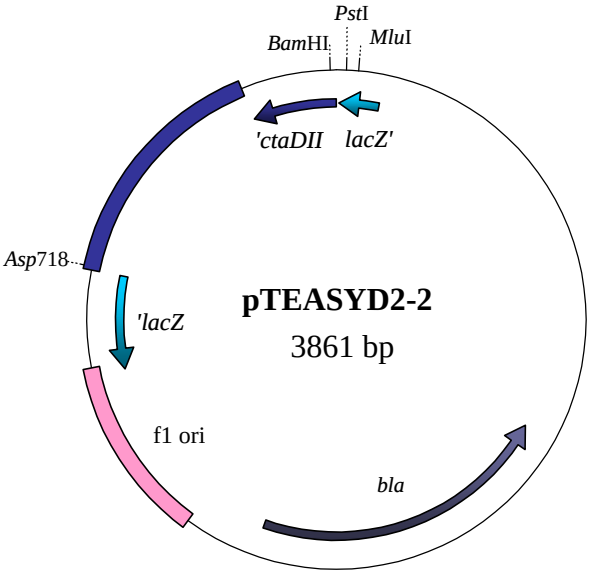

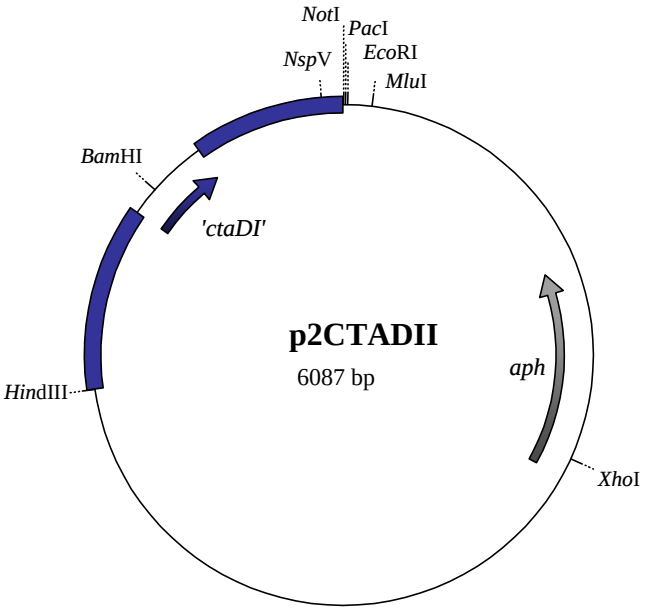

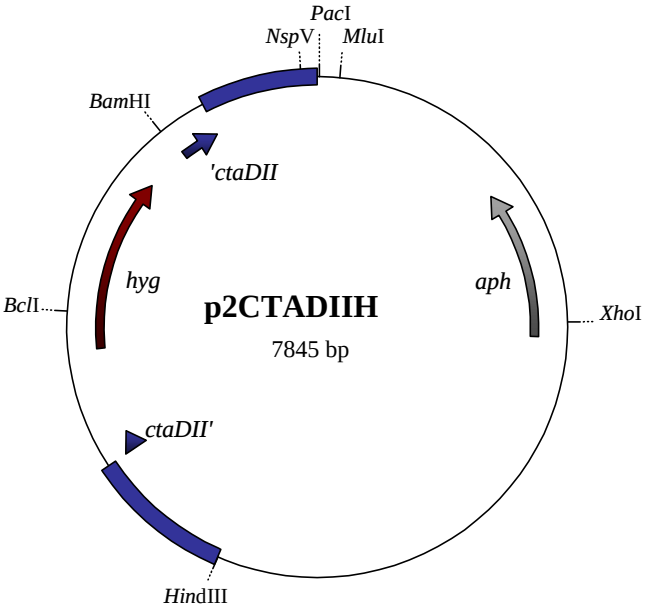

For construction of M. smegmatis ctaDII knockout vector

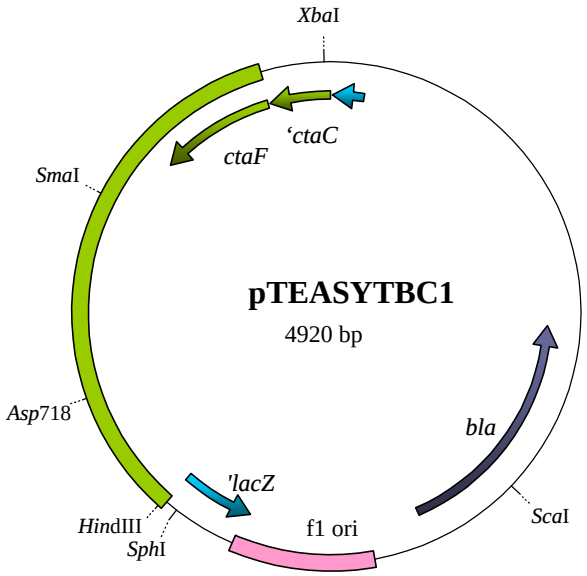

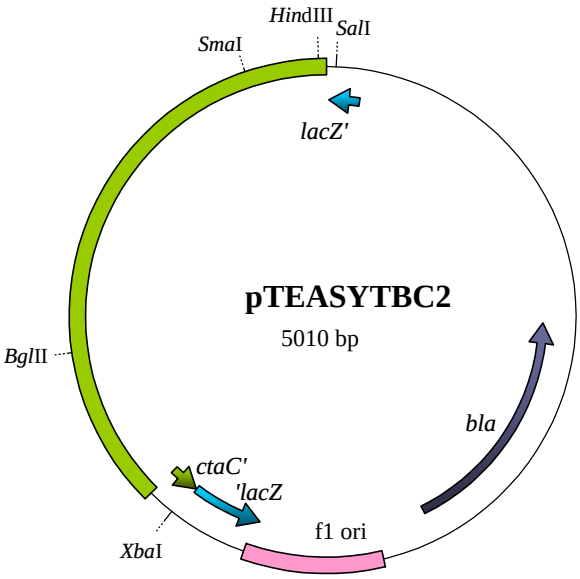

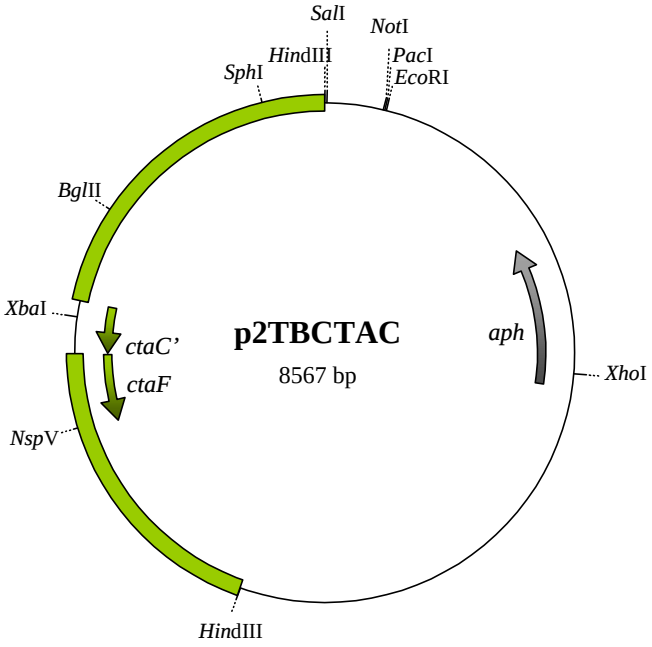

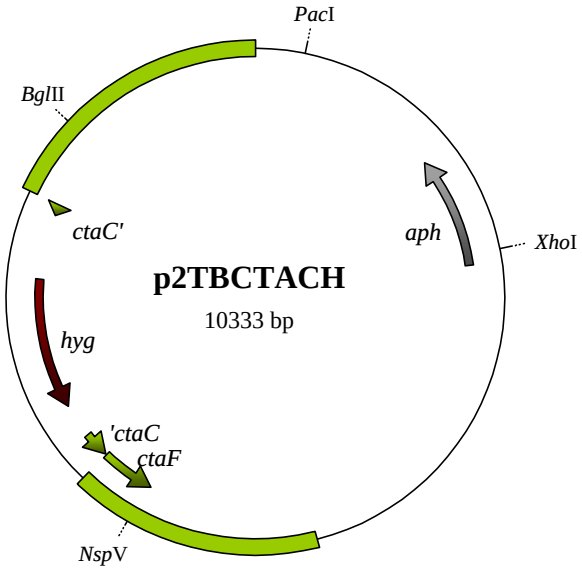

For construction of M. tuberculosis ctaC knockout vector

APPENDIX D: DNA microarray supplementary information

Table D1. *M. smegmatis* Δ*qcrCAB*::*hyg* genes induced during growth at 21% oxygen as analyzed on the partial-genome amplicon array (Table from produced from Dr D. Powell's analyses)

ID	Gene	TIGR name	Function (as per Leproma & Tuberculist)	M	P value	Class
ribA	*ribA2*	MSMEG3082	Probable riboflavin biosynthesis protein	-2.301	0.0020	7
ML2274		MSMEG3498	Probable conserved secreted protein	-1.914	0.0072	3
mihF	*mihF*	MSMEG3063	Putative integration host factor	-1.764	0.0003	2
glgC	*glgC*	MSMEG5067	glucose-1-phosphate adenyl-transferase	-1.753	0.0072	7
ML1835		MSMEG6527	CHP	-1.556	0.0030	10
ML0510		MSMEG3035	CHP	-1.444	0.0004	10
ML0886		MSMEG4257	possible glycosyl transferase	-1.430	0.0024	7
ML1312		MSMEG4598	CHP	-1.229	0.0001	10
argD-g	*argD*	MSMEG2446	probable acetylornithine aminotransferase	-1.027	0.0033	7
gabD-q	*gabD*	MSMEG2554	probable aldehyde dehydrogenase	-1.005	0.0052	7
Rv3134c	*uspL*	MSMEG5230	Universal stress protein	-0.990	0.0098	10
Rv1623c	*cydA*	MSMEG3243	Cytochrome bd oxidase subunit I	-0.931	0.0069	7
ML1926		MSMEG0828	putative tuberculin-related protein	-0.915	0.0058	3
Rv1592c		MSMEG3205	CHP	-0.878	0.0016	10
ML1783		MSMEG4344	possible transcriptional regulatory protein	-0.849	0.0080	9
PPE-b	*PPE*	MSMEG0063	PPE family domain	-0.807	0.0003	6
ML0663		MSMEG2085	CHP	-0.804	0.0016	10
argD-e	*argD*	MSMEG2971	probable acetylornithine aminotransferase	-0.767	0.0030	7
atpH	*atpH*	MSMEG4925	ATP synthase delta chain	-0.741	0.0024	7
ML0990		MSMEG2732	CHP	-0.701	0.0066	10
glpD-a	*glpD*	MSMEG6721	glycerol-3-phosphate dehydrogenase	-0.683	0.0017	7
menD	*menD*	MSMEG1225	bifunctional menaquinone biosynthesis protein	-0.677	0.0072	7
Rv3841	*bfrB*	MSMEG6385	bacterioferritin	-0.660	0.0062	7
bccA-c		MSMEG1807	biotin carboxy carrier protein & transferase	-0.641	0.0017	1
purM	*purM*	MSMEG5766	phosphoribosylformylglycinamidine cyclo-ligase	-0.635	0.0082	7
fas	*fas*	MSMEG0552	fatty acid synthase	-0.633	0.0015	
lpqF	*lpqF*	MSMEG6050	probable conserved lipoprotein	-0.617	0.0062	3
ML0759	*fbiA*	MSMEG1829	probable F420 biosynthesis protein	-0.611	0.0015	7
gabD-y	*gabD*	MSMEG1497	succinate-semialdehyde dehydrogenase	-0.600	0.0075	7

ID	Gene	TIGR name	Function (as per Leproma & Tuberculist)	M	P value	Class
glnA2-f	*glnA2*	MSMEG2596	probable glutamine synthetase	-0.593	0.0026	7
ML1094		MSMEG1104	short chain type dehydrogenase/ reductase	-0.590	0.0024	7
ML0596-a	*csd*	MSMEG4531	probable cysteine desulfurase	-0.576	0.0020	7
ML2203		MSMEG3807	CHP	-0.552	0.0020	10
ML2289		none	CHP	-0.537	0.0020	10
sdhC	*sdhC*	MSMEG1669	succinate dehydrogenase	-0.528	0.0082	7
lysX	*lysX*	MSMEG6531	lysyl-tRNA synthetase	-0.501	0.0070	2
phoT	*phoT*	MSMEG2124	phosphate transport ATP-binding protein	-0.496	0.0066	3
ML2053	*adhA*	MSMEG0251	probable alcohol dehydrogenase	-0.477	0.0041	7
uvrD2	*uvrD2*	MSMEG1956	ATP-dependent DNA helicase	-0.476	0.0051	2
gabD-e	*gabD*	MSMEG6662	aldehyde dehydrogenase family protein	-0.469	0.0062	7
folK	*folK*	MSMEG6064	hydroxymethyldihydropteridine phosphokinase	-0.443	0.0071	7
miaA	*miaA*	MSMEG6675	tRNA delta(2)-isopentenylpyrophosphate transferase	-0.383	0.0100	7

[a] M, log base 2 of the fold ratio
[b] Functional class as per Tuberculist: 1, Lipid metabolism; 2, Information pathways; 3, Cell wall & cell processes; 6, PE/PPE; 7, Intermediary metabolism & respiration; 9, Regulatory proteins; 10, Conserved hypotheticals

Table D2. *M. smegmatis* Δ*qcrCAB*::*hyg* genes repressed during growth at 21% oxygen as analyzed on the partial-genome amplicon array (Table from produced from Dr D. Powell's analyses)

ID	Gene	TIGR name	Function	M	P value	Class
lytB2	*lytB*	MSMEG5208	probable LytB-related protein, LytB2	3.316	0.0002	3
xseA	*xseA*	MSMEG5210	exo-deoxyribonuclease VII, large subunit	2.737	0.0003	2
ML2088-a		MSMEG4807	putative cytochrome P450	2.039	0.0004	7
ctpC-a		MSMEG5384	cadmium-translocating P-type ATPase	1.789	0.0081	3
rpoT	*sigA*	MSMEG2759	RNA polymerase sigma factor, SigA	1.513	0.0000	2
rplE	*rplE*	MSMEG1464	ribosomal protein L5	1.198	0.0002	2
ML2661-e	*fadD7*	MSMEG3702	Fatty acid CoA ligase, FadD7	1.197	0.0051	1
fpg	*fpg*	MSMEG2417	formamidopyrimidine-DNA glycosylase	0.961	0.0078	7
ML1750		MSMEG2202	CHP	0.922	0.0098	10
uvrB	*uvrB*	MSMEG3820	excinuclease ABC, B subunit	0.843	0.0057	2
Rv1009	*rpfB*	MSMEG5419	probable resuscitation-promoting factor B, RpfB	0.835	0.0027	3
uspE	*uspB*	MSMEG4462	probable sugar ABC transporter	0.810	0.0024	3
ML0115		MSMEG6327	CHP	0.807	0.0051	10

ID	Gene	TIGR name	Function	M	P value	Class
ML2661-h	*fadD7*	MSMEG4041	Fatty acid CoA ligase, FadD7	0.805	0.0002	1
Rv2393		MSMEG4522	CHP	0.771	0.0041	10
ML2491-c		MSMEG4370	CHP	0.760	0.0033	10
ML0815		MSMEG1939	transcriptional regulator, TetR family domain	0.725	0.0002	9
rpsL	*rpsL*	MSMEG1393	ribosomal protein S12	0.724	0.0066	2
ML0691-b	*dacB*	MSMEG1659	probable D-alanyl-alanine carboxypeptidase	0.720	0.0005	3
ML0729		MSMEG1810	CHP	0.674	0.0039	10
ML0093	*glfT*	MSMEG5323	bifunctional UDP-galactofuranosyl transferase	0.668	0.0085	3
gatA-b	*gatA*	MSMEG1078	glutamyl-tRNA (GLN) amidotransferase	0.668	0.0024	2
atpD-c	*atpD*	MSMEG4939	probable ATP synthase Beta chain	0.660	0.0009	7
trpS	*trpS*	MSMEG1655	tryptophanyl-tRNA synthetase	0.655	0.0020	2
mce1A-a	*mce1A*	MSMEG6500	host cell invasion	0.650	0.0026	0
ML2549		MSMEG0428	CHP	0.628	0.0029	10
ML2620-b	*mmpL3*	MSMEG4733	conserved transmembrane transport protein	0.624	0.0024	3
pdc-a	*pdc*	MSMEG4455	probable pyruvate decarboxylase	0.590	0.0027	7
ML1115	*lprB*	MSMEG1390	possible lipoprotein	0.581	0.0031	3
ML0174	*mprA*	MSMEG5468	DNA-binding response regulator (persistence)	0.580	0.0016	9
umaA2-a	*umaA*	MSMEG1199	possible mycolic acid synthase	0.476	0.0041	1
ML1698		MSMEG5185	conserved membrane protein	0.464	0.0033	3
ML2140		MSMEG5666	transcriptional regulator, marR family	0.460	0.0070	9
ML2377	*mmpS4*	MSMEG0373	conserved membrane protein	0.455	0.0073	3
ML0243-b	*pks16*	MSMEG5415	putative polyketide synthase	0.440	0.0081	1
ung	*ung*	MSMEG3668	probable uracil-DNA glycosylase	0.422	0.0079	2

Table D3. Genes up-regulated in response to CPZ in the Δ*qcrCAB*::*hyg* mutant (TIGR full genome oligonucleotide array

Name on array	Gene	Description (TIGR)	LR	STDEV	Closest H37Rv Hit (BLAST)a	
					Rv #	E-value
ORFA09082		transcriptional regulator, TetR family domain	7.05	0.17	Rv0302	[1e-06]
ORFA04432	*ald*	alanine dehydrogenase	5.60	1.03	Rv2780	[1e-156]
ORFA10783		hypothetical protein	4.79	0.22	Rv3300c	[2.1]
ORFA03112*		S30AE family protein	4.63	0.42	Rv3241c	[3e-89]
ORFA10805		seq ID no 1F, putative	4.62	2.35	Rv0203	[6e-08]
ORFA06467		FxsA cytoplasmic membrane protein family	4.20	0.87	Rv2053c	[1e-05]
ORFA09393		hypothetical protein	3.97	2.45	Rv0538	[0.11]
ORFA02973		conserved hypothetical protein	3.95	1.13	Rv2719c	[0.077]
ORFA00682*		hypothetical protein	3.78	0.48	Rv1628c	[0.87]
ORFA04487		Helix-turn-helix domain protein	3.62	1.17	Rv2745c	[1e-34]
ORFA08694		conserved hypothetical protein|	3.51	1.72	Rv1072	[3e-82]
ORFA06043		integral membrane protein [imported]	3.46	1.94	Rv1861	[4e-07]
ORFA02952		conserved hypothetical protein	3.22	1.66	Rv2181	[0.004]
ORFA11060		hypothetical protein	3.21	2.24	Rv2228c	[0.55]
ORFA10188*	*uvrA*	hypothetical protein	3.19	0.89	Rv1638	[0.52]
ORFA04589*	*sigB*	mysB sigma factor	3.15	1.06	Rv2710	[1e-166]
ORFA05950*	*bfrA*	bacterioferritin	3.14	0.89	Rv1876	[3e-78]
ORFA05222		transcriptional regulator, ArsR family domain	3.07	0.80	Rv1460	[6e-88]
ORFA05225		Uncharacterized protein family (UPF0051)	3.07	1.88	Rv1462	[1e-177]
ORFA00963*		STAS domain protein	2.98	0.40	Rv0516c	[2e-22]
ORFA05224		Pps1 sans inteine	2.97	0.43	Rv1461	[1e-129]
ORFA02971		hypothetical protein	2.92	0.57	Rv2391	[0.37]
ORFA02906*		desA3	2.89	2.72	Rv3229c	[1e-94]
ORFA08326		conserved hypothetical protein	2.87	0.35	Rv1249c	[2e-76]
ORFA02904*		oxidoreductase	2.86	2.54	Rv3230c	[2e-41]
ORFA02957	*usfY*	conserved hypothetical protein	2.68	0.38	Rv3288c	[7e-19]
ORFA01713*		Flavin-binding monooxygenase-like subfamily	2.62	1.10	Rv3049c	[0.0]
ORFA02972		putative membrane protein	2.58	0.11	Rv2566	[4.8]
ORFA00111		putative transposase	2.39	0.68	Rv2839c	[0.036]
ORFA09026*	*pepD*	heat shock protein HtrA, putative	2.28	0.71	Rv0983	[1e-129]
ORFA03236		CsbD-like family	2.24	0.43	Rv2176	[3.7]
ORFA06545*		COG0464:ATPases of the AAA+ class	2.15	1.30	Rv2115c	[0.0]
ORFA08264		Heavy-metal-associated domain, putative	2.15	1.58	Rv1856c	[0.70]
ORFA05227		MW07	2.13	1.50	Rv1463	[1e-121]
ORFA00897		transposase, putative	2.02	0.53	Rv0755	[0.001]
ORFA10770		hypothetical protein	1.95	1.12	No_Hit	No_Hit
ORFA00617*		MaoC domain protein	1.92	0.20	Rv0241c	[1e-112]
ORFA03205	*rhlE*	rhlE	1.86	0.98	Rv3211	[1e-177]
ORFA06532*		Protein of unknown function (DUF797) family	1.80	0.35	Rv2111c	[3e-14]

Name on array	Gene	Description (TIGR)	LR	STDEV	Closest H37Rv Hit (BLAST)a	
					Rv #	E-value
ORFA03454*	*fadE23*	fadE23	1.67	0.50	Rv3140	[1e-168]
ORFA07028*		SEQ ID NO 45F	1.64	0.71	Rv2169c	[2e-44]
ORFA04061*		4-aminobutyrate aminotransferase	1.59	0.63	Rv3329	[6e-52]
ORFA08327*	*sucA*	2-oxoglutarate dehydrogenase E1 component	1.56	0.67	Rv1248c	[0.0]
ORFA03313		hypothetical protein	1.50	0.07	Rv2284	[0.088]
ORFA06530*	*prcB*	proteasome beta subunit	1.46	0.15	Rv2110c	[1e-112]
ORFA05419*	*cydA*	appC	1.36	0.46	Rv1623c	[0.0]
ORFA01621		conserved hypothetical protein	1.26	0.43	Rv0483	[0.39]
ORFA07027		conserved hypothetical protein TIGR00242	1.25	0.04	Rv2166c	[2e-70]
ORFA10275	*furA*	furA	1.24	0.00	Rv1909c	[3e-45]

6. REFERENCES

Alexeeva, S., K. J. Hellingwerf, and M. J. Teixeira de Mattos. 2002. Quantitative assessment of oxygen availability: perceived aerobiosis and its effect on flux distribution in the respiratory chain of *Escherichia coli*. J. Bacteriol. **184:**1402-1406.

Alexeeva, S., K. J. Hellingwerf, and M. J. Teixeira de Mattos. 2003. Requirement of ArcA for redox regulation in *Escherichia coli* under microaerobic but not anaerobic or aerobic conditions. J. Bacteriol. **185:**204-209.

Altschul, S. F., W. Gish, W. Miller, E. W. Myers, and D. J. Lipman. 1990. Basic local alignment search tool. J. Mol. Biol. **215:**403-410.

Andersen, P., and T. M. Doherty. 2005. The success and failure of BCG– implications for a novel tuberculosis vaccine. Nat. Rev. Microbiol. **3:**656-662.

Andries, K., P. Verhasselt, J. Guillemont, H. W. H. Göhlmann, J.-M., Neefs, H. Winkler, J. Van Gestel, P. Timmerman, M. Zhu, E. Lee, P. William, D. de Chaffoy, E. Huitric, S. Hoffner, E. Cambau, C. Truffot-Pernot, N. Lounis, and V. Jarlier. 2004. A diarylquinoline drug active on the ATP synthase of *Mycobacterium tuberculosis*. Science **307:**223-227.

Ashour, J., and M. K. Hondalus. 2003. Phenotypic mutants of the intracellular actinomycete *Rhodococcus equi* created by in vivo *Himar1* transposon mutagenesis. J. Bacteriol. **185:**2644-2652.

Bacon, J., B. W. James, L. Wernisch, A. Williams, K. A. Morley, G. J. Hatch, J. A. Mangan, J. Hinds, N. G. Stoker, P. D. Butcher, and P. D. Marsh. 2004. The influence of reduced oxygen availability on pathogenicity and gene expression in *Mycobacterium tuberculosis*. Tuberculosis **84:**205-217.

Bagchi, G., Mayuri, and J. S. Tyagi. 2003. Hypoxia-responsive expression of *Mycobacterium tuberculosis Rv3134c* and *devR* promoters in *Mycobacterium smegmatis.* Microbiology **149:**2303-2305.

Baker, S. C., S. J. Ferguson, B. Ludwig, M. D. Page, O.-M. H. Richter, and R. J. M. Van Spanning. 1998. Molecular genetics of the genus *Paracoccus*: metabolically versatile bacteria with bioenergetic flexibility. Microbiol. Mol. Biol. Rev. **62:**1046-1078.

Ballel, L., R. A. Field, K. Duncan, and R. J. Young. 2005. New small-molecule synthetic antimicrobials. Antimicrob. Agents Chemother. **49:**2153-2163.

Barry, C. E., III. 2001. *Mycobacterium smegmatis*: an absurd model for tuberculosis? Response from Barry III. Trends Microbiol. **9:**473-474.

Baruah, A., B. Lindsey, Y. Zhu, and M. M. Nakano. 2004. Mutational analysis of the signal-sensing domain of ResE histidine kinase from *Bacillus subtilis*. J. Bacteriol. **186:**1694-1704.

Bebbington, K. J., and Williams, H. D. 2001. A role for DNA supercoiling in the regulation of the cytochrome *bd* oxidase of *Escherichia coli*. Microbiology **147:**591-598.

Belevich, I. V. B. Borisov, J. Zhang, K. Yang, A. A. Konstantinov, R. B. Gennis, and M. I. Verkhovsky. 2005. Time-resolved electrometric and optical studies on cytochrome *bd* suggest a mechanism of electron-proton coupling in the di-heme active site. Proc. Natl. Acad. Sci. USA **102:**3657-3662.

Betts, J. C., P. T. Lukey, L. C. Robb, R. A. McAdam, and K. Duncan. 2002. Evaluation of a nutrient starvation model of *Mycobacterium tuberculosis* persistence by gene and protein expression profiling. Mol. Microbiol. **43:**717-731.

Blondelet-Rouault, M.H., J. Weiser, A. Lebrihi, P. Branny, and J.L. Pernodet. 1997. Antibiotic resistance gene cassettes derived from the interposon for use in *E. coli* and *Streptomyces.* Gene **190:**315-317.

Blower, S. M., and T. Chou. 2004. Modeling the emergence of 'hot zones': tuberculosis and the amplification dynamics of drug resistance. Nat. Med. **10:**1111-1116.

Bock, A., and R. Gross. 2002. The unorthodox histidine kinases BvgS and EvgS are responsive to the oxidation status of a quinone electron carrier. Eur. J. Biochem. **269:**3479-3484.

Borisov, V. B., E. Forte, A. A. Konstantinov, R. K. Poole, P. Sarti, and A. Giuffrè. 2004. Interaction of the bacterial terminal oxidase cytochrome *bd* with nitric oxide. FEBS Lett. **576:**201-204.

Boshoff, H. I. M., T. G. Myers, B. R. Copp, M. R. McNeil, M. A. Wilson, and C. E. Barry, III. 2004. The transcriptional responses of *Mycobacterium tuberculosis* to inhibitors of metabolism: novel insights into drug mechanisms of action. J. Biol. Chem. **279:**40174-40184.

Boshoff, H. M. I., and C. E. Barry. 2005. Tuberculosis – metabolism and respiration in the absence of growth. Nat. Rev. Microbiol. **3:**70-80.

Bott, M., and A. Niebisch. 2003. The respiratory chain of *Corynebacterium glutamicum*. J. Biotech. **104:**129-153.

Bränden, M., H. Sigurdson, A. Namslauer, R. B. Gennis, P. Adelroth, and P. Brzezinski. 2001. On the role of the K-proton transfer pathway in cytochrome *c* oxidase. Proc. Natl. Acad. USA **98:**5013-5018.

Brekasis, D., and M.S.B. Paget. 2003. A novel sensor of NADH/NAD^+ redox poise in *Streptomyces coelicolor* A3(2). *EMBO J.* **22:**4856-4865.

Brennan, M. J. 2005. The tuberculosis vaccine challenge. Tuberculosis **85:**7-12.

Brennan, P. J., and H. Nikaido. 1995. The envelope of mycobacteria. Ann. Rev. Biochem. **64:** 29-63.

Brodin, P., I. Rosenkrands, P. Andersen, S. T. Cole, and R. Brosch. 2004. ESAT-6 proteins: protective antigens and virulence factors? Trends Microbiol. **12:**500-508.

Brodin, P., M. I. de Jonge, L. Majlessi, C. Leclerc, M. Nilges, S. T. Cole, and R. Brosch. 2005. Functional analysis of ESAT-6, the dominant T-cell antigen of *Mycobacterium tuberculosis*, reveals key residues involved in secretion, complex-formation, virulence and immunogenicity. J. Biol. Chem. in press.

Chandel, N. S., D. S. McClintock, C. E. Feliciano, T. M. Wood, J. A. Melendez, A. M. Rodriguez, and P. T. Schumacker. 2000. Reactive oxygen species generated at

mitochondrial complex III stabilize hypoxia-inducible factor-1apha during hypoxia: a mechanism of O_2 sensing. J. Biol. Chem. **275:**25130-25138.

Cohen, T., B. Sommers, and M. Murray. 2003. The effect of drug resistance on the fitness of *Mycobacterium tuberculosis*. Lancet Infect. Dis. **3:**13-21.

Cohen, T., and M. Murray. 2004. Modeling epidemics of multidrug-resistant *M. tuberculosis* of heterogeneous fitness. Nat. Med. **10:**1117-1121.

Cole, S. T., R. Brosch, J. Parkhill, T. Garnier, C. Churcher, D. Harris, S. V. Gordon, K. Eiglmeier, S. Gas, C. E. Barry, III, F. Tekaia, K. Badcock, D. Basham, D. Brown, T. Chillingworth, R. Connor, R. Davies, K. Devlin, T. Feltwell, S. Gentles, N. Hamlin, S. Holroyd, T. Hornsby, K. Jagels, A. Krogh, J. McLean, S. Moule, L. Murphy, K. Oliver, J. Osborne, M. A. Quali, M. A. Rajandream, J. Rogers, S. Rutter, K. Seeger, J. Skelton, R. Squares, S. Squares, J. E. Sulston, J. Taylor, S. Whitehead, B. G. Barrell. 1998. Deciphering the biology of *Mycobacterium tuberculosis* from the complete genome sequence. Nature **393:**537-544.

Cole, S. T., K. Eiglmeier, J. Parkhill, K. D. James, N.R. Thomson, P. R. Wheeler, N. Honore, T. Garnier, C. Churcher, D. Harris, K. Mungall, D. Basham, D. Brown, T. Chillingworth, R. Connor, R. M. Davies, K. Devlin, S. Duthoy, T. Feltwell, A. Fraser, N. Hamlin, S. Holroyd, T. Hornsby, K. Jagels, C. Lacroix, J. Maclean, S. Moule, L. Murphy, K. Oliver, M. A. Quail, M. A. Rajandream, K. M. Rutherford, S. Rutter, K. Seeger, S. Simon, M. Simmonds, J. Skelton, R. Squares, S. Squares, K. Stevens, K. Taylor, S. Whitehead, J. R. Woodward, and B. G. Barrell. 2001. Massive gene decay in the leprosy bacillus. Nature **409:**1007-1011.

Cooper, C. E. 2002. Nitric oxide and cytochrome oxidase: substrate, inhibitor or effector?. Trends Biochem. Sci. **27:**33-39.

Corbett, E. L., C. J. Watt, N. Walker, D. Maher, B. G. Williams, M. C. Raviglione, and C. Dye. 2003. The growing burden of tuberculosis: global trends and interactions with the HIV epidemic. Arch. Intern. Med. **163:**1009-1021.

Cosma, C. L., O. Humbert, and L. Ramakrishnan. 2004. Superinfecting mycobacteria home to established tuberculous granulomas. Nat. Immunol. **5:**828-835.

Cruciat, C.-M., S. Brunner, F. Baumann, W. Neupert, and R. A. Stuart. 2000. The cytochrome bc_1 and cytochrome *c* oxidase complexes associate to form a single supracomplex in yeast mitochondria. J. Biol. Chem. **275:**18093-18098.

Cunningham, A. F., and C. L. Spreadbury. 1998. Mycobacterial stationary phase induced by low oxygen tension: cell wall thickening and localization of the 16-kiloDalton α-crystallin homolog. J. Bacteriol. **180:**801-808.

Dahl, J. L., C. N. Krause, H. I. Boshoff, B. Doan, K. Foley, D. Avarbock, G. Kaplan, V. Mizrahi, and C. E. Barry III. 2003. The role of Rel_{MTb}-mediated adaptation to stationary phase in long-term persistence of *Mycobacterium tuberculosis* in mice. Proc. Natl. Acad. Sci. USA **100:**10026-10031.

Daniel, J., C. Deb, V. S. Dubey, T. D. Sirakova, B. Abomoelak, H. R. Morbidoni, and P. E. Kolattukudy. 2004. Induction of a novel class of diacylglycerol acyltransferases and triacylglycerol accumulation in *Mycobacterium tuberculosis* as it goes into a dormancy-like state in culture. J. Bacteriol. **186:**5017-5030.

Dannenberg, A. M., Jr, and G. A. W. Rook. 1994. Pathogenesis of pulmonary tuberculosis: an interplay of tissue-damaging and macrophage-activating immune response- dual mechanisms that control bacillary multiplication, p459-483. *In* B. R. Bloom (ed.), Tuberculosis: pathogenesis, protection, and control. American Society for Microbiologists, Washington, DC.

Darrouzet, E., and F. Daldal. 2002. Movement of the iron-sulfur subunit beyond the *ef* loop of cytochrome *b* is required for multiple turnovers of the bc_1 complex but not for single turnover Q_o site catalysis. J. Biol. Chem. **277:**3471-3476.

Dasgupta, N., V. Kapur, K. K. Singh, T. K. Das, S. Sachdeva, and K. Jyothisri. 2000. Characterization of a two-component system, *devR-devS*, of *Mycobacterium tuberculosis*. Tuberc. Lung Dis. **80:**141-159.

de Gier, J. W., M. Lubben, W. N. Reijnders, C. A. Tipker, D. J. Slotboom, R. J. van Spanning, A. H. Stouthamer, and J. van der Oost. 1994. The terminal oxidases of *Paracoccus denitrificans.* Mol. Microbiol. **13:**183-196.

Dick, T., B. H. Lee, and B. Murugasu-Oei. 1998. Oxygen depletion induced dormancy in *Mycobacterium smegmatis.* FEMS Microbiol. Lett. **163:**159-164.

Dudoit, S., and Y. H. Yang. 2003. Bioconductor R packages for exploratory analysis and normalization of cDNA microarray data, p. 45-65. *In* P. Parmigiani, E.S. Garrett, R.A. Irizarry, and S.L. Zeger, (ed.), The analysis of gene expression data: methods and software. Springer Verlag, New York.

Finnerty, W. R. 1992. The biology and genetics of *Rhodococcus.* Ann. Rev. Microbiol. **46:**193-218.

Fleischmann, R. D., D. Alland, J. A. Eisen, L. Carpenter, O. White, J. Peterson, R. DeBoy, R. Dodson, M. Gwinn, D. Haft, E. Hickey, J. F. Kolonay, W. C. Nelson, L. A. Umayam, M. Ermolaeva, S. L. Salzberg, A. Delcher, T. Utterback, J. Weidman, H. Khouri, J. Gill, A. Mikula, W. Bishai, W. R. Jacobs Jr, J. C. Venter, and C. M. Fraser. 2002. Wole-genome comparison of *Mycobacterium tuberculosis* clinical and laboratory strains. J. Bacteriol. **184:**5479-5490.

Flint, J. L., J. C. Kowalski, P. V. Karnati, and K. M. Derbyshire. 2004. The RD1 virulence locus of *Mycobacterium tuberculosis* regulates DNA transfer in *Mycobacterium smegmatis*. Proc. Natl. Acad. Sci. USA **101:**12598-12603.

Florczyk, M. A., L. A. McCue, A. Purkayastha, E. Currenti, M. J. Wolin, and K. A. McDonough. 2003. A family of *acr*-coregulated *Mycobacterium tuberculosis* genes shares a common DNA motif and requires Rv3133c (*dos*R or *dev*R) for expression. Infect. Immun. **71:**5332-5343.

Flynn, J. L., and J. Chan. 2001. Tuberculosis: latency and reactivation. Infect. Immun. **69:**4195-4201.

Flynn, J. L., and J. Chan. 2005. What's good for the host is good for the bug. Trends Microbiol. **13:**98-102.

Fortune, S. M., A. Jaeger, D. A. Sarracino, M. R. Chase, C. M. Sassetti, D. R. Sherman, B. R. Bloom, and E. J. Rubin. 2005. Mutually dependent secretion of proteins required for mycobacterial virulence. Proc. Natl. Acad. Sci. USA **102:**10676-10681.

Galamba, A., K. Soetaert, X.-M. Wang, J. De Bruyn, P. Jacobs, and J. Content. 2001. Disruption of *adhC* reveals a large duplication in the *Mycobacterium smegmatis* mc^2155 genome. Microbiology **147:**3281-3294.

Garcia-Horsman, J. A., B. Barquera, J. Rumbley, J. Ma, and R. B. Gennis. 1994. The superfamily of heme-copper respiratory oxidases. J. Bacteriol. **176:**5587-5600.

Geadle, J., and J. Ratcliffe. 2001. Hypoxia, p.1-9. *In* Encyclopedia of Life Sciences, Nature Publishing Group, London, UK.

Gennis, R. B. 1998. How does cytochrome oxidase pump protons? Proc. Natl. Acad. Sci. USA **95:**12747-12749.

Georgellis, D., O. Kwon, and E. C. C. Lin. 2001a. Quinones as the redox signal for the Acr two-component system of bacteria. Science **292:**2314-2316.

Georgellis, D., O. Kwon, E. C. C. Lin, S. M. Wong, and B. J. Akerley. 2001b. Redox signal transduction by the ArcB sensor kinase of *Haemophilus influenzae* lacking the PAS domain. J. Bacteriol. **183:**7206-7212.

Ghanekar, K., A. McBride, O. Dellagostin, S. Thorne, R., Mooney, and J. McFadden. 1999. Stimulation of transposition of the *Mycobacterium tuberculosis* insertion sequence IS*6110* by exposure to microaerobic environment. Mol. Microbiol. **33:**982-993.

Glickman, M. S., and W. R. Jacobs, Jr. 2001. Microbial pathogenesis of *Mycobacterium tuberculosis*: dawn of a discipline. Cell **104:**477-485.

Gomez, M, L. Doukhan, G. Nair, and I. Smith. 1998. *sigA* is an essential gene in *Mycobacterium smegmatis.* Mol. Microbiol. **29:**617-628.

Goodfellow, M., and D. E. Minnikin. 1977. Nocardioform bacteria. Ann. Rev. Micobiol. **31:**159-180.

Gordhan, B. G., and T. Parish. 2001. Gene replacement using pretreated DNA. Methods Mol. Med. **54:**77-92.

Gordhan, B. G., D. A. Smith, H. Alderton, R. A. McAdam, G. J. Bancroft, and V. Mizrahi. 2002. Construction and phenotypic characterization of an auxotrophic mutant

of *Mycobacterium tuberculosis* defective in L-arginine biosynthesis. Infect. Immun. **70:**3080-3084.

Grabbe, R. and R. A. Schmitz. 2003. Oxygen control of *nif* gene expression in *Klebsiella pneumoniae* on NifL reduction at the cytoplasmic membrane by electrons derived from the reduced quinone pool. Eur. J. Biochem. **270:**1555-1566.

Green, J., and M. S. Paget. 2004. Bacterial redox sensors. Nat. Rev. Microbiol. **2:**954-966.

Grode, L., P. Seiler, S. Baumann, J. Hess, V. Brinkmann, A. N. Eddine, P. Mann, C. Goosmann, S. Bandermann, D. Smith, G. J. Bancroft, J.-M. Reyrat, D. van Sooligen, B. Raupach, and S. H. E. Kaufmann. 2005. Increased vaccine efficacy against tuberculosis of recombinant *Mycobacterium bovis* bacille Calmette-Guérin mutants that secrete listeriolysin. J. Clin. Invest. doi:10.1172/JCI24617.

Hanahan, D. 1983. Studies on transformation of *Escherichia coli* with plasmids. J. Mol. Biol. **166:**557-580.

Hansford, R. 2001. Oxidative phosphorylation, p.1-8. *In* Encyclopedia of Life Sciences, Nature Publishing Group, London, UK.

Hederstedt, L. 2003. Complex II is complex too. Science **299:**671-672.

Himpens, S., C. Locht, and P. Supply. 2000. Molecular characterization of the mycobacterial SenX3-RegX3 two-component system: evidence for autoregulation. Microbiology **146:**3091-3098.

Horwitz, M. A., G. Harth, B. J. Dillon, and S. Masleša-Galić. 2005. Enhancing the protective efficacy of *Mycobacterium bovis* BCG vaccination against tuberculosis by boosting with the *Mycobacterium tuberculosis* major secretory protein. Infect. Immun. **73:**4676-4683.

Hou, J. Y., J. E. Graham, and J. E. Clark-Curtiss. 2002. *Mycobacterium avium* genes expressed during growth in human macrophages detected by selected capture of transcribed sequences (SCOTS). Infect. Immun. **70:**3714-3726.

Husson, R. N., B. E. James, and R. A. Young. 1990. Gene replacement and expression of foreign DNA in mycobacteria. J. Bacteriol. **172:**519-524.

Ishikawa, J., A. Yamashita, Y. Mikami, Y. Hoshino, H. Kurita, K. Hotta, T. Shiba, and M. Hattori. 2004. The complete genome sequence of *Nocardia farcinica* IFM 10152. Proc. Natl. Acad. Sci. USA **101:**14925-14930.

Jacobs, W. R. Jr, G. V. Kalpana, J. D. Cirillo, L. Pascopella, S. B. Snapper, R. A. Udani, W. Jones, R. G. Barletta, and B. R. Bloom. 1991. Genetic systems for mycobacteria. Methods Enzymol. **204:**537-555.

Kana, B. D., E. A. Weinstein, D. Avarbock, S. S. Dawes, H. Rubin, and V. Mizrahi. 2001. Characterization of the *cyaAB*-encoded cytochrome *bd* oxidase from *Mycobacterium smegmatis.* J. Bacteriol. **183:**7076-7086.

Karakousis, P. C., T. Yoshimatsu, G. Lamichhane, S. C. Woolwine, E. L. Nuermberger, J. Grosset, and W. R. Bishai. 2004. Dormancy phenotype displayed by extracellular *Mycobacterium tuberculosis* within artificial granuloma in mice. J. Exp. Med. **200:**647-657.

Kendall, S. L., F. Movahedzadeh, S. C. G. Rison, L. Wernisch, T. Parish, K. Duncan, J. C. Betts, and N. G. Stoker. 2004. The *Mycobacterium tuberculosis doRS* two-component system is induced by multiple stresses. Tuberculosis **84:**247-255.

Krzywinska, E., J. Krzywinski, and J. S. Schorey. 2004. Naturally occurring horizontal gene transfer and homologous recombination in *Mycobacterium.* Microbiology **150:**1707-1712.

Kwast, K. E., P. V. Burke, B. T. Staahl, and R. O. Poyton. 1999. Oxygen sensing in yeast: evidence for the involvement of the respiratory chain in regulating the transcription of a subset of hypoxic genes. Proc. Nat. Acad. Sci. **96:**5446-5451.

Kusumoto, K., M. Sakiyama, J. Sakamoto, S. Noguchi, and N. Sone. 2000. Menaquinol oxidase activity and primary structure of cytochrome *bd* from the amino-acid fermenting bacterium *Corynebacterium glutamicum.* Arch. Microbiol. **173:**390-397.

Larsen, M. H. 2000. Appendix 1. p313-320. *In* G. F. Hatfull, W. R. Jacobs, Jr (ed.), Molecular genetics of mycobacteria. ASM Press, Washington, D.C.

Lenaerts, A. J., V. Gruppo, K. S. Marietta, C. M. Johnson, D. K. Driscoll, N. M. Tompkins, J. D. Rose, R. C. Reynolds, and I. M. Orme. 2005. Preclinical testing of the nitroimidazopyran PA-824 for activity against *Mycobacterium tuberculosis* in a series of in vitro and in vivo models. Antimicrob. Agents Chemother. **49:**2294-2301.

Lewis, K. N., R. Liao, K. M. Guinn, M. J. Hickey, S. Smith, M. A. Behr, and D. R. Sherman. 2003. Deletion of RD1 from *Mycobacterium tuberculosis* mimics Bacille Calmette-Guérin attenuation. J. Infect. Dis. **187:**117-123.

Liu, X., and P. de Wulf. 2004. Probing the ArcA~P modulon of *Escherichia coli* by whole-genome transcriptional analysis and sequence-recognition profiling. J. Biol. Chem. **279:**12588-12597.

Maholtra, V., D. Sharma, V. D. Ramanathan, H. Shakila, D. K. Saini, S. Chakravorty, T. K. Das, Q. Li, R. F. Silver, P. R. Narayanan, and J. S. Tyagi. 2004. Disruption of response regulator gene, *devR*, leads to attenuation in virulence of *Mycobacterium tuberculosis.* FEMS. Microbiol. Lett. **231:**237-245.

Malpica, R., B. Franco, C. Rodriguez, and D. Georgellis. 2004. Identification of a quinone-sensitive redox switch in the ArcB sensor kinase. Proc. Natl. Acad. Sci. USA **101:**13318-13323.

Matsoso, L. G., B. D. Kana, P. K. Crellin, D. J. Lea-Smith, A. Pelosi, D. Powell, S. S. Dawes, H. Rubin, R. L. Coppel, and V. Mizrahi. 2005. Function of the cytochrome bc_1-aa_3 branch of the respiratory network in mycobacteria and network adaptation occurring in response to its disruption. J. Bacteriol. **187:**6300-6308.

Mayuri, G. Bagchi, T. K. Das, J. S. Tyagi. 2002. Molecular analysis of the dormancy response in *Mycobactrium smegmatis*: expression analysis of genes encoding the DevR-DevS two-component system, R3134c and chaperone α-crystallin homologues. FEMS Microbiol. Lett. **211:**231-237.

Miyatake, H., M. Mukai, S. Y. Park, S. Adachi, K. Tamura, H. Nakamura, K. Nakamura, T. Tsuchiya, T. Iizuka, and Y. Shiro. 2000. Sensory mechanism of oxygen sensor FixL from *Rhizobium meliloti*: crystallographic, mutagenesis and resonance Raman spectroscopic studies. J. Mol. Biol. **301:**415-431.

Monack, D. M., A. Mueller and S. Falkow. 2004. Persistent bacterial infections: the interface of the pathogen and host immune response. Nat. Rev. Microbiol. **2:**747-765.

Morris, R. P., L. Nguyen, J. Gatfield, K. Visconti, K. Nguyen, D. Schnappinger, S. Ehrt, Y. Liu, L. Heifets, J. Pieters, G. Schoolnik, and C. J. Thompson. 2005. Ancestral antibiotic resistance in *Mycobacterium tuberculosis*. Proc. Natl. Acad. Sci. USA **102:**12200-12205.

Murray, J. P., and E. J. Rubin. 2005. New genetic approaches shed light on TB virulence. Trends Microbiol. **13:**366-372.

Muttucumaru, D. G. N., G. Roberts, J. Hinds, R. A. Stabler, and T. Parish. 2004. Gene expression profile of *Mycobacterium tuberculosis* in a non-replicating state. Tuberculosis **84:**239-246.

Nantapong, N., A. Otufuji, C. T. Migita, O. Adachi, H. Toyama, and K. Matsushita. 2005. Electron transfer ability from NADH to menaquinone and from NADPH to oxygen of type II NADH dehydrogenase of *Corynebacterium glutamicum*. Biosci. Biotechnol. Biochem. **69:**149-159.

Niebisch, A., and M. Bott. 2001. Molecular analysis of the cytochrome bc_1-aa_3 branch of the *Corynebacterium glutamicum* respiratory chain containing an unusual diheme cytochrome c_1. Arch. Microbiol. **175:**282-294.

Niebisch, A., and M. Bott. 2003. Purification of a cytochrome bc_1-aa_3 supercomplex with quinol activity from *Corynebacterium glutamicum*. Identification of a fourth subunit of cytochrome aa_3 oxidase and mutational analysis of diheme cytochrome c_1. J. Biol. Chem. **278:**4339-4346.

Nolden, L., G. Beckers, and A. Burkovski. 2002. Nitrogen assimilation in *Corynebacterium diphtheriae*: pathways and regulatory cascades. FEMS Microbiol. Lett. **208:**287-293.

O'Gaora, P., S. Barnin, C. Hayward, E. Filley, G. Rook, D. Young, and J. Thole. 1997. Mycobacteria as immunogens: development of expression vectors for use in multiple mycobacterial species. Med. Princ. Prac. **6:**91-96.

Oh, J-II, and S. Kaplan. 2000. Redox signalling: globalization of gene expression. EMBO J. **19:**4237-4247.

Oh, J-II, and S. Kaplan. 2002. Oxygen adaptation: the role of the CcoQ subunit of the cbb_3 cytochrome *c* oxidase of *Rhodobacter sphaeroides* 2.4.1. J. Biol. Chem. **277:**16220-16228.

Ortalo-Magne, A., A. Lemassu, M-A. Laneelle, F. Bardou, G. Silve, P. Gounon, G. Marchal, and M. Daffe. 1996. Identification of the surface-exposed lipids on the cell envelopes of *Mycobacterium tuberculosis* and other mycobacterial species. J. Bacteriol. **178:**456-461.

Osyczka, A., C. C. Moser, and P. L. Dutton. 2004. Novel cyanide inhibition at cytochrome c_1 of *Rhodobacter capsulatus* cytochrome bc_1. Biochim. Biophys. Acta **1655:**71-76.

O'Toole, R., M. J. Smeulders, M. C. Blokpoel, E. J. Kay, K. Lougheed, and H. D. Williams. 2003a. A two-component regulator of universal stress protein expression and adaptation to oxygen starvation in *Mycobacterium smegmatis*. J. Bacteriol. **185:**1543-1554.

O'Toole, R., and H. D. Williams. 2003b. Universal stress proteins and *Mycobacterium tuberculosis*. Res. Microbiol. **187:**5023-5028.

Otten, M. F., D. M. Stork, W. N. M. Reijnders, H. V. Westerhoff, and R. J. M. van Spanning. 2001a. Regulation of expression of terminal oxidases in *Paracoccus denitrificans*. Eur. J. Biochem. **268:**2486-2497.

Otten, M. F., J. van der Oost, V. N. M. Reijnders, H. V. Westerhoff, B. Ludwig, and R. J. M. van Spanning. 2001b. Cytochromes C_{550}, C_{552}, and C_1 in the electron transport network of *Paracoccus denitrificans*: redundant or subtly different in function? J. Bacteriol. **183:**7017-7026.

Ouchane, S., I. Agalidis, and C. Astier. 2002. Natural inhibitors of the ubiquinol cytochrome *c* oxidoreductase of *Rubrivivax gelatinosus*: sequence and functional analysis of the cytochrome bc_1 complex. J. Bacteriol. **184:**3815-3822.

Parish, T., and N.G. Stoker. 2000. Use of a flexible cassette method to generate a double unmarked *Mycobacterium tuberculosis tlyA plcABC* mutant by gene replacement. Microbiology **146:**1969-1975.

Parish, T., D. A. Smith, G. Roberts, J. Betts, and N. G. Stoker. 2003. The *senX3-regX3* two-component regulatory system of *Mycobacterium tuberculosis* is required for virulence. Microbiology **149:**1423-1435.

Park, H. D., K.M. Guinn, M.I. Harrell, R. Liao, M.I. Voskuil, M. Tompa, G.K. Schoolnik, and D.R. Sherman. 2003. Rv3133c/*dosR* is a transcription factor that mediates the hypoxic response of *Mycobacterium tuberculosis*. Mol. Microbiol. **48:**833-843.

Payne, W. J. 2001. Anaerobic respiration, p1-7. *In* Enzyclopedia of life sciences. Nature Publishing Group, London, United Kingdom.

Pedulla, M. L., and G. F. Hatfull. 1998. Characterization of the *mIHF* gene of *Mycobacterium smegmatis.* J. Bacteriol. **180:**5473-5477.

Poole, R. K., and G. M. Cook. 2000. Redundancy of aerobic respiratory chains in bacteria? Routes, reasons and regulation. Adv. Microb. Physiol. **43:**165-224.

Purkayastha, A., L. A. McCue, K. A. McDonough. 2002. Identification of a *Mycobacterium tuberculosis* putative classical nitroreductase gene whose expression is coregulated with that of the *acr* gene within macrophages, in standing versus shaking cultures, and under low oxygen conditions. Infect. Immun. **70:**1518-1529.

Raitio, M., J. M. Pispa, T. Metso, and M. Saraste. 1990. Are there isoenzymes of cytochrome *c* oxidase in *Paracoccus denitrificans*? FEBS Lett. **261:**431-435.

Raviglione, M. C. 2003. The TB epidemic from 1992 to 2002. Tuberculosis **83:**4-14.

Renshaw, P. S., K. L. Lightbody, V. Veverka, F. W. Muskett, G. Kelly, T. A. Frekiel, S. V. Gordon, R. G. Hewinson, B. Burke, J. Norman, R. A. Williamson, and M. D. Carr. 2005. Structure and function of the complex formed by the tuberculosis virulence factors CFP-10 and ESAT-6. EMBO J. **24:**2491-2498.

Reyrat, J.-M., and D. Kahn. 2001. *Mycobacterium smegmatis*: an absurd model for tuberculosis? Trends Microbiol. **9:**472-473.

Rickman, L., J. W. Saldanha, D. M. Hunt, D. N. Hoar, M. J. Colston, J. B. Millar, and R. S. Buxton. 2004. A two-component signal transduction system with a PAS domain-containing sensor is required for virulence of *Mycobacterium tuberculosis* in mice. Biochem. Biophys. Res. Commun. **314:**259-267.

Roberts, D. M., R. P. Liao, G. Wisedchaisri, W. G. J. Hol, and D. R. Sherman. 2004. Two sensor kinases contribute to the hypoxic response of *Mycobacterium tuberculosis*. J. Biol. Chem. **279:**23082-23087.

Roehm, K.-H. 2001. Electron carriers: proteins and cofactors in oxidative phosphorylation, p.1-8. *In* Encyclopedia of Life Sciences, Nature Publishing Group, London, UK.

Rohdich, F., S. Hecht, K. Gärtner, P. Adam, C. Krieger, S. Amslinger, D. Arigoni, A. Bacher, and W. Eisenreich. 2002. Studies on the nonmevalonate terpene biosynthetic pathway: Metabolic role of IspH (LytB) protein. *Proc. Natal. Acad. Sci. USA* **99:**1158-1163.

Rook, G. A. W., K. Dheda, and A. Zumla. 2005. Immune response to tuberculosis in developing countries: implications for new vaccines. Nat. Rev. Immunol. **5:**661-667.

Rosenkrands, I., R. A. Slayden, J. Crawford, C. Aagaard, C. E. Barry III, and P. Andersen. 2002. Hypoxic response of *Mycobacterium tuberculosis* studied by metabolic labeling and proteome analysis of cellular and extracellular proteins. J. Bacteriol. **184:**3485-3491.

Saini, D. K., V. Malhotra, D. Dey, N. Pant, T. K. Das, and J. S. Tyagi. 2004. DevR-DevS is a bonafide two-component system of *Mycobacetrium tuberculosis* that is hypoxia-responsive in the absence of the DNA-binding domain of DevR. Microbiology **150:**865-875.

Sakamoto, J., T. Shibata, T. Mine, R. Miyahara, T. Torigoe, S. Noguchi, K. Matsushita, and N. Sone. 2001. Cytochrome *c* oxidase contains an extra charged amino

acid cluster in a new type of respiratory chain in the amino-acid-producing bacterium *Corynebacterium glutamicum*. Microbiology **147:**2865-2871.

Salgame, P. 2005. Host innate and Th1 responses and the bacterial factors that control *Mycobacterium tuberculosis* infection. Curr. Opinion Immunol. **17:**374-380.

Sambrook, J., and D.W. Russell. 2001. Molecular cloning: a laboratory manual, 3rd ed. Cold Spring Harbor Laboratory Press, Cold Spring Harbor, N. Y.

Sassetti C. M., D. H. Boyd, and E. J. Rubin. 2003. Genes required for mycobacterial growth defined by high density mutagenesis. Mol. Microbiol. **48:**77-84.

Schau, M., Y. Chen, and F. M. Hulett. 2004. *Bacillus subtilis* YdiH is a negative regulator of the *cydABCD* operon. J. Bacteriol. **186:**4585-4595.

Schnappinger, D., S. Ehrt, M. I. Voskuil, Y. Liu, J. A. Mangan, I. M. Monahan, G. Dolganov, B. Efron, P. D. Butcher, C. Nathan, and G. K. Schoolnik. 2003. Transcriptional adaptation of *Mycobacterium tuberculosis* within macrophages: insights into the phagosomal environment. J. Exp. Med. **198:**693-704.

Schuler, F., T. Yano, S. D. Bernardo, T. Yagi, V. Yankovskaya, T. P. Singer, and J. E. Casida. 1999. NADH-quinone oxidoreductase: PSST subunit couples electron transfer from iron-sulfur cluster N2 to quinone. Proc. Natl. Acad. Sci. USA **96:**4149-4153.

Shen, Y., L. Shen, P. Sehgal, D. Huang, L. Qiu, G. Du, N. L. Letvin, and Z. W. Chen. 2004. Clinical latency and reactivation of AIDS-related mycobacterial infections. J. Virol. **78:**14023-14032.

Sherman, D. R., M.I. Voskuil, D. Schnappinger, R. Liao, M.I. Harrell, and G.K. Schoolnik. 2001. Regulation of the *Mycobacterium tuberculosis* hypoxic response gene encoding α-crystallin. Proc. Nat. Acad. Sci. **98:**7534-7539.

Smyth, G. K. 2004. Linear models and empirical Bayes methods for assessing differential expression in microarray experiments. Statistical Applications in Genetics and Molecular Biology **3:** Article 3.

Smyth, G. K., J. Michaud, and H. S. Scott. 2005. Use of within-array replicate spots for assessing differential expression in microarray experiments. Bioinformatics 0: 2701 (Epub ahead of print).

Snapper, S. B., R. E. Melton, T. Mustafa, T. Keiser, and W. R. Jacobs, Jr. 1990. Isolation and characterization of efficient plasmid transformation mutants of *Mycobacterium smegmatis*. Mol. Microbiol. **4:**1911-1919.

Solomon, E. P., L. Berg, D. W. Martin, and C. Villee. 1993. Biology, third edition, p.162-180., Saunders College Publishing, USA.

Sone, N., K. Nagata, H. Kojima, J. Tajima, Y. Kodera, T. Kanamaru, S. Noguchi, and Sakamoto. 2001. A novel hydrophobic diheme *c*-type cytochrome: purification from *Corynebacterium glutamicum* and analysis of the *qcrCBA* operon encoding three subunit proteins of a putative cytochrome reductase complex. Biochim. Biophys. Acta **1503:**279-290.

Sone, N., M. Fukuda, S. Katayama, A. Jyoudai, M. Syugyou, S. Noguchi, and J. Sakamoto. 2003. *QcrCAB* operon of a nocardia-form actinomycete *Rhodococcus rhodochrous* encodes cytochrome reductase complex with diheme cytochrome *cc* subunit. Biochim. Biophys. Acta **1557:**125-131.

Stewart, G. R., B. D. Robertson and D. B. Young. 2003. Tuberculosis: a problem with persistence. Nat. Rev. Microbiol. **1:**97-105.

Stover, C. K., V. F. de la Cruz, T. R. Fuerst, J. E. Burlein, L. A. Benson, L. T. Bennett, G. P. Bansal, J. F. Young, M. H. Lee, and G. F. Hatfull. 1991. New use of BCG for recombinant vaccines. Nature **351:**456-460.

Sturr, M. G., T. A. Krulwich, and D. B. Hicks. 1996. Purification of a cytochrome *bd* terminal oxidase encoded by the *Escherichia coli app* locus from a Δ*cyo* Δ*cyd* strain complemented by genes from *Bacillus firmus* OF4. J. Bacteriol. **176:**1742-1749.

Swem, D. L., and C. E. Bauer. 2002. Coordination of ubiquinol oxidase and cytochrome cbb_3 oxidase expression by multiple regulators in *Rhodobacter capsulatus*. J. Bacteriol. **184:**2815-2820.

Swem, L. R., B. J. Kraft, D. L. Swem, A. T. Setterdahl, S. Masuda, D. B. Knaff, J. M. Zaleski, and C. E. Bauer. 2003. Signal transduction by the global regulator RegB is mediated by a redox-active cysteine. EMBO J. **22:**4699-4708.

Timm, J., F. A. Post, L. G. Bekker, G. B. Walther, H. C. Wainwright, R. Manganelli, W. T. Chan, L. Tsenova, B. Gold, I. Smith, G. Kaplan, and J. D. McKinney. 2003. Differential expression of iron-, carbon-, and oxygen-responsive mycobacterial genes in the lungs of chronically infected mice and tuberculosis patients. Proc. Natl. Acad. Sci. USA **100:**14321-14326.

Tran, S. L., and G. M. Cook. 2005. The F_1F_0 –ATP synthase of *Mycobacterium smegmatis* is essential for growth. J. Bacteriol. **187:**5023-5028.

Tsang, W. Y., L. C. Sayles, L. I. Grad, D. B. Pilgrim, and B. D. Lemire. 2001. Mitochondrial respiratory chain deficiency in *Caenorhabditis elegans* results in developmental arrest and increased life span. J. Biol. Chem. **276:**32240-32246.

Tyagi, J. S., and D. Sharma. 2002. *Mycobacterium smegmatis* and tuberculosis. Trends Microbiol. **10:**68-69.

van der Oost, J., T. Haltia, M. Raitio, and M. Saratse. 1991. Genes encoding for cytochrome *c* oxidase in *Paracoccus denitrificans.* J. Bioenerg. Biomembr. **23:**257-267.

van der Oost, J., M. Schepper, A. H. Stouthamer, H. V. Westerhoff, R. J. M. van Spanning, and J.-W. L. de Gier. 1995. Reversed electron transfer through the bc_1 complex enables cytochrome *c* oxidase mutant ($\Delta aa_3/cbb_3$) of *Paracoccus denitrificans* to grow on methylamine. FEBS Lett. **371:**267-270.

van Helden, P. D. 2003. The economic divide and tuberculosis. EMBO reports **4:**524-528.

Vilchèze, C., T. R. Weisbrod, B. Chen, L. Kremer, M. H. Hazbón, F. Wang, D. Alland, J. C. Sacchettini, and W. R. Jacobs, Jr. 2005. Altered $NADH/NAD^+$ ratio mediates coresistance to isoniazid and ethionamide in mycobacteria. Antimicrob. Agents Chemother. **49:**708-720.

Volkman, H. E., H. Clay, D. Beery, J. C. W. Chang, D. R. Sherman, and L. Ramakrishnan. 2004. Tuberculous granuloma formation is enhanced by a *Mycobacterium tuberculosis* virulence determinant. PloS Biology **2:**1946-1956.

Voskuil, M. I., D. Schnappinger, K.C. Visconti, M.I. Harrell, G.M. Dolganov, D.R. Sherman, and Schoolnik, G. K. 2003. Inhibition of respiration by nitric oxide induces a *Mycobacterium tuberculosis* dormancy program. J. Exp. Med. **198:**705-713.

Voskuil, M.I., K.C. Visconti, and G.K. Schoolnik. 2004. *Mycobacterium tuberculosis* gene expression during adaptation to stationary phase and low oxygen dormancy. Tuberculosis **84:**281-227.

Wallis, R. S. 2005. Reconsidering adjuvant immunotherapy for tuberculosis. Clin. Infect. Dis. **41:**201-208.

Warner, D. F. 2005. Ph.D. thesis. University of the Witwatersrand, Johannesburg, South Africa.

Wayne, L. G., and L. G. Hayes. 1996. An in vitro model for sequential study of shiftdown of *Mycobacterium tuberculosis* through two stages of nonreplicating persistence. Infect. Immun. **64:**2062-2069.

Wayne, L. G., and Sohaskey, L. G. 2001. Nonreplicating persistence of *Mycobacterium tuberculosis*. Annu. Rev. Microbiol. **55:**139-163.

Weinstein, E. A., T. Yano, L.-S. Li, D. Avarbock, A. Avarbock, D. Helm, A. A. McColm, K. Duncan, J. T. Lonsdale, and H. Rubin. 2005. Inhibitors of type II NADH:menaquinone oxidoreductase represent a class of antitubercular drugs. Proc. Natl. Acad. Sci. USA **102:**4548-4553.

Wikström, M. 2001. Cytochrome *c* oxidase, p.1-8. *In* Encyclopedia of Life Sciences, Nature Publishing Group, London, UK.

Wikström, M. 2002. Cytochrome *c* oxidase, p1-8. *In* Encyclopedia of Life Sciences, Nature Publishing Group, London, UK.

Wikström, M. 2004. Cytochrome *c* oxidase: 25 years of the elusive proton pump. Biochim. Biophys. Acta **1655:**241-247.

Williams, B. G., and C. Dye. 2003. Antiretroviral drugs for tuberculosis control in the era of HIV/AIDS. Science **301:**1535-1537.

Winstedt, L., and C. von Wachenfeldt. 2000. Terminal oxidases of *Bacillus subtilis* strain 168: one quinol oxidase, cytochrome aa_3 or cytochrome *bd*, is required for aerobic growth. **182:**6557-6564.

Wren, B. W., S. M. Colby, R. R. Cubberly, and M. J. Pallen. 1992. Degenerate PCR primers for the amplification of fragments from genes encoding response regulators from a range of pathogenic bacteria. FEMS Microbiol. Lett. **99:**287-292.

Yang, Y. H., S. Dudoit, P. Luu and T. P. Speed. 2001. Normalisation for cDNA microarray data, p. 141-152. *In* M. L. Bittner, Y. Chen, A. N. Dorsel, and E. R. Dougherty (ed.), Microarrays: optical technologies and informatics. Proceedings of SPIE, vol 4266. San Jose, California.

Yankovskaya, V., R. Horsefield, S. Törnroth, C. Luna-Chavez, H. Miyoshi, C. Leger, B. Byrne, G. Cecchini, and S. Iwata. 2003. Architecture of succinate dehyrogenase and reactive oxygen species generation. Science **299:**700-704.

Yuan, Y., D. D. Crane, and C. E. Barry, III. 1996. Stationary phase-associated expression in *Mycobacterium tuberculosis*: function of the mycobacterial α-crystallin homolog. J. Bacteriol. **178:**4484-4492.

Zahrt, T. C., and V. Deretic. 2001. *Mycobacterium tuberculosis* signal transduction system required for persistent infections. Proc. Natl. Acad. Sci. USA **98:**12706-12711.

Zhang, Z., L. Huang, V. M. Shulmeister, Y.-I. Chi, K. K. Kim, L.-W. Hung, A. R. Crofts, E. A. Berry, and S.-H. Kim. 1998. Electron transfer by domain movement in cytochrome bc_1. Nature **392:**677-684.

Zhang, J., P. Hellwig, J. P. Osborne, and R. B. Gennis. 2004. Arginine 391 in subunit I of the cytochrome *bd* quinol oxidase from *Escherichia coli* stabilizes the reduced form of the hemes and is essential for quinol oxidase activity. J. Biol. Chem. **279:**53980-53987.

Zientz, E., J. Bongaerts, and G. Unden. 1998. Fumarate regulation of gene expression in *Escherichia coli* by the DcuSR (*dcuSR* genes) two-component regulatory system. J. Bacteriol. **180:**5421-5425.

JOURNAL OF BACTERIOLOGY, Sept. 2005, p. 6300–6308 Vol. 187, No. 18
0021-9193/05/$08.00+0 doi:10.1128/JB.187.18.6300–6308.2005

Function of the Cytochrome bc_1-aa_3 Branch of the Respiratory Network in Mycobacteria and Network Adaptation Occurring in Response to Its Disruption†

Limenako G. Matsoso,[1] Bavesh D. Kana,[1] Paul K. Crellin,[2] David J. Lea-Smith,[2] Assunta Pelosi,[2] David Powell,[3] Stephanie S. Dawes,[1] Harvey Rubin,[4] Ross L. Coppel,[2] and Valerie Mizrahi[1]*

MRC/NHLS/WITS Molecular Mycobacteriology Research Unit, DST/NRF Centre of Excellence in Biomedical TB Research, School of Pathology, National Health Laboratory Service, and University of the Witwatersrand, Johannesburg, South Africa[1]; Department of Microbiology, Monash University, and ARC Centre for Structural and Functional Microbial Genomics, Monash, Australia[2]; Department of Computer Science and Software Engineering, Monash University, and the Victorian Bioinformatics Consortium, Monash, Australia[3]; and Division of Infectious Diseases, Department of Medicine, University of Pennsylvania, Philadelphia, Pennsylvania 19104[4]

Received 29 April 2005/Accepted 15 June 2005

The aerobic electron transport chain in *Mycobacterium smegmatis* can terminate in one of three possible terminal oxidase complexes. The structure and function of the electron transport pathway leading from the menaquinol-menaquinone pool to the cytochrome bc_1 complex and terminating in the aa_3-type cytochrome *c* oxidase was characterized. *M. smegmatis* strains with mutations in the bc_1 complex and in subunit II of cyctochome *c* oxidase were found to be profoundly growth impaired, confirming the importance of this respiratory pathway for mycobacterial growth under aerobic conditions. Disruption of this pathway resulted in an adaptation of the respiratory network that is characterized by a marked up-regulation of *cydAB*, which encodes the bioenergetically less efficient and microaerobically induced cytochrome *bd*-type menaquinol oxidase that is required for the growth of *M. smegmatis* under O_2-limiting conditions. Further insights into the adaptation of this organism to rerouting of the electron flux through the branch terminating in the *bd*-type oxidase were revealed by expression profiling of the bc_1-deficient mutant strain using a partial-genome microarray of *M. smegmatis* that is enriched in essential genes. Although the expression profile was indicative of an increase in the reduced state of the respiratory chain, blockage of the bc_1-aa_3 pathway did not induce the sentinel genes of *M. smegmatis* that are induced by oxygen starvation and are regulated by the DosR two-component regulator.

The ability of *Mycobacterium tuberculosis* to grow and persist in its human host and to establish and maintain a state of latent tuberculosis infection from which it can reactivate to cause disease is critical to its extraordinary success as a pathogen. This remarkable competence is attributable to *M. tuberculosis*'s ability to adapt physiologically to the environmental conditions encountered during the course of an infection. These conditions are thought to include restricted nutrient availability and oxidative and nitrosative stress imposed by the host immune response (10, 37, 39, 41).

Of these, the mechanism of physiological adaptation to O_2 restriction has been most intensively investigated. These studies have revealed that gradual depletion of O_2 from cultures of *M. tuberculosis* leads to progression of this organism through two stages of nonreplicating persistence, confirming that its replication requires the availability of O_2 (41). Of particular importance was the observation that a rapid shift from an aerobic environment to an oxygen-deficient one resulted in bacterial death, indicating that ordered metabolic shutdown is necessary for adaptation to hypoxia or anoxia. Recent studies that have utilized transcriptional profiling to explore the metabolic changes that occur in *M. tuberculosis* in response to inhibiting aerobic electron flow by O_2 depletion (5, 23, 31, 39) and by other means (5, 39) have revealed intriguing insights into the respiratory network of *M. tuberculosis* that underscore the need to investigate its function and regulation at a molecular level (6).

Mycobacteria possess a branched aerobic respiratory chain in which electrons flow from NADH dehydrogenase and succinate dehydrogenase complexes into the menaquinone-menaquinol pool, from where they are transferred either to an aa_3-type cytochrome *c* oxidase (CcO) via the cytochrome bc_1 complex or directly to the cytochrome *bd*-type menaquinol oxidase (6, 16, 42). The branch terminating in the *bd*-type oxidase was shown to be important for microaerobic respiration in *M. smegmatis* (16) and as such is functionally analogous to *bd*-type oxidase-terminating branches in other organisms (25). In contrast, little is currently known about the CcO-terminating branch in mycobacteria. Genome comparisons suggest that its structure resembles those of other nocardio-

* Corresponding author. Mailing address: Molecular Mycobacteriology Research Unit, NHLS, P. O. Box 1038, Johannesburg 2000, South Africa. Phone: 2711 4899370. Fax: 27 11 4899001. E-mail: mizrahiv@pathology.wits.ac.za.

† Supplemental material for this article may be found at http://jb.asm.org/.

TABLE 1. Strains and plasmids used in this study

Strain or plasmid	Characteristics[a]	Source or reference
M. tuberculosis H37Rv	Laboratory strain ATCC 27294	Laboratory collection
M. smegmatis		
mc^{2}155	High-frequency transformation mutant of ATCC 607	34
Δ*qcrCAB*::*hyg*	*qcrCAB* deletion-replacement mutant of mc^{2}155; Hyg^r	This work
Δ*ctaC*::*hyg*	*ctaC* deletion-replacement mutant of mc^{2}155; Hyg^r	This work
ctaDI$^{+/-}$	Derivative of mc^{2}155 with one wild-type *ctaDI* and one Δ*ctaD*::*hyg* allele	This work
Δ*ctaDII*::*hyg*	*ctaDII* deletion-replacement mutant of mc^{2}155; Hyg^r	This work
mc^{2}155::pBK4	mc^{2}155 carrying pBK4 integrated at *cyd* locus; Km^r	16
Δ*qcrCAB*::*hyg*::pBK4	Δ*qcrCAB*::*hyg* carrying pBK4 integrated at *cyd* locus; Hyg^r Km^r	This work
Plasmids		
pGEM3Z(+)f	*E. coli* cloning vector; Ap^r	Promega
pGEMTeasy	*E. coli* cloning vector for cloning PCR products; Ap^r	Promega
pCR2.1-TOPO	*E. coli* vector for cloning PCR products; Km^r Ap^r	Invitrogen
p2NIL	*E. coli* vector for cloning homologous recombination substrates; Km^r	22
pGOAL17	Vector carrying P_{Ag85}-*lacZ* P_{hsp60}-*sacB* PacI marker cassette; Ap^r	22
pIJ963	*E. coli* vector carrying *hyg* cassette	2
pBK4	p2NIL containing the *M. smegmatis cydA′*::*lacZ* fusion cassette; Hyg^r	16
pQCRTBKO	Knockout vector carrying *M. tuberculosis* Δ*qcrCAB* allele; Hyg^r Km^r	This work
pCTACTBKO	Knockout vector carrying *M. tuberculosis* Δ*ctaC*::*hyg* allele; Hyg^r Km^r	This work
pQCRSMKO	Knockout vector carrying *M. smegmatis* Δ*qcrCAB*::*hyg* allele; Hyg^r Km^r	This work
pCTADISMKO	Knockout vector carrying *M. smegmatis* Δ*ctaDI*::*hyg* allele; Hyg^r Km^r	This work
pCTADIISMKO	Knockout vector carrying *M. smegmatis* Δ*ctaDII*::*hyg* allele; Hyg^r Km^r	This work
pCTACSMKO	Knockout vector carrying *M. smegmatis* Δ*ctaC*::*hyg* allele; Hyg^r Km^r	This work

[a] Ap^r, ampicillin resistance; Hyg^r, hygromycin resistance; Km^r, kanamycin resistance.

form actinomycetes, such as *Corynebacterium glutamicum* (7, 18, 19, 29, 35) and *Rhodococcus rhodochrous* (36), which are distinguished by the fact that the cytochrome c_1 (QcrC) in these organisms is a distinct, diheme *c*-type cytochrome (18, 35).

A resulting feature of note inferred from studies in *C. glutamicum* (7, 19) is that the mycobacterial bc_1 complex and the cytochrome aa_3 oxidase would be expected to form a supercomplex. We have adopted a genetic approach to investigate the function of the bc_1-aa_3 branch in mycobacteria and, in this paper, report the construction of mutations in *M. smegmatis* genes encoding the bc_1 complex and the aa_3-type CcO. The results of this study demonstrate the importance of the cytochrome bc_1-aa_3 branch for mycobacterial growth and suggest that the disruption of this pathway is accompanied by an adaptation of the respiratory network that is characterized by constitutive up-regulation of the menaquinol oxidase, cytochrome *bd*-type menaquinol oxidase, and some genes previously shown to be induced by hypoxia, such as *uspL* (5, 20, 23, 31) and Rv1592c (5, 23, 31), but not of sentinel, DosR-regulated genes (20).

MATERIALS AND METHODS

Bacterial strains and plasmids. The strains and plasmids used in this study are shown in Table 1. The vectors pQCRTBKO and pCTACTBKO were used for knockout of *qcrCAB* and *ctaC*, respectively, in *M. tuberculosis*, whereas pQCRSMKO, pCTADSMKO, pCATD2SMKO, and pCATCSMKO were used for knockout of the *qcrCAB*, *ctaDI*, *ctaDII*, and *ctaC* genes, respectively, in *M. smegmatis*. A deletion allele of *M. tuberculosis qcrCAB* was constructed by ligating the 3,147-bp upstream ScaI/PstI fragment (containing the 5′-terminal 240 bp of *qcrC*) to the 3,256-bp downstream PstI fragment (containing the 3′-terminal 800 bp of *qcrB*) in p2NIL (22), thus eliminating an internal, 2,734-bp region from the *qcrCAB* operon. The *hyg-lacZ-sacB* marker cassette from pGOAL19 (22) was cloned in the PacI site of the resulting plasmid to produce pQCRTBKO.

Deletion alleles of the remaining genes were constructed by PCR amplification of 5′- and 3′-flanking regions using the primer pairs shown in Table 2. In the case of the *M. smegmatis* genes, the PCR primers were designed based on the open reading frame sequences identified in the preliminary genome sequence of strain mc^{2}155 from the Institute for Genomic Research (http://www.tigr.org/ufmg/). The flanking regions were cloned in pGEMTeasy or pCR2.1-TOPO before simultaneously subcloning both fragments in p2NIL (22). The deletion alleles were marked by the insertion of a hygromycin resistance gene at the junction site before introduction of the *lacZ-sacB* marker cassette from pGOAL17 (22) in the PacI site of p2NIL (22). The knockout vectors were electroporated into *M. tuberculosis* or *M. smegmatis* and mutant selection was carried out as previously described (3, 14, 22).

Bacterial culture conditions. *Escherichia coli* DH5α used for cloning procedures was grown in Luria broth (LB) or agar (LA) containing 100 μg/ml ampicillin, 50 μg/ml kanamycin, or 200 μg/ml hygromycin where necessary. *M. smegmatis* strains were grown in LB or MADC-Tw [Middlebrook 7H9 broth (Difco) supplemented with 0.085% NaCl, 0.2% glucose, 0.2% glycerol, and 0.05% Tween 80] or on LA. *M. tuberculosis* strains were grown in Middlebrook 7H9 medium supplemented with Middlebrook ADC (Difco), 0.2% glycerol, and 0.05% Tween 80 in roller bottles or as stirred cultures. Antibiotic supplements were as follows: kanamycin, 10 μg/ml (solid medium) or 25 μg/ml (liquid medium), and hygromycin, 50 μg/ml.

For growth of cultures of wild-type and mutant strains of *M. smegmatis* in shaking flasks, starter cultures at an optical density at 600 nm (OD_{600}) of ~0.013 were prepared by diluting a preculture (OD_{600} ~2.0) in 100 ml of MADC-Tw, and incubating at 37°C with shaking (350 rpm). Optical density was monitored at 3-h intervals over a period of 42 to 60 h. Oxystatic growth of *M. smegmatis* strains was carried out in a New Brunswick Scientific Bioflow 110 fermentor in batch cultures. This system is similar to the Braun BIOSTAT B system employed by Kana et al. (16), with the exception that the rotometer allowed the air supply to be controlled from 0 to 150 ml/min, and agitation speeds ranged from 50 to 1200 rpm.

Oxystatic culturing of reporter strains was carried out as follows. The fermentor was autoclaved with 990 ml of Middlebrook 7H9 and 2 ml of glycerol. Glucose and NaCl were added as the vessel cooled down, to bring the final volume to 1 liter. The vessel was allowed to equilibrate overnight, before the dissolved-O_2 probe was calibrated. The 0% air saturation level was set by sparging the medium with 100% nitrogen and the 100% air saturation level was set by sparging with 100% compressed air. The medium was inoculated with 200 ml of a preculture (OD_{600} = 2.0) to yield a starting culture of ca. 10^7 CFU/ml. To

TABLE 2. Oligonucleotides and probes used in this study

Gene(s)	Oligonucleotide	Oligonucleotide pairs used to construct knockout vector	
		Sequence (5′–3′)[a]	Region amplified
M. smegmatis qcrCAB	QCRF1	GGGCCGGAAGCttATGGGAACGGCTGGGAAGGT	878-bp product including 114 bp of 5′ end of *qcrC*
	QCRR1	CTGCCAGACgGATCcGCAGCAGAAGCCCTGCTGACA	
	QCRF2	CGCTCACCGgGATCcCGCATGCGTCCGAGCACA	863-bp product including 104 bp of 3′ end of *qcrB*
	QCRR2	GCTGTCGGgtACCTGTGCGCTGGGCGTGGC	
M. smegmatis ctaC	CTACF1	TTCGGGACGAgGTACCGCGTCACCTCGGGTGC	1,038-bp product including 130 bp of 5′ end of *ctaC*
	CTACR1	TTGCCTCAGGGGgGATcCCCGTTGGCCAGCCGAGT	
	CTACF2	CAAGGCCTACATgGATCcGCGCAACGCCGG	1,100-bp product including 139 bp of 3′ end of *ctaC*
	CATCR2	TCACGCGCGACGAGAAGCttTACCGACGCCACG	
M. smegmatis ctaDI	CTAD1F1	ACCTCGTCGgGTACCGAGGCAGGCAGCCCGGCG	883-bp product including 114 bp of 3′ end of *ctaDI*
	CTAD1R1	ACTACCCGCACATGGTCGAGCGGATcCGGGCCGA	
	CTAD1F2	TGAACAGCGCCAgGAtcCCGCCGACCAGGAAGAA	787-bp product including 69 bp of 5′ end of *ctaDI*
	CTAD1R2	AATACGACGGCTGCGCGTCCGAAgCTtCGGGCAG	
M. smegmatis ctaDII	CTAD2F1	ACCCGGAGGaaGCTtGCTGGCTGTGTCCGGCGCT	859-bp product including 217 bp of 5′ end of *ctaDII*
	CTAD2R1	AACTGCAGGCCGGGATCCGCCAACTCGGTGCGGA	
	CTAD2F2	TCACGGTCGAgGATCCGTGGGGCTACGGCAACT	844-bp product including 239 bp of 3′ end of *ctaDII*
	CGCGTTTGGgGTAccTCTCCAGATCCCAACCGA		
M. tuberculosis ctaC	TBCTACF1	GGCCATCTCGTGGAAGCttCTACCCAGGTCC	1,903-bp product including 221 bp of 3′ end of *ctaC*
	TBCTACR1	TCGTGGGCCACTGCGtCtAGATGTGTGGCAC	
	TBCTACF2	AGCATTGCTGCGAGCGCCAGCTcTaGAAGACCAC	1,994-bp product including 111 bp of 5′ end of *ctaC*
	TBCTACR2	GTACTTGGTGGTGGTACGGGTaAgCTTGGCGCCC	

[a] Restriction sites used for cloning are underlined (HindIII, BamHI, KpnI), and bases changed to introduce the site are given in lowercase letters.

produce cultures for use in microarray analyses, a total culture volume of 2 liters was used.

***cyd* expression analysis using a *lacZ* reporter.** To monitor *cyd* expression in a cytochrome bc_1-deficient background, a reporter strain was constructed by electroporation of plasmid pBK4 into the Δ*qcrCAB*::*hyg* mutant, where pBK4 is a suicide plasmid carrying a *cydA′*::*lacZ* transcriptional fusion that expresses the *lacZ* gene under the control of the *cyd* promoter (16). Single crossovers were selected on media containing kanamycin and 5-bromo-4-chloro-3-indolyl-β-D-galactopyranoside (X-Gal) and site specificity of recombination at the *cyd* locus was confirmed by Southern blot analysis. β-Galactosidase activity assays were performed as described by Kana et al. (16). To determine statistical significance, unpaired *t* tests were performed using GraphPad Instat version 3.00 (http://www.graphpad.com).

RNA purification and labeling for DNA microarrays. RNA was extracted as described by Betts et al. (1). RNA from the control experiment (2 μg) was labeled with Cy3-dCTP (Amersham Pharmacia Biotech), whereas that from the subject (4 μg) was labeled with Cy5-dCTP using previously described methods (4).

Construction of a partial-genome amplicon array of *M. smegmatis* mc²155. A partial *M. smegmatis* array of 1,822 genes was constructed to analyze the transcriptional profile of the two samples. Selection was on the basis of homology with the functional genes of *Mycobacterium leprae* (9), as established via tblastn analysis. A total of 1,327 *M. leprae* genes demonstrated homology to one or more genes in *M. smegmatis*. Preliminary sequence data were obtained from the Institute for Genomic Research website at http://www.tigr.org. In addition, 99 homologs of selected *M. tuberculosis* genes were added to the array (8). Included in this list were homologs of respiratory pathway genes (including *cydA*, *cydB*, *ctaDII*, and MSMEG5584) and of those that are hypoxically inducible (31).

PCR primers with equivalent melting temperatures were designed using PRIMER3 software to amplify internal segments of each gene ranging in size from 100 to 1,000 bp (28) (source code available at http://fokker.wi.mit.edu/primer3/). Primers were synthesized by PROLIGO Australia Pty Ltd. PCR products were produced by a MWG Biotech Roboamp 4200 thermocycler in 96-well plates using the amplification protocol of 94°C for 2 min, 30 cycles of 94°C for 30 s, 60°C for 30 s, and 72°C for 1 min, followed by 72°C for 5 min. Amplicons were evaluated by agarose gel electrophoresis with only six primer pairs not amplifying single products of the right size. Products were purified in Millipore multiscreen 96-well filtration plates and resuspended in 50% dimethyl sulfoxide (Sigma). The microarrays were printed in triplicate on Corning Gaps II slides using a Genetic Microsystems Inc. GMS 417 Arrayer. Slides were hydrated at 100°C for 5 s, cross-linked using a Stratagene UV Stratalinker 1800, baked at 80°C for 2 h, and boiled for 2 min prior to storage. The MIAME (Minimum Information About a Microarray Experiment) compliance file can be downloaded at http://vbc.med.monash.edu.au/~powell/M.smegmatis.

Microarray hybridization and data analysis. The amplicon array slides were washed in 95°C deionized water (2 min), rinsed in 95% ethanol, and quick-dried by centrifugation (500 rpm, 5 min) prior to hybridization. The slides were prehybridized for 1 h at 42°C in a buffer containing 5× SSC (1× SSC is 0.15 M NaCl plus 0.015 M sodium citrate), 1% bovine serum albumin, and 0.1% sodium dodecyl sulfate (SDS). Labeled probes were mixed with blocking reagents (4 μg yeast tRNA, 1.9 μg herring sperm DNA) and made up to a total of 24 μl in hybridization buffer (5× SSC, 25% formamide, 0.1% SDS). Samples were denatured at 98°C for 2 min, snap-cooled on ice, and applied to the array. Hybridization was carried out under a glass coverslip in a humidified slide chamber (Corning) submerged in a 42°C water bath for approximately 16 h. Coverslips were removed in wash buffer I (1× SSC, 0.05% SDS) and slides were washed once in buffer I and twice in buffer II (0.1× SSC) for 2 min each at room temperature before being dried by centrifugation (500 rpm, 5 min). Slides were scanned using a GenePix 4000B instrument (Axon Instruments) and the resulting images were analyzed using GenePix Pro 4.0 software (Axon Instruments). Each experiment was performed using three biological replicates. Since each amplicon was spotted in triplicate on the array, a total of nine data points were obtained for each open reading frame.

Image analysis and quantification were performed using Imagene 6.0 (BioDiscovery). Spots found to be poor were flagged and removed from the analysis. Subsequent analysis was done using Bioconductor (11) and Limma (32). Spot intensities were background corrected by subtracting the background median from the foreground mean. Any resulting nonpositive values were replaced with half the minimum of all positive corrected intensities for that array. The normalization to remove various biases involved two parts. First, each array was normalized independently using print-tip loess normalization (43). Second, diagnostic plots suggested a variation in scale between arrays, so the log-ratios were scaled in such a way that each array had the same median-absolute-deviation (MAD). The normalized data were then used to fit a linear model (43) for each gene using generalized least-squares, which takes into account the correlation between duplicate spots (33). The coefficient of the fitted model for each gene describes the inferred difference in RNA expression between wild-type and mutant cells. Empirical Bayes was then used to calculate the moderated *t*

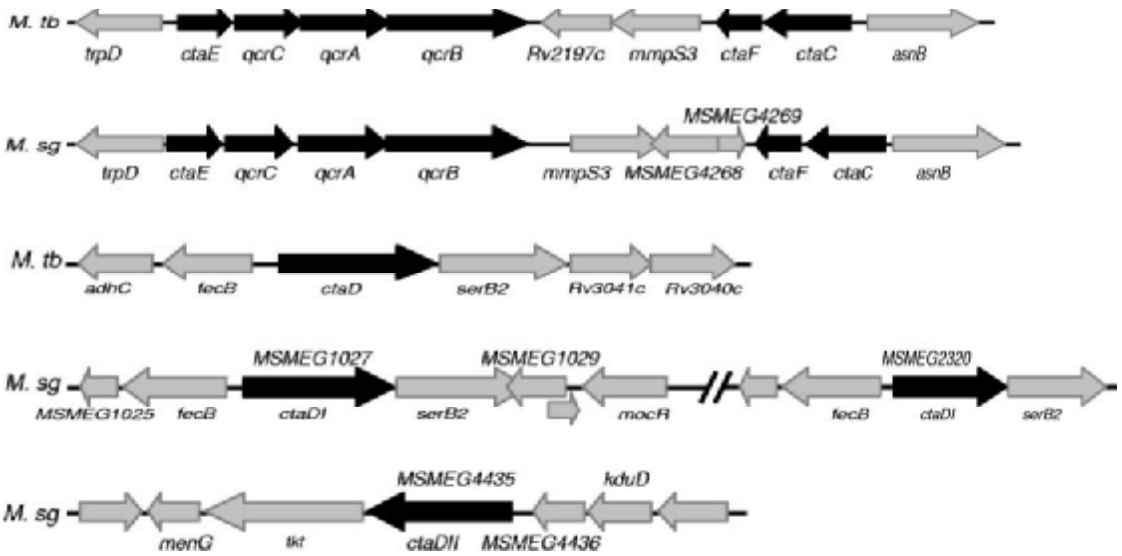

FIG. 1. Genomic organization of bc_1-aa_3 respiratory pathway genes in mycobacteria. The arrows denote the respiratory pathway (black) and neighboring genes (gray). The gene annotation for *M. tuberculosis* H37Rv is taken from Tuberculist (http://genolist.pasteur.fr/TubercuList/), and the annotation for *M. smegmatis* mc^{2}155 is from the TIGR Comprehensive Microbial Resource (http://www.tigr.org/tigr-scripts/CMR2/CMRHomePage.spl).

statistics and associated *P* values. The *P* values were adjusted for multiple testing using false-discovery-rate. At a cutoff of 1% false-discovery-rate, 78 genes were found to be differentially expressed; this corresponds to less than one expected false-positive.

RESULTS

Targeted knockout of genes in the cytochrome bc_1-aa_3 respiratory pathway in *M. tuberculosis*. To investigate the role of the cytochrome bc_1-aa_3 branch in aerobic respiration in *M. tuberculosis*, the *qcrCAB*-encoded menaquinol-cytochrome *c* oxidoreductase was targeted for disruption by allelic exchange mutagenesis using an unmarked Δ*qcrCAB* allele delivered on a suicide plasmid (22). Both up- and downstream single crossovers were obtained. However, no double crossovers were recovered following counterselection against an upstream single crossover; all Km^s clones analyzed (20 of 20) were wild-type revertants generated by second crossover events on the same side of the deletion mutation (data not shown).

To increase the likelihood of identifying potentially growth-impairing mutations in this pathway, allelic exchange mutagenesis was attempted using a *hyg*-marked deletion-replacement allele of the *M. tuberculosis ctaC* gene, which encodes subunit II of CcO. The counterselection plates containing sucrose and hygromycin were incubated at 37°C for more than twice the normal length of time (54 versus 21 days) before colonies were picked for screening. However, no double crossovers were recovered; all clones obtained from upstream (25 of 25) and downstream single crossovers (40 of 40) were Km^r, suggesting that they were all spontaneous *sacB* mutants.

Targeted knockout of genes in the cytochrome bc_1-aa_3 pathway in *M. smegmatis*. Genes in the corresponding pathway of *M. smegmatis* were identified by BLAST searches of the unfinished genome sequence of strain mc^{2}155 (http://www.tigr.org/ufmg/) using the corresponding *M. tuberculosis* genes as query sequences. This analysis revealed the presence of three *ctaD* homologues encoding subunit I of cytochrome *c* oxidase in *M. smegmatis*, two of which are identical but differ from the third. The two identical homologues are located within a region of the genome of mc^{2}155 that is duplicated (12) and was recently shown by genome sequence analysis to be 52 kb in length and flanked by IS*1096* elements (http://www.tigr.org/tigr-scripts/CMR2/CMRHomePage.spl). This duplicated *ctaD* homologue, which is designated herein as *ctaDI*, shows 86% identity with *M. tuberculosis ctaD* at the amino acid level and is located in the same chromosomal context as *M. tuberculosis ctaD* (Fig. 1; MSMEG1027 and MSMEG2320). The second homologue, *ctaDII*, shares 85% identity with *M. tuberculosis ctaD* at the amino acid level but is located in a different chromosomal context (Fig. 1; MSMEG4435).

The duplication of *ctaDI* was confirmed by allelic exchange mutagenesis using a knockout vector carrying a Δ*ctaDI*::*hyg* allele (pCTADISMKO). Southern blot analysis of double crossovers revealed the presence of two cross-hybridizing bands of 4.6 and 2.6 kb, which correspond to the wild-type (*ctaDI*) and Δ*ctaDI*::*hyg* alleles, respectively (Fig. 2; *ctaDI*$^{+/-}$ strain). However, attempts to create a null *ctaDI* mutant of *M. smegmatis* by inactivation of the second copy of *ctaDI* in the *ctaDI*$^{+/-}$ strain failed to produce double crossovers, suggesting that this gene may be essential (data not shown). In contrast, a Δ*ctaDII*::*hyg* mutant of mc^{2}155 was readily obtained (data not shown). This strain displayed no discernible growth phenotype under aerobic conditions (data not shown), suggesting that the *ctaDII* gene is dispensable for the growth of *M. smegmatis*.

In contrast to the results obtained in *M. tuberculosis*, viable Δ*qcrCAB*::*hyg* and Δ*ctaC*::*hyg* mutants of *M. smegmatis* were obtained by allelic exchange mutagenesis (Fig. 2). However, both strains exhibited a marked reduction in growth rate in aerated liquid cultures compared to their parental wild type even though they achieved comparable cell densities in stationary phase (Fig. 3A). The growth defect of the mutant strains

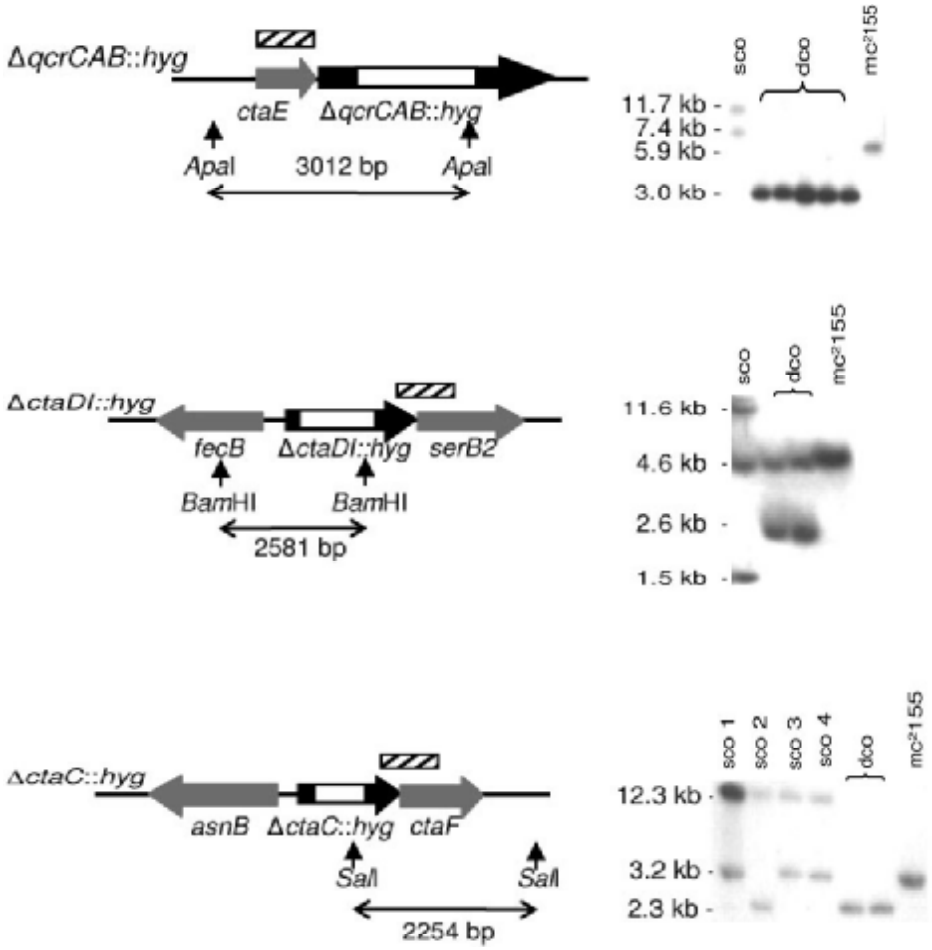

FIG. 2. Targeted knockout of bc_1-aa_3 respiratory pathway genes in *M. smegmatis* mc²155. Each panel shows a schematic representation of the mutant allele. The gene(s) in which internal deletions were made is denoted by a black arrow, the *hyg* gene is denoted by a white block, and neighboring genes are shown as gray arrows. The positions of the restriction enzymes used for Southern blot analysis shown on the right of each panel are indicated by vertical arrows, and the hybridization probes used in the analysis are shown as hatched boxes above each map. Chromosomal DNA from up- and downstream single-crossover (sco) recombinants, double crossovers (dco), and the parental wild type (mc²155) was digested with ApaI (*qcrCAB*), BamHI (*ctaDI*), or SalI (*ctaC*) and hybridized with the corresponding probe shown above the restriction map (hatched box).

was even more pronounced on solid medium (LA), with pinprick colonies taking a minimum of 6 days to appear (Fig. 3B). Both strains displayed visibly altered colony morphology, were highly variable in size, and continued to appear up to 2 weeks after plating.

Overexpression of cytochrome *bd* oxidase compensates for loss of the bc_1 complex. In prior work, we showed that *M. smegmatis* possesses a *cydAB*-encoded cytochrome *bd*-type menaquinol oxidase, which is induced under microaerobic conditions (16). To investigate the effect of loss of the bc_1 complex on expression of cytochrome *bd*-type menaquinol oxidase, we constructed a reporter strain that carried a *cydA′*::*lacZ* transcriptional fusion (16) site-specifically integrated at the *cyd* locus of the Δ*qcrCAB*::*hyg* mutant. Levels of β-galactosidase in the resulting Δ*qcrCAB*::*hyg*::pBK4 strain were analyzed under aerobic and microaerobic conditions and were compared with those observed in the control, mc²155::pBK4, in which the same transcriptional fusion was integrated at the *cyd* locus of the parental wild type. In both strains, the *lacZ* gene is under control of the *cyd* promoter.

Induction of *cyd* gene expression was observed in wild-type *M. smegmatis* under microaerobic conditions (Fig. 4), in agreement with previous results (16). Importantly, a marked increase in expression of the *cyd* operon was observed in the Δ*qcrCAB*::*hyg* mutant over the air saturation range tested (1 to 21%). The difference in the level of *cyd* expression between the wild-type and mutant strain was significant under all conditions tested ($P < 0.0001$). However, comparison of *cyd* expression levels in the mutant strain under conditions of varying O_2 availability revealed no significant induction under microaerobic conditions above the basal expression level observed under full aeration. These results suggest that the loss of cytochrome bc_1 resulted in constitutive overproduction of the *bd*-type oxidase.

Expression profiling of the bc_1 (Δ*qcrCAB*::*hyg*) mutant. To gain further insight into the effects of rerouting aerobic elec-

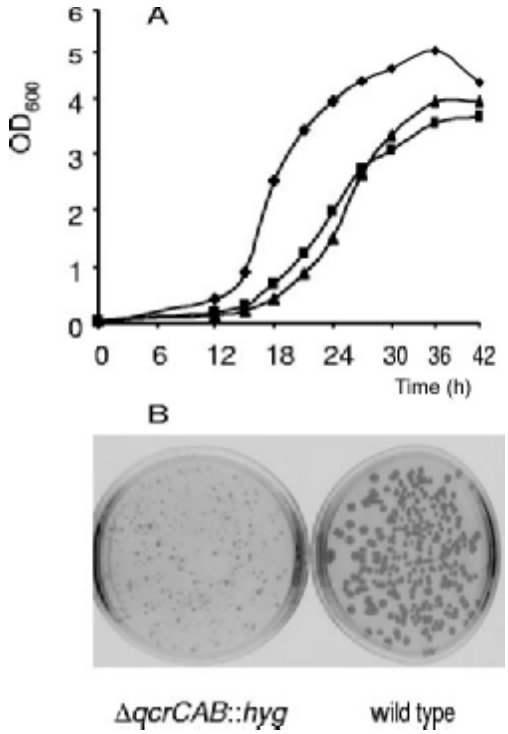

FIG. 3. Growth of the Δ*qcrCAB*::*hyg* and Δ*ctaC*::*hyg* mutants of *M. smegmatis* under aerobic conditions. (A) Growth in liquid medium. Strains were grown at 37°C in shaking flasks (350 rpm) in MADC-Tw medium, and growth was monitored by the absorbance at 600 nm (OD_{600}). ▲, Δ*qcrCAB*::*hyg*; ■, Δ*ctaC*::*hyg*; ◆, wild-type mc^2155. (B) Growth on solid medium. Strains were grown oxystatically (21% air saturation) in MADC-Tw in a bioreactor, and aliquots were withdrawn and plated on LA. Plates were incubated at 37°C for 3 days (wild type) or 6 to 8 days (mutant).

tron flow through the cytochrome *bd*-type menaquinol oxidase-terminating branch, expression profiling of aerobically grown cultures of the Δ*qcrCAB*::*hyg* mutant was carried out using a partial-genome amplicon array of *M. smegmatis*. In this experiment, Cy5-labeled cDNA from cultures of the mutant strain grown oxystatically at full aeration (21% pO_2) was hybridized against Cy3-labeled cDNA from the wild-type control cultured under identical conditions. A total of 78 genes were found to be differentially expressed, of which 42 were up- and 36 were down-regulated. The top-ranked differentially expressed genes are listed in Table 3, and the complete list is provided in the supplemental material (Table S1).

The majority of the up-regulated genes (52%) are involved in intermediary metabolism and respiration. Importantly, the presence of *cydA* in this group of differentially expressed genes was independently validated by the marked induction of *cyd* expression in the mutant strain, as deduced using the *cydA'*::*lacZ* reporter assay (Fig. 4). Other up-regulated genes included *uspL* and the *M. smegmatis* homolog of Rv1592c (MSMEG3205), which were previously shown to be induced in response to hypoxia in *M. tuberculosis* (*uspL* and Rv1592c) (5, 23, 31) and in *M. smegmatis* (*uspL*) (20). The marked up-regulation of *mihF* in the bc_1 mutant was also notable, as this gene is up-regulated in *M. smegmatis* just prior to stationary phase and may be involved in the expression of genes required for stationary-phase survival (24).

In contrast, many of the down-regulated genes are involved in information pathways (transcription and DNA repair) and in cell wall and cell processes. The most highly down-regulated gene was *lytB* (MSMEG5208). This gene is involved in the nonmevalonate pathway for the biosynthesis of terpenoids (27) and its down-regulation may thus affect the biosynthesis of menaquinone in the bc_1 mutant. The principal σ factor-encoding gene, *sigA* (13), was also markedly down-regulated in the bc_1 mutant, which is significant in light of the down-regulation of *sigA* that occurs in *M. tuberculosis* during anaerobiosis (6, 17).

DISCUSSION

Function of the cytochrome bc_1-aa_3 branch of the respiratory network in mycobacteria. A genetic approach was employed to investigate the function of the cytochrome bc_1-aa_3 branch of the respiratory network in mycobacteria. Allelic exchange mutagenesis was used to generate viable mutants of *M. smegmatis* lacking either subunit II (CtaC) of the aa_3-type CcO or the entire bc_1 complex (QcrCAB). These mutants were profoundly impaired for growth and in this respect resemble the corresponding bc_1-aa_3 pathway mutants of *C. glutamicum*, which displayed similar growth impairment in glucose minimal medium (7, 18). Together, these observations confirm that the bc_1-aa_3 pathway is the major respiratory route in actinomycetes grown under standard, aerobic culturing conditions.

Two distinct *ctaD* alleles were identified in the genome of *M. smegmatis*, *ctaDI* and *ctaDII*. CtaD is the only CcO subunit encoded by distinct alleles in *M. smegmatis*. Inactivation of *ctaDII* conferred no growth phenotype on *M. smegmatis*, confirming its dispensability for growth under the conditions tested. In contrast, a null *ctaDI* mutant lacking both copies of the *ctaDI* gene could not be recovered. The viability of other bc_1-aa_3 pathway mutants in *M. smegmatis* suggests that our

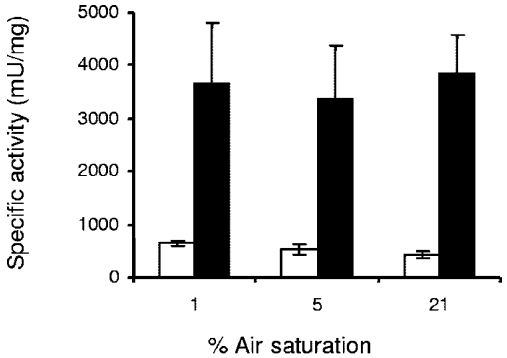

FIG. 4. Effect of cytochrome bc_1 disruption on expression of the *cyd* operon in *M. smegmatis*. Expression of the *cyd* operon was assessed using a previously described *lacZ* reporter under control of the *cyd* promoter (16) that was integrated at the *cyd* locus in the wild-type (open bars) and Δ*qcrCAB*::*hyg* (black bars) strains. The specific activity of the reporter gene product (β-galactosidase) was assessed at 21, 5, and 1% air saturation, as described under Materials and Methods. All assays were performed in duplicate and the data shown represent the averages and standard deviation of at least two independent experiments.

TABLE 3. Differentially expressed genes in aerobically grown Δ*qcrCAB*::*hyg* mutant of *M. smegmatis*

Genes and ID[a]	Gene	TIGR annotation[b]	Function[c]	*M*[d]	*P*	Class[e]
Upregulated genes						
ribA	*ribA2*	MSMEG3082	Probable riboflavin biosynthesis protein	−2.301	0.0020	7
ML2274		MSMEG3498	Probable conserved secreted protein	−1.914	0.0072	3
mihF	*mihF*	MSMEG3063	Putative integration host factor	−1.764	0.0003	2
glgC	*glgC*	MSMEG5067	Glucose-1-phosphate adenyl-transferase	−1.753	0.0072	7
ML1835		MSMEG6527	CHP	−1.556	0.0030	10
ML0510		MSMEG3035	CHP	−1.444	0.0004	10
ML0886		MSMEG4257	Possible glycosyltransferase	−1.430	0.0024	7
ML1312		MSMEG4598	CHP	−1.229	0.0001	10
argD-g	*argD*	MSMEG2446	Probable acetylornithine aminotransferase	−1.027	0.0033	7
gabD-q	*gabD*	MSMEG2554	Probable aldehyde dehydrogenase (NAD dependent)	−1.005	0.0052	7
Rv3134c	*uspL*	MSMEG5230	Universal stress protein	−0.990	0.0098	10
Rv1623c	*cydA*	MSMEG3243	Cytochrome *bd* oxidase subunit I	−0.931	0.0069	7
ML1926		MSMEG0828	Putative tuberculin-related protein	−0.915	0.0058	3
Rv1592c		MSMEG3205	CHP	−0.878	0.0016	10
Downregulated genes						
lytB2	*lytB*	MSMEG5208	Probable LytB-related protein, LytB2	3.316	0.0002	3
xseA	*xseA*	MSMEG5210	Exo-deoxyribonuclease VII, large subunit	2.737	0.0003	2
ML2088-a		MSMEG4807	Putative cytochrome P450	2.039	0.0004	7
ctpC-a		MSMEG5384	Cadmium-translocating P-type ATPase	1.789	0.0081	3
rpoT	*sigA*	MSMEG2759	RNA polymerase sigma factor, SigA	1.513	0.0000	2
rplE	*rplE*	MSMEG1464	Ribosomal protein L5	1.198	0.0002	2
ML2661-e	*fadD7*	MSMEG3702	Fatty acid coenzyme A ligase, FadD7	1.197	0.0051	1
fpg	*Fpg*	MSMEG2417	Formamidopyrimidine-DNA glycosylase	0.961	0.0078	7
ML1750		MSMEG2202	CHP	0.922	0.0098	10

[a] Gene identifier as defined in the MIAME compliance file (http://vbc.med.monash.edu.au/≈powell/M.smegmatis).
[b] TIGR annotation (http://www.tigr.org/tigr-scripts/CMR2/CMRHomePage.spl).
[c] Function as per Tuberculist and Leproma (http://genolist.pasteur.fr). CHP, conserved hypothetical protein.
[d] Log_2 of the fold ratio.
[e] Functional classification as per Tuberculist and Leproma: 1, lipid metabolism; 2, information pathways; 3, cell wall and cell processes; 6, PE/PPE; 7, intermediary metabolism and respiration; 9, regulatory proteins; 10, conserved hypotheticals.

failure to recover a null *ctaD1* mutant was unlikely to be due to the essentiality of this gene but could be due to polar effects of the Δ*ctaDI*::*hyg* mutation on the downstream *serB2* gene, which may be essential (30).

We could only identify distinct *ctaD* alleles in the genome of *M. smegmatis* and not in any other sequenced mycobacterial species (http://www.tigr.org/tigr-scripts/CMR2/CMRHomePage.spl; http://genolist.pasteur.fr). However, two or more *ctaD* alleles were also identified in the genomes of several other completely sequenced actinobacteria (http://www.ncbi.nlm.nih.gov/sutils/genom_table.cgi), including *Streptomyces*, and *Nocardia* species. *Paracoccus denitrificans* has similarly been found to contain two distinct *ctaD* genes (26, 38), suggesting that the presence of multiple *ctaD* genes is a reasonably common occurrence in bacterial genomes. In *P. denitrificans*, the *ctaDI* and *ctaDII* genes appear to be functionally interchangeable, implying the existence of CcO isoenzymes (26). Importantly, the microarray analysis suggested that *ctaDII* (MSMEG4435) is expressed in *M. smegmatis* under aerobic conditions. However, the extent (if any) of functional redundancy and/or interchangeability of the *M. smegmatis ctaD* alleles has yet to be determined.

The failure to recover allelic exchange mutants in the bc_1-aa_3 pathway of *M. tuberculosis* H37Rv suggests that the mutants were either severely attenuated or nonviable under the conditions tested. This conclusion is supported by the underrepresentation of transposon mutations in genes encoding the bc_1 complex (*qcrCAB*) and the CcO (*ctaC*, *ctaD*, *ctaE*) in high-density mutagenized libraries of *M. tuberculosis*, as determined by transcription site hybridization (30).

Up-regulation of *cyd* occurs in response to disruption of the bc_1-aa_3 respiratory pathway. In *M. smegmatis*, inactivation of the bc_1-aa_3 pathway at the level of the bc_1 complex or the CcO (data not shown) resulted in pronounced up-regulation of the *bd*-type terminal oxidase encoded by the *cydABDC* operon. Analogous observations have been made in *P. denitrificans*, where changes in electron distribution caused by blockage of a respiratory pathway affected the activities of terminal oxidase promoters (21). The viability of the *ctaC* and *qcrCAB* mutants of *M. smegmatis* attests to the adaptability of the respiratory network in this organism, which allows its energy requirements to be met by increased activity of the bioenergetically less efficient *bd*-type oxidase. In addition to *cydAB*, genes encoding a second putative *bd*-type oxidase have also been identified in *M. smegmatis* (MSMEG5584 and MSMEG5585) (16). The microarray analysis confirmed that MSMEG5584 is expressed in *M. smegmatis* grown aerobically, but unlike *cydA*, this gene was not differentially expressed in response to blockage of the bc_1-aa_3 pathway.

The apparent essentiality of the bc_1-aa_3 pathway in *M. tuberculosis* may be due to an inability of its aerobic respiratory network to adapt in a manner analogous to that of *M. smegmatis*. However, *cyd* gene expression in *M. tuberculosis* has been shown to be highly responsive to interference with the machinery that maintains the proton motive force, as evidenced by its upregulation by inhibitors of CcO and chemicals

that affect its maturation (5), by growth on palmitate (5), during adaptation to hypoxia (5, 40), and by protonophores (5). We therefore conclude that respiratory adaptation by *cyd* upregulation probably does occur in *M. tuberculosis* in response to disruption of the bc_1-aa_3 pathway, but the consequence of single-route electron flow to the bioenergetically less efficient cytochrome *bd*-type menaquinol oxidase (15) in this slow-growing mycobacterium may be such that mutant colonies might not be detectable under the conditions employed in this study (up to 54 days of incubation).

Other adaptations to rerouting of the electron flux through cytochrome *bd* oxidase. A broader view of the consequences of rerouting of the electron flux through the cytochrome *bd*-type menaquinol oxidase-terminating branch was obtained from comparative expression profiling of the bc_1 mutant and its parental wild type using a partial-genome microarray of *M. smegmatis* that is enriched for essential genes. In addition to *cydA*, two other genes known to be induced by hypoxia were also upregulated in the bc_1 mutant, *uspL* (MSMEG5230) and the homolog of Rv1592c (MSMEG3205). Interestingly, UspL is a member of the DosR regulon of *M. smegmatis* (20).

Although the partial-genome array also contained other genes identified by O'Toole et al. (20) as being hypoxically induced and regulated by DosR, including *hspX* (MSMEG3937), *uspM* (MSMEG3957), *dosS* (MSMEG5226), *dosR* (MSMEG5229) and *acg* (MSMEG5231), these genes were not found to be differentially expressed in the bc_1 mutant. Therefore, although the results of microarray analysis were suggestive of an overall increase in the reduced state of the respiratory chain, blockage of electron transport via the bc_1-aa_3 pathway by deletion of the bc_1 complex did not induce the DosR regulon of *M. smegmatis*. This observation suggests that the molecular signal(s) generated by deletion of the bc_1 complex is distinct from that generated by O_2 starvation, although some genes may respond to both, e.g., *cydA* (16) and *uspL* (this study). Current work is aimed at using the respiratory mutant strains as tools for investigating these molecular signals and their transduction pathways.

ACKNOWLEDGMENTS

This work was supported by grants from the Howard Hughes Medical Institute (International Research Scholar's grants to V.M. and R.L.C.), the Medical Research Council of South Africa, the National Research Foundation of South Africa, the World Health Organization TDR, the Australian National Health and Medical Research Council, the Australian Research Council, and the NIH (#AI43420 to H.R.).

Preliminary sequence data were obtained from the Institute for Genomic Research website at http://www.tigr.org. We thank Marty Voskuil and David Sherman for helpful discussions.

REFERENCES

1. **Betts, J. C., P. T. Lukey, L. C. Robb, R. A. McAdam, and K. Duncan.** 2002. Evaluation of a nutrient starvation model of *Mycobacterium tuberculosis* persistence by gene and protein expression profiling. Mol. Microbiol. **43:** 717–731.
2. **Blondelet-Rouault, M. H., J. Weiser, A. Lebrihi, P. Branny, and J. L. Pernodet.** 1997. Antibiotic resistance gene cassettes derived from the interposon for use in *E. coli* and *Streptomyces*. Gene **190:**315–317.
3. **Boshoff, H. I. M., and V. Mizrahi.** 1998. Purification, gene cloning, targeted knockout, overexpression, and biochemical characterization of the major pyrazinamidase from *Mycobacterium smegmatis*. J. Bacteriol. **180:**5809–5814.
4. **Boshoff, H. I. M., M. B. Reed, C. E. Barry III, and V. Mizrahi.** 2003. DnaE2 polymerase contributes to in vivo survival and the emergence of drug resistance in *Mycobacterium tuberculosis*. Cell **113:**183–193.
5. **Boshoff, H. I. M., T. G. Myers, B. R. Copp, M. R. McNeil, M. A. Wilson, and C. E. Barry III.** 2004. The transcriptional responses of *Mycobacterium tuberculosis* to inhibitors of metabolism: novel insights into drug mechanisms of action. J. Biol. Chem. **279:**40174–40184.
6. **Boshoff, H. I. M., and C. E. Barry.** 2005. Tuberculosis –metabolism and respiration in the absence of growth. Nat. Rev. Microbiol. **3:**70–80.
7. **Bott, M., and A. Niebisch.** 2003. The respiratory chain of *Corynebacterium glutamicum*. J. Biotech. **104:**129–153.
8. **Cole, S. T., R. Brosch, J. Parkhill, T. Garnier, C. Churcher, D. Harris, S. V. Gordon, K. Eiglmeier, S. Gas, C. E. Barry, III, F. Tekaia, K. Badcock, D. Basham, D. Brown, T. Chillingworth, R. Connor, R. Davies, K. Devlin, T. Feltwell, S. Gentles, N. Hamlin, S. Holroyd, T. Hornsby, K. Jagels, A. Krogh, J. McLean, S. Moule, L. Murphy, K. Oliver, J. Osborne, M. A. Quail, M. A. Rajandream, J. Rogers, S. Rutter, K. Seeger, J. Skelton, R. Squares, S. Squares, J. E. Sulston, J. Taylor, S. Whitehead, and B. G. Barrell.** 1998. Deciphering the biology of *Mycobacterium tuberculosis* from the complete genome sequence. Nature **393:**537–544.
9. **Cole, S. T., K. Eiglmeier, J. Parkhill, K. D. James, N. R. Thomson, P. R. Wheeler, N. Honore, T. Garnier, C. Churcher, D. Harris, K. Mungall, D. Basham, D. Brown, T. Chillingworth, R. Connor, R. M. Davies, K. Devlin, S. Duthoy, T. Feltwell, A. Fraser, N. Hamlin, S. Holroyd, T. Hornsby, K. Jagels, C. Lacroix, J. Maclean, S. Moule, L. Murphy, K. Oliver, M. A. Quail, M. A. Rajandream, K. M. Rutherford, S. Rutter, K. Seeger, S. Simon, M. Simmonds, J. Skelton, R. Squares, S. Squares, K. Stevens, K. Taylor, S. Whitehead, J. R. Woodward, and B. G. Barrell.** 2001. Massive gene decay in the leprosy bacillus. Nature **409:**1007–1011.
10. **Dahl, J. L., C. N. Krause, H. I. Boshoff, B. Doan, K. Foley, D. Avarbock, G. Kaplan, V. Mizrahi, H. Rubin, and C. E. Barry III.** 2003. The role of Rel_{Mtb}-mediated adaptation to stationary phase in long-term persistence of *Mycobacterium tuberculosis* in mice. Proc. Natl. Acad. Sci. USA **100:**10026–10031.
11. **Dudoit, S., and Y. H. Yang.** 2003. Bioconductor R packages for exploratory analysis and normalization of cDNA microarray data, p. 45–65. *In* P. Parmigiani, E. S. Garrett, R. A. Irizarry, and S. L. Zeger, (ed.), The analysis of gene expression data: methods and software. Springer Verlag, New York, NY.
12. **Galamba, A., K. Soetaert, X.-M. Wang, J. De Bruyn, P. Jacobs, and J. Content.** 2001. Disruption of *adhC* reveals a large duplication in the *Mycobacterium smegmatis* mc^2155 genome. Microbiology **147:**3281–3294.
13. **Gomez, M., L. Doukhan, G. Nair, and I. Smith.** 1998. *sigA* is an essential gene in *Mycobacterium smegmatis*. Mol. Microbiol. **29:**617–628.
14. **Gordhan, B. G., and T. Parish.** 2001. Gene replacement using pretreated DNA. Methods Mol. Med. **54:**77–92.
15. **Hansford, R.** 2001. Oxidative phosphorylation, p. 1–8. *In* Encyclopedia of life sciences. Nature Publishing Group, London, United Kingdom.
16. **Kana, B. D., E. A. Weinstein, D. Avarbock, S. S. Dawes, H. Rubin, and V. Mizrahi.** 2001. Characterization of the *cydAB*-encoded cytochrome *bd* oxidase from *Mycobacterium smegmatis*. J. Bacteriol. **183:**7076–7086.
17. **Kendall, S. L., F. Movahedzadeh, S. C. G. Rison, L. Wernisch, T. Parish, K. Duncan, J. C. Betts, and N. G. Stoker.** 2004. The *Mycobacterium tuberculosis dosRS* two-component system is induced by multiple stresses. Tuberculosis **84:**247–255.
18. **Niebisch, A., and M. Bott.** 2001. Molecular analysis of the cytochrome bc_1-aa_3 branch of the *Corynebacterium glutamicum* respiratory chain containing an unusual diheme cytochrome c_1. Arch. Microbiol. **175:**282–294.
19. **Niebisch, A., and M. Bott.** 2003. Purification of a cytochrome bc_1-aa_3 supercomplex with quinol oxidase activity from *Corynebacterium glutamicum*. Identification of a fourth subunit of cytochrome aa_3 oxidase and mutational analysis of diheme cytochrome c_1. J. Biol. Chem. **278:**4339–4346.
20. **O'Toole, R., M. J. Smeulders, M. C. Blokpoel, E. J. Kay, K. Lougheed, and H. D. Williams.** 2003. A two-component regulator of universal stress protein expression and adaptation to oxygen starvation in *Mycobacterium smegmatis*. J. Bacteriol. **185:**1543–1554.
21. **Otten, M. F., D. M. Stork, W. N. M. Reijnders, H. V. Westerhoff, and R. J. M. Van Spanning.** 2001. Regulation of expression of terminal oxidases in *Paracoccus denitrificans*. Eur. J. Biochem. **268:**2486–2497.
22. **Parish, T., and N. G. Stoker.** 2000. Use of a flexible cassette method to generate a double unmarked *Mycobacterium tuberculosis tlyA plcABC* mutant by gene replacement. Microbiology **146:**1969–1975.
23. **Park, H. D., K. M. Guinn, M. I. Harrell, R. Liao, M. I. Voskuil, M. Tompa, G. K. Schoolnik, and D. R. Sherman.** 2003. Rv3133c/*dosR* is a transcription factor that mediates the hypoxic response of *Mycobacterium tuberculosis*. Mol. Microbiol. **48:**833–843.
24. **Pedulla, M. L., and G. F. Hatfull.** 1998. Characterization of the *mIHF* gene of *Mycobacterium smegmatis*. J. Bacteriol. **180:**5473–5477.
25. **Poole, R. K., and G. M. Cook.** 2000. Redundancy of aerobic respiratory chains in bacteria? Routes, reasons and regulation. Adv. Microb. Physiol. **43:**165–224.
26. **Raitio, M., J. M. Pispa, T. Metso, and M. Saraste.** 1990. Are there isoenzymes of cytochrome *c* oxidase in *Paracoccus denitrificans*? FEBS Lett. **261:** 431–435.
27. **Rohdich, F., S. Hecht, K. Gärtner, P. Adam, C. Krieger, S. Amslinger, D. Arigoni, A. Bacher, and W. Eisenreich.** 2002. Studies on the nonmevalonate

terpene biosynthetic pathway: Metabolic role of IspH (LytB) protein. Proc. Natl. Acad. Sci. USA **99:**1158–1163.
28. **Rozen, S., and H. Skaletsky.** 2000. Primer3 on the WWW for general users and for biologist programmers. Methods Mol. Biol. **132:**365–386.
29. **Sakamoto, J., T. Shibata, T. Mine, R. Miyahara, T. Torigoe, S. Noguchi, K. Matsushita, and N. Sone.** 2001. Cytochrome *c* oxidase contains an extra charged amino acid cluster in a new type of respiratory chain in the amino-acid-producing Gram-positive bacterium *Corynebacterium glutamicum*. Microbiology **147:**2865–2871.
30. **Sassetti, C. M., D. H. Boyd, and E. J. Rubin.** 2003. Genes required for mycobacterial growth defined by high density mutagenesis. Mol. Microbiol. **48:**77–84.
31. **Sherman, D. R., M. I. Voskuil, D. Schnappinger, R. Liao, M. I. Harrell, and G. K. Schoolnik.** 2001. Regulation of the *Mycobacterium tuberculosis* hypoxic response gene encoding α-crystallin. Proc. Natl. Acad. Sci. USA **98:**7534–7539.
32. **Smyth, G. K.** 2004. Linear models and empirical Bayes methods for assessing differential expression in microarray experiments. Stat. Appl. Genet. Mol. Biol. **3:**1–26.
33. **Smyth, G. K., J. Michaud, and H. S. Scott.** 2005. Use of within-array replicate spots for assessing differential expression in microarray experiments. Bioinformatics **0:**2701 (Epub ahead of print).
34. **Snapper, S. B., R. E. Melton, T. Mustafa, T. Keiser, and W. R. Jacobs, Jr.** 1990. Isolation and characterization of efficient plasmid transformation mutants of *Mycobacterium smegmatis*. Mol. Microbiol. **4:**1911–1919.
35. **Sone, N., K. Nagata, H. Kojima, J. Tajima, Y. Kodera, T. Kanamaru, S. Noguchi, and J. Sakamoto.** 2001. A novel hydrophobic diheme *c*-type cytochrome: Purification from *Corynebacterium glutamicum* and analysis of the *qcrCBA* operon encoding three subunit proteins of a putative cytochrome reductase complex. Biochim. Biophys. Acta **1503:**279–290.
36. **Sone, N., M. Fukuda, S. Katayama, A. Jyoudai, M. Syugyou, S. Noguchi, and J. Sakamoto.** 2003. *QcrCAB* operon of a nocardia-form actinomycete *Rhodococcus rhodochrous* encodes cytochrome reductase complex with diheme cytochrome *cc* subunit. Biochim. Biophys. Acta **1557:**125–131.
37. **Timm, J., F. A. Post, L. G. Bekker, G. B. Walther, H. C. Wainwright, R. Manganelli, W. T. Chan, L. Tsenova, B. Gold, I. Smith, G. Kaplan, and J. D. McKinney.** 2003. Differential expression of iron-, carbon-, and oxygen-responsive mycobacterial genes in the lungs of chronically infected mice and tuberculosis patients. Proc. Natl. Acad. Sci. USA **100:**14321–14326.
38. **van der Oost, J., T. Haltia, M. Raitio, and M. Saratse.** 1991. Genes encoding for cytochrome *c* oxidase in *Paracoccus denitrificans*. J. Bioenerg. Biomembr. **23:**257–267.
39. **Voskuil, M. I., D. Schnappinger, K. C. Visconti, M. I. Harrell, G. M. Dolganov, D. R. Sherman, and G. K. Schoolnik.** 2003. Inhibition of respiration by nitric oxide induces a *Mycobacterium tuberculosis* dormancy program. J. Exp. Med. **198:**705–713.
40. **Voskuil, M. I., K. C. Visconti, and G. K. Schoolnik.** 2004. *Mycobacterium tuberculosis* gene expression during adaptation to stationary phase and low-oxygen dormancy. Tuberculosis **84:**281–327.
41. **Wayne, L. G., and C. D. Sohaskey.** 2001. Nonreplicating persistence of *Mycobacterium tuberculosis*. Annu. Rev. Microbiol. **55:**139–163.
42. **Weinstein, E. A., T. Yano, L.-S. Li, D. Avarbock, A. Avarbock, D. Helm, A. A. McColm, K. Duncan, J. T. Lonsdale, and H. Rubin.** 2005. Inhibitors of type II NADH:menaquinone oxidoreductase represent a class of antitubercular drugs. Proc. Natl. Acad. Sci. USA **102:**4548–4553.
43. **Yang, Y. H., S. Dudoit, P. Luu, and T. P. Speed.** 2001. Normalisation for cDNA microarray data, p. 141–152. *In* M. L. Bittner, Y. Chen, A. N. Dorsel, and E. R. Dougherty (ed.), Microarrays: optical technologies and informatics. Proceedings of the International Society for Optical Engineering, vol. 4266. International Society for Optical Engineering, San Jose, California.

TABLE S1. Genes differentially expressed in aerobically grown Δ*qcrCAB*::*hyg* mutant of *M. smegmatis*

ID[a]	Gene	TIGR annotation[b]	Function[c]	M[d]	P value	Class[e]
Upregulated genes						
ribA	*ribA2*	MSMEG3082	Probable riboflavin biosynthesis protein	-2.301	0.0020	7
ML2274		MSMEG3498	Probable conserved secreted protein	-1.914	0.0072	3
mihF	*mihF*	MSMEG3063	Putative integration host factor	-1.764	0.0003	2
glgC	*glgC*	MSMEG5067	glucose-1-phosphate adenyl-transferase	-1.753	0.0072	7
ML1835		MSMEG6527	CHP	-1.556	0.0030	10
ML0510		MSMEG3035	CHP	-1.444	0.0004	10
ML0886		MSMEG4257	possible glycosyl transferase	-1.430	0.0024	7
ML1312		MSMEG4598	CHP	-1.229	0.0001	10
argD-g	*argD*	MSMEG2446	probable acetylornithine aminotransferase	-1.027	0.0033	7
gabD-q	*gabD*	MSMEG2554	probable aldehyde dehydrogenase (NAD-dependent)	-1.005	0.0052	7
Rv3134c	*uspL*	MSMEG5230	Universal stress protein	-0.990	0.0098	10
Rv1623c	*cydA*	MSMEG3243	Cytochrome *bd* oxidase subunit I	-0.931	0.0069	7
ML1926		MSMEG0828	putative tuberculin-related protein	-0.915	0.0058	3
Rv1592c		MSMEG3205	CHP	-0.878	0.0016	10
ML1783		MSMEG4344	possible transcriptional regulatory protein	-0.849	0.0080	9
PPE-b	*PPE*	MSMEG0063	PPE family domain	-0.807	0.0003	6
ML0663		MSMEG2085	CHP	-0.804	0.0016	10
argD-e	*argD*	MSMEG2971	probable acetylornithine aminotransferase	-0.767	0.0030	7
atpH	*atpH*	MSMEG4925	ATP synthase delta chain	-0.741	0.0024	7
ML0990		MSMEG2732	CHP	-0.701	0.0066	10
glpD-a	*glpD*	MSMEG6721	glycerol-3-phosphate dehydrogenase	-0.683	0.0017	7
menD	*menD*	MSMEG1225	bifunctional menaquinone biosynthesis protein	-0.677	0.0072	7
Rv3841	*bfrB*	MSMEG6385	bacterioferritin	-0.660	0.0062	7

bccA-c		MSMEG1807	biotin carboxy carrier protein biotin carboxyl transferase	-0.641	0.0017	1
purM	*purM*	MSMEG5766	phosphoribosylformylglycinamidine cyclo-ligase	-0.635	0.0082	7
fas	*fas*	MSMEG0552	fatty acid synthase	-0.633	0.0015	
lpqF	*lpqF*	MSMEG6050	probable conserved lipoprotein	-0.617	0.0062	3
ML0759	*fbiA*	MSMEG1829	probable F420 biosynthesis protein	-0.611	0.0015	7
gabD-y	*gabD*	MSMEG1497	succinate-semialdehyde dehydrogenase	-0.600	0.0075	7
glnA2-f	*glnA2*	MSMEG2596	probable glutamine synthetase	-0.593	0.0026	7
ML1094		MSMEG1104	short chain type dehydrogenase/ reductase	-0.590	0.0024	7
ML0596-a	*csd*	MSMEG4531	probable cysteine desulfurase	-0.576	0.0020	7
ML2203		MSMEG3807	CHP	-0.552	0.0020	10
ML2289		none	CHP	-0.537	0.0020	10
sdhC	*sdhC*	MSMeg1669	succinate dehydrogenase	-0.528	0.0082	7
lysX	*lysX*	MSMEG6531	lysyl-tRNA synthetase	-0.501	0.0070	2
phoT	*phoT*	MSMEG2124	phosphate transport ATP-binding protein	-0.496	0.0066	3
ML2053	*adhA*	MSMEG0251	probable alcohol dehydrogenase	-0.477	0.0041	7
uvrD2	*uvrD2*	MSMEG1956	ATP-dependent DNA helicase	-0.476	0.0051	2
gabD-e	*gabD*	MSMEG6662	aldehyde dehydrogenase family protein	-0.469	0.0062	7
folK	*folK*	MSMEG6064	2-amino-4-hydroxy-6-hydroxymethyldihydropteridine pyrophosphokinase	-0.443	0.0071	7
miaA	*miaA*	MSMEG6675	probable tRNA delta(2)-isopentenylpyrophosphate transferase	-0.383	0.0100	7
Downregulated genes						
lytB2	*lytB*	MSMEG5208	probable LytB-related protein, LytB2	3.316	0.0002	3
xseA	*xseA*	MSMEG5210	exo-deoxyribonuclease VII, large subunit	2.737	0.0003	2
ML2088-a		MSMEG4807	putative cytochrome P450	2.039	0.0004	7
ctpC-a		MSMEG5384	cadmium-translocating P-type ATPase	1.789	0.0081	3

rpoT	*sigA*	MSMEG2759	RNA polymerase sigma factor, SigA	1.513	0.0000	2
rplE	*rplE*	MSMEG1464	ribosomal protein L5	1.198	0.0002	2
ML2661-e	*fadD7*	MSMEG3702	Fatty acid CoA ligase, FadD7	1.197	0.0051	1
fpg	*fpg*	MSMEG2417	formamidopyrimidine-DNA glycosylase	0.961	0.0078	7
ML1750		MSMEG2202	CHP	0.922	0.0098	10
uvrB	*uvrB*	MSMEG3820	excinuclease ABC, B subunit	0.843	0.0057	2
Rv1009	*rpfB*	MSMEG5419	probable resuscitation-promoting factor B, RpfB	0.835	0.0027	3
uspE	*uspB*	MSMEG4462	probable sugar ABC transporter	0.810	0.0024	3
ML0115		MSMEG6327	CHP	0.807	0.0051	10
ML2661-h	*fadD7*	MSMEG4041	Fatty acid CoA ligase, FadD7	0.805	0.0002	1
Rv2393		MSMEG4522	CHP	0.771	0.0041	10
ML2491-c		MSMEG4370	CHP	0.760	0.0033	10
ML0815		MSMEG1939	transcriptional regulator, TetR family domain	0.725	0.0002	9
rpsL	*rpsL*	MSMEG1393	ribosomal protein S12	0.724	0.0066	2
ML0691-b	*dacB*	MSMEG1659	probable D-alanyl-alanine carboxypeptidase	0.720	0.0005	3
ML0729		MSMEG1810	CHP	0.674	0.0039	10
ML0093	*glfT*	MSMEG5323	bifunctional UDP-galactofuranosyl transferase	0.668	0.0085	3
gatA-b	*gatA*	MSMEG1078	probable glutamyl-tRNA (GLN) amidotransferase	0.668	0.0024	2
atpD-c	*atpD*	MSMEG4939	probable ATP synthase Beta chain	0.660	0.0009	7
trpS	*trpS*	MSMEG1655	tryptophanyl-tRNA synthetase	0.655	0.0020	2
mce1A-a	*mce1A*	MSMEG6500	host cell invasion	0.650	0.0026	0
ML2549		MSMEG0428	CHP	0.628	0.0029	10
ML2620-b	*mmpL3*	MSMEG4733	possible conserved transmembrane transport protein	0.624	0.0024	3
pdc-a	*pdc*	MSMEG4455	probable pyruvate decarboxylase	0.590	0.0027	7
ML1115	*lprB*	MSMEG1390	possible lipoprotein	0.581	0.0031	3
ML0174	*mprA*	MSMEG5468	DNA-binding response regulator (persistence)	0.580	0.0016	9
umaA2-a	*umaA*	MSMEG1199	possible mycolic acid synthase	0.476	0.0041	1

ML1698		MSMEG5185	conserved membrane protein	0.464	0.0033	3
ML2140		MSMEG5666	transcriptional regulator, marR family	0.460	0.0070	9
ML2377	*mmpS4*	MSMEG0373	conserved membrane protein	0.455	0.0073	3
ML0243-b	*pks16*	MSMEG5415	putative polyketide synthase	0.440	0.0081	1
ung	*ung*	MSMEG3668	probable uracil-DNA glycosylase	0.422	0.0079	2

[a] Gene identifier as defined in the MIAME compliance file (http://vbc.med.monash.edu.au/ powell/M.smegmatis).

[b] TIGR annotation (http://www.tigr.org/tigr-scripts/CMR2/CMRHomePage.spl)

[c] Function as per Tuberculist and Leproma (http://genolist.pasteur.fr).

[d] Log_2 of the fold ratio

[e] Functional classification as per Tuberculist and Leproma. 1, Lipid metabolism; 2, Information pathways; 3, Cell wall cell processes; 6, PE/PPE; 7, Intermediary metabolism respiration; 9, Regulatory proteins; 10, Conserved hypotheticals.